

**INVESTIGATION OF DOWNFLOW HANGING SPONGE
(DHS) SYSTEM USING BACTERIAL AND FUNGAL
CULTURES AS A POST TREATMENT FOR THE UASB
EFFLUENT OF A TAPIOCA STARCH WASTEWATER**

Patcharin Racho

A Thesis Submitted in Partial Fulfillment of the Requirements for the

Degree of Doctor of Philosophy in Environmental Engineering

Suranaree University of Technology

Academic Year 2009

**การศึกษาระบบ DOWNFLOW HANGING SPONGE (DHS)
โดยใช้เชื้อแบคทีเรียและราเพื่อบำบัดน้ำทิ้งจากระบบ UASB
ในอุตสาหกรรมแป้งมันสำปะหลัง**

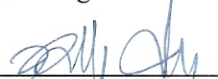
นางสาวพัชรินทร์ ราโช

วิทยานิพนธ์นี้เป็นส่วนหนึ่งของการศึกษาตามหลักสูตรปริญญาวิศวกรรมศาสตรดุษฎีบัณฑิต
สาขาวิชาวิศวกรรมสิ่งแวดล้อม
มหาวิทยาลัยเทคโนโลยีสุรนารี
ปีการศึกษา 2552

**INVESTIGATION OF DOWNFLOW HANGING SPONGE (DHS)
SYSTEM USING BACTERIAL AND FUNGAL CULTURES
AS A POST TREATMENT FOR THE UASB EFFLUENT
OF A TAPIOCA STARCH WASTEWATER**

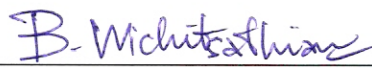
Suranaree University of Technology has approved this thesis submitted in partial fulfillment of the requirements for the Degree of Doctor of Philosophy

Thesis Examining Committee



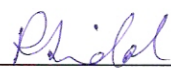
(Asst. Prof. Dr. Sudjit Karuchit)

Chairperson



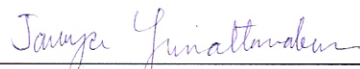
(Asst. Prof. Dr. Boonchai Wichitsathian)

Member (Thesis Advisor)



(Asst. Prof. Dr. Ranjna Jindal)

Member



(Asst. Prof. Dr. Jareeya Yimratanabovorn)

Member



(Dr. Piyarat Premanoch)

Member



(Prof. Dr. Sukit Limpijumnong)

Vice Rector for Academic Affairs



(Assoc. Prof. Dr. Vorapot Khompis)

Dean of Institute of Engineering

พัชรินทร์ ราโช : การศึกษาระบบ DOWNFLOW HANGING SPONGE (DHS) โดยใช้เชื้อแบคทีเรียและราเพื่อบำบัดน้ำทิ้งจากระบบ UASB ในอุตสาหกรรมแป้งมันสำปะหลัง (INVESTIGATION OF DOWNFLOW HANGING SPONGE (DHS) SYSTEM USING BACTERIAL AND FUNGAL CULTURES AS A POST TREATMENT FOR THE UASB EFFLUENT OF A TAPIOCA STARCH WASTEWATER) อาจารย์ที่ปรึกษา : ผู้ช่วยศาสตราจารย์ ดร.บุญชัย วิจิตรเสถียร, 309 หน้า.

การศึกษาระบบ Downflow hanging sponge (DHS) เพื่อเป็นระบบบำบัดขั้นหลังให้กับระบบ UASB ในการบำบัดน้ำเสียอุตสาหกรรมที่มีความเข้มข้นของสารอินทรีย์และไนโตรเจนสูง แต่โดยทั่วไประบบกรองชีวภาพจำเป็นต้องควบคุมค่าภาระบรรทุกสารอินทรีย์ให้ต่ำและคงที่ เนื่องจากในภาวะบรรทุกสารอินทรีย์สูงจะสนับสนุนการเจริญเติบโตของจุลชีพกลุ่มเฮเทอโรโทรฟทำให้มวลชีวภาพในระบบสูงจึงเกิดการอุดตันขึ้นกรองได้ อีกทั้งการล้างย้อนไม่สามารถทำได้ในระบบ DHS ดังนั้นการศึกษานี้จึงมีวัตถุประสงค์เพื่อพัฒนาระบบ DHS โดยใช้เชื้อรา (FDHS) และแบคทีเรีย (BDHS) เป็นจุลชีพในการเป็นบำบัดน้ำทิ้งจากระบบ UASB ในอุตสาหกรรมแป้งมันสำปะหลัง การศึกษาทำการเปรียบเทียบประสิทธิภาพระบบ FDHS และ BDHS ด้วยการประเมินการกำจัดสารอินทรีย์และไนโตรเจน ค่าคงที่ทางจลศาสตร์ และลักษณะของตะกอน อีกทั้งทำการประเมินผลกระทบขององค์ประกอบของฟิล์มตรึงต่อการทำงานของจุลชีพ และความเข้มข้นของสารอินทรีย์ในระบบ DHS โดยแบ่งการทดลองออกเป็น 3 ช่วงเวลาซึ่งมีระยะเวลาในการกักเก็บใน RUN I เท่ากับ 4 ชั่วโมง และใน RUN II และ RUN III เท่ากับ 1 ชั่วโมง จากผลการศึกษาพบว่าประสิทธิภาพการกำจัดสารอินทรีย์ของระบบ FDHS สูงกว่าระบบ BDHS ในทุกช่วงของการศึกษา โดยมีประสิทธิภาพการกำจัดค่าบีโอดีทั้งหมด (TBOD) ในช่วง 83-95% ส่วนประสิทธิภาพการกำจัดไนโตรเจนของระบบ BDHS พบสูงสุดใน RUN I โดยสามารถกำจัดไนโตรเจนทั้งหมดได้ประมาณ 68% แต่ระบบ FDHS ไม่สามารถกำจัดไนโตรเจนด้วยกระบวนการไนตริฟิเคชันและดีไนตริฟิเคชันได้ อีกทั้งจากการศึกษาค่าคงที่ทางจลศาสตร์พบอัตราการเจริญเติบโตของจุลชีพ (μ_{max}) สูงสุดในระบบ FDHS ส่วนที่ 1 ซึ่งเป็นส่วนที่สามารถกำจัดค่า TBOD ได้สูงสุดเช่นกัน ส่วนการศึกษาองค์ประกอบของตะกอนพบว่าค่าของแข็งระเหยง่าย (VSS) ในตะกอนที่อยู่ในตัวกลางฟองน้ำของระบบ FDHS มีค่าค่อนข้างคงที่แสดงถึงความสามารถในการย่อยสลายตะกอนเกิดได้ค่อนข้างดีจึงทำให้เกิดสมดุลของตะกอนขึ้นในระบบ และการเกิดเส้นใยของเชื้อราทำให้โครงสร้างของระบบฟิล์มตรึงหลวมและการถ่ายเทมวลของอาหารและออกซิเจนเข้าสู่ภายในฟิล์มตรึงเกิดได้ดี อีกทั้งการศึกษายังพบว่าระบบ DHS ทั้งสองระบบมีเสถียรภาพเมื่อมีการเปลี่ยนแปลงค่า HLR ทำให้ระบบ DHS เป็นระบบที่มีประสิทธิภาพในการเป็นระบบบำบัดน้ำเสียขั้นหลังระบบ UASB

การศึกษาด้วยแบบจำลองทางคณิตศาสตร์ทำการศึกษาโดยการประยุกต์ใช้ Unified multi-components cellular automaton (UMCCA) model เพื่อประเมินค่าความหนาแน่นของฟิล์มตรึงจากองค์ประกอบที่เป็นของแข็ง จากผลการศึกษาพบว่าฟิล์มตรึงในระบบ BDHS มีความหนาแน่นสูงกว่าระบบ FDHS ทั้งหมดในทุกส่วนของถึงปฏิกิริยา โดยเกิดเนื่องจากอัตราการตายของจุลชีพในระบบ FDHS ต่ำกว่าระบบ BDHS จึงเกิดการสะสมของเซลล์ที่ตายแล้วในฟิล์มตรึงได้มากกว่า และเมื่อนำค่าความหนาแน่นไปประเมินค่าความสัมพันธ์ของการถ่ายเทมวลในฟิล์มตรึง (f_D) พบว่ามีแนวโน้มที่ตรงกันกับค่าความหนาแน่น โดยด้านบนของฟิล์มตรึงซึ่งมีอายุน้อยกว่าและมีโครงสร้างไม่แน่นอนมีค่า f_D สูงกว่าด้านล่างแต่มีค่าความหนาแน่นต่ำและยังพบว่าค่า f_D ทั้งหมดของระบบ FDHS สูงกว่าระบบ BDHS และค่าความพรุนของฟิล์มตรึงมีค่าลดลงตามระดับความลึกของฟิล์มตรึงอีกด้วย อีกทั้งผลการศึกษายังให้ความชัดเจนในการอธิบาย โครงสร้างของฟิล์มตรึงที่มีผลกระทบต่ออัตราการถ่ายเทมวลและการย่อยสลายภายในฟิล์มตรึง ซึ่งนำไปสู่การควบคุมเงื่อนไขในการเดินระบบให้มีความเหมาะสม

สาขาวิชา วิศวกรรมสิ่งแวดล้อม

ปีการศึกษา 2552

ลายมือชื่อนักศึกษา



ลายมือชื่ออาจารย์ที่ปรึกษา



ลายมือชื่ออาจารย์ที่ปรึกษาร่วม



PATCHARIN RACHO : INVESTIGATION OF DOWNFLOW HANGING SPONGE (DHS) SYSTEM USING BACTERIAL AND FUNGAL CULTURES AS A POST TREATMENT FOR THE UASB EFFLUENT OF A TAPIOCA STARCH WASTEWATER. THESIS ADVISOR : ASST. PROF. BOONCHAI WICHITSATHIAN, Ph.D., 309 PP.

DOWNFLOW HANGING SPONGE / FUNGAL BIOFILM / BACTERIAL BIOFILM / TAPIOCA STARCH WASTEWATER / BIOFILM DENSITY

Investigations were carried out to evaluate the performance of downflow hanging sponge (DHS) system as a post treatment for industrial wastewater effluents containing high organic and nitrogen concentration. In general, it is important to keep the organic waste load for biofilter constant and as low as possible because a high heterotroph bacteria combined with biofilm detachment may clog a biofilter, backwashing is not possible in DHS system. Thus, the objective of this research was to develop two DHS systems using mixed fungal culture (FDHS) and mixed bacterial culture (BDHS) systems, and to examine their potential for improving the quality of UASB effluents from a tapioca starch wastewater treatment process. This study attempted to compare the performance of the FDHS and BDHS systems by systematically evaluating organic and nitrogen removal, the biokinetic coefficients and sludge characteristics. Effect of biofilm compositions on the microbial activity and effluent organic matter concentrations were also investigated. The whole experimental period was divided into three runs (RUN I, RUN II and RUN III) with the hydraulic retention time (HRT) at 4 h, 1 h and 1 h, respectively and the organic loading rates (OLR) fluctuating in the range of 1.0-3.6 kgTBOD/m³-d. The organic removal efficiency of FDHS system was higher than BDHS system during three runs, ranging 83%-95%. The highest total nitrogen removal efficiency was found during RUN I about

68% for BDHS system. But nitrogen was not significantly removed in FDHS system by and nitrification and denitrification. Values of biokinetic coefficients of aerobic heterotrophs indicated that substrate utilization rate (r_x) and maximum specific growth rate (μ_{\max}) were higher in the first segment of fungal culture in FDHS system. Moreover, the VSS concentration in retained sludge of FDHS system remained almost constant suggesting that the degradation of old biomass nearly balanced the accumulation of the fresh one. Filamentous fungi formed the loose biofilm that presented sufficient high substrate and oxygen mass transport. Furthermore, two DHS systems exhibited substantial stability with respect to fluctuations in hydraulic loading that the proposed two DHS systems can be promising post treatment for UASB effluents.

The unified multi-component cellular automaton (UMCCA) model was applied for the quantitative simulation of the biofilm's composite density. The biofilm mass transport evaluation provided an empirical relationship between relative diffusivity (f_D) and biofilm density (ρ). All simulated results indicated that BDHS biofilms were denser than FDHS biofilms. This can be explained by the biomass decay rates (k_d) of FDHS system were lower than BDHS system. The relative diffusivity (f_D) values decreased with an enhanced biofilm density. The top, where the biofilm was young and irregular, had high f_D values that cause of small composite density. Also f_D values of all segments of FDHS system were higher than BDHS system. And, results show porosity decreased along the biofilm depth or the density was increased. Furthermore, the results of this study are helpful in obtaining a clearly physical description of biofilm structure affects mass transport and biodegradation in biofilms. That leads to suitable operating condition control.

School of Environmental Engineering

Academic Year 2009

Student's Signature P. Racho.

Advisor's Signature B. Widitsathian

Co-advisor's Signature R. del

ACKNOWLEDEMENTS

The author wishes to express her profound gratitude to her advisor, Asst. Prof. Dr. Boonchai Wichisathian, for his valuable guidance, advice and support throughout this study. She is gratefully thanked to her co-advisor, Asst. Prof. Dr. Ranjna Jindal from Mahidol University, for her valuable advice. Special thanks are extended to Asst. Prof. Dr. Sudjit Karuchit, Asst. Prof. Dr. Jareeya Yimrattanabovorn and Dr. Piyarat Premanoch for their valuable suggestions, comments and guidance given as members of the examination committee. She would like to express their sincere gratitude towards National Research Council of Thailand (NRCT) for funding this research.

She appreciates the active support of the staff members of the School of Environmental Engineering at Suranaree University of Technology (SUT), as well as to all her friends for their kind help, suggestions, and assistance throughout the period of this study.

Last but not the least, she would like to acknowledge the heartfelt gratitude she feels towards her family for their support and encouragement throughout her course of study at Suranaree University of Technology and reaffirms her faith in the all mighty.

Patcharin Racho

TABLE OF CONTENTS

	Page
ABSTRACT (THAI)	I
ABSTRACT (ENGLISH).....	III
ACKNOWLEDGEMENTS.....	V
TABLE OF CONTENTS	VI
LIST OF TABLES.....	XV
LIST OF FIGURES	XXIV
SYMBOLS AND ABBREVIATIONS.....	XXIX
CHAPTER	
I INTRODUCTION	1
1.1 Statement of the Problem	1
1.2 Background Information.....	3
1.2.1 Combinations of UASB and Downflow Hanging Sponge (DHS) System.....	3
1.2.2 The Unified Multi-Component Cellular Automaton (UMCCA) Model.....	4
1.3 Objectives of the Study.....	5
1.4 Scopes of the Study	5
II LITERATURE REVIEWS	7
2.1 Tapioca Starch Industry	7
2.2 Tapioca Starch Wastewater Characteristics	7

TABLE OF CONTENTS (Continued)

	Page
2.3 Conventional Methods of Tapioca Starch Wastewater Treatments	8
2.4 Main Limitations of Anaerobic Systems	11
2.4.1 Main Limitations of Anaerobic Systems	12
2.4.2 Limitation Regarding Nitrogen and Phosphorus	13
2.4.3 Limitation Regarding Microbiological Indicators	14
2.5 Advantages of the Combined (Anaerobic/Aerobic) System	14
2.6 Post Treatment Options for Effluent Enhancement.....	16
2.7 Downflow Hanging Sponge (DHS) Processes	18
2.7.1 Type of DHS Reactor	18
2.7.2 DHS Sludge Characteristics	20
2.7.3 Factors Affect on DHS System Performances.....	22
2.8 Past Studies of DHS System.....	24
2.8.1 Performance Comparison of DHS System and Other Post Treatment Systems.....	27
2.9 Application of Fungi in Wastewater Treatment	31
2.9.1 Domestic Sewage.....	32
2.9.2 Sludge Treatment.....	36
2.9.3 Decolorization of Wastewater	38
2.9.4 Agroindustrial and Food Processing Effluents	40
2.9.5 Metal Containing Effluents.....	42
2.9.6 Biological Nutrient Removal.....	44

TABLE OF CONTENTS (Continued)

	Page
2.10 The Advantages of Fungi.....	46
2.11 Biokinetic Coefficients Determination.....	48
2.11.1 Growth of Microorganism	48
2.11.2 Respirometric Method	50
2.12 Biofilm Composition and Density	56
2.12.1 Biofilm Compositions	56
2.12.2 Biofilm Compositions under the Unified Theory.....	58
2.12.3 Unified Theory for EPS, SMP, and Inert and Active Biomass	59
2.12.4 Biofilm Density	61
2.13 Mathematical Modeling of Biofilms.....	62
2.13.1 Mathematical Modeling Conceptual.....	62
2.13.2 Model Selection	66
2.14 The Unified Multiple Component Cellular Automaton (UMCCA) Model.....	70
2.14.1 Application of the Unified Multi-Component Cellular Automaton (UMCCA) Model	73
2.14.2 Trends predicted by the UMCCA Model for a Biofilm including Active Biomass and EPS	74
2.15 Influence of Microbial Growth Rate/Substrate Transport Rate (G Number) on Biofilm Structure	75

TABLE OF CONTENTS (Continued)

	Page
2.16 Rationales of the Study and Proposed Treatment System.....	77
2.16.1 Need of Downflow Hanging Sponge (DHS) System.....	77
2.16.2 Need of Fungal Culture for Organic Removal	78
2.16.3 Need of Bacterial Culture for Nitrogen Nutrient Removal.....	79
2.16.4 Need of the UMCCA Model.....	80
III METHODOLOGY	81
3.1 The UASB effluent Sampling Site	81
3.2 Sponge Characteristics.....	83
3.3 Enrichment of Seed Mixed Fungal and Bacterial Sludge.....	83
3.4 Experimental Setup of DHS System.....	86
3.5 Organic Loading Rate (OLR) Variation Study.....	87
3.6 Biokinetic Coefficients Determination	88
3.7 Investigation for Biodegradable COD Fractions	93
3.8 Material Balance Calculation Methods	94
3.9 Identifying Cultures	95
3.10 Sludge Characteristics	96
3.10.1 Microorganisms Morphology	96
3.10.2 Extracellular Polymeric Substances (EPS)	96
3.10.3 Active Biomass Concentrations.....	97

TABLE OF CONTENTS (Continued)

	Page
3.11 Analytical Methods.....	98
3.12 Application of the UMCCA Model for Biofilm	
Composition and Density in Two DHS Systems.....	99
3.12.1 Computer Environment.....	102
3.12.2 System Definition	103
3.12.3 Initial and Boundary Conditions.....	104
3.12.4 Model Variables.....	107
3.12.5 Mass Balance Equations	110
3.12.6 Mass Balance Equations	112
3.13 Dynamics of Biofilm Compositions and Density.....	113
IV EXPERIMENTAL RESULTS AND DISCUSSION.....	113
4.1 UASB Effluent Characterizations.....	115
4.2 Sludge Enrichment and Acclimatization	115
4.2.1 COD Removal.....	115
4.2.2 Biomass.....	117
4.3 Sponge Media Characteristics	118
4.4 Immobilized Biomass Preparation.....	119
4.4.1 Immobilization of Microorganisms onto	
Sponge Media	120
4.4.2 Retained Biomass and Treatment Efficiencies	120
4.5 Tracer Study.....	121

TABLE OF CONTENTS (Continued)

	Page
4.6 DHS Treatment Efficiency	125
4.6.1 Dissolved Oxygen (DO) Profiles	125
4.6.2 pH	126
4.6.3 TSS removal	128
4.6.4 Organic Matter Removal	128
4.6.5 Nitrogen Removal.....	133
4.6.6 Effect of Recirculation on DHS Efficiency	136
4.7 COD Fractions and Organic Biodegradation.....	139
4.8 Mass Balances	141
4.8.1 COD and Nitrogen Assimilation in Sludge.....	142
4.8.2 COD and Nitrogen Mass Balances	144
4.8.3 Denitrification Potential in DHS Systems	146
4.9 Biokinetic Parameters	147
4.10 Dominant Culture in DHS Sludge	148
4.11 Sludge Characteristics	149
4.11.1 Retained Sludge	150
4.11.2 Viable Cell Concentrations.....	151
4.11.3 Extracellular Polymeric Substances (EPS).....	152
4.11.4 Dead Cell Fractions	154
4.11.5 Sludge Retention Time (SRT)	155
4.11.6 Sludge Morphology	156

TABLE OF CONTENTS (Continued)

	Page
4.12 Effect of Extracellular Polymeric Substance (EPS) on Effluent Organic Matter Concentrations	159
4.13 Effect of Treatment Loading on Sludge Compositions	160
4.14 Problem and Limitation of DHS Systems	164
4.14.1 The Development of Predators	164
4.14.2 Filter Clogging.....	165
4.15 Operating Cost Analysis	166
V MATHEMATICAL MODELING OF BIOFILM	
COMPOSITION AND DENSITY DYNAMICS.....	167
5.1 Application of the UMCCA Model for Biofilm Composition and Density in Two DHS Systems.....	167
5.1.1 Simulated Dynamics of Biofilm Compositions	167
5.1.2 Biofilm Composite Density Simulation.....	179
5.2 Influence of Biofilm Density on Mass Transport.....	182
5.2.1 Relative Diffusivity (f_D).....	183
5.3 Biofilm Porosity by Simulation	186
5.4 Model Validation.....	189
5.4.1 Comparison of the UMCCA Model Results with Laspidou and Rittmann (2004b) Study.....	189
5.4.2 Comparison of the Simulated Biofilm Compositions and Density with some Previous Studies.....	193

TABLE OF CONTENTS (Continued)

	Page
5.5 Summary.....	201
5.5.1 The UMCCA Model	201
5.5.2 Mass Transport Approach.....	204
VI CONCLUSIONS AND RECOMMENDATIONS.....	206
6.1 Conclusions.....	206
6.1.1 Experimental Results	206
6.1.2 Mathematical Modeling of Biofilm Compositions and Density Dynamics.....	209
6.2 Recommendations.....	210
REFERENCES.....	213
APPENDICES.....	229
APPENDIX A EXPERIMENTAL DATA OF TRACER STUDY.....	229
APPENDIX B EXPERIMENTAL DATA OF ORGANIC REMOVAL EFFICIENCY.....	235
APPENDIX C EXPERIMENTAL DATA OF NITROGEN REMOVAL EFFICIENCY.....	259
APPENDIX D EXPERIMENTAL RESULTS OF COD FRACTION STUDY	274
APPENDIX E EXPERIMENTAL DATA OF BIOKINETIC PARAMETERS.....	279
APPENDIX F EXPERIMENTAL DATA OF SLUDGE SLUDGE CHARACTERISTICS	282

TABLE OF CONTENTS (Continued)

	Page
APPENDIX G THE UNIFIED MULTI-COMPONENT CELLULAR AUTOMOTAN (UMCCA) MODEL	292
APPENDIX H EXPERIMENTAL DATA OF TRACER STUDY.....	298
APPENDIX I LIST OF PUBLICATIONS.....	304
BIOGRAPHY	309

LIST OF TABLES

Table	Page
2.1 Tapioca starch wastewater characteristics	9
2.2 Previous studies on anaerobic wastewater treatment of tapioca wastewater	10
2.3 Tapioca starch wastewater from extraction step and effluent UASB characteristics.....	12
2.4 The previous aerobic processes options for a post treatment in tapioca starch industry	18
2.5 Typical removal efficiencies and operating condition of UASB+DHS system treatment for domestic wastewater	28
2.6 Average effluent concentrations and typical removal efficiencies of the main pollutants of interest in domestic sewage	29
2.7 Typical characteristics of UASB reactor and various post treatment systems, expressed as per capita values	30
2.8 Example of fungi used in wastewater treatment systems, optimal conditions and the effect of fungal pretreatment.....	33
2.9 Comparison of whole and sectioned biofilms	63
2.10 Features by which various types of models of biofilm system differ. Model codes are: (A) analytical, (PA) pseudo-analytical, (N1) 1-D numerical and (N2/N3) 2-D/3-D numerical	69
3.1 Operating conditions for fungal and bacterial culture enrichments.....	84
3.2 The operating conditions of DHS systems during three runs	88

LIST OF TABLES (Continued)

Table	Page
3.3 Operating conditions of the respirometric experiment of fugal and bacterial cultures	92
3.4 Parameters and analytical methods.....	98
3.5 Parameter values for illustrating the trends of the UMCCA model for FDHS system	107
3.6 Parameter values for illustrating the trends of the UMCCA model for BDHS system.....	108
3.7 Nomenclature for all components in the UMCCA model.....	109
3.8 Equations for all components in the UMCCA model.....	111
4.1 The UASB effluent characteristics form tapioca starch industry	114
4.2 Physical characteristics of sponge media	119
4.3 Actual HRT, dispersion numbers and fractions of dead volume of DHS system by tracer study	123
4.4 Average dissolved oxygen concentration in segment effluent of FDHS and BDH system	126
4.5 Overall process performance of BDHS and FDHS systems	127
4.6 Organic and nitrogen loading profiles along the four segments during three runs	132
4.7 Mass flows of COD and nitrogen assimilation in cells	143
4.8 Total COD mass balance in two DHS systems	145
4.9 Nitrogen mass balance in two DHS systems	145
4.10 Denitrification potential of two DHS systems.....	146

LIST OF TABLES (Continued)

Table	Page
4.11 Biokinetic coefficients of FDHS and BDHS sludge during RUN I	147
4.12 Retained sludge concentrations in sponge media of two DHS systems	150
4.13 Retained sludge, Extracellular polymeric substances (EPS), viable cell and dead concentrations of two DHS sludge	153
4.14 Sludge retention time of two DHS systems	155
4.15 Soluble EPS concentrations in the DHS effluents	160
4.16 Total chemical cost requirement for each treatment system	166
4.17 The operating of IWA activated sludge model No. 1 (ASM 1) was operated with inflow rate 300 m ³ /d	166
5.1 The run termination time (<i>Bioage</i>) sufficient in 280 μm of the biofilm depth	174
5.2 Comparison of S_{max} and K_s values	176
5.3 Simulated average composite biofilm density in each segment of FDHS and BDHS systems.....	181
5.4 Simulated average relative diffusivity (f_D) in each segment of FDHS and BDHS systems.....	185
5.5 Simulated average porosities (ε_f) in each segment of FDHS and BDHS systems	188
5.6 The comparison of the variables range for whole biofilm depth and the average values from the model output with Lapidou and Rittmann (2004b) results.....	192

LIST OF TABLES (Continued)

Table	Page
5.7 Parameters values used in the UMCCA model to simulate the experiments of Bishop et al. (1995) and Zhang and Bishop (2001)	194
5.8 The group statistics and independent samples t test of simulated and experimental data of Zhang and Bishop (2001) for original substrate	196
5.9 The group statistics and independent samples t test of simulated and experimental data of Zhang and Bishop (2001) for active biomass	198
5.10 Statistical analytical of biofilm density through the model validation within the biofilm thickness 52-130 μm	202
5.11 Statistical analytical of biofilm density through the model validation within the biofilm thickness 130-240 μm	203
A.1 The experimental data of tracer study at HRT = 0.9 h	230
A.2 The experimental data of tracer study at HRT = 1.7 h	231
A.3 The experimental data of tracer study at HRT = 2.6 h	232
A.4 The experimental data of tracer study at HRT = 6.9 h	233
A.5 The experimental data of tracer study at HRT = 11.5 h	234
B.1 SCOD removal efficiencies monitoring of two DHS systems during all experimental study	236
B.2 Experimental results of TCOD, TBOD, SCOD and SBOD concentrations of two DHS influents (RUN I).....	244
B.3 Experimental results of TCOD, TBOD, SCOD and SBOD concentrations in segment 1 effluent of two DHS systems (RUN I).....	245

LIST OF TABLES (Continued)

Table	Page
B.4 Experimental results of TCOD, TBOD, SCOD and SBOD concentrations in segment 2 effluent of two DHS systems (RUN I)	246
B.5 Experimental results of TCOD, TBOD, SCOD and SBOD concentrations in segment 3 effluent of two DHS systems (RUN I)	247
B.6 Experimental results of TCOD, TBOD, SCOD and SBOD concentrations in segment 4 effluent of two DHS systems (RUN I)	248
B.7 Experimental results of TCOD, TBOD, SCOD and SBOD concentrations of two DHS influents (RUN II)	249
B.8 Experimental results of TCOD, TBOD, SCOD and SBOD concentrations in segment 1 effluent of two DHS systems (RUN II).....	250
B.9 Experimental results of TCOD, TBOD, SCOD and SBOD concentrations in segment 2 effluent of two DHS systems (RUN II).....	251
B.10 Experimental results of TCOD, TBOD, SCOD and SBOD concentrations in segment 3 effluent of two DHS systems (RUN II).....	252
B.11 Experimental results of TCOD, TBOD, SCOD and SBOD concentrations in segment 4 effluent of two DHS systems (RUN II).....	253
B.12 Experimental results of TCOD, TBOD, SCOD and SBOD concentrations of two DHS influents (RUN III)	254
B.13 Experimental results of TCOD, TBOD, SCOD and SBOD concentrations in segment 1 effluent of two DHS systems (RUN III)	255
B.14 Experimental results of TCOD, TBOD, SCOD and SBOD concentrations in segment 2 effluent of two DHS systems (RUN III)	256

LIST OF TABLES (Continued)

Table	Page
B.15 Experimental results of TCOD, TBOD, SCOD and SBOD concentrations in segment 3 effluent of two DHS systems (RUN III)	257
B.16 Experimental results of TCOD, TBOD, SCOD and SBOD concentrations in segment 4 effluent of two DHS systems (RUN III)	258
C.1 Nitrogen concentrations of influent of two DHS systems during RUN I.....	260
C.2 Nitrogen concentrations of segment 1 effluent of two DHS systems during RUN I.....	261
C.3 Nitrogen concentrations of segment 2 effluent of two DHS systems during RUN I.....	262
C.4 Nitrogen concentrations of segment 3 effluent of two DHS systems during RUN I.....	263
C.5 Nitrogen concentrations of segment 4 effluent of two DHS systems during RUN I.....	264
C.6 Nitrogen concentrations of influent of two DHS systems during RUN II.....	265
C.7 Nitrogen concentrations of segment 1 effluent of two DHS systems during RUN II.....	266
C.8 Nitrogen concentrations of segment 2 effluent of two DHS systems during RUN II.....	267
C.9 Nitrogen concentrations of segment 3 effluent of two DHS systems during RUN II.....	268
C.10 Nitrogen concentrations of segment 4 effluent of two DHS systems during RUN II.....	269

LIST OF TABLES (Continued)

Table	Page
C.11 Nitrogen concentrations of influent of two DHS systems during RUN III	270
C.12 Nitrogen concentrations of segment 1 effluent of two DHS systems during RUN III	271
C.13 Nitrogen concentrations of segment 2 effluent of two DHS systems during RUN III	272
C.14 Nitrogen concentrations of segment 3 effluent of two DHS systems during RUN III	273
C.15 Nitrogen concentrations of segment 4 effluent of two DHS systems during RUN III	274
D.1 Experimental results of COD fractionation of BDHS system during RUN I.....	276
D.2 Experimental results of COD fractionation of FDHS system during RUN I.....	277
D.3 Experimental results of COD fractionation of BDHS system during RUN II.....	278
D.4 Experimental results of COD fractionation of FDHS system during RUN II.....	279
D.5 Experimental results of COD fractionation of BDHS system during RUN III	280
D.6 Experimental results of COD fractionation of FDHS system during RUN III	281
E.1 Experimental data of biokinetic parameters of BDHS system.....	282

LIST OF TABLES (Continued)

Table	Page
E.2 Experimental data of biokinetic parameters of BDHS system.....	281
F.1 Experimental data of retained sludge concentrations during RUN I.....	283
F.2 Experimental data of retained sludge concentrations during RUN II	284
F.3 Experimental data of retained sludge concentrations during RUN III.....	285
F.4 EPS concentrations in sludge during RUN I.....	286
F.5 EPS concentrations in sludge during RUN II.....	288
F.6 EPS concentrations in sludge during RUN III	290
G.1 Statistical analysis of data output for the segment 1 of FDHS system (<i>Bioage</i> 45 days).....	294
G.2 Statistical analysis of data output for the segment 2 of FDHS system (<i>Bioage</i> 180 days).....	294
G.3 Statistical analysis of data output for the segment 3 of FDHS system (<i>Bioage</i> 180 days).....	295
G.4 Statistical analysis of data output for the segment 4 of FDHS system (<i>Bioage</i> 180 days).....	295
G.5 Statistical analysis of data output for the segment 1 of BDHS system (<i>Bioage</i> 245 days).....	296
G.6 Statistical analysis of data output for the segment 2 of BDHS system (<i>Bioage</i> 65 days).....	297
G.7 Statistical analysis of data output for the segment 3 of BDHS system (<i>Bioage</i> 145 days).....	298

LIST OF TABLES (Continued)

Table	Page
G.8 Statistical analysis of data output for the segment 4 of BDHS system (<i>Bioage</i> 105 days).....	297
H.1 TSS removal efficiency of FDHS and BDHS systems during RUN I.....	299
H.2 TSS removal efficiency of FDHS and BDHS systems during RUN II	299
H.3 TSS removal efficiency of FDHS and BDHS systems during RUN III.....	300
H.4 pH values efficiency of FDHS and BDHS systems during RUN I	301
H.5 pH values efficiency of FDHS and BDHS systems during RUN II.....	302
H.6 pH values efficiency of FDHS and BDHS systems during RUN III.....	301
H.7 Dissolved oxygen profiles of FDHS and BDHS systems during RUN I	302
H.8 Dissolved oxygen profiles of FDHS and BDHS systems during RUN II	303
H.9 Dissolved oxygen profiles of FDHS and BDHS systems during RUN III.....	303

LIST OF FIGURES

Figure	Page
2.1	Flow diagram of tapioca starch manufacturing 8
2.2	Tapioca starch wastewater treatment technology 17
2.3	Application types of DHS reactors 20
2.4	Growth curve of microorganism in a culture 49
2.5	The effects of a limiting substrate on the specific growth rate 50
2.6	Schematic diagram of respirometer 51
2.7	Recorder chart with a typical respirogram 52
2.8	Oxygen uptake rate (OUR) response in respirometer 53
2.9	Schematic representation of the unified model for active biomass, EPS, SMP and inert biomass 61
2.10	Four compartments typically defined in biofilm system: bulk liquid, boundary layer, biofilm substratum 66
2.11	Spatial biomass distribution and equal line substrate concentration in 2D simulations at different G values 76
3.1	Flow chart showing different stages of experimental study 82
3.2	UASB reactor and the sampling site 83
3.3	Mixed fungal and bacterial sludge enrichment processes 85
3.4	Schematic diagram of experimental setup 87
3.5	The segment of two DHS systems and sponge media 88
3.6	Experimental setups for RUN I, RUN II and RUN III 89
3.7	Experimental setup for the respirometric tests 91

LIST OF FIGURES (Continued)

Figure	Page
3.8 Biokinetics coefficients study processes	92
3.9 Division of COD fractions in two DHS systems	94
3.10 Schematic of electron flows dealing with original substrate and active biomass. Kinetic forms are shown for each flow. All flows are expressed in mg-COD/L-d.....	101
3.11 Schematic of electron flows for BAP and UAP utilization. Kinetic forms are shown for each flow. All flows are expressed in COD/L-d.....	103
3.12 Flowchart of the solution strategy for the UMCCA model	105
3.13 Flowchart of CA algorithm of the UMCCA model.....	106
4.1 Time profiles of BOD/COD ratio of UASB effluents	114
4.2 COD removal and F/M ratio profiles in fungal sludge.....	116
4.3 COD removal and F/M ratio profiles in bacterial sludge	117
4.4 MLSS concentrations of two cultures during acclimatization processes	118
4.5 The SEM photo of the sponge media	119
4.6 SEM photos of microbes immobilized on sponge media	120
4.7 The profiles of retained biomass in sponge media	121
4.8 The variation curve of tracer concentrations in relation to elapsed times	124
4.9 C-curve of simulation dispersion in closed vessels	124
4.10 Dissolved oxygen profiles of two DHS systems	126
4.11 SCOD removal profiles of FDHS system during three runs	129

LIST OF FIGURES (Continued)

Figure	Page
4.12 SCOD removal profiles of BDHS system during three runs	129
4.13 Organic removal profiles in two DHS systems during three runs	130
4.14 Nitrogen profiles of BDHS systems in two runs	134
4.15 Effect of recirculation flows on organic removal of two DHS systems	137
4.16 Effect of recirculation flows on organic removal of two DHS systems	138
4.17 The carbonaceous material characterizations of two DHS systems	140
4.18 Dominant cultures in FDHS sludge	148
4.19 Dominant cultures in BDHS sludge	149
4.20 Extracellular polymeric substances (EPS) concentrations in two DHS systems.....	152
4.21 Sludge Morphology of BDHS System by SEM Photos	157
4.22 Sludge Morphology of FDHS System by SEM Photos.....	158
4.23 The fractions of two DHS sludge compositions	162
5.1 Simulated soluble organic donor substrate (S) profiles along the biofilm depth in four segments of FDHS and BDHS systems	168
5.2 Simulated soluble organic donor substrate (S) profiles along the biofilm depth in four segments of FDHS and BDHS systems	169
5.3 Simulated residual or inert biomass (X_{res}) profiles along the biofilm depth in four segments of FDHS and BDHS systems	170
5.4 Simulated extracellular polymeric substances (EPS) profiles along the biofilm depth in four segments of FDHS and BDHS systems	171

LIST OF FIGURES (Continued)

Figure	Page
5.5 Simulated utilization-associated product (<i>UAP</i>) profiles along the biofilm depth in four segments of FDHS and BDHS systems	172
5.6 Simulated biomass-associated product (<i>BAP</i>) profiles along the biofilm in four segments of FDHS and BDHS systems	173
5.7 Simulated composite densities along the biofilm depth of BDHS system	180
5.8 Simulated composite densities along the biofilm depth of FDHS system.....	181
5.9 Simulated relative diffusivity (f_D) along the biofilm depth of BDHS system	184
5.10 Simulated relative diffusivity (f_D) along the biofilm depth of FDHS system.....	184
5.11 Simulated biofilm porosity of BDHS system along the biofilm depth.....	187
5.12 Simulated biofilm porosity of FDHS system along the biofilm depth	187
5.13 Simulated profiles of six biofilm components along the biofilm depth using parameter values of the UMCCA model presented in this study (termination time = 24.5 days).....	190
5.14 Simulated profiles of six biofilm components along the biofilm depth by Lapidou and Rittmann (2004b) study (termination time=24.5 days).....	191
5.15 Modeling results for SCOD profile throughout the biofilm depth and experimental data of Zhang and Bishop (2001) for the 1,420 μm of thickness layer	195

LIST OF FIGURES (Continued)

Figure	Page
5.16 Modeling results for active biomass profile throughout the biofilm depth and experimental data of Zhang and Bishop (2001) for the 1,420 μm of thickness layer	197
5.17 Modeling results for composite density and experimental data of Bishop et al. (1995) for the 52-130 μm of thickness layer.....	199
5.18 Modeling results for composite density and experimental data of Bishop et al. (1995) for the 130-240 μm of thickness layer.....	200
6.1 Recommendation of two DHS systems in tapioca starch industry.....	211
G.1 Example of the part of 2-D physical space of the model.....	293

SYMBOLS AND ABBREVIATIONS

b	First-order endogenous decay rate coefficient
B	Rate of secondary consolidation to total consolidation
BAP	Dimensionless concentration of BAP
bap	Concentration of BAP concentration
bap_{\max}	Maximum BAP concentration
b_{det}	Biofilm detachment coefficient
Bioage	“Age” of each biofilm compartment
CompDen	Composite density of biofilm
d	Dimension of each square grid space element
D	Dimension donor substrate
d_{\max}	Maximum donor substrate concentration
D_S	Diffusion coefficient
EPS	Dimensionless concentration of EPS
eps	Concentration of EPS
eps_{\max}	Maximum EPS packing density
f_D	Biodegradable fraction of active biomass
k_I	UAP formation rate coefficient
K_{BAP}	Half maximum rate concentration for BAP utilization
K_D	Half maximum rate concentration for utilization
k_{ESP}	EPS formation coefficient
k_{hyd}	EPS formation coefficient
K_O	Half maximum rate concentration for O ₂ consumption
K_S	Half maximum rate concentration for utilization of original substrate
K_{UAP}	Half maximum rate concentration for UAP utilization

SYMBOLS AND ABBREVIATIONS (Continued)

O_2	Oxygen concentration
$O_{2,max}$	Maximum oxygen concentration
\hat{q}_{BAP}	Maximum specific BAP utilization rate
\hat{q}_D	Maximum specific substrate utilization rate for donor substrate
\hat{q}_S	Maximum specific substrate utilization rate for original substrate
\hat{q}_{UAP}	Maximum specific UAP utilization rate
S	Dimension concentration of original donor substrate
s	Concentration of original donor substrate
s_{max}	Maximum concentration of electron donor substrate
t_c	Consolidation time
UAP	Dimensionless concentration of UAP
uap	Concentration of UAP
uap_{max}	Maximum concentration of UAP
U_c	Consolidation ratio
x	Biofilm width
X	Dimensionless biofilm
X_a	Dimensionless density of active biomass
x_a	Dimensionless density of active biomass
$x_{a,max}$	Active biomass density
X_{res}	Maximum active biomass packing density
x_{res}	Dimensionless density of true residual inert biomass
$x_{res,max}$	Maximum residual inert biomass packing density
Y_P	True yield for SMP (UAP and BAP) utilization
Y_S	True yield for SMP (UAP and BAP) utilization

SYMBOLS AND ABBREVIATIONS (Continued)

z	Biofilm depth
Z	Dimensionless biofilm depth
∂t_b	Time steps used for biomass growth
∂t_s	Time step usage for relaxation of S
η	Creep constant
λ	1 st order decay coefficient for dissolved oxygen in the biofilm
ρ_{BAP}	Utilization rate of BAP
ρ_D	Utilization rate of any donor
ρ_S	Utilization rate of substrate
ρ_{UAP}	Utilization rate of UAP

CHAPTER I

INTRODUCTION

1.1 Statement of the Problem

High rate anaerobic reactors are becoming increasingly popular for the treatment of tapioca starch processing wastewater because of their low operation costs, smaller space requirements, high organic removal efficiency and low sludge production, combined with a net energy benefit through the production of biogas. These reactors' operations are based on the immobilization of high concentrations of biogas. Among the various anaerobic reactors developed so far, the UASB reactor ([Lettinga and Hulshoff, 1991](#)) has been found to be relatively superior because it neither requires added substratum as in anaerobic filters, nor effluent recirculation as in fluidized bed reactors. However, the effluents of UASB reactor still contained a relatively high residual COD, and the nitrogen nutrient contents based on the COD:N ratio that seems to be very high for heterotroph microorganism utilization. Thereby, the organic and nitrogen nutrient removal process would be required before effluents discharged to receiving waters. Further, for the UASB effluent characteristics, treatment efficiency of nitrification-denitrification is considered poor at $BOD/TKN < 2.5$ or $BOD/NH_3 < 4$ and $COD/TKN < 5$ ([Grady, et al., 1999](#)). In order to ensure successful removal of ammonia in the nitrification-denitrification process, an external carbon source would be necessary, which could further increase the operational costs.

Accordingly, it is strongly recommended to use DHS system for post-treatment of anaerobic pre-treated sewage (Tawfik et.al., 2006a). Thus, Downflow Hanging Sponge (DHS) system offers an attractive method to treat UASB effluents from tapioca starch industry. However, the UASB effluent in tapioca starch industry is too fluctuated and higher concentration than domestic wastewater. When high amounts organic matter are present in a biofilter, the fast growing heterotrophic bacteria will 'out-space' the slow growing nitrifiers from the aerobic zone in the biofilm as they compete for oxygen and space. And in general, higher contents of organic in the system resulted in higher heterotroph organism population. It is important to keep the organic waste load for biofilter constant and as low as possible because a high heterotroph bacteria combined with biofilm detachment ("sloughing") may clog a biofilter, backwashing is not possible in DHS system.

Several researches recommended that fungi have a wide range of enzymes, and are capable of metabolizing complex mixtures of organic compounds such as particulate matters and dead cells (Tripathi et al., 2007; Thanh and Simard, 1973; Mannan et al., 2005; Tung et al., 2004; Guest and Smith, 2002). Recently, emphasis has been made on treatment of wastewater with fungi because they are capable of rapid growth on a variety of substances (Karim and Sistrunk, 1984). Fungi based on organic and nitrogen reduction system have the potential to overcome issues associated with the Downflow Hanging Sponge (DHS) treatment system, while maintaining or improving performances. However, several questions need to be addressed by a systematic research plan. Comprehensive investigations concerning reactor configurations, biokinetics coefficient, structure and mass transport of fungal and bacterial biofilms through the DHS reactor performance have been carried out.

1.2 Background Information

1.2.1 Combinations of UASB and Downflow Hanging Sponge (DHS) System

All industries are increasingly required to reduce their impact on the environment. Adequate treatment of food processing effluents is assuming increasing importance. Many local authorities are now insisting that industries undertake some form of effluent treatment so as to protect the environment. One research group has been developing a wastewater treatment system as a cost-effective and easy maintenance method at the Nagaoka University in Japan, by combining an anaerobic UASB reactor as pre-treatment unit and an aerobic Downflow Hanging Sponge (DHS) reactor as a post treatment unit. The combinations of UASB and various configuration of DHS have been developed and evaluated over two decades period already for various type of wastewater, including domestic wastewater or sewage (Agrawal et al., 1997; Machdar et al., 1997; Araki et al., 1999; Mechdar et al., 2000; Uemura et al., 2002; Tandukar et al., 2005; Tandukar et al., 2006a; Tandukar et al., 2006b; Tawfik et al., 2006a; Tawfik et al., 2006b; Chuang et al., 2007), actual dye wastewater (Ohashi et al., 2006) as well as in wastewater reuse in small communities (Vigneswaran et al., 2003). These results of all these researchers suggested DHS system to be an excellent system for post-treatment of anaerobically pre-treated sewage. The main advantages of using DHS systems include: a rapid and dense colonization of biomass, a high specific surface area of the packing material which can reach up to $2,400 \text{ m}^2/\text{m}^3$ and 97% porosity, a sufficiently long biomass retention time allowing the application of a higher loading rate, a high process stability and no oxygen requirement and a low production of waste sludge (Tawfik et al., 2006a). Also, the high entrapment capacity of the DHS system and the retain of a high biomass concentration of 34 g VSS/L are the main reasons for the higher COD removal, nitrification process and *F. coliform* removal as compared to a series of RBC's treating UASB reactor effluent. Furthermore, the DHS system is not only superior to the

conventional trickling filter, but also to other post-treatment systems, such as, activated sludge process, sequencing batch reactor (SBR), and aerobic filter with regard to COD removal, nitrification efficiency and *F. coliform* removal for domestic wastewater treatment processes. Accordingly, it is strongly recommended to use DHS system for post-treatment of anaerobic pre-treated sewage (Tawfik et al., 2006a). Thus, Downflow Hanging Sponge (DHS) system offers an attractive method to treat UASB effluents from tapioca starch industry.

1.2.2 The Unifies Multi-Component Cellular Automaton (UMCCA) Model

Biofilm diffusion is the main parameter must concern in biofilm system. Mass transport in biofilms is influenced by the biofilm structure which in turn is influenced by the local availability of substrate. A quantitative understanding of how biofilm structure is linked to mass transport is essential for our understanding of biofilms. Two main approaches can be used to relate biofilm structure to mass transport. One approach is can be obtained from direct imaging of biofilms or from mathematical modeling (Horn and Morgenroth, 2006). The unified multi-component cellular automaton (UMCCA) was developed which purpose to quantify composite density that relationships among three solid species—active cells, EPS, and residual inert biomass, three soluble species—original substrate, utilization associated products (UAP), and biomass associated products (BAP), and electron acceptor, such as oxygen. The suitability of this combination for representing the structure of a heterogeneous biofilm has been demonstrated. An advantage of this approach is that it can provide a fast and accurate model solution with readily available computing resources, such as a high-capacity personal computer.

1.3 Objectives of the Study

The overall aim of this study was to evaluate the performances of fungal and bacterial downflow hanging sponge system for residual organics removal during post

treatment of starch wastewater effluents from an UASB reactor. Therefore, the specific objectives of proposed research were as follow:

1.3.1 To investigate and evaluate the performances of the Downflow Hanging Sponge using mixed fungal (FDHS) and mixed bacterial (BDHS) cultures as a post treatment for treating UASB effluent from tapioca starch industry.

1.3.2 To obtain the biokinetic coefficients and identify the dominant genus of mixed fungal and mixed bacterial cultures on Downflow Hanging Sponge (DHS) system.

1.3.3 To evaluate the factors influencing the biofilm density through sludge characteristics and its components.

1.3.4 To investigate the biofilm mass transport through its density under simulated conditions using Unified Multiple Component Cellular Automaton (UMCCA) model.

1.4 Scopes of the Study

In order to achieve the above mentioned objectives, the scopes of this study to be carried out were included:

1.4.1 The pilot scale experiment of DHS systems were conducted at a site near F4 laboratory building of Suranaree University of Technology. Investigation was carried out with tapioca starch industrial wastewater effluent from a full-scale UASB reactor at the General Starch Co., Ltd. In Khon-Buri district of Nakhon Ratchasima province in the northeastern part of Thailand, fed to two DHS reactors.

1.4.2 Performances of both FDHS and BDHS reactors were optimized varying the organic (OLR) and hydraulic (HLR) loading rates. All operational conditions were evaluated in terms of organic and nitrogen removal efficiencies.

1.4.3 Biokinetic coefficients were investigated through oxygen uptake rate by respirometric technique that was used for calculating biokinetic parameters of biomass.

1.4.4 The sludge characteristics and biofilm components were analyzed to understand their relationship with biofilm density in the DHS reactor. The biofilm components including the three solid species (active bacteria, inert or dead biomass produced by death and decay, and extracellular polymeric substances (EPS)) and three soluble components (soluble substrate, substrate utilization association product (UAP) and biomass association product (BAP)) were investigated in the sludge.

1.4.5 The Unified Multiple Component Cellular Automaton (UMCCA) model was used to predict density and quantitatively the heterogeneity of biofilms including with three solid species and three soluble components that occur over time and deeper in the biofilms.

CHAPTER II

LITERATURE REVIEWS

2.1 Tapioca Starch Industry

There are about 60 large and medium starch factories in Thailand (Loha et al., 2003). Tapioca is grown throughout the tropical parts and is one of the important starchy root crops in the tropic. The main products of tapioca roots are pellets, chips and starch (flour). Tapioca starch production was found to produce the wastewater in large quantity producing. The tapioca starch industry causes water pollution from its wet processing operation. Figure 2.1 shows the flow diagram of starch production from tapioca. The combined wastewater chiefly comprises the streams from root washer and separators in the manufacturing processes. After rasping the hydrogen cyanide in roots is set free and dissolved in water used for washing.

2.2 Tapioca Starch Wastewater Characteristics

Tapioca starch is an important agro-based product found in many parts of the world. The starch extraction process involves preprocessing of tapioca roots, starch extraction, separation, and drying. It also generates large volumes of wastewater up to 20-60 m³/ton starch produced. Water pollution problems related the tapioca starch industries are serious. The wastewater is highly organic and acidic by nature with chemical oxygen demand (COD) up to 25,000 mg/L and pH between 3.8 and 5.2 as the results from several researches are shown in Table 2.1. It also contains biodegradable starch suspended solids up to 4,000 mg/L (Annachhatre, A. P. and Amornkeaw, A., 2001; Annachhatre A. P. and Amatya, P. L., 2000).

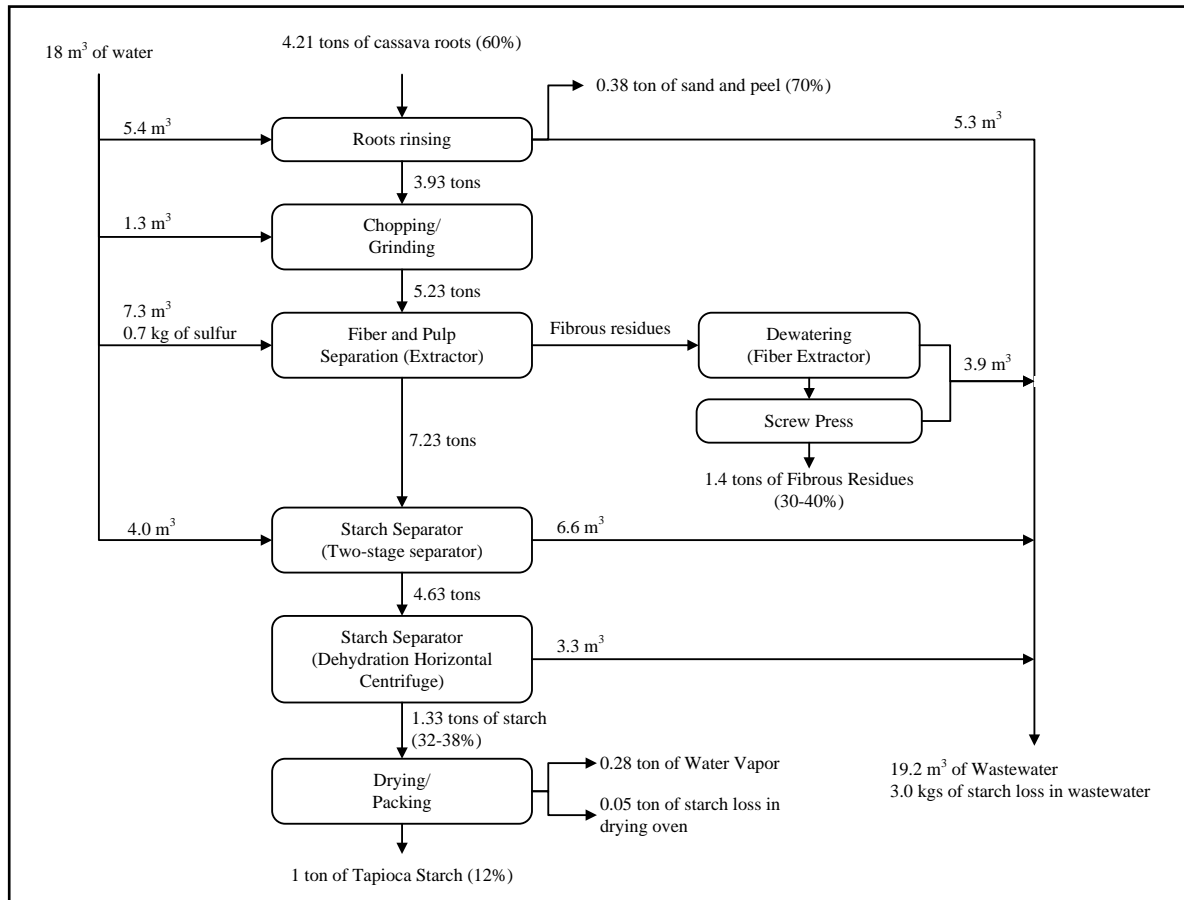


Figure 2.1 Flow diagram of tapioca starch manufacturing (Chavalparit, O. et al., 2009).

2.3 Conventional Methods of Tapioca Starch Industry Wastewater Treatment

The tapioca starch industry causes water pollution problems from cassava roots' wet processing operation. In general, tapioca starch wastewater is highly organic and contains minute suspended solids and dissolved solids. The volume of combined wastewater generated per 1 ton of starch production is 30-50 m³ and is highly concentrated. The tapioca starch wastewater is acidic in nature due to the release of some prussic acids by the tapioca roots and the use of sulfuric acid in extraction processes (Amatya, 1996).

Table 2.1 Tapioca starch wastewater characteristics

Manufacturing processes wastewater	Washing step	Extraction step	Extraction step	Combined wastewater	Combined wastewater	Combined wastewater
pH	5-6	4-6	3-4	4-5	4-5	-
TSS (g/L)	10-13	4-8	1-2	2-4	6-9	3-8
COD _t (g/L)	4-8	12-19	13-16	14-25	22-25	4-27
COD _f (g/L)	-	-	-	10-25	-	-
BOD ₅ (g/L)	-	-	10-13	-	13-16	2-14
TKN (mg/L)	-	-	259-462	85-250	85-180	60-298
Org-N (mg/L)	-	-	196-392	-	-	-
NH ₃ -N (mg/L)	67-85	161-187	63-77	-	-	-
Total P (mg/L)	-	-	39-73	-	50-85	41-235
Ortho-PO ₄ ⁻	-	-	-	25-48	-	-
CN ⁻ (mg/L)	-	4-7	30-36	10	-	-
BOD:COD	-	-	0.8	-	0.6	0.5
References	Hein et al. (1999)		Mai et.al. (2004)	Annachatre and Amornkeaw (2001)	Polprasert, C. and Chatsanguthai, S. (1988)	Reampim, J. (2002)

In the past, most of tapioca starch factories in Thailand treated their wastewater using series of anaerobic and facultative ponds. The major environmental problem caused by the practice was obnoxious odor of sulfide generated from the pond system. In fact, this odor had not been a serious in the past due to the remoteness of the factory-locations. With growing population, the areas around the factories have transformed into residential areas and thus the odor has turned out to be an objectionable problem. Beside this, more stringent environmental pollution control on the effluent discharges demands the improvement in the efficiencies of the wastewater treatment plants (Amatya, 1996).

Anaerobic wastewater treatment technology has become exceeding popular worldwide in tapioca starch industry, which can be operating at high operating at organic loading rate (OLR). Variations of anaerobic wastewater treatments are applicable to tapioca wastewater as summarized in Table 2.2. A deep discussion on the evolution and

applicability of anaerobic technology for the treatment of tapioca starch is presented elsewhere, where several favorable characteristics of anaerobic processes are highlighted, such as high organic removal efficiency, low cost, operational simplicity, no energy consumption, and low sludge production, combined with a net energy benefit through the production of biogas. These advantages, associated with the favorable environmental conditions in warm-climate regions, where high temperatures prevail practically throughout the year, have contributed to establish the anaerobic systems, particularly the UASB reactors, in an outstanding position ([Annachatre and Amornkeaw, 2001](#); [Annachatre and Amatya, 2000](#); [Chernicharo, 2006](#)).

Table 2.2 Previous studies on anaerobic wastewater treatment of tapioca wastewater

Treatments	OLR (kgCOD/m ³ -d)	HRT (d)	COD removal (%)	References
UASB	33-40	0.5	94-98	Hein et al. (1999)
UASB	10-16	0.2	>95	Annachatre and Amatya (2000)
UASB	28-43	0.3	84-90	Mai et al. (2004)
AFF	2-10	2-4	70-80	Chaiprasert, C. et al. (2003)
AFF	2-3	3	89	Barana and Cereda (2000)
Anaerobic contactor	-	1-10	32-80	Reampim, J. (2002)
Anaerobic pond	2-3	10	57	Polprasert, C. and Chatsanguthai, S. (1989)
Anaerobic attached growth waste stabilization pond	-	8	60-70	Rukvichitkul, T. (2002)

Among the various anaerobic reactors developed so far, the UASB reactor has been found to be relatively superior because it neither requires added substratum as in anaerobic filters nor effluent recirculation as fluidized bed reactors.

Evidences from literature indicate the UASB system achieved COD conversion efficiency more than 95% at OLR 10-16 kgCOD/m³-d and gas productivity of 5-8 m³/m³-d were obtained. Also, experiments showed tapioca wastewater contained up to 10 mg/L of cyanide yielded satisfactory cyanide removal of approximately 93 to 98% (Annachhatre and Amatya, 2000; Annachhatre and Amornkaew, 2001; Hein et al., 1999 and Mai et al., 2004) as COD removal efficiency and operating conditions are shown in Table 2.2. Although, high rate treatment processes offer an attractive treatment alternative, process start-up is one hurdle that must be overcome before steady process operation can be achieved. They are also sensitive to suspended solids (SS). SS inhibits sludge granulation in UASB reactor or may even lead to sudden wash out of the sludge bed. A separate settling pretreatment system for SS removal has been recommended. Other researchers have suggested restricting the SS level below 1,000 mg/L or pre-acidification of SS (Annachhatre and Amatya, 2000).

2.4 Main Limitations of Anaerobic Systems

In spite of their great advantages, anaerobic reactors hardly produce effluents that comply with usual discharge standards established by environmental agencies. Therefore, the effluents from anaerobic reactors usually require a post-treatment step as a means to adapt the treated effluent to the requirements of the environmental legislation and protect the receiving water bodies. The main role of the post-treatment is to complete the removal of organic matter, as well as to remove constituents little affected by the anaerobic treatment, such as nutrients (N and P) and pathogenic organisms (viruses, bacteria, protozoans and helminths) (Chernicharo, 2006).

2.4.1 Limitation Regarding Organic Matter

Limitations imposed by environmental agencies for BOD are usually expressed in terms of effluent discharge standards and minimum removal efficiencies. These constraints are probably the cause that has mostly limited the use of anaerobic systems (without post-treatment) for tapioca starch wastewater treatment (typical values in Table 2.3). In view of the limitations imposed by the environmental legislation for the effluent BOD concentration, or also when the receiving body has limited capacity for assimilating the effluent from the treatment plant (which is frequently the case), it is usually necessary to use aerobic treatment to supplement the anaerobic stage. However, there are situations in which the combination of different anaerobic processes can meet less restrictive requirements regarding efficiency and concentration of the final effluent. Obviously, the application of these combined anaerobic systems is conditioned to an appropriate dilution capacity of the receiving body.

Table 2.3 Tapioca starch wastewater from extraction step and effluent UASB characteristics

Parameters/References	Mai et.al. (2004)	Sima-Inter Products Co.,Ltd. ^(a)	General Starch Co.,Ltd. ^(b)
pH	7-8	7-8	7-8
TSS (mg/L)	120-320	500-1,000	300-500
TCOD (mg/L)	1,005-2,650	734-1,600	400-1,500
TBOD ₅ (mg/L)	-	-	320-600
TKN (mg/L)	57-95	200-250	141-250
Org-N (mg/L)	15-31	5-7	5-11
NH ₃ -N (mg/L)	36-68	195-243	130-245
Total P (mg/L)	12-60	5-8	4-6
COD/TKN	25	4	2
COD:N:P	100:4:2	100:25:1	100:49:1

Remark: ^{a,b}field surveys of tapioca starch wastewater treatment in two factories of in Nakhon Ratchasima Province, Thailand

In this sense, in situations in which the receiving body presents a good dilution capacity, the adoption of less restrictive discharge standards could enable the construction of simpler and more economical treatment plants in several small cities by means of a more intensive use of anaerobic reactors, particularly UASB reactors. At a later stage, if it becomes necessary to produce a better quality effluent, a complementary treatment unit can be built after some years. The high costs of sophisticated treatment systems, designed exclusively to meet BOD discharges standards, make their construction at a single stage unfeasible for most cities located in developing countries. On the other hand, the construction in stages could be decisive and that systems consisting of UASB reactor and a post-treatment unit become the most feasible ones regarding technical and economical criteria.

2.4.2 Limitation Regarding Nitrogen and Phosphorus

The discharge of nutrients into surface water bodies may cause increased algal biomass as a result of the eutrophication process (abnormal algae growth due to the nutrients discharged). The problem can be even worsened due to the decreased oxygen levels, by means of the nitrification processes, when at least 4.0 kg of dissolved oxygen are consumed for each kg of ammonia discharged into the receiving body (Grady et al., 1999).

In cases in which nutrient removal is required to meet the quality standards of the receiving water body, the use of anaerobic processes preceding a complementary aerobic treatment for biological nutrient removal should be analyzed very carefully, once anaerobic systems present good biodegradable organic matter removal, but practically no N and P removal efficiency. This certainly causes a negative effect on biological treatment systems aiming at good nutrient removal, because the effluent from the anaerobic reactor will have N/COD and P/COD ratios much higher than the values desired for the good performance of biological nutrient removal processes. When the purpose of the treatment plant is also a good nitrogen removal, the anaerobic reactor should be used to treat initially

only a part of the influent raw sewage (possibly no more than 50–70%), and the remaining part (30–50%) should be directed to the complementary biological treatment, aiming at nitrification and denitrification, so that there is enough organic matter for the denitrification step. In this case, the great advantage of the use of the anaerobic reactor is to receive and stabilize the sludge generated in the complementary treatment, eliminating the need for an anaerobic sludge digester (Chernicharo, 2006).

2.4.3 Limitation Regarding Microbiological Indicators

Regarding the microbiological indicators, low faecal coliform removal efficiencies have been reported in anaerobic reactors, usually amounting to around only 1 log-unit. Regarding other types of microorganisms, such as viruses and protozoans (mainly *Giardia* and *Cryptosporidium*), there are few references covering their reduction or elimination in anaerobic reactors. The removal of helminth eggs in anaerobic reactors, particularly in UASB reactors, has been reported as amounting to 60–90%, being therefore insufficient to produce effluents that may be used in irrigation. However, it should be mentioned that these limitations are not exclusive of anaerobic reactors, but are a characteristic of most compact wastewater treatment systems. As the risk of human contamination by ingestion or contact with water containing pathogenic organisms is high, many times it may be necessary to disinfect the effluents. This fact becomes even more serious due to the poor sanitary conditions in developing countries. On the other hand, the low investments in health and sanitation make the population of these countries bearers of several diseases that can be transmitted by faeces and, consequently, by the sewage generated by this population.

2.5 Advantages of the Combined (Anaerobic/Aerobic) System

In comparison with a conventional wastewater treatment plant consisting of primary sedimentation tank followed by aerobic biological treatment (activated sludge, trickling

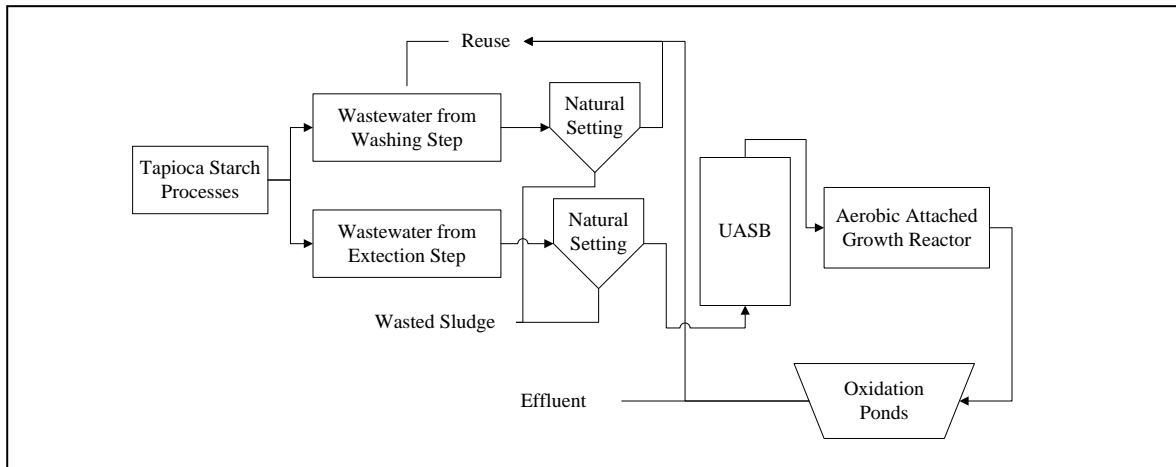
filter, submerged aerated biofilter or biodisc), with the primary and secondary sludge passing through sludge thickeners and anaerobic digesters prior to dewatering, a treatment consisting of a UASB reactor followed by aerobic biological treatment (with the secondary sludge directed to thickening and digestion in the UASB reactor itself and then straight to dewatering), can present the following advantages ([Chernicharo, 2006](#)):

- the primary sedimentation tanks, sludge thickeners and anaerobic digesters, as well as all their equipment, can be replaced with UASB reactors, which do not require the use of equipment. In this configuration, besides their main sewage treatment function, the UASB reactors also accomplish the aerobic sludge thickening and digestion functions, requiring no additional volume;
- power consumption for aeration in activated sludge systems preceded by UASB reactors will be substantially lower compared to conventional activated sludge systems, and especially extended aeration systems;
- thanks to the lower sludge production in anaerobic systems and to their better dewaterability, sludge volumes to be disposed of from anaerobic/aerobic systems will be much lower than those from aerobic systems alone. According to studies carried out by [Pontes \(2003\)](#), a 30% VSS destruction can be reached when secondary sludge produced in a trickling filter is returned to a UASB reactor. When the mass balance is performed, the total sludge production in a combined UASB/Trickling Filter system can be 30–50% lower than in a conventional trickling filter system.
- the construction cost of a treatment plant with UASB reactor followed by aerobic biological treatment usually amounts 50–80% of the cost of a conventional treatment plant (20–50% investment savings). In addition, due to the simplicity, smaller sludge production and lower power consumption of the combined anaerobic/ aerobic system, the operational costs also represent an even greater advantage. Savings on

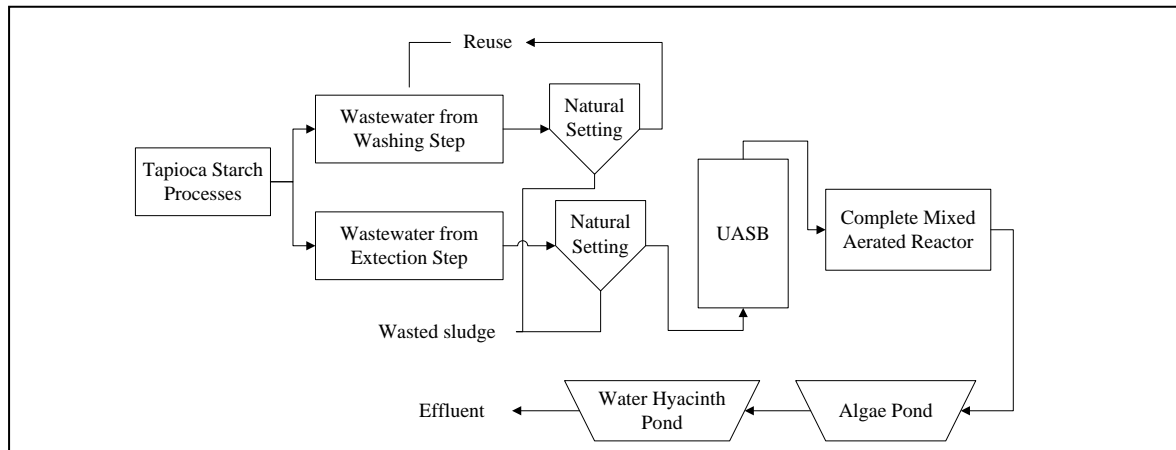
operation and maintenance costs are usually in the range of 40–50% in relation to a conventional treatment plant.

2.6 Post Treatment Options for Effluent Quality Enhancement

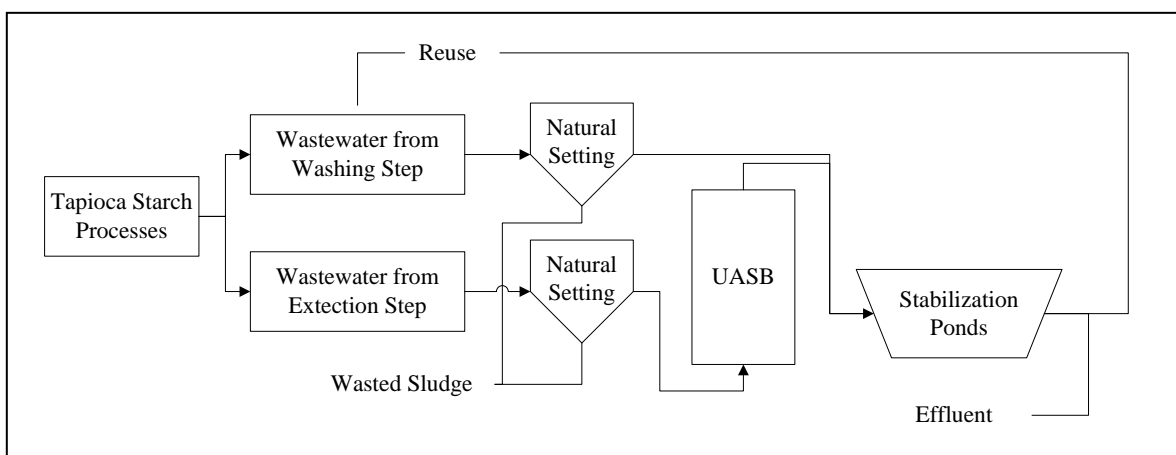
Nowadays, there exist a lot of studies related to the treatments of tapioca wastewater by anaerobic and aerobic processes, such as anaerobic fixed bed reactor, methanogenic reactor, acidification reactor, UASB reactor, attached growth reactor, oxidation pond system and others. But there seems little be done on the study for whole system, from original wastewater to the effluent of system, which can meet the local effluent standard. [Hein et al. \(1999\)](#) reported the treatment system from a large scale factory in a laboratory scale treatment system including primary sedimentation, UASB reactor and aeration tank using attached growth reactor give high treatment efficiencies, with influent COD reduced from 11,077-19,083 mg/L to less than 87 mg/L in the effluent of aeration tank. The full scale oxidation pond system is used as a post treatment, with HRT of 12-20 days. This final effluent COD of pond system is lower than 10 mg/L, so the effluent can be used for agriculture or reused for the factory, as flow diagram in Figure 2.2(a) and operating condition in Table 2.4. [Mai et al. \(2004\)](#) were investigated treatment technology as follow in Figure 2.2(b) and Table 2.4, the upflow anaerobic process (UAF) is responsible for the reduction of SS, and hydrolysis a portion of organic matter. The UASB reactor (as the treatment system) is responsible for the reduction of organic matter. The aeration tank is responsible for the reminder of organic matter. And aquatic plant pond is responsible for the remainder of organic matter, nitrogen and phosphorus removal. Moreover, Figure 2.2(c) illustrates flow diagram from field surveys of tapioca starch wastewater treatment in two factories of in Nakhon Ratchasima Province, Thailand. The UASB effluents were treated by stabilization pond system. That is not the effective process and still high area using.



(a) The treatment technology investigated by Hein et al. (1999).



(b) The treatment technology investigated by Mai et al. (2004).



(c) Two tapioca starch factories of the researchers survey

Figure 2.2 Tapioca starch wastewater treatment technology

Table 2.4 The previous aerobic processes options for a post treatment
in tapioca starch industry

Treatments	OLR (kgCOD/m ³ -d)	HRT (d)	COD removal (%)	References
RBC	0.3-1.6	0.3-1.1	69-97	Radwan and Ramanujam (1996)
Activated sludge	0.5-1.4	1.4-4.2	>90	Oliverira et al. (2001)
Attached growth reactor	1-1.4	0.5	83-87	Hein et al. (1999)
Aerated pond	2.1	0.5	93-97	Mai et al. (2004)

2.7 Downflow Hanging Sponge (DHS) Processes

A downflow hanging sponge (DHS) reactor was proposed and developed as a novel and low cost post treatment for UASB treating sewage ([Tandukar et al., 2005](#)). The principle of this system is the use of polyurethane sponge as a medium to retain biomass. The concept is somewhat similar to that of tricking filter, except that the that the packing material is sponge, which has a void space of more than 90%, resulting in a significant increase in entrapped biomass and thus longer SRT. As the sponge in a DHS is not submerged and freely hung/placed in air, oxygen is dissolved into the wastewater when it flows down the reactor and therefore there is no need for external aeration or any other energy inputs. Moreover, production of excess sludge from DHS is negligible as longer SRT provides ample time for autolysis of sludge in the system itself.

2.7.1 Types of DHS Reactor

Since the emergence of the first DHS proto-type a decade ago, it has been modified to newer configurations, making it simple, more cost effective and suitable for real-scale application. Cube type DHS, called the “first generation DHS” (Figure 2.3a), was the first of its type, and was like a rosary of cube shaped sponges that hung freely in the air ([Agrawal et al., 1997](#); [Mechdar et al., 1997](#)). The system exhibited good efficiency

in removing organics and nitrogenous compounds, when applied as a post treatment unit for UASB treating sewage. However, the configuration was not compatible for real-scale application. To overcome this drawback, a better arrangement of sponges was worked out, which was called “curtain-type DHS” or the second generation DHS” (Figure 2.3b). Based on these findings, a demonstration-scale “second generation DHS” has been constructed and is under continuous monitoring in Karnal, India, since the year 2002. The project was undertaken by the government of India under the Yamuna Action Plan [Tandukar et al. \(2006a\)](#). Yet other designs of DHS were conceptualized bringing forth the “third generation” and the “fourth generation” DHS reactors. These newer generations were modified to make them simpler in construction and maintenance, lowering the cost at same time. The third generation DHS was more like a tricking filter, packing medium being replaced by small sponge units put inside a net-like plastic cover. The construction was simple as sponge units were randomly packed inside a reactor container (Figure 2.3c). [Tandukar et al. \(2005\)](#) and [Tandukar et al. \(2006a\)](#) describe the “fourth generation DHS” in terms of performance and material balance along with sludge characteristics (Figure 2.3d). Construction of this reactor is discussed in a later section. The design is peculiar in enhancing dissolution of air into the wastewater and in avoiding possible clogging of the reactor due to sudden washout from UASB. Additionally, it is simple and easy to construct.

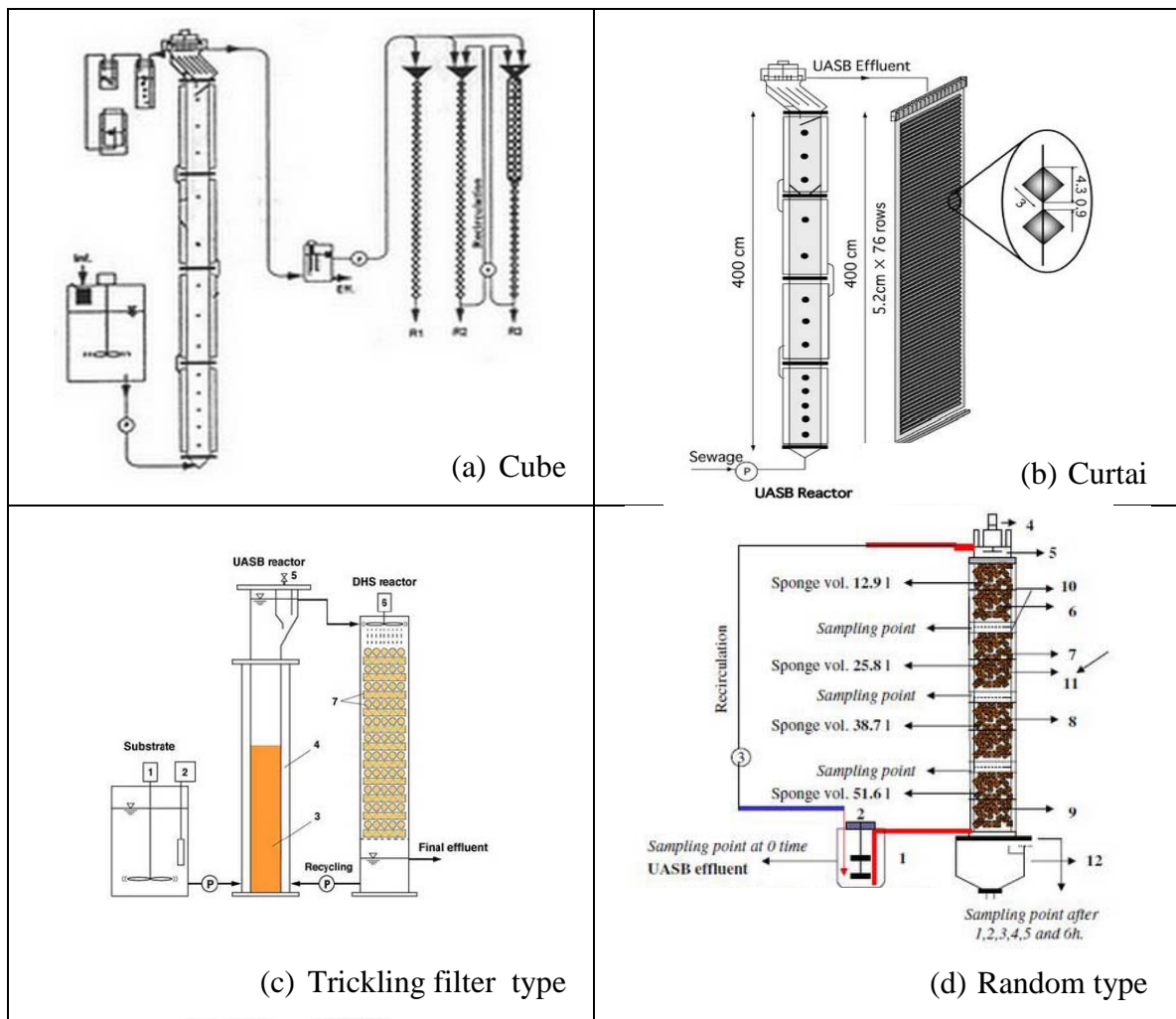


Figure 2.3 Application types of DHS reactors

2.7.2 DHS Sludge Characteristics

Development of biomass and its quantification has been illustrated by [Tandukar et al. \(2005\)](#). The DHS was started up without any inoculums. Biomass growth and accumulation in the DHS attained a steady state after around eight months of operation. Afterwards, the biomass concentration in the sponge remained almost stable with around 34 gSS/L or 26 gVSS/L of sponge volume, which is 5-20 times higher than that a conventional activated sludge system. More than 90% of void space and reticulated structure of sponge forms an appropriate colonization matrix and attachment site for microorganisms.

Dens accumulation of biomass prolongs the SRT of the system, which then provides enough time for self-degradation of sludge in the reactor itself, minimizing the production of excess sludge. Excess sludge from the DHS was that accumulated in the clarifier, which was withdraw periodically. Mass balance of the curtain type DHS system showed that only 6% of the total influent COD was eluted as excess sludge (Tandukar et al., 2006b). Also, the excess sludge production DHS system was negligible. Endogenous respiration of DHS sludge was high compared to other aeration systems. The specific oxygen utilization rate for endogenous respiration was 6.5 gDO/kgVSS-h for the sludge harvested from the upper part of DHS curtain (near inlet) and 4.8 gDO/kgVSS-h for the sludge harvested from the lower part (near outlet). The values were higher than that of activated sludge system or submerged membranes treating domestic sewage. The value of endogenous respiration for sludge harvested from the membrane was in the range of 1.92-2.16 gO₂/kgVSS-h. For the returned sludge from activated sludge system it was in the range of 3-8 gO₂/kgVSS-h. High endogenous respiration of DHS sludge suggests that the sludge accumulation was near balance with the degradation of sludge in the reactor itself, thus minimizing excess sludge production. Further, sludge was also being utilized as a carbon source during denitrification. Observed sludge yield for DHS was calculated to be 0.27-0.40 mgVSS/mgBOD_{utilized}, which is less compared to other aerobic systems treating domestic sewage. The observed sludge yield for other aerobic system like activated sludge system varies from 0.6 to 1.2 mgVSS/mgBOD_{utilized} that depending upon the substrate loading. The value for aerated biofilter also average around 0.37 mgVSS/mgBOD due to long SRT and higher degradation of old sludge in the system (Tandukar et al., 2006a). However, several questions need to be addressed by a systematic research plan, the most important being the optimized operating conditions, biokinetic coefficients, sludge composition, mass transport and dominant microorganism in DHS biomass.

2.7.3 Factors Affecting on DHS System Performancy

The DHS system was more like a trickling, packing medium being replaced by small sponge units put inside a net-like plastic cover. Overlong history of use, a large data base has been assembled describing the factors affecting the performance of the trickling filter process by [Grady et al. \(1999\)](#) and [Eding et al. \(2006\)](#) could be summarized down (Table 2.8):

(a) *Process Loading*: The performance of any biochemical operation is affected by the process loading, i.e. the amount of substrate applied per unit time per unit mass of biomass. In suspended growth systems the process loading is expressed as the solids retention time (SRT) or process loading factor, i.e. F/M ratio. When high amounts of easily degradable organic matter are present in a biofilter, the fast growing heterotrophic bacteria will 'out-space' the slow growing nitrifiers from the aerobic zone in the biofilm as they compete for oxygen and space. When high amounts of easily degradable organic matter are present in a biofilter, the fast growing heterotrophic bacteria will 'out-space' the slow growing nitrifiers from the aerobic zone in the biofilm as they compete for oxygen and space. In literature, minimum and maximum hydraulic surface loading rates (HSL; m^3/m^2 filter cross-section/day) are reported for trickling filters. The upper and lower limits for HSL vary with specific surface area and media type. Head loss or removal of bacteria from the plastic media limits the increase of hydraulic surface loading. A minimum HSL is necessary to keep the complete filter surface area wet and may be needed to control the concentration of grazing organisms in a trickling filter. Minimum hydraulic loading rates reported for trickling filters are 32–55 $\text{m}^3/\text{m}^2/\text{day}$ and maximum hydraulic loading rates reported are 72–188 $\text{m}^3/\text{m}^2/\text{day}$.

(b) *Recirculation*: The term recirculation refers to the return of trickling filter effluent, either prior to or following secondary clarification, back to trickling filter influent. The primary purpose of recirculation is to uncouple the hydraulic and organic

loading rates. Another purpose for recirculation applies when a high-strength wastewater is being treated. As literature suggested that oxygen limitations may be expected in trickling filters whenever the concentration of biodegradable organic exceeds about 250 mg/L as COD.

(c) *Media Depth*: Trickling filters have been constructed with a wide range of media depths. Depths are generally around 2 m for rocking media, with a typical range of 1 to 2.5m. Depths up to 12 m have been used for high-rate media, but a maximum depth of about 6.7 m is often used because of media structural consideration.

(d) *Temperature*: Temperature is another factor whose impact on trickling filter performance has historically been poorly understood. Ample full-scale evidence exists demonstrating that the performance of trickling filter can decline significantly during periods of cold weather.

(e) *Ventilation*: Resistance to air flow through a properly designed trickling filter is quite low, and thus only a small motive force is required to induce it. Natural draft ventilation operates very effectively as long as the temperature and humidity differences between the air inside and outside the trickling filter are sufficiently large to generate the air inside and outside the trickling filter are sufficiently large to generate the needed force.

(f) *Distributor Configuration*: Several wastewater distribution systems have been used, including fixed nozzles with or without periodic dosing and rotary distributors with or without speed control. Experience indicates that the distributor type significantly affects the hydraulic flow pattern and the biofilm thickness within the trickling filter. Both of these factors significantly affect trickling filter performance.

(g) *Wastewater Characteristics*: As with all biochemical operations, the characteristics of wastewater being treated affect the performance of a trickling filter. The more easily biodegradable the wastewater, the higher the organic loading that can be

applied while still achieving acceptable effluent quality. There are limits of course, because ultimately, the rate of oxygen transfer will control the rate at which organic matter can be removed and oxidized. Just as in the activated sludge process, various wastewater components are removed by a variety of mechanisms. Readily biodegradable substrate is removed by diffusion through the biofilm to microorganisms which biodegrade it. Slowly biodegradable substrates are initially removed by flocculation and entrapment mechanisms, just like in the activated sludge process. They are then hydrolyzed by extracellular enzymes before they are biodegraded.

(h) *Total Suspended Solids*: Particulate matter may also be problematic for biofilters in negatively affecting nitrification through clogging, occupation of the surface area by bacteria biomass as well as the through the addition of organic. Particles can easily attach onto the biofilm surface leading to thicker biofilms; however, these biofilms do not necessarily result in higher nitrification rates. Degradation of organic solids in the biofilm may compete with nitrification thus lowering the overall nitrification capacity of the trickling filter.

2.8 Past Studies of DHS System

The first research team of aerobic post treatment process named DHS reactor (Cube type DHS) is [Machdar et al. \(1997\)](#) with the aim of the study was to investigated the feasibility of the proposed system. Over six months experiment by feeding sewage their proposed system achieved 94% of COD_t removal, 81% of COD_s removal and nearly perfect SS and total BOD removal at overall HRT 8.3 h (7 h in UASB and 1.3 h in DHS). The reactor was capable of performing high (73-78% of NH_3-N removal) nitrification. That found to be the system was capable of organic removal also nitrification. With evidence from literature who applied Fluorescence In-Situ Hybridization (FISH) to investigate the presence ratio of *Nitrosomonas* and *Nitrobacter* cells to total cells that was

found to be 1.4% and 0.18%, respectively. Cells concentrations of both nitrifying bacteria were in good agreement with the magnitudes of ammonia-oxidizing and nitrite-oxidizing activities evaluated from batch tests (Araki et al., 1999).

Machadar et al. (2000) is original the second generation of DHS reactor proposed sewage treatment system. They described a long term experiment to assess the process performance of the whole combined system receiving actual sewage, with an emphasis on nitrification behavior of DHS post treatment unit. After successful performance in the COD and nitrogen removal by DHS, Uemura et al. (2002) were study about the suitability of the UASB-DHS combined system for pathogenic removal with curtain type DHS. The results were superior to the conventional activated sludge process in the reduction of fecal coliforms, but in the reductions of total RNA coliphages, the system showed somewhat less removal efficiency. Moreover, Turdukar et al. (2006a) evaluated for 3.5 years of the system regarding the applicability of curtain type DHS process to further treat the effluent of UASB treating domestic sewage. Behavior of DHS system in response to hydraulic and organic shock loads was also investigated. The observation suggested that DHS has a capability to cope with higher organic shock loads, with rapid recovery. However, the performance of the reactor especially in terms of nitrogen removal deteriorated during the organic shock load.

The third generation of DHS system (random type) investigated by Tawfik et al. (2006a). Performances of the combined system for sewage treatment at an average wastewater temperature of 15 °C have been investigated for 6 months. The results showed that a combined system operated at a total HRT of 10.7 h and total SRT of 88 days represents a cost effective sewage treatment process. The average total COD and total BOD₅ concentrations measured in the final effluent of the total system (UASB+DHS) amounted to 43 and 3.0 mg/L, respectively, corresponding to the overall removal efficiency of 90% for total COD and 98% for total BOD₅. The total process provided a final effluent

containing a low concentration of 12 mg/L for TSS. Eighty-six percent of ammonia was eliminated at space loading rate of 1.6 kg COD/m³-d and HRT of 2.7 h. The removal of *F. coliform* in the UASB reactor only amounted to 0.86 log₁₀. On the other hand, the *F. coliform* concentration dropped substantially, i.e. by 2.6 log₁₀ in the DHS system resulting only 2.7×10³/100 mL in the final effluent. The calculated average sludge production was indeed very low only 6.0 g TSS/d corresponding to sludge yield coefficient of 0.09 g TSS/g total COD removed, for DHS system.

And, the forth generation (tricking filter type DHS) was developed to overcome a few shortcomings of its predecessors (Tandukar et al., 2005). This reactor was designed to further enhance the treatment efficiency and simplify the construction process in real scale, especially for the application in developing countries. Configuration of the reactor was modified to enhance the dissolution of air into the wastewater and to avert the possible clogging of the reactor especially during sudden washout from the UASB reactor. The whole system was operated at a total HRT of 8 h (UASB 6 h + DHS 2 h) for a period of over 600 days. The combined system was able to remove 96% of unfiltered BOD. Likewise, *F.coli* were removed by 3.45 log with the final count of 10³ to 10⁴ MPN/100ml. Nutrient removal by the system was also satisfactory. The summarized performances of DHS processes were showed in Table 2.5. The high entrapment capacity of the DHS system and the retain of a high biomass concentration of 34 g VSS/L are the main reasons for the higher COD removal, nitrification process and *F. coliform* removal as compared to a series of RBC's treating UASB reactor effluent (Tawfik et al., 2005).

Several literatures suggest DHS system is not only superior to the conventional trickling filter (Chernicharo and Nachimento, 2001), but also to other post-treatment systems, such as, activated sludge process, sequencing batch reactor (SBR) (Torres and Foresti, 2001), and submerge aerated filter (Gonçalves et al., 1999) with regard to COD removal, nitrification efficiency and *F. coliform* removal as summarized results in Table 2.5

and 2.6. Accordingly, it is strongly recommended to use DHS system for post-treatment of anaerobically pre-treated sewage. So far most of the research work on the DHS system has been with sewage wastewater treatment (Agrawal et al., 1997; Machdar et al., 1997; Araki et al., 1999; Mechdar et al., 2000; Uemura et al., 2002; Tandukar et al., 2005; Tawfik et al., 2006a; Tawfik et al., 2006b; Chuang et al., 2007). Only one has been reported on actual dye wastewater treatment using DHS system (Ohashi et al., 2006).

2.8.1 Performance Comparison of DHS System and Other Post Treatment Systems

This part of the study focuses on post-treatment options for the anaerobic treatment of tapioca starch industry. Initially, the main limitations of anaerobic systems regarding carbon and nutrient removal are presented. In sequence, the advantage of combined anaerobic/aerobic treatment and the main post treatment options currently in use are discussed, including its economy apart from the level of social and educational conditions. Tables 2.6 and 2.7 (Chernicharo 2006; Tawfik et al., 2006a) and Tandukar et al., 2007) present a comparative analysis between the main systems applied to the post-treatment of effluents from UASB reactors, as follows:

- Quantitative comparison (Table 2.6): average effluent concentrations and typical removal efficiencies of the main pollutants of interest in domestic sewage
- Quantitative comparison (Table 2.7): typical characteristics of the main sewage treatment systems, expressed in per-capita values.

Table 2.5 Typical removal efficiencies and operating condition of UASB+DHS system treatment for domestic wastewater

Type of DHS reactors	UASB				DHS			Overall Efficiencies			References	
	HRT (h)	Influent		Effluent		HRT (h)	Effluent		SRT (d)	TSS (%)		TCOD (%)
		TSS (mg/L)	TCOD (mg/L)	TSS (mg/L)	TCOD (mg/L)		TSS (mg/L)	TCOD (mg/L)				
1. Cube type	7	235	672	75	144	1.3	ND	70	>170	100	94	Machdar et al. (1997)
2. Cube type	7	235	672	75	144	1.3	ND	40	-	100	94	Araki et al. (1999)
3. Curtain type	6	138	393	56	161	2	51	59	-	79	84	Machdar et al. (2000)
4. Trickling filter type	6	262	240	66	78	2	17	46	88	93	91	Turdukar et al. (2005)
5. Random type	8	255	492	47	178	2.7	12	72	178	94	90	Tawfik et al. (2006a)
6. Curtain type	6	134	373	75	167	1.3	40	69	167	70	94	Turdukar et al. (2006a)

Remark: ND is not detection

Table 2.6 Average effluent concentrations and typical removal efficiencies of the main pollutants of interest in domestic sewage

Systems	Average quality of effluent							Average removal efficiency						
	BOD ₅ (mg/L)	COD (mg)	TSS (mg/L)	NH ₄ -N (mg/L)	Total N (mg/L)	Total P (mg/L)	FC (log units)	BOD ₅ (%)	COD (%)	TSS (%)	NH ₄ -N (%)	Total N (%)	Total P (%)	FC (log units)
1. UASB reactor	70-100	180-270	60-100	>15	>20	>4	10 ⁶ -10 ⁷	60-75	55-70	65-80	<50	<60	<35	1-2
2. UASB + Activated Sludge	20-50	60-150	20-40	5-15	>20	>4	10 ⁶ -10 ⁷	83-93	75-88	87-93	50-85	<60	<35	1-2
3. UASB + Submerge aerated biofilter	20-50	60-150	20-40	5-15	>20	>4	10 ⁶ -10 ⁷	83-93	75-88	87-93	50-85	<60	<35	1-2
4. UASB + high rate trickling filter	20-60	70-180	20-40	>15	>20	>4	10 ⁶ -10 ⁷	83-93	73-88	87-93	<50	<60	<35	1-2
5. UASB + anaerobic filter	40-80	100-200	30-60	>15	>20	>4	10 ⁶ -10 ⁷	75-87	70-80	80-90	<50	<60	<35	1-2
6. UASB + dissolved air floatation	20-50	60-100	10-30	>20	>30	1-2	10 ⁶ -10 ⁷	83-93	83-90	90-97	<30	<30	75-88	1-2
7. UASB + polishing ponds	40-70	100-180	50-80	10-15	15-20	<4	10 ² -10 ⁴	77-87	70-83	73-83	50-65	50-65	>50	3-5
8. UASB + overland flow	30-70	90-180	20-60	10-20	>15	>4	10 ⁴ -10 ⁶	77-90	70-85	80-93	35-65	<65	<35	2-3
9. UASB + DHS system	4-30	32-92	4-32	3-15	12-24	-	<10 ⁴	94.3	89.7	94.8	59.9	55.9	-	4

Source: Adapted from Chernicharo (2006); Tawfik et al. (2006a) and Tandukar et al. (2007)

Table 2.7 Typical characteristics of UASB reactor and various post treatment systems, expressed as per capita values

Systems	Land requirements (m ² /inhab)	Power for aeration		Sludge volume		Cost	
		Install power (W/inhab.year)	Consumed power (kWh/inhab.year)	Liquid sludge to be treated (l/inhab.year)	Dewatered sludge to be disposed of (l/inhab.year)	Construction (US\$/inhab)	Operation and maintenance (US\$/inhab.year)
1. UASB reactor	0.03-0.10	0	0	70-220	10-35	12-20	1.0-1.5
2. UASB + Activated Sludge	0.08-0.2	1.8-3.5	14-20	180-400	15-60	30-45	2.5-5.0
3. UASB + Submerge aerated biofilter	0.05-0.15	1.8-3.5	14-20	180-400	15-55	25-40	2.5-5.0
4. UASB + high rate trickling filter	0.1-0.2	0	0	180-400	15-55	25-35	2.0-3.0
5. UASB + anaerobic filter	0.05-0.15	0	0	150-300	10-50	20-30	1.5-2.2
6. UASB + dissolved air floatation	0.05-0.15	1.0-1.5	8-12	300-470	25-75	25-35	2.5-3.5
7. UASB + polishing ponds	1.5-2.5	0	0	150-250	10-35	15-30	1.8-3.0
8. UASB + overland flow	1.5-3.0	0	0	70-220	10-35	20-35	2.0-3.0
9. UASB + DHS system	0.1-0.2	0	0	12-27	1-4	25-35 ^(a)	2.0-3.0 ^(b)
<p>Remark: Construction, operation and maintenance costs based Brazilian experience (basis: year 2002) a, b were taken from the cost as same as UASB + high rate trickling filter combined wastewater treatment system</p>							

Source: Adapted from [Chernicharo \(2006\)](#); [Tawfik et al. \(2006a\)](#) and [Tandukar et al. \(2007\)](#)

2.9 Application of Fungi in Wastewater Treatment

Fungi usually are saprophytic organisms and are classified by their mode of reproduction. As saprophytes they obtain their nourishment from the degradation of dead organic matter. Most fungi are free-living and include yeast, molds, and mushrooms. Most fungi are strict aerobes and can tolerate a low pH and a low nitrogen environment. Although fungi grow over a wide range of pH values (2-9), the optimum pH for most species of fungi is 5.6, and their nitrogen nutrient requirement for growth is approximately one-half as much as that for bacteria. In the activated sludge process filamentous fungi may proliferate and contribute to settle ability problems in secondary clarifiers. The proliferation of filamentous fungi is associated with low pH (<6.5) and low nutrients. Although filamentous fungi contribute to settle ability problems in the activated sludge process, the presence of a large and diverse population of fungi is desired for the treatment of some industrial wastewaters and composting of organic wastes. Fungi have the ability to degrade cellulose, tolerate low nutrient levels, and grow in the presence of low pH conditions (Gerardi, 2006).

Fungi are recognized for their superior aptitudes to produce a large variety of extracellular proteins, organic acids and other metabolites, and for their capacities to adapt to severe environmental constraints. For example, *Aspergillus niger* is the prototypical fungus for the production of citric acid, homologous proteins (esp. enzymes) and heterologous proteins. Moreover, *Phanerochaete chrysosporium* is the model of white-rot fungi for the production of peroxidases. Beyond the production of such relevant metabolites, fungi have been attracting a growing interest for the biotreatment (removal or destruction) of wastewater ingredients such as metals, inorganic nutrients and organic compounds. The focus of this review therefore concerns the use of fungi to remove or degrade various wastewater constituents. Some instances of synthetic wastewaters are reported, but only the contributions of fungal biomass in the biological treatment.

Moreover, researchers recognized the potential use of fungi in wastewater treatment during the late 1950s to early mid 1960s (Geust and Smith, 2002). Recently, emphasis has been made on treatment of wastewater with fungi because they are capable of rapid growth on a variety of substances (Karim and Sistrunk, 1984). Moreover, microscopic fungi can perform nitrification and denitrification under laboratory conditions. Evidence from the literature indicates the fungi based on biological wastewater could be efficient as summarized in Table 2.8.

2.9.1 Domestic Sewage

Domestic sewage contains carbon and nutrient sources that can be removed by fungal biomass. In an early investigation, Thanh and Simard (1973) demonstrated the capacities of seventeen fungal biomasses to remove phosphates (84.1%), ammonia (73.3%), total nitrogen (68.1%) and chemical oxygen demand (COD) (39.3%). They obtained fungal growth on this effluent with an accumulation of biomass (451.2 mg/L) that contained protein (47% g/g). There was variability in fungal capacities as to the removal of pollutants. In fact, *Trichothecium roseum* was the best in phosphate removal (97.5%), whilst *Epicoccum nigrum*, *Geotrichum candidum* and *Trichoderma sp.* were the best in the removal of ammonia (84%), total nitrogen (86.8%) and COD (72.3%), respectively. Concerning cell-protein production, *Paecilomyces carneus* had the highest ratio of protein to biomass (92.5%). However, this fungus did not grow very well on domestic sewage. In our laboratory, domestic wastewater pretreatment by a strain of *A. niger* has been investigated under transient conditions. This fungal biomass removed about 72% of COD and 65% of protein. Despite the differences between the bioprocess investigated in these two studies, COD and protein removal rates are in the same order. The overall feasibility of domestic wastewater treatment under sewer-simulating conditions has been explored recently both experimentally and by simulation. The heat treatment liquor (HTL) of an activated sludge was decolourised by *Coriolus hirsutus*.

Table 2.8 Example of fungi used in wastewater treatment systems, optimal conditions and the effect of fungal pretreatment.

Effluents	Fungi	Treatments	
		Reactor and medium handing	Parameters
Domestic sewage	<i>Penicillium c.</i> , <i>Steganosporium p.</i> , <i>Arthriniium a.</i> , <i>Fusarium o.</i> , <i>Cladosporium h.</i> , <i>Cladosporium c.</i> , <i>Scopulariopsis b.</i> , <i>Mucor h.</i> , <i>Trichothecium r.</i> , <i>Epicoccum n.</i> , <i>Helminthosporium s.</i> , <i>Ulocladium atrum</i> , <i>Geotricum c.</i> , <i>Trichocladium a.</i> , <i>Paecilomyces c.</i> , <i>Trichoderma sp.</i> , <i>Chrysosporium p.</i>	Shake-flask	COD (72.3%); Phosphates (97.5%); Total N (86.8%); Dry matter (684 mg/L); Protein content (205 mg/L)
	<i>Aspergillus niger</i>	Stirred tanks reactor in series	COD (72%); N-total (65.4%)
	<i>Coriolus hirsutus</i>	Continuous immobilized bioreactor; addition (nutrient (NH ₄ (100 mg/L), NO ₃ (100 mg/L); MnSO ₄); Co-substrate (glucose, 0.5%)	Decolorization (80%, 2 d); MnP (60 U/L); MIP (40 U/L)
Starch Processing Effluents	<i>A. oryzae</i> ; <i>Rhizopus arrhizus</i> ; <i>Trichoderma viride</i> ; <i>T. reesei</i> ; <i>G. candidum</i> ; <i>A. terreus</i> ; <i>R. oligosporus</i>	Shake-flask, air lift bioreactor (45 L); addition of nutriment (NH ₄) ₂ SO ₄ ; Urea; NH ₄ NO ₃ ; NaNO ₃ ; K ₂ HPO ₄ ; KH ₂ PO ₄)	TOC (44-88%); SS (95%); starch hydrolysis (53-100%); biomass (2-5.6 g/L); protein (48.8% of biomass weight); COD (97.8%); glucoamylase (3.94 U/mL)
	<i>A. niger</i> ; <i>A. oryzae</i>	Shake-flask	COD (90%); biomass and amylase production

Source: Adapted from (Coulibaly et al., 2003).

Table 2.8 Example of fungi used in wastewater treatment systems, optimal conditions and the effect of fungal pretreatment (Continued).

Effluents	Fungi	Treatments	
		Reactor and medium handling	Parameters
Starch Processing Effluents	<i>A. niger</i> , <i>P. simplicissimum</i> , <i>Geotrichum sp.</i> , <i>Fusarium verticillioides</i> , <i>Rhizoctonia solani</i> , <i>Aquathanatephorus pendulus</i> ;	Shake-flask, presence of co-ions, biomass (produced)	<i>A. niger</i> (Cu (91%); Zn (70%))
	<i>A. niger</i> , <i>A. flavus</i> , <i>A. fumigatus</i> ; <i>R. Arrhizus</i> ; <i>A. terrus</i>	Shake-flask; presence of co-ions, biomass (industrial waste, produced)	Metal removal (82-100%)
	<i>Mucor meihi</i>	Shake-flask; biomass (industrial waste), dilution (1-20)	Sorption (0.7-1.15 mmol/g)
	<i>A. niger</i>	Shake-flask; presence of co-ions, biomass (produced)	Metal removal (75%)
Distillery Wastewaters	<i>P. chrysosporium</i> ; <i>G. candidum</i> ; <i>C. versicolor</i> ; <i>Mycelia sterilia</i>	Dilution (50%)	Decolorization (53%, 10 d); growth rates inhibition below 50% of dilution; decoloration of melanoidins (80%) by <i>P. chrysosporium</i> JAG-40
	<i>A. niger</i> ; <i>A. awamori</i>	Shake-flask; continuous bubble reactor; co-substrate (sucrose, fructose, glucose); MgSO ₄ (1 g/L); KH ₂ PO ₄ (0.5 g/L); NH ₄ NO ₃ (1.8 g/L); peptone (5%); rice (3%)	OMW (decolorization (69%, 3-4 d); COD (78%)) Thin stillage (protease (200 U ml ⁻¹); biomass (30 g l ⁻¹))
	<i>C. hirsutus</i>	Shake-flask; continuous immobilized polyurethane-foam reactor; MnSO ₄ ; co-substrate (glucose, ethanol)	Decolorization (76%, 2 d); TOC (45%);

Source: Adapted from (Coulibaly et al., 2003).

Table 2.8 Example of fungi used in wastewater treatment systems, optimal conditions and the effect of fungal pretreatment (Continued).

Effluents	Fungi	Treatments	
		Reactor and medium handing	Parameters
Wood Processing Wastewater	<i>P. chrysosporium</i> ; <i>Phanerochaete flavido-alba</i>	Shake-flask; co-substrate (glucose); Mn (0.3 mg l ⁻¹); culture age	Decolorization (88%), LiP (450 nmol min ⁻¹ ml ⁻¹); MnP (800 nmol min ⁻¹ ml ⁻¹)
	<i>P. chrysosporium</i> ; <i>Ganoderma australe</i> ; <i>Coriolopsis gallica</i> ; <i>Paecilomyces variotii</i>	Shake-flask	<i>P. chrysosporium</i> (decolorization, 50%, 7 d; lignin pyrolysis compounds, 57% reduction); <i>G. australe</i> (decolorization, 50%, 7 d; lignin derivated compounds 48% increased); <i>C. gallica</i> (decolorization, 48%, 7 d; ligninderivated compounds 77% reduction); <i>P. variotii</i> (decolorization, 85%, 7 d; lignin derivated compounds 78% reduction)
	; <i>T. versicolor</i>	Shake-flask; continuous feeding bioreactor; culture age; dilution 30%); SO ₄ Mn (23 mg l ⁻¹); co-substrate (glucose, 0.3%; sucrose; starch; ethanol, carboxymethyl-cellulose; pulp and bagasse pith)	Decolorization (90 %, 9 d) Lacc (700 U l ⁻¹ , 10 d); MnP (25 U l ⁻¹ , 7 d); phenols (90%); COD (69%)

Source: Adapted from (Coulibaly et al., 2003).

This fungal strain exhibited a strong ability to decolourise HTL (70%) with an accumulation of manganese independent peroxidase (MIP) and manganese peroxidase (MnP). Optimising the culture medium by adding nitrogen and carbon sources and improving the biomass quality resulted in increased colour removal capacity by *C. hirsutus*. Although fungal applications have shown good capacities on sewage treatment, they are still underutilized in practice. This could be explained, in part, by a widespread *a priori* assumption that fungal strains do not perform as well as bacteria.

2.9.2 Sludge Treatment

Among the various global environmental hazards, sewage sludge is one of the greatest contributors to waste generation, with a typical person generating over 15 liter of sewage sludge per week and 50 g of dry solids per day. Proper management and safe disposal of wastewater sludge is a serious bottleneck at the wastewater treatment plant. Therefore, attention has been focused on non-hazardous, environmental friendly, and sustainable techniques through bioremediation, or biological-based treatment of wastewater sludge and disposal. Therefore, bioconversion/biodegradation might be a potentially effective measure for proper waste management (Molla et al., 2002).

Alam et al. (2003) selected the filamentous fungal strains such as *Penicillium corylophilum* (P), *Aspergillus niger* (A), *Trichoderma harzianum* (T) and *Phanerochaete chrysosporium* (PC) isolated from its relevant sources (wastewater, sewage sludge and sludge cake) for compatible/incompatible mixed cultures. The results of the present study showed that the combinations of P/A, P/PC and A/PC showed compatible growth and the rest of the combinations (P/T, A/T and T/PC) were incompatible cultures. A maximum production of dry biomass and dry filter cake were recorded in the compatible mixed culture of *P. corylophilum* and *A. niger* (P/A). A maximum reduction of COD (90%) and a decreased filtration time of treated sludge were observed in the case of P/A microbial mixed culture.

[Mannan et al. \(2005\)](#) presented the design to evaluate the potential of microbial adaptation and its affinity to biodegradation as well as bioconversion of soluble/insoluble (organic) substances of domestic wastewater treatment plant (DWTP) sludge (activated domestic sludge) under natural/non-sterilized conditions. The two filamentous fungi, *Penicillium corylophilum* and *Aspergillus niger* were used to achieve the objectives. It observed *P. corylophilum* was the better strain compared to *A. niger* for the bioconversion of domestic activated sludge through adaptation. The visual observation in plate culture showed that about 95–98% of cultured microbes (*P. corylophilum* and *A. niger*) dominated in treated sludge after 2 days of treatment. In this study, it was also found that the *P. corylophilum* was capable of removing 94% of COD and 99% of turbidity of filtrate with minimum dose of inoculums of 10% v/v in DWTP sludge (1% w/w). The pH level was lower (acidic condition) in the fungal treatment and maximum reduction of COD and turbidity was observed (at lower pH). The results for specific resistance to filtration (SRF) showed that the fungi played a great role in enhancing the dewaterability and filterability.

[Fakhru'l-Razi and Molla \(2007\)](#) studied on a promising biological, sustainable, non-hazardous, safe and environmental friendly management and disposal technique of domestic wastewater sludge is global expectation. Fungal entrapped biosolids as a result of prior fungal treated raw wastewater sludge was recycled to evaluate its performance as inoculums for bioseparation/bioconversion of supplemented sludge in view of continuous as well as scale up wastewater sludge treatment. Encouraging results were achieved in bioseparation of suspended solids and in dewaterability/filterability of treated domestic wastewater sludge. Fungal entrapped biosolids offered 98% removal of total suspended solids (TSS) in supplemented sludge treatment at 6 day without nutrient (wheat flour, WF) supply. Consequently, 99% removal of turbidity and 87% removal of COD were achieved in supernatant of treated sludge. Furthermore, the present result is addressing a potential

avenue of probable solution for expected management and disposal of domestic wastewater sludge in future.

2.9.3 Decolorization of Wastewater

The effluents of pharmaceutical industries, dyeing, printing, photographs, textile and cosmetics contain dyes. For example, over 7×10^7 tons dyes are produced annually worldwide, of which about 10% are lost in industrial effluent. Wastewaters from textile industries are a complex mixture of many polluting substances such as organochlorine-based pesticides, heavy metals, pigments and dyes. Their compositions have been discussed in detail by O'Neill et al. (1999). The majority of these dyes are slowly removed by the WWTP, because of their toxicities to indigenous microorganisms. Dye removal from wastewaters by established WWTP processes are expensive and need careful application. Furthermore, following anaerobic digestion, nitrogen-containing dyes are transformed into aromatic amines that are more toxic and mutagenic than the parent molecules. To overcome these difficulties, fungi are being investigated for their potential to decolourise effluents. Among them, the most widely studied are the white-rot fungi *P. chrysosporium* (a model, primarily laboratory organism) and *T. versicolor* (a promising organism for industrial applications).

Nowadays other fungi have also shown some capacities to remove dyes from industrial effluents. Dyes are removed by fungi by biosorption, biodegradation and enzymatic mineralisation (LiP, MnP, manganese independent peroxidase (MIP), Lacc). However, one or more of these mechanisms could be involved in colour removal, depending on the fungus used. Other fungal biomasses applied to the decolourisation of raw textile effluents include *Botrytis cinerea*, *Endothiella aggregata*, *Geotrichum fici*, *R. oryzae*, *Tremella fuciformis*, *Xeromyces bisporus*, *Hirschioporus larincinus*, *Inonotus hispidus*, *Phebia tremellosa* and *C. versicolor*. It is reported that raw effluents can only partially be decolourised upon fungal treatment (maximum of 49-80% but often much less).

For example, a complex mixture of real textile effluents containing many reactive dyes could be decolourised upon partial dilution by using the agaric white-rot fungus *Clitocybula duseinii*. The weak decolourisation of these effluents by complete cultures could be explained by the influences of temperature, pH, salts, inhibitory molecules (sulphur compounds, surfactants, heavy metals, bleaching chemicals), carbon and nutrients within these solutions. Concerning enzymatic (Lacc, LiP, MnP) degradations, these reactions are quite complicated, involving numerous low molecular weight cofactors that serve as redox mediators. These cofactors, in addition to the enzymes themselves, influence fungal colour removal rates (Coulibaly et al., 2003).

Furthermore, there has been an intensive research on fungal decolorization of dye wastewater. It is becoming a promising alternative to replace or supplement present treatment processes. Based on Fu and Viraraghvan (2001) reviews, there were many fungal strains capable of decolorizing dye wastewater. Decolorization by living cells involves more complex mechanisms such as intracellular, extracellular oxidases and biosorption, than by dead cells. Concurrent to application of fungi in large scale wastewater treatment, Hai et al., (2006) developed a novel submerged microfiltration membrane fungi reactor for treatment of textile wastewater that ensures permeate quality while avoiding membrane fouling. Accomplishment of excellent stable pollutant removal (99% color and 97% TOC removal) along with the alleviation of the membrane fouling problem by employing a reasonable chemical cleaning dose presents the proposed novel system as attractive one.

Blázquez et al. (2007) also established the operational conditions for the continuous treatment process of the metal complex dye Grey Lanaset G (150 mg/L), in a fluidised bed bioreactor using air pulses with retained pellets of the white rot fungus *Trametes versicolor* has been carried out. Although the bioreactor operated under non-growth conditions, the fungus activity related to laccase production was maintained. Decolourization was highly efficient (>80%) for the different HRT ranging from 18 to 120

h, and the dye removal rates ranged from 6.73 to 1.16 mg/L-h. No direct relationship between decolourization and extracellular enzyme activity was found, and high enzyme activities were not necessary to obtain high decolourization percentages. The treated effluent fulfils the environmental quality standards in relation to colour, so it could be discharged into a municipal wastewater treatment plant if necessary.

In another studies, [Dhouib et al \(2006\)](#); [Ahmadi et al. \(2006\)](#) and [Eusébio et al. \(2007\)](#) applied fungi reactor for treating olive mill wastewater (OMW). Degradation of the phenolic compounds responsible for the organic load and black color of the OMW is the limiting step in the treatment of this wastewater, i.e., conventional biological processes for the purification of OMW are ineffective. Stringent environmental regulations impose increasing efforts towards the development of new technologies and improved methods for reduction of the biorecalcitrant organics in wastewaters, such as OMW. Use of white-rot fungi to degrade the phenolics in the OMW has been reported by several investigators. In the case of *Phanerochaete chrysosporium* as the most studied fungus, the ability to degrade these types of compounds are known to be due to the expression and activation of the lignin-degrading enzymatic system.

2.9.4 Agroindustrial and Food Processing Effluents

Industries of olive oil, tapioca starch, distillery (molasses), cotton bleaching, pulp and paper processing produce several billion litres of coloured, often toxic and harmful wastewaters over the world annually. Those effluents have strong concentrations of COD (10-200 g/L), phenol and its derivatives (0.5-8 g/L) and often contain proteins, cyanides, chlorinated lignin compounds and dyes. The large amount of lignin derivatives of these effluents is responsible of their dark-brown color. The phenolic compounds of such wastewaters exert some bactericidal effects on wastewater treatment plant (WWTP) microorganisms. Fungal pretreatment (Table 2.8) of these effluents under aerobic conditions makes it possible to obtain phenol reduction (51-100%), good Decolorization

(31-100%), biochemical oxygen demand (BOD) reduction up to 85.4%, and enzyme production. Amendment of olive mill wastewater (OMW) composition (addition of co-substrate, nutrients, salts) influences the removal of COD, phenols and colors (Coulibaly et al., 2003).

Food processing wastewater is very amenable to treatment by fungi because of their inherent ability to effectively degrade complex polymers such as cellulose, hemicellulose, and lignin materials and produce high value fungal biomass. The highly dewaterable fungal biomass can be used as a source of protein and biochemicals. The ability of fungi to grow at low pH is a desirable property as it not only eliminates the need to increase the pH of many acidic food processing wastewater during treatment, but also minimizes the bacterial contamination (Jasti, et al., 2006).

Jasti et al. (2006) investigated the corn processing wastewater was treated by attached growth system of *Rhizopus oligosporus* fungi. The effects of HRT and plant-based components in the support media were evaluated in 1 L reactors under non-aseptic conditions. Plastic composite support (PCS) tubes, composed of 50% (w/w) polypropylene (PP) and 50% (w/w) agricultural products were used as support media or, as a test, PP only. A maximum COD removal of 78% was achieved at a 5 h HRT with a biomass yield of 0.44 gVSS/gCOD_{removed}. The biomass yield increased to 0.48 gVSS/gCOD_{removed} while COD removal reduced to 70% at a 2.5 h HRT.

Specifically, starch is a polysaccharide widely occurring in nature as a reserve of stored energy in many plants and also occurs extensively in waste materials produced from food processing plants starch processing waste is produced in large quantities and causes pollution problems. Biotechnological treatment of food processing can produce valuable products, such as microbial biomass protein, while also purifying the effluent (Jin et al., 1999). In a previous work reported, the biotechnological treatment of food processing wastewater can convert pollutant into valuable products such as single cell

protein, together with purifying the effluent. In cassava starch processing wastewater, the major organic components such as starch residue, free sugars and the sugar formed by the amylolytic organisms present in effluent can be used as substrates for the generation of microbial biomass rich in protein. *Aspergillus oryzae*, a filamentous fungus which has apparently been an essential part of oriental food production for centuries, is known to have a wide range of enzymes, and is capable of metabolizing complex mixtures of organic compounds occurring in most wastes. Processing a high amylolytic enzymes activity, *A. oryzae* has been determined to be suitable cultures for treatment of the starch processing wastewater. Another advantage of *A. oryzae* is safe production of harmless products. Fungal biomass is abundant in protein and can be used as additive for animal feeding. *A. oryzae* does not produce aflatoxins or any other carcinogenic metabolites (Tung et al., 2004).

2.9.5 Metal Containing Effluents

Metallurgical industries, mining, surfaces cleaning, waste incinerators produce large wastewater polluted by metals. Dissolved metals escaping into the environment pose a serious health hazard. Because they accumulate in living tissues throughout the food chain, which has human at its top. There is a need to remove heavy metals before they enter the complex ecosystem. Physicochemical treatments evolved in much diluted water-containing metals (precipitation, electrochemical, flocculation, coagulation, ion exchange) are expensive. Utilization of biomasses in general and particularly that of fungi are considered to be best alternatives for those waters purification. Indeed, the purification of the water containing metals by fungal biomass is cheaper and it presents the following advantages: (i) production of residual small volume; (ii) possibility of valorisation of fungal waste biomasses from industrial fermentations; (iii) fast removal and (iv) easy installation of the process (Coulibaly et al., 2003).

Fungal biomasses walls are composed of macromolecules (chitin, chitosan, glucan, lipid, phospholipides), which contain carboxyl groups (RCOOH), amino groups (R_2NH , $R-NH_2$), phosphates, lipids, melanin, sulphates ($R-OSO_3^-$) and hydroxides (OH). Those functional groups are metals sorption sites. Fungi remove metals essentially by adsorption, chemisorptions (ion exchange), complexation, coordination, chelation, physical adsorption and micro-precipitation. There are also possible oxydo-reduction taking place in the biosorbent. When metals are removed by ionic exchange, they generally replace K^+ , Mg^{2+} , Ca^{2+} and H^+ contained in biomasses. Table 2.8 gives a synthesis of some works on metals removal from wastewaters by some fungi. Biomasses used to remove metals from wastewaters are generally produced against few residual biomasses from fermentation. Metals sequestrations by fungi are influenced by the mineral and organic compositions content of the medium in which biomasses are produced. Biomasses granulometries and physiological states (living or dead), co-ions, metals concentrations and physical parameters (temperature, pH, ionic force, presence of others metals) influence also metals removal from polluted waters. Metals by fungi from various raw effluents (gold mining effluent, tanning effluent, swine water, polluted lake waters) are sometimes completely removed. However, these outputs depend on the metal and fungus involved. To increase fungal biomasses removal capacities, some of them undergo physicochemical treatments (soda or acidic treatments, insertion of functional groupings, heat treatment. A simple detergent and alkaline solutions treatment of *M. rouxii* biomass was sufficient to obtain an increase in its adsorption capacity. Fungal biomasses that have sequestered metals can be regenerated following their washing with HNO_3 (0.05 N) and/or with Ca^{2+} , Mg^{2+} and K^+ (0.1 M) (Coulibaly et al., 2003).

2.9.6 Biological Nutrient Removal

Nitrification and denitrification have long been considered solely a bacteria based process. Consequently, biological wastewater treatment has focused on bacteria excluding the effect of other microorganisms. More recently it has been recognized that other microorganisms are capable of fostering nitrification and denitrification. Of significant interest are the filamentous fungi. Literature suggests there may be potential advantages of fungi over bacteria in terms of rate reaction, stoichiometry, and resistance to inhibition (Guest and Smith, 2002).

- *Nitrification:*

Since the early 1930s it has been established that fungi have the ability to perform nitrification. Early studies indicated the ability in a narrow range of species with limited ability to use urea or ammonia as an energy source in the nitrification process. More recently, a much broader range of fungi have been identified to carry out nitrification as well as use urea and ammonia as an oxidizable nitrogen energy and nutrient source. One recent study notes fungal nitrification was 1 to 4 orders of magnitude greater than nitrification by autotrophic nitrifying bacteria. Studies conducted to date are essentially limited to pure cultures in a defined medium. Studies report production of nitrite and nitrate but not the overall removal or rate of removal from the medium. An assessment of the ability of fungi to replace or supplement bacterial nitrification in a biological nitrogen reduction (BNitR) system appears to be an important and potentially beneficial area for advanced research (Geust and Smith, 2002). In recent years, more evidence has been forthcoming to support the suggestion that heterotrophic nitrification may be more common than has so far been realized.

Hirsch et al. (1961) studied the formation of nitrite and nitrate by actinomycetes (Group of Gram positive, mainly soil bacteria) and fungi under various conditions. This study also found that fungi had the ability to nitrify; however, the main

product again was nitrate. Several findings from this study are worth noting. First, when the pH of the medium dropped below 5.0, nitrification was inhibited; however, growth of the fungi was not affected. Second, fungi carried out oxidation of ammonia.

[Falih and Wainwright \(1995\)](#) recently tested the ability of a wide range of filamentous fungi and yeasts to oxidize urea or ammonium. Their results showed that, with the exception of two species, all fungi oxidized ammonium or urea to nitrate. Fungi studied included *Phanerochaete chrysosporium*, *Hymenoscyphus ericae*, *Pythium oligandrum*, *Rhizomucor pusillus*, *Aspergillus oryzae*, *Mucor strictus*, *Fusarium solani*, *Aspergillus niger*, *Cladosporium herbarum*, *Penicillium chrysogenum*, *Penicillium notatum*, *Penicillium expansum*, *Geotrichum candidum*, *Williopsis californica*, and two unidentified soil yeasts.

[Kurakov and Popov \(1996\)](#) studied the nitrifying activity and phytotoxicity of 40 strains of 13 species of fungi. Forty-five percent of strains tested showed nitrifying activity. The study found that fungi showed 1 to 4 orders of magnitude greater resistance to nitrification inhibitors and 1 to 4 orders of magnitude greater formation of nitrates and nitrites than autotrophic nitrifying bacteria.

- *Denitrification*

Up until 1990, denitrification was considered solely a bacterial process; however, several species of fungi have been shown to have the ability of denitrification. To date, research in this area has been confined to biochemical and molecular genetic studies by a research group at the University of Tsukuba, Tsukuba, Japan. The current hypothesis for the origins of fungal denitrification is a horizontal gene transfer event from bacteria to fungi. Fungal denitrifiers can be split into two groups depending on the type of denitrification system they employ: a group that produces nitrite oxide reductase cytochrome P-450 (P-450Nor) and codenitrification ([Guest and Smith, 2002](#)).

Fungal denitrification shows a unique characteristic that has yet to be identified in bacteria, co-denitrification. In co-denitrification, fungi can utilize nitrogen compounds other than nitrate/nitrite in the production of nitrous oxide or nitrogen gas. In experiments with [^{15}N]-azide and [^{14}N]-nitrite, it was found that the nitrous oxide produced was a mixture of $^{14}\text{N}^{14}\text{NO}$ and $^{15}\text{N}^{14}\text{NO}$ and nitrogen gas was $^{15}\text{N}^{15}\text{N}$. Both azide and nitrite nitrogen was converted to nitrogen gas. Azide and other nitrogen nucleophiles normally inhibit the microbial denitrification processes. However, fungi are only temporarily inhibited. Addition of azide alone does not result in denitrification. Nitrite must be present for co-denitrification to occur. Co-denitrification also provides an explanation for the greater resistance of fungi to inhibitory compounds. What needs to be explored is the number and type of nitrogen containing compounds that fungi can co-denitrify (Guest and Smith, 2002).

2.10 The Advantages and Disadvantages of Fungi

Literatures suggest there may be potential advantages of fungi in wastewater treatments as summarized below:

- (i) Literature suggests there may be potential advantages of fungi over bacteria in terms of rate reaction, stoichiometry, and resistance to inhibition.
- (ii) Successful waste control by use of fungi has been reported by previous workers. They reported that many of these fungi grow rapidly on sugar cane and sugar beet molasses as well as on crude raw plant materials. There are many reasons for using fungi in biological process (Thanh and Simard, 1973).
- (iii) Fungi inherent ability to effectively degrade complex polymers such as cellulose, hemi-cellulose, and lignin materials and produce high value fungal biomass (Jasti et al., 2006)

(iv) Some fungi are regarded as safe agents and can decompose starch and protein; *Apergillus oryzea*, *Aspergillus niger*, and *Aspergillus flavus* (Hwang et al., 2004).

(v) The filaments of fungi are suitable for tangling around biofiltered materials (Hwang et al., 2004). Specifically, the three-dimensional reticular structure of polyurethane foam (sponge) was benefit to filamentous fungi growth in spreading mycelia taking nutrients and oxygen effectively (Goa, et al., 2006).

(vi) Fungi complete nitrification in a single step. A simpler treatment system reduces the number of possibilities for failure. For large scale systems found in wastewater treatment, simplicity is always preferred as long as the performance criteria are achieved. But bacterial nitrification is a two-stage process requiring two groups of bacteria. The bacterial system relies on diffusion of an intermediate compound to the second bacteria. The two groups of nitrifiers have different growth rates and also show different sensitivities to inhibitory compounds (Guest and Smith, 2002).

(vii) Soil fungi nitrifiers have greater resistance (1 to 4 orders of magnitude) to inhibitory compounds than bacterial nitrifiers. Wastewater treatment plants receiving significant quantities of industrial effluents could be provided with a robust treatment option. In addition to nitrification inhibitors, fungi also show greater resistance to heavy metals than many of the bacterial species. Several explanations can be offered on the ability of fungi to resist inhibitory compounds. First, mycelial growth may provide greater protection to sensitive organelles of fungi. The larger surface area would act in the same manner as the extra polysaccharide matrix of a biofilm; a type of adsorption matrix. Second, fungi are eukaryotic cells, which contain significantly more genes than bacteria providing other methods for dealing with inhibitory compounds. In either case, the net result is the potential for a BNitR system to operate with a greater stability even in the presence of inhibitory compounds (Guest and Smith, 2002).

(viii) The production of greater end products of nitrification (1 to 4 orders of magnitude), nitrates and nitrites (Kurakov and Popov 1996). This should hold true for wastewater, the benefits in a nutrient removal system would be reduction in the size of the aeration (nitrification) compartment of a BNR system.

(ix) The evidence has been come clear from literature reviews are that a species of fungi that perform nitrification also has been identified as being capable denitrification.

2.11 Biokinetic Coefficients Determination

2.11.1 Growth of Microorganism

Jackson and Edwards (1975) estimated specific growth rates of microorganisms in a culture by the following expressions (Figure 2.4):

$$\frac{dX}{dt} = \mu X \quad (2.1)$$

$$X = X_0 e^{\mu(t-t_0)} \quad (2.2)$$

$$\ln X = \mu(t - t_0) + \ln X_0 \quad (2.3)$$

$$\mu = \frac{\ln X - \ln X_0}{t - t_0} \quad (2.4)$$

where

X	=	Biomass concentration at the time t (mg/L)
X_0	=	Biomass concentration at the time t_0 (mg/L)
μ	=	Specific growth rate (L/h)

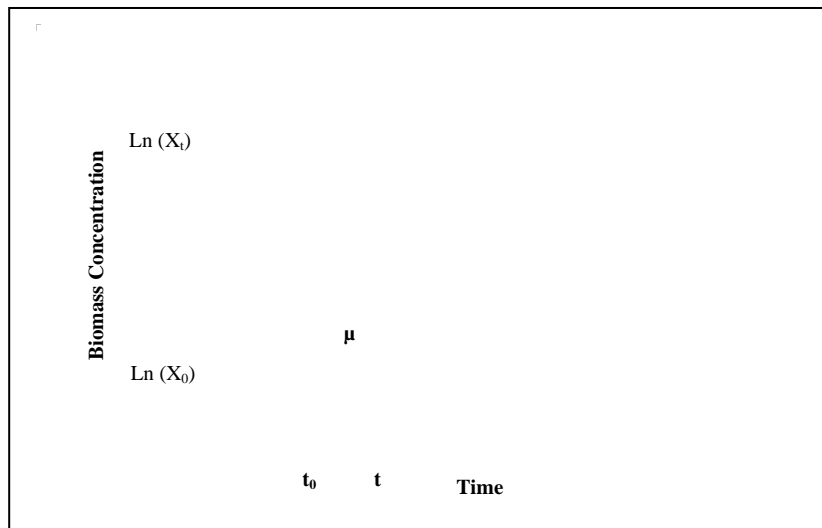


Figure 2.4 Growth curve of microorganism in a culture

Generally, Monod's model is used to estimate different biokinetic reactions between microorganisms and the substrate in a continuous culture (Metcalf and Eddy, 1991). According to this model, specific growth can be related to substrate by the following relations (Figure 2.5):

$$\mu = \mu_m \frac{S}{S + K_S} \quad (2.5)$$

where

- μ = Specific growth rate of microorganism (d^{-1})
- μ_m = Maximum specific growth rate (d^{-1})
- K_S = Half-velocity constant or Monod constant (mg/L)

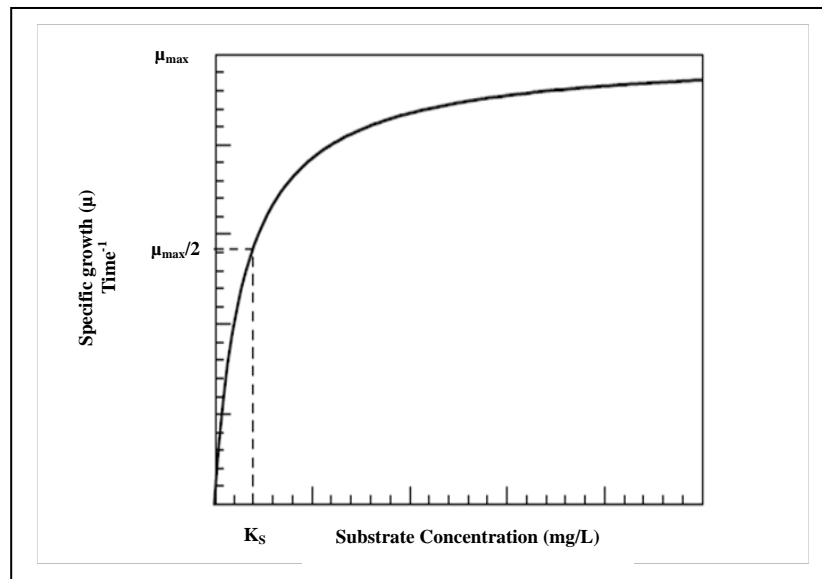


Figure 2.5 The effects of a limiting substrate on the specific growth rate

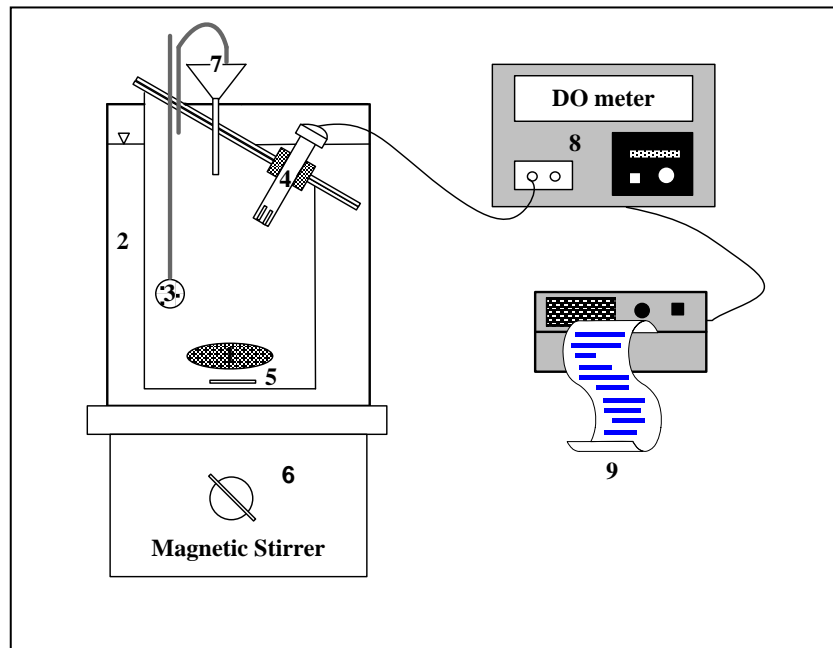
2.11.2 Respirometric Method

The respirometry measurement technique is used to measure the biochemical oxygen uptake rate (OUR) under well-defined experimental conditions. The respirometers are based on measuring the rate at which biomass takes up dissolved oxygen from the liquid phase. Assessment of wastewater components is often referred to as wastewater characterization. The procedures for characterization involve a combination of physicochemical and biodegradation tests. Using this method, the biodegradable components in the wastewater can be quantified (Vanrolleghem et al., 1999).

a. Respirometer

In principle, the respirometer consists of an oxygen electrode, DO meter, recorder, respirometric reactor and water jacket vessel to maintain a constant temperature. It is placed on a magnetic mixer in order to obtain a complete mixing of the reactor volume. A ceiling of the respirometric cell is oblique, so that the air bubbles can easily escape from the cell. The expansion funnel is used for adding the substrate solution

and for escaping air bubbles during periods of aeration. A cross-sectional area of the funnel stalk is small enough to minimize oxygen absorption during the measurement (Figure 2.6).



- | | | |
|-----------------------|-----------------|---------------------|
| 1. Respirometric cell | 2. Water jacket | 3. DO probe |
| 4. Air diffuser | 5. Magnetic bar | 6. Expansion funnel |
| 7. DO meter | 8. Recorder | |

Figure 2.6 Schematic diagram of respirometer (Witchitsatian, 2004)

b. Experimental Procedure

An expected concentration of endogenous activated sludge is transferred into the respirometry and aerated to increase the dissolved oxygen concentration to 6-8 mg/L. When these concentrations are reached, the aeration is stopped. A slow decrease in oxygen concentration is due to heterotrophic endogenous respiration. A typical respirogram is shown in Figure 2.7, and can be interpreted as follows (Cech et al., 1984).

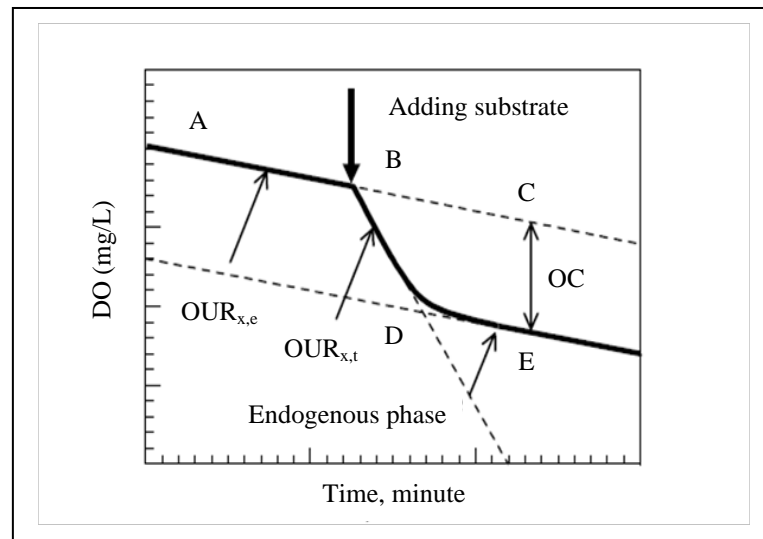


Figure 2.7. Recorder chart with a typical respirogram (Cech et al., 1984).

During the endogenous phase of respiration, heterotrophic microorganisms utilize oxygen at a constant rate over a relatively long period of time, as demonstrated by the line AB-C. At time B, a small volume of concentrated substrate solution is injected into the cell by means of a hypodermic syringe. Addition of a limited amount of substrate to the respirometry reactor causes a temporary increasing respiration rate, as shown by the lines B-D. This line is a maximum-value tangent to the curve B-E. It represents the constant total respiration rate at the substrate concentration S added. When the substrate concentration decreases with time, the respiration rate also decreases. When the substrate has been removed (at point E) the respiration rate returns to a value (line D-E), which is equal to, or perhaps slightly different from, the original endogenous rate.

When the measurement of one concentration is finished, a new dose of substrate can be injected into the cell and a next respirogram is recorded (Cech et al., 1984). In order to evaluate a respirogram, the endogenous respiration rate ($OUR_{x,e}$), the total respiration rate (OUR_t) and net oxygen consumption (OC) are calculated. The line section CE is equal to net oxygen consumption (Figure 2.7). If the OC value is higher than 4 mg/L O_2 , the determination of OC is conducted using Ekama et al. (1986) method (Figure 2.8). The high

OC value occurs when a high substrate concentration is introduced. This method is normally used for determination of COD fraction (i.e. biodegradable COD/total COD).

In this test a preselected volume of wastewater of known total COD is mixed with a preselected volume of mixed liquor of known MLVSS concentration in a batch reactor. After mixing, the OUR is measured approximately every 5 to 10 minutes until OUR attains to a constant value that is approximate or equal to OUR in the endogenous phase (Ekama et al., 1986). The respirogram is obtained by plotting the curve of OUR and time (Figure 2.8).

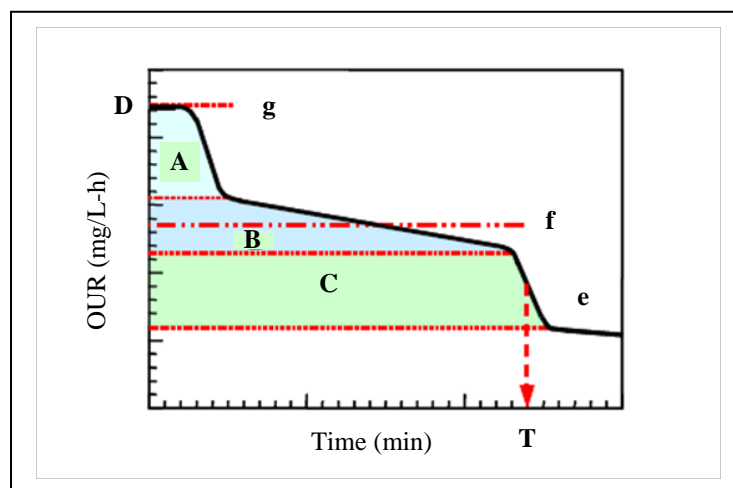


Figure 2.8 OUR response in respirometer (Ekama, et al., 1986)

where

Area A: This area gives the concentration of Readily Biodegradable COD (RBCOD) oxidized by the biomass. This is useful for assessing the amount of volatile fatty acids (VFA) that needs to be added in a biological phosphorus removal plant.

Area B: This area represents the amount of less readily biodegradable material being oxidized.

Area C: This area shows the amount of oxygen being used to convert ammonia into oxidized nitrate (nitrification).

Area D: The area under the whole curve shows the total oxygen demand of the liquor. This is the total amount of oxygen which must be supplied to the sludge to achieve full treatment.

OUR at line e: The respiration rate at the end of the curve, when at least 95% of the organic waste has been treated, is the endogenous respiration rate. This rate is proportional to the activity of the biomass.

OUR at line f: This rate is termed the Average Viability, and it is the average respiration rate for the period where nitrification and the breakdown of less readily biodegradable substrates are occurring.

OUR at line g: This is the maximum respiration rate observed at the start-up of the respiration cycles. At this point all oxidative reactions take place, including the oxidation of carbon and nitrogen compounds and the uptake of phosphates.

Time T: The time for the sample to reach an endogenous respiration rate. This is a direct method to determine the minimum HRT required to achieve at least 95% treatment efficiency.

Specific OUR of substrate oxidation at a substrate concentration S ($OUR_{x,ox}$) is given by:

$$OUR_{x,ox} = OUR_{x,t} - OUR_{x,e} \quad (2.6)$$

where:

$$OUR_{x,t} = \text{Total respiration rate (mg O}_2\text{/mg VSS.h)}$$

$$OUR_{x,e} = \text{Endogenous respiration rate (mg O}_2\text{/mg VSS .h)}$$

Further specific substrate removal rate at a substrate concentration S (R_x) is given by:

$$R_x = \frac{OUR_{x,ox}}{OC/S} \quad (2.7)$$

where

R_x = Substrate removal rate (mg COD removed/mg VSS.h)

OC = Net oxygen consumption (mg O₂/L)

S = Substrate concentration (mg COD/L)

OC is then equal to the area between the OUR curve and the second plateau level where the OUR decreases rapidly and levels off ($OC = Area A + area B$) (Figure 2.8).

Biomass yield coefficient (Y) is expressed as:

$$Y = \frac{1}{f} \left(1 - \frac{OC}{S} \right) \quad (2.8)$$

and the specific growth rate (μ) as:

$$\mu = Y \cdot R_x \quad (2.9)$$

where

μ = Specific growth rate (h⁻¹)

f = COD/VSS ratio of the sludge (mg COD/mg VSS)

Y = Yield coefficient (mg VSS/mg COD removed)

2.12 Biofilm Compositions and Density

2.12.1 Biofilm Compositions

Biofilms are typically heterogeneous structures consisting of living cells, dead cells and cells debris in a matrix of extracellular polysaccharide (EPS) attached the surface (the substratum) (Lapidou and Rittmann, 2004a). Many biofilms may essentially be considered to be layered, with an aerobic layer overlying an anoxic or anaerobic layer. Biofilm properties change with biofilm depth because transfer limitations on dissolved oxygen (DO) and nutrient and because of biological processes. Zhang and Bishop (1994) found the biofilm density's total solid changed from 15 mg/cm³ in the top layers to 105 mg/cm³ in the bottom layers and biofilm porosity changed from 84 to 93% porous in the top layers and from 58-67% in the bottom layers. The biofilms they studied had a typical feed COD of 350-700 mg/L. Biofilms grown under different operating conditions may be having different physical properties.

EPS are predominant components of biofilms. In typical of biofilm, 95% mass is water and 5% is dry material; up to 90% of biofilm organic carbon is EPS material. Because EPS is key constituent of biofilm, biofilm properties such as density, porosity, strength, elasticity, frictional resistance, thermal conductivity, and metabolic activity may be greatly influenced by EPS composition and quantities. EPS is believed to have many important functions in biofilm attachment and activated sludge floc formation. In particular research, Zhang and Bishop (2001) have been conducted on the spatial distribution of EPS along the depth of biofilm, important information that one needs to evaluate the heterogeneity of biofilm structure. Heterotrophic biofilms were grown in a rotating drum biofilm reactor fed with synthetic wastewater with a COD of 150 mg/L. Biofilm was found to be heterogeneously structured, represented not only spatial distribution of EPS yields but

also by clearly defined aerobic/anoxic zones, increased density, decreased porosity, decreased soluble COD concentrations and decreased viable biomass concentrations along the biofilm depth. Thicker biofilms exhibited greater soluble COD concentrations, EPS yields, and viable biomass than thinner biofilms. The EPS yields in the biofilms are proportionally related to the amount of viable biomass present, and viable biomass loses its ability to produce EPS at deeper sections because of its lower microbial activity resulting from lower nutrient availability. Also, it is possible that the naturally produced EPS was consumed as substrate in the deeper layer, where more readily degradable organics were absent. The results of the spatial distribution of EPS yields gained in this paper provide helpful information to achieve a more complete description of heterogeneous biofilm structure. New biofilm models need to be developed to incorporate the EPS information to accurately reflect the heterogeneity of biofilm.

Also, [Yun et al. \(2006\)](#) research base on EPS visualization and quantification, it was also found that EPS, key membrane foulants were spread out more uniformly in the anoxic biofilm in spite of lower amount of EPS compared to that in the aerobic biofilm. The difference in biofilm structure between the aerobic and anoxic MBR was investigated by comparing structural parameters. The aerobic biofilm showed a large porosity ($0.77 > 0.63$) than the anoxic biofilm. The porosity indicates that anoxic biofilm was less porous, which explains the much faster rate of fouling in the anoxic MBR compared to that in the aerobic MBR. EPS were first extracted from the biofilm at three points (aerobic at 2 kPa, aerobic 30 kPa & anoxic 30 kPa) using heating methods. The amount of polysaccharides, known as main components of EPS matrix in the biofilm was then determined. When comparing the amount of EPS in each biofilm, it is also necessary to take into account the bio-volume of each biofilm. Thus, EPS concentrations were expressed as the specific weight (mg-polysaccharide). The total weight of polysaccharide extracted from each point was 5.12 (aerobic at 2 kPa), 16.5 (aerobic 30 kPa) and 2.5 mg-

polysaccharide (anoxic 30 kPa), respectively. The polysaccharide content per unit biomass, e.g., specific weight, was increased with operating time from 35 to 55 mg-polysaccharide/g-MLVSS even under the same aerobic phase. Moreover, more rapid membrane fouling rate was observed not at point 1 but at point 2. This result shows that the more EPS in the biofilm, the greater is the membrane fouling in an aerobic MBR also observed this phenomenon. To reveal this contradictory phenomenon, the spatial distribution of EPS inside the biofilm was identified by means of lectin-stained biofilm images. A sequence of Confocal Laser Scanning Microscopy (CLMS) images of a biofilm with optical sections in step size of 1 μm from the bottom to the top. The confocal images of anoxic biofilm showed that they were highly spread out and the distribution of polysaccharide was more uniform than in the aerobic biofilm, which might result in a greater hydraulic barrier. This conclusion is also supported by porosity computed from biofilm images. Although, this porosity represents only the polysaccharides excluding the effects of other types of EPS and cells on the porosity of the biofilm, it allowed us to confirm that a more uniformly spread out of polysaccharide having smaller porosity gives rise to a greater loss of filterability. In summary, not only the amount of EPS but also the spatial distribution of EPS inside the biofilm may affect membrane filterability.

2.12.2 Biofilm Compositions under the Unified Theory

Most bacteria produce extracellular polymeric substrates (EPS) of biological origin that participate in the formation of microbial aggregates whether the bacteria grow in suspended cultures or in biofilms. The microbial biofilm or floc consists of bacterial cells enveloped by matrix of large polymeric molecules, the EPS. By definition, EPS are located at outside the cell surface. Their composition may be controlled by different processes, such as active secretion, shedding of cell surface material, cell lysis, and adsorption from the environment. Some of the functions of the EPS matrix are adhesion to surfaces, aggregation of bacterial cells in flocs and biofilms, stabilization of the biofilm structure,

formation of a protective barrier that provide resistance to biocides or other harmful effects, retention of water, sorption of exogenous organic compounds for the accumulation of nutrients from the environment, and accumulation of enzymatic activities, such as digestion of exogenous macromolecules for nutrient acquisition. A modern concept is that EPS allow microorganisms to live continuously at high-cell densities in stable mixed population communities. In other words, the EPS matrix is a medium allowing cooperation and communication among cell in microbial aggregates. Stable close proximity of the bacteria requires that the cells be held together by EPS (Laspidou and Rittmann, 2002a). Other microbial products, the soluble microbial products (SMP), are defined as soluble cellular components that are released during cell lysis, diffuse through the cell membrane, are lost during synthesis, or are excreted for some purpose. They have moderate formula weight and are biodegradable. SMP are important because they are ubiquitously present and usually form the majority of the effluent COD and BOD from biological treatment processes. SMP can be subdivided into two categories: substrate utilization-associated products (UAP), which are produced directly during substrate metabolism, and biomass, presumably as part of decay (Laspidou and Rittmann, 2002a). A common theme of EPS and SMP is that they are microbial produced organic materials that contain electrons and carbon, but are not active cells. This common theme is important, because diversion of electrons and carbon affects cell yield and growth rate. The traditional view is that all electron-donor oxygen demand (OD) is either shunted to the electron acceptor to generate energy or is converted to biomass. However, when a significant part of OD is shunted to EPS or SMP formation, the OD available for synthesizing active biomass is reduced, and active biomass yield and specific growth rate decline. Therefore, ignoring EPS and/or SMP can lead to a general overestimation of cellular growth rates (Laspidou and Rittmann, 2002a).

2.12.3 Unified Theory for EPS, SMP, and Inert and Active Biomass

[Lapidou and Rittmann \(2002a\)](#) now develop a unified theory for how EPS, SMP, active and inert biomass are related. This theory culminates with a schematic of electron flow that shows how substrate electrons are diverted to create all products that have been observed by the two different groups. They organized the unified theory through six hypotheses for how SMP, EPS, active and inert biomass are related. They state each hypothesis provide, supporting evidence and identify its effects on kinetic modeling when effects are direct.

Hypothesis 1: SMP and soluble EPS are identical in system in which hypothesis of particulate organic substrates is not important.

Hypothesis 2: Bound EPS are hydrolyzed to form BAP.

Hypothesis 3: The growth associated part of soluble EPS is the same as UAP.

Hypothesis 4: Soluble EPS polymerizes to bound EPS.

Hypothesis 5: The formation of bound EPS is growth associated and produced in direct proportion to substrate utilization.

Hypothesis 6: The SMP school of thought includes part of the bound EPS in the newly formed active biomass and another part in the inert biomass.

Figure 2.9 shows a schematic of electron flow that reflects our unified theory of how active biomass relate to each other. All mechanisms described in the six hypotheses are reflected in the figure:

- all soluble EPS are either UAP and BAP; in other words, soluble EPS and SMP are the same
- bound EPS are hydrolyzed to form BAP
- UAP are formed directly from and in proportion to substrate utilization
- bound EPS are formed directly during and in proportion to substrate utilization

- active biomass, as defined by the SMP school, is composed of bound EPS is included with inert biomass
- true dead cell residue is produced as part of endogenous decay of biomass and comprises part of inert biomass and
- BAP and UAP cycle back to become electron-donor substrate cells, since they are biodegradable

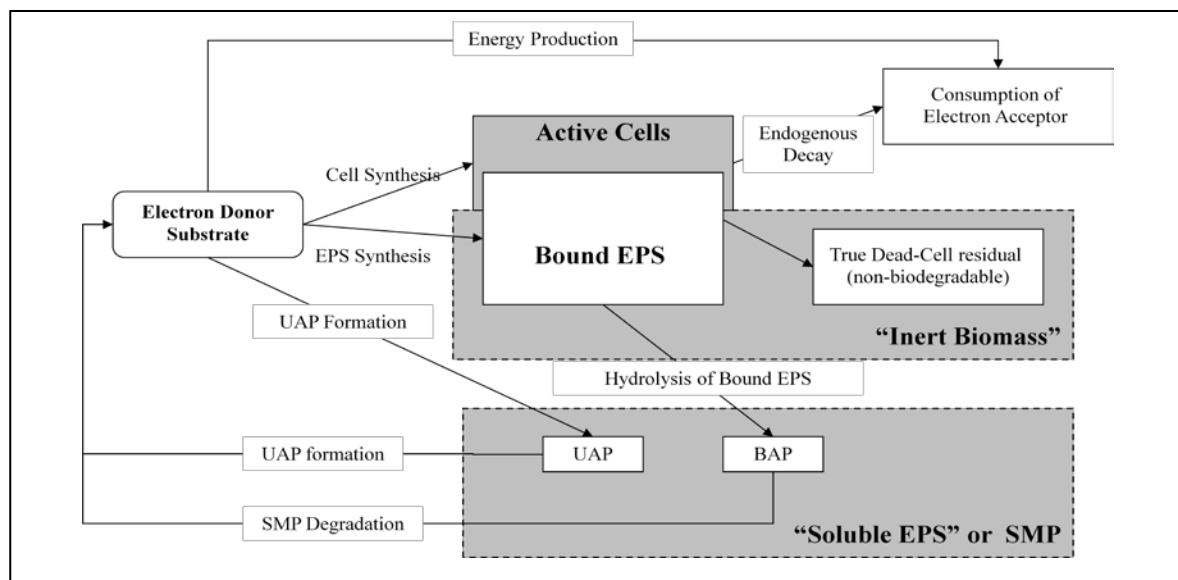


Figure 2.9. Schematic representation of the unified model for active biomass, EPS, SMP and inert biomass (Lapidou and Rittmann, 2002a)

2.12.3 Biofilm Density

Biofilm reactors are extensively used for biotechnological applications such as wastewater treatment and enzyme production. In these reactors, the substrates required for internal consumption in the biofilm are mainly transported via diffusion. This diffusional mass transfer rate usually determines the propagation and substrate utilization rates of the microorganisms within the biofilm. The performance of a biofilm reactor may

be estimated by developing an appropriate 'diffusion-reaction' model for the biofilm ([Şeker et al., 1995](#)).

The evaluation of the performance of a biofilm reactor always requires the biofilm density and thickness, since reaction rate and total consumption are directly dependent on these parameters. In the literature, it has generally been assumed that the density is constant and is independent of biofilm thickness. However, past studies discovered that the biofilm density depended on its thickness and reached a maximum value at a biofilm thickness consistent with the active thickness. The reductions in the biofilm density observed with increasing thickness, although they observed no region of increasing density possibly due to an overdeveloped biofilm thickness. Moreover, the biofilm density approached a maximum value as the substrate loading rate increased at a constant shear stress. It was also noted that the film thickness associated with a given shear stress was also a function of the substrate loading, i.e., of the net growth rate, which influenced the biofilm density ([Şeker et al., 1995](#)). Several workers have measured the biofilm density and others have attempted to study the influence of factors on biofilm thickness and density, including microbial species as details illustrate in Table 2.9 ([Zhang and Bishop, 1994a](#)).

2.13 Mathematical Modeling of Biofilms

Over 90% of bacterial biomass exists in the form of biofilms. The ability of bacteria to attach to surfaces and to form biofilms often is an important competitive advantage for them over bacteria growing in suspension. Some biofilms are "good" in natural and engineered systems; they are responsible for nutrient cycling in nature and are used to purify waters in engineering processes. Other biofilms are "bad" when they cause fouling and infections of humans and plants. Whether we want to promote good biofilms

or eliminate bad biofilms, we need to understand how they work and what works to control those (Eberli et al., 2006).

Table 2.9 Comparison of whole and sectioned biofilms (Zhang and Bishop, 1994a)

Sample No. & Layer No.	Biofilm size (cm×cm×µm)	Bacterial Counts (CFU of MPN/cm ³ biofilm)				Density (mg/cm ³)		INT Activity (%)
		HPC	FPC	NH ₄ ⁺	NO ₂ ⁻	TS	TVS	
F1.layer 1	1.2×0.9×550	1.7×10 ¹⁰	5.9×10 ⁸	2.0×10 ²	9.4×10 ²	16.4	13	82
F1.layer 2	1.2×0.9×250	9.3×10 ¹⁰	3.7×10 ⁹	2.0×10 ³	3.3×10 ⁴	36.1	28.5	38
F1.layer 3	1.2×0.9×250	5.6×10 ¹⁰	2.2×10 ¹⁰	1.0×10 ⁴	5.5×10 ⁴	58.9	45.6	16
F1.layer 4	1.2×0.9×370	1.0×10 ¹⁰	7.5×10 ⁹	2.3×10 ³	5.5×10 ⁴	93.7	77.0	8
F1. total	1.2×0.9×1420	3.5×10 ¹⁰	6.8×10 ⁹	2.8×10 ³	1.8×10 ⁴	47.5	38.1	43.2
Control 1	1.25×0.9×1510	2.2×10 ⁹	9.4×10 ⁸	2.2×10 ³	9.7×10 ³	48.3	38.4	35
F2.layer 1	1.2×0.9×350	2.7×10 ¹⁰	2.6×10 ⁸	5.5×10 ¹	9.3×10 ²	18.1	12.5	80
F2.layer 2	1.2×0.9×150	1.9×10 ¹⁰	6.8×10 ⁹	6.5×10 ²	3.6×10 ⁴	55.2	35.7	40
F2.layer 3	1.2×0.9×150	8.0×10 ¹⁰	1.9×10 ¹⁰	1.2×10 ³	5.5×10 ⁴	68.3	42.2	21
F2.layer 4	1.2×0.9×50	1.9×10 ¹⁰	1.5×10 ¹⁰	1.7×10 ²	1.5×10 ²	87.7	68.2	7
F2. total	1.2×0.9×700	3.6×10 ¹⁰	6.7×10 ⁹	4.4×10 ²	2.0×10 ⁴	41.8	27.8	26.4
Control 2	1.3×0.9×680	6.7×10 ⁹	1.3×10 ⁹	2.4×10 ³	6.5×10 ³	39.9	29.3	34.2

Remark: HPC = heterotrophic plate count; FPC = facultative plate count; NH₄⁺ = ammonium oxidizer; NO₂⁻ = nitrite oxidizer; INT = the tetrazolium dye reduction method.

Biofilms consist of cells immobilized in an organic polymer matrix of microbial origin. The structure of a biofilm has only recently received more attention. Although it was known in the past that biofilms are not uniform in time or space, frequently it was assumed that biofilms were homogeneous. With a more detailed analysis of biofilms it is however apparent that a wide variety of biofilm structures exist. Biofilm studies are either performed at a macroscopic level (i.e. measuring general properties of biofilms formed in a reactor or system) or microscopically (i.e. using microscopy and micro-electrodes). A microscopic study has the disadvantage that it is difficult to link it with the overall system

dynamics, whereas a macroscopic study is difficult to interpret unless a very well defined experimental system is available (Loosdrecht et al., 2002).

2.13.1 Mathematical Modeling Conceptual

A mathematical model is a systematic attempt to translate the conceptual understanding of a real-world system into mathematical terms. A model is a valuable tool for testing our understanding of how a system works. Creating and using a mathematical model require six steps (Eberli et al., 2006).

1. The important variables and processes acting in the system are identified.
2. The processes are represented by mathematical expressions
3. The mathematical expressions are combined together appropriately in equations.
4. The parameters involved in the mathematical expressions are given values appropriate for the system being modeled.
5. The equations are solved by a technique that fits the complexity of the equations.
6. The model solution outputs properties of the system that are represented by the model's variables.

Modeling is a powerful tool for studying biofilm processes, as well as for understanding how to encourage good biofilms or discourage bad biofilms. A mathematical model is the perfect means to connect the different processes to each other and to weigh their relative contributions

Mathematical models come in many forms that can range from very simple empirical correlations to sophisticated and computationally intensive algorithms that describe three dimensional (3D) biofilm morphology. The best choice depends on the type

of biofilm system studied, the objectives of the model user, and the modeling capability of the user (Eberi et al., 2006).

- Starting in the 1970s, several mathematical models were developed to link substrate flux into the biofilm to the fundamental mechanisms of substrate utilization and mass transport. The major goal of these first-generation mechanistic models was to describe mass flux into the biofilm and concentration profiles within the biofilm of one rate-limiting substrate. The models assumed the simplest possible geometry (a homogeneous “slab”) and biomass distribution (uniform), but they captured the important phenomenon that the substrate concentration can decline significantly inside the biofilm.

- Beginning in the 1980s, mathematical models began to include different types of microorganisms and non-uniform distribution of the biomass types inside the biofilm. These second-generation models still maintained a simplified 1-dimensional (1D) geometry, but spatial patterns for several substrates and different types of biomass were added. A main motivation for these models was to evaluate the overall flux of substrates and metabolic products through the biofilm surface.

- Starting in the 1990s and carrying to today, new mathematical models are being developed to provide mechanistic representations for the factors controlling the formation of complex 2- and 3-d biofilm morphologies. Features included in these third-generation mathematical models usually are motivated by observations made with the powerful new tools for observing biofilms in experimental systems. Today, all of the model types are available to someone interested in incorporating mathematical modeling into a program of biofilm research or application. Which model type to choose is an important decision.

- The third-generation models can produce highly detailed and complex descriptions of biofilm geometry and ecology; however, they are computationally intense and demand a high level of modeling expertise. The first generation models, on the other

hand, can be implemented quickly and easily—often with a simple spreadsheet – but cannot capture all the details. The “best” choice depends on the intersection of the user’s modeling capability, biofilm system, and modeling goal.

2.13.2 Model Selection

The first step in creating or choosing a biofilm model is to identify the essential features of the biofilm system. Features are organized into a logical hierarchy that is illustrated in Figure 2.10 (Eberl et al., 2006).

- Compartments define the different sections of the biofilm system. For example, the biofilm itself is distinguished from the overlying water and the substratum to which it is attached. A mass-transport boundary layer often separates the biofilm from the overlying water.

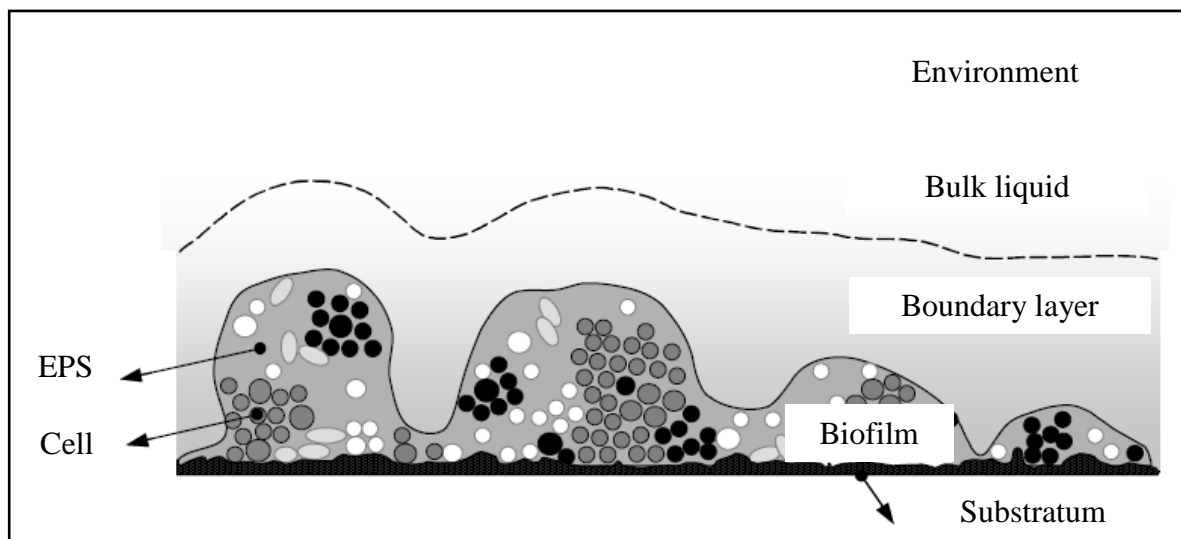


Figure 2.10 Four compartments typically defined in biofilm system: bulk liquid, boundary layer, biofilm and substratum (Eberl et al., 2006).

- Within each compartment are components, which can include the different types of biomass, substrates, products, and any other material that is important to

the model. The biomass is often divided into one or more active microbial species, inert cells, and extracellular polymeric substances (EPS).

- The components can undergo transformation, transport, and transfer processes. For example, substrate is consumed, and this leads to the synthesis of new active biomass. Also, active biomass decays to produce inert.
- All processes affecting each component in each compartment are mathematically linked together into a mass balance equation that contains rate terms and parameters for each process.

Because most biofilms are complex systems, a biofilm model that attempts to capture all the complexity would need to include (i) mass balance equations for all processes occurring for all components in all compartments, (ii) continuity and momentum equations for the fluid in all compartments, and (iii) defined conditions for all variables at all system boundaries. Implementing such a model is impractical, maybe impossible. Therefore, even the most complex biofilm models existing today contain many simplifying assumptions. Most biofilm models today capture only a small fraction of the total complexity of a biofilm system, but they are highly useful. Thus, simplifications are necessary and a natural part of modeling. In fact, the “golden rule” of modeling is that a model should be as simple as possible, and only as complex as needed ([Eberli et al., 2006](#)).

Good simplifying assumptions are identified by a careful analysis of the characteristics of a specific system. These good assumptions become part of the model structure; in other words, they serve as guidance for the selection of the model. The models found in the literature can be differentiated by their assumptions, which depend on the objectives of the modeling effort and the desired type of modeling output. Thus, a user that is searching for a model to simulate specific features of a biofilm system should begin by evaluating the type of assumptions used in creating the models ([Eberli et al., 2006](#)).

One of the objectives of the IWA Task Group on Biofilm Modeling was a comparison of characteristic biofilm models using benchmark problems. A main purpose was to analyze the significance of simplifying assumptions as a prelude for providing guidance on how to select a model (Eberli et al., 2006).

The models used by the Task Group can be grouped into four distinct categories according to the level of simplifying assumptions used: namely, analytical (A), pseudoanalytical (PA), 1D numerical (N1), and 2D/3D numerical (N2/N3). As a baseline, all model types normally can represent biofilms having the following features: (i) the biofilm compartment is homogeneous, with fixed thickness and attached to an impermeable flat surface, (ii) only one substrate limits the growth kinetics, (iii) only one microbial species is active, (iv) the bulk liquid compartment is completely mixed, and (v) the external resistance to mass transfer of dissolved components is represented with a boundary layer compartment with a fixed thickness (Eberli et al., 2006).

Table 2.10 identifies other features that can be incorporated into certain models and that differentiate among the model types. A plus sign (+) means that the feature can be simulated, a minus sign (-) indicates that the model cannot simulate that feature, and a zero (o) indicates that the model may be able to simulate the feature, but with restrictions. In general, the flexibility and complexity of the models is lower on the left hand side of the table and increases towards the right hand side (Eberli et al., 2006).

Biofilm models can be used to provide information at macro-scale or micro-scale. *Macroscale* outputs include substrate removal rates, biomass accumulation in the biofilm and biomass loss from the system. Typical *micro-scale* outputs are the spatial distributions of substrates and microbial species in the biofilm (Eberli et al., 2006).

Selecting a model is intimately related to the modeling objectives and the modeling capability of the user of the model. Common quantitative objectives are the calculation of substrate removal, biomass production and detachment rates, or the quantity

of biomass present in a given biofilm system. In engineering applications, biofilm models also are employed to optimize the operation of existing biofilm reactors and to design new reactors. In research, they serve as tools to fill gaps in our knowledge, as they help to identify unknown processes and to provide insight into the mechanisms of these processes. The capability of the user relates to the computing power available and, equally important, to the user's capacity for understanding the model. A model that cannot be formulated or solved by the user is of no value, whether or not it addresses the objectives well.

Simplifying assumptions are related to making the modeling objective mesh with the user capability. For instance, if the objective is to describe the performance of a biofilm system at the macroscale, then the various compartments and processes do not need to be described in too much of a microscale. A lot of microscale detail makes the model difficult to create and computing-intensive. For example, a 1d model with only one type of active biomass may be completely adequate to estimate the flux of one substrate averaged over square meters (Eberl et al., 2006).

Table 2.10 Features by which various types of models of biofilm system differ.

Model codes are: (A) analytical, (PA) pseudo-analytical, (N1)

1-D numerical and (N2/N3) 2-D/3-D numerical.

Feature	A	PA	N1	N2/N3
Development over time (i.e., dynamic)	-	-	+	+
Heterogeneous biofilm structure	-	-	0	+
Multiple substrate	0	0	+	+
Multiple microbial species	0	0	+	+
External mass transfer limitation predicted	0	0	+	+
Hydrodynamics computed	-	-	-	+

Source: (Eberl et al., 2006)

If the objective is to model micro-scale processes (e.g., the interaction between microbial cells and EPS in the biofilm or 3d physical structures at the μm -scale), the number and type of processes occurring in each compartment of the biofilm need to be represented in microscale detail. For example, a 2d or 3d model is necessary if understanding the physical structure of the biofilm at the μm -scale is the modeling objective, while a multi-species model is necessary if the objective is to understand how ecological diversity develops. When microscale detail is required, the size of the system being modeled will need to be small in order to make the model's solution possible. Although many processes always take place in a biofilm, it is not necessary to include every one, depending on the objectives. For example, the spatial distribution of the particulate components can be specified by an *a priori* assumption, instead of predicted by the model, if the goal is to predict substrate flux for a known biofilm. Then, the model needs not include the processes of microbial growth and loss. On the other hand, when the objective is to predict the distribution of microbial species within the biofilm or to calculate the expected biofilm thickness at steady state, then microbial growth and detachment processes are essential (Eberl et al., 2006).

2.14 The Unified Multiple Component Cellular Automaton

(UMCCA) Model

The morphological characterizations of biofilms (biofilm thickness, biofilm density, and biofilm surface shape) are very important for the stability and performance of a biofilm reactor. Intensive research in the past has revealed a wide variety in biofilm structure, but the relationship between environmental conditions and biofilm structure has been not been considered theoretically. For aerobic processes a small biofilm thickness ($<150 \mu\text{m}$) is favorable due to the smaller diffusion resistance and, moreover thicker biofilms are sensitive to sloughing phenomena. The control and therefore understanding of biofilm

thickness and structure is then an important aspect for a stable operation of biofilm processes. Biofilm surface shape is also an important parameter for the stability of the reactor. These factors also affect considerably the biomass hold-up and mass transfer in a biofilm reactor. Especially in particle biofilm processes fluffy biofilms and outgrowth lead to instabilities. However, suspended organic particles in wastewater are filtrated easier by fluffy and porous biofilms. The biofilm density has a direct effect on the achievable biomass concentration in the reactor; therefore, it will directly affect the conversion of substrate. Hence, establishing and modeling the factors that control biofilm thickness, density, and surface shape is important for overall performance of the reactor. In fact of biofilms are very heterogeneous system, containing cells distributed in a non-uniform manner, and polymers. Moreover, a liquid phase exists in the pores and channels developed in the hydrogel matrix. Therefore, to simulate the development of a structurally heterogeneous biofilm, discrete methods such as cellular automata are required ([Picioreanu et al., 1998](#)).

CA models have been used for a long time in physics as theoretical models for studying physical phenomena when complex boundary conditions are encountered. Because the states of the variables of CA models are discrete, they can be implemented entirely using logical operations; thus, CA models have the potential to eliminate any numerical artifacts that can appear in the computation due to rounding or truncation of real numbers. A classic example of the use of CA in physics is the microscopic modeling of diffusion. Because diffusion is a macroscopic manifestation of Brownian motion, it is possible to simulate it as a random walk of particles in a lattice. The characteristics of locality, uniformity, and spatial regularity of CA algorithms make them ideal for simulations on parallel computers or specially designed cellular automata machines ([Pizarro et al., 2005](#)). An approach that has provided new insight into the factors that influence biofilm structure has been the use of cellular automata (CA) simulations. CA

simulations of biofilms represent cells as discrete units that replicate stochastically in a two- or three-dimensional domain according to a set of rules, and they are effective at simulating the heterogeneity in biofilms. A general feature of CA models of biofilms is their ability to dynamically generate a range of observed biofilm morphologies using a minimal set of assumptions about cell behavior; however, computational time constraints have limited most models to two dimensions. An approach to improving computational efficiency has been to decouple solute transport from stochastic bacterial growth by the use of numerically solved, partial differential equations to describe substrate diffusion. This method allows the CA model to extend to three dimensions more easily, but does so at the expense of losing heterogeneity in the solute concentration profile. Another new trend in CA biofilm models is an individual-based modeling approach, which allows for variability in each of the cells in the simulation. Overall, CA models have been employed (Chang et al., 2003).

Consequently, [Lospidou and Rittmann \(2004a\)](#) presented a mechanistic, multi-component model—the Unified Multiple Cellular Automaton (UMCCA) model—that predicts quantitatively the biofilm’s heterogeneity for many components of a biofilm system: three solid species (active bacteria, inert or dead biomass produced by death and decay, and extracellular polysaccharides (EPS)) and three soluble components (soluble substrate and two types of soluble microbial products (SMP)). This model builds on our unified theory, which reconciles the apparently disparate findings about active and inert biomass, EPS, and SMP. The model presented here is the biofilm adaptation of our multicomponent mathematical model that quantifies the unified theory. Our biofilm model represents a growing biofilm using a CA approach in which the biofilm grows in a two-dimensional domain of compartments. One key feature is that the UMCCA model produces a “composite density” that changes in time and space in the biofilm.

2.14.1 Application of the Unified Multi-Component Cellular Automaton

(UMCCA) Model

One main goal of this model is to compute a “composite density,” or the density that includes active biomass, inert biomass, and EPS. This composite density corresponds to what is measured experimentally by total solids, volatile solids, or dry weight. To do this, the UMCCA model incorporates not only active biomass but also EPS and residual inert biomass formed as a result of cell decay and lysis. The composite density can vary in time and in space, according to how its three components vary. Because each of the components is represented separately, the UMCCA model also computes the distribution of the different components in time and space. This makes it possible to compare the results of UMCCA model runs to experimental data on each component, such as those existing for viable biomass. The second goal is to incorporate the consolidation phenomenon into the model in a realistic, yet simple manner that is based on the well-established theory from the consolidation field. Consolidation allows the UMCCA model to describe the increases in biomass density that occurs over time and deeper in the biofilm. Finally, a third goal of the UMCCA model is to find an improved system for distributing newly formed biomass. Specifically, excess biomass in a compartment must be distributed in a way that is optimum in terms of the distance the biomass has to move until it finds an empty compartment in which it can be placed. Because biomass does not advert or diffuse, the CA algorithm has rules that allow the excess biomass to move out of a full compartment and into a nearby compartment that has room to accept it. Although previous CA algorithms have such rules, the UMCCA model incorporates a more efficient and realistic set of rules.

2.14.2 Trends predicted by the UMCCA model for a biofilm including active biomass and EPS

The UMCCA model by [Laspidou and Rittmann \(2004a\)](#) includes unique new features for modeling biofilms in multiple dimensions: (a) It distinguishes among active biomass, residual inert biomass, and EPS according to the unified model of [Laspidou and Rittmann \(2002a,b\)](#); (b) It includes two types of soluble microbial products, also according to [Laspidou and Rittmann \(2002a,b\)](#); (c) It includes for the first time the time dependent consolidation of the biomass; and (d) It uses a more efficient CA algorithm to distribute excess biomass to unoccupied compartments. The five cases presented here illustrate general trends predicted by the UMCCA model, as well as effects particular to the conditions of each case. They summarized the general trends and then the particular trends. It will be valuable to look for these trends in the results of existing and new research on biofilm structure. They evaluated some of the trends by comparison to existing results in [Laspidou and Rittmann \(2004b\)](#).

(a) *General trends*

All outputs of the UMCCA model showed five general trends. First, the concentration profiles for the two soluble microbial products are opposite the profile for original substrate, since they are produced in the biofilm and must diffuse out the top surface. Second, the top of the biofilm is dominated by active biomass and EPS, while the bottom is dominated by residual inert biomass. Within the top layers, active biomass has a much higher concentration than EPS. Third, the top of all biofilms is quite “fluffy,” since the newly synthesized biomass has not had time to fill in the top compartments and consolidate. Fourth, the peak of the composite density does not correspond to the peak of active biomass. Finally, the biomass concentration has considerable local heterogeneity in the vertical and lateral directions, even when the soluble species have generally flat profiles that vary only in the vertical direction ([Laspidou, 2003](#)).

(b) *Particular effects*

Having the substrate concentration is near and below K_s or having a low dissolved-oxygen concentration promotes the formation of the cluster-and-channel structure. Then, a cluster that protrudes above other clusters (due to random effects) experiences a higher substrate (or oxygen) concentration and gains a growth rate advantage. Low substrate (or oxygen) concentration also slows the biofilm growth rate, giving the biofilm more time to consolidate to higher overall biomass density and become more inert. A high specific detachment rate also favors the cluster-and-channel structure and maintains relatively open channels near the substratum. The high surface detachment rate accentuates the growth-rate benefit for a protruding cluster. It also keeps the biofilm less dense overall, but with a lower proportion of residual inert biomass. Consolidation shows two dramatic trends. First, it makes the biofilm denser overall, and this slows its vertical expansion rate. Second, consolidation increases the local heterogeneity in all biomass types (Laspidou, 2003).

2.15 Influence of Microbial Growth Rate/Substrate Transport Rate (G Number) on Biofilm Structure

Growth of bacterial colonies in biofilms is the result of substrate conversion into biomass. Because, in the present model, the limiting nutrient is transported from the bulk liquid to the cells only by diffusion, as a result of external and internal mass transfer resistance, a gradient of substrate will form. Each microbial cell will “see” a different environment; i. e., bacteria situated on top biofilm layers get more substrate than those living in deeper layers. The lower the substrate transport rate (or higher the consumption rate) the steeper the gradient. Therefore, the biofilm structure was determined by dimensionless criteria defined (as in classical chemical reaction engineering) as ratios between the rates of relevant processes (external and internal transport, substrate

conversion, biomass growth, biofilm detachment, etc.). The ratio of biomass growth rate to substrate transport (G) is one of the most important parameters in the biofilm system. It is clear that the G (growth) group represents, in one parameter, the factors that many researchers have found to affect the biofilm structure as shown in Figure 5.10 (Lapidou 2003; Picioreanu et al., 1998b).

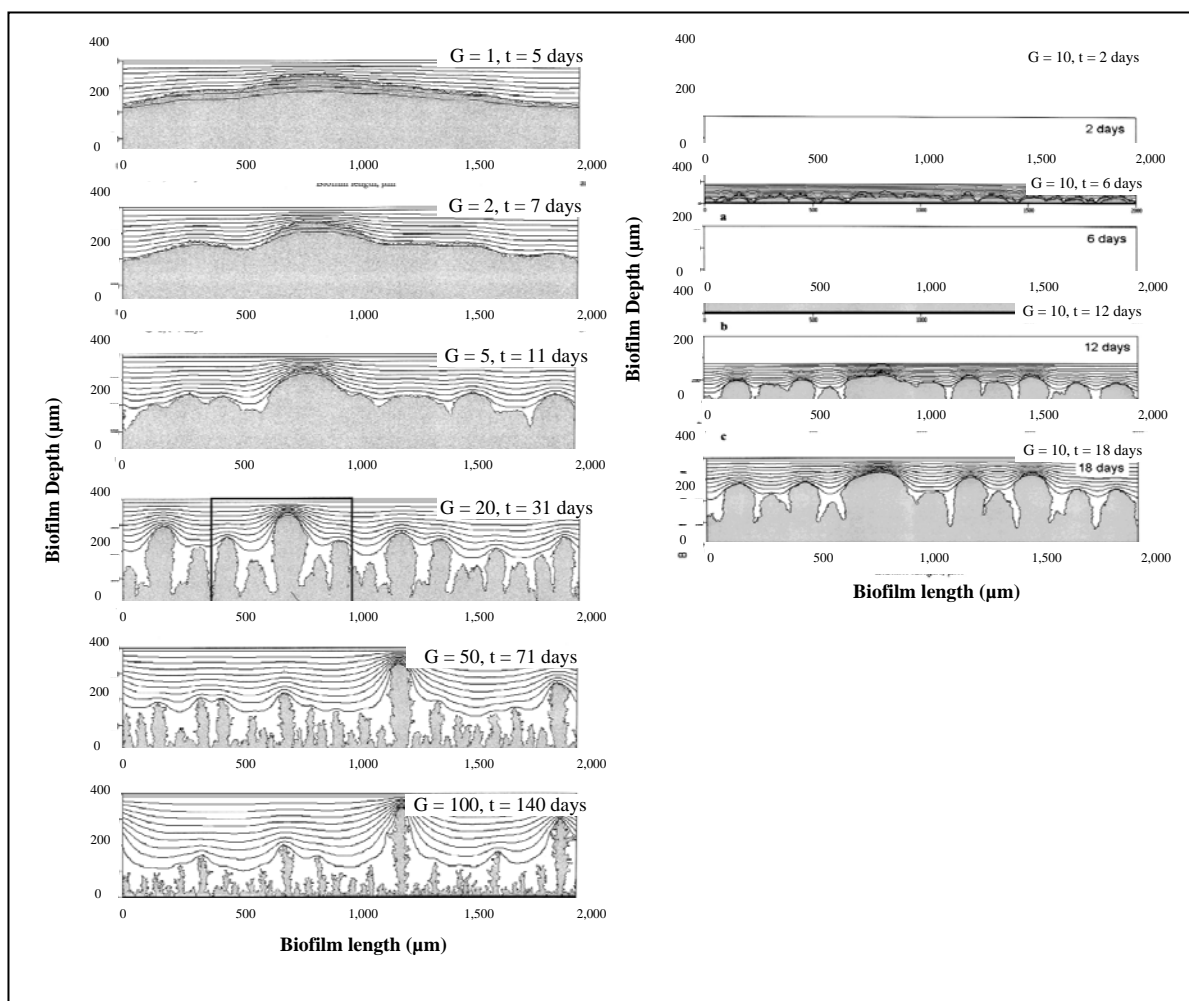


Figure 2.11 Spatial biomass distribution and equal line substrate concentration in 2D simulations at different G values (Picioreanu et al., 1998b)

The cluster effect for low S was predicted by the model of [Picioreanu et al. \(1998b\)](#), who defined the G group as the ratio of maximum biomass growth rate to the maximum substrate transport rate, as follows:

$$G = \frac{\text{maximum biomass growth rate}}{\text{maximum substrate transport rate}} = L_z^2 \frac{Y_s \overset{\Delta}{q}_s X_{a,\max}}{D_s S_{\max}} \quad (2.21)$$

where, L_z is the length of the grid along the z direction. A high G is a “transport–limited regime,” and a low G is a “growth-limited regime.” G increases as S_{\max} decreases, as long as S_{\max} is not in the saturation, or zero-order, region of the Monod relationship.

2.16 Rationales of the Study and Proposed Treatment System

2.16.1 Need of Downflow Hanging Sponge (DHS) System

A downflow hanging sponge (DHS) reactor was proposed and developed as a novel and low cost post treatment for UASB treating sewage ([Tandukar et al., 2005](#)). The principle of this system is the use of polyurethane sponge as a medium to retain biomass. As the sponge in a DHS is not submerged and freely hung/placed in air, oxygen is dissolved into the wastewater when it flows down the reactor and therefore there is no need for external aeration or any other energy inputs. Several literatures suggest DHS system is not only superior to the conventional trickling filter ([Chernicharo and Nachimento., 2001](#)), but also to other post-treatment systems, such as, activated sludge process, sequencing batch reactor (SBR) ([Torres and Foresti, 2001](#)), and submerge aerated filter ([Gonçalves et al., 1999](#)) with regard to COD removal, nitrification efficiency and F. coliform removal as summarized results in Table 2.5 and 2.6.

Accordingly, it is strongly recommended to use DHS system for post-treatment of anaerobically pre-treated sewage. So far most of the research work on the DHS system has been with sewage wastewater treatment (Agrawal et al., 1997; Machdar et al., 1997; Araki et al., 1999; Mechdar et al., 2000; Uemura et al., 2002; Tandukar et al., 2005; Tawfik et al., 2006a; Tawfik et al., 2006b; Chuang et al., 2007) and one on actual dye wastewater treatment system (Ohashi et al., 2006). However, the UASB effluent in tapioca starch industry is too fluctuated and higher concentration than domestic wastewater. When high amounts organic matter are present in a biofilter, the fast growing heterotrophic bacteria will 'out-space' the slow growing nitrifiers from the aerobic zone in the biofilm as they compete for oxygen and space. And in general, higher contents of organic in the system resulted in higher heterotroph organism population. It is important to keep the organic waste load for biofilter constant and as low as possible because a high heterotroph bacteria combined with biofilm detachment ("sloughing") may clog a biofilter, backwashing is not possible.

2.16.2 Need of Fungal Culture for Organic Removal

The UASB effluent contained high amount of biologically resistant organics. Readily biodegradable substrate is removed by diffusion through the biofilm to microorganisms which biodegrade it. Slowly biodegradable substrates are initially removed by flocculation and entrapment mechanisms, just like in the activated sludge process. Literatures suggested that the residual COD of anaerobic effluent may be comprised of residual non-degraded substrate, intermediate volatile fatty acids (VFA) and soluble microbial products (SMP). In well operated systems only a small fraction of the effluent COD is usually due to VFAs, while SMP account for 85-100% of residual COD. These SMP may not be readily biodegradable, or may even be refractory, and comprise a wide variety of organic compounds distributed across a broad spectrum of molecular weight (MW). They are then hydrolyzed by extracellular enzymes before they are

biodegraded. Several researches recommended that fungi have a wide range of enzymes, and are capable of metabolizing complex mixtures of organic compounds such as particulate matters and dead cells (Tripathi et al., 2007; Thanh and Simard, 1973; Mannan et al., 2005; Tung et al., 2004; Guest and Smith, 2002). Moreover, the efficient immobilization of fungal could also be due to the dispersed filaments (filamentous growth). Fungal culture also has potential application as immobilized cell systems which, because of their shape, may not require cross-linking or entrapment (Tung et al., 2004). Fungi and filamentous microorganisms formed as loose filamentous granular and biofilm that presence the sufficient high in substrate and oxygen mass transport.

2.16.3 Need of Bacterial Culture for Nitrogen Nutrient Removal

Total effluent nitrogen comprises ammonia, nitrate, particulate organic nitrogen, and soluble organic nitrogen. The biological processes that primarily remove nitrogen are nitrification and denitrification. During nitrification ammonia is oxidized to nitrite by one group of autotrophic bacteria, most commonly *Nitrosomonas*. Nitrite is then oxidized to nitrate by another autotrophic bacteria group, the most common being *Nitrobacter*. Denitrification involves the biological reduction of nitrate to nitric oxide, nitrous oxide, and nitrogen gas. Both heterotrophic and autotrophic bacteria are capable of denitrification. The most common and widely distributed denitrifying bacteria are *Pseudomonas* species, which can use hydrogen, methanol, carbohydrates, organic acids, alcohols, benzoates, and other aromatic compounds for denitrification (Metcalf and Eddy, 2003). Although, some literature suggested that fungi have capable in nitrogen nutrient removal but most experiences were study on laboratory scale. That has several questions need to be addressed by a systematic research plan, reactor configuration and complete denitrification.

2.16.4 Needs of UMCCA Model

Biofilm diffusion is the main parameter must concern in biofilm system. Mass transport in biofilms is influenced by the biofilm structure which in turn is influenced by the local availability of substrate. A quantitative understanding of how biofilm structure is linked to mass transport is essential for our understanding of biofilms. Solute transport in biofilms is the result of diffusion in the denser aggregates and potentially convective transport within pores and water channels. Diffusion has been shown to dominate mass transport in many biofilm systems. Two main approaches can be used to relate biofilm structure to mass transport. One approach is to explicitly describe the complex three-dimensional structure of the different biofilm components where the three-dimensional structure can be obtained from direct imaging of biofilms or from mathematical modeling ([Horn and Morgenroth, 2006](#)). The unified multi-component cellular automaton (UMCCA) was developed which purpose to quantify composite density that relationships among three solid species—active cells, EPS, and residual inert biomass, three soluble species—original substrate, utilization associated products (UAP), and biomass associated products (BAP), and electron acceptor, such as oxygen. The suitability of this combination for representing the structure of a heterogeneous biofilm has been demonstrated. An advantage of this approach is that it can provide a fast and accurate model solution with readily available computing resources, such as a high-capacity personal computer.

CHAPTER III

METHODOLOGY

The overall studies were divided into 3 main parts; (1) preliminary study, (2) pilot scale of fungal and bacterial downflow hanging sponge (DHS) reactors study and (3) mathematical modeling of biofilm mass transport in two DHS systems. The details of each stage are shown in Figure 3.1.

3.1 The UASB Effluent Sampling Site

The UASB effluent was obtained the full scale UASB plant that installed at the General Starch Co., Ltd. in Khon-Buri district of Nakhon Ratchasima province in north eastern part of Thailand as shown in Figure 3.2 (a). The UASB reactor has 4,000 m³, 23 m diameter, 11 m high, working volume consisting of a 3,428 m³ column portion and a 52 m³ gas/solid separator (GSS). The GSS portion is modified by equipping with inclined plates type settle to enhance separation of sludge from evolve biogas and effluent system. The UASB effluent were collected from overflow weirs on the top of the UASB reactor as shown in Figure 3.1(b) and stored at 4°C for maximum 1 month during used in experimental study.

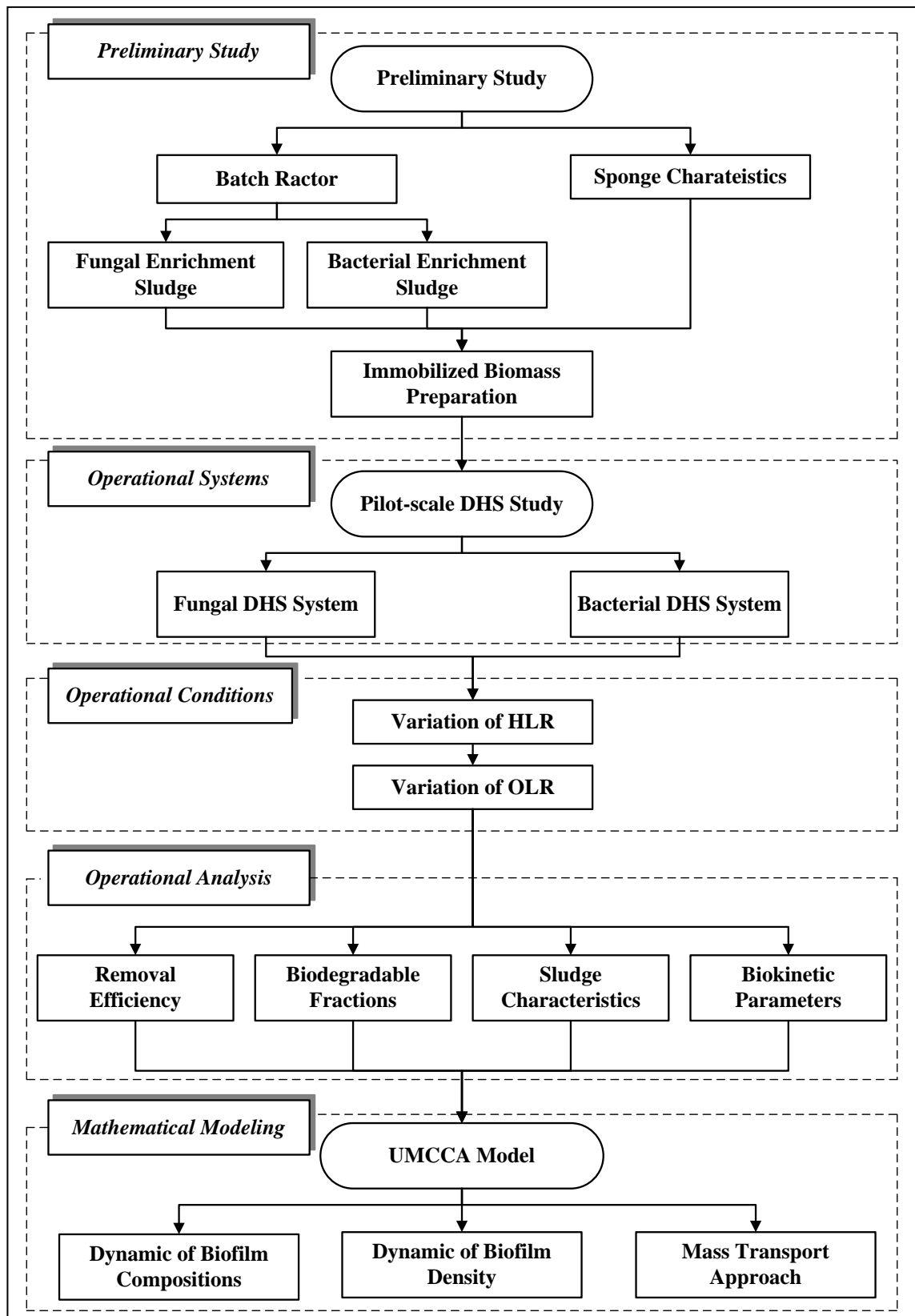


Figure 3.1 Flow chart showing different stages of experimental study



(a) UASB reactor

(b) Sampling site

Figure 3.2 UASB reactor and the sampling site

3.2 Sponge Characteristic

Characterization of packing materials was carried out according to Test Methods for the Examination of Composition and Compost (TMECC, 2002). The following properties were compared in each case: specific surface area, material density, void ratio and pore size. Specific area and material density were determined by BET technique in a Micrometrics, model ASAP 2010, apparatus and a Micrometrics, model AccPyc 1330, apparatus, respectively. Pore sizes and void ratio of sponge media were determined by scanning electron microscopy (SEM) in a JEOL, model JSM 6400, apparatus.

3.3 Enrichment of Seed Mixed Fungal and Bacterial Sludge

The initial seed sludge was isolated from the bottom sediment of an equalization tank from a tapioca starch factory. The enrichment process was carried out cultivate naturally mixed fungi and bacteria in the seed sludge. The 5 L of seed sludge was added into each polyethylene tank that contained 31 L of the UASB effluent, so a total volume of 36 L for wastewater and sludge mixture with 1,500 mg/L of initial MLSS. Figure 3.3 and

Table 3.1 illustrate the procedure and operation control conditions for enrichment of mixed fungal and bacterial sludge. The wastewater was thoroughly mixed by a diffused aeration system and pH was adjusted to 4.0 ± 0.2 , which is the optimum pH for mixed fungi growth that can prevent bacterial contamination (Dan et al., 2003; Tung et al., 2004 and Wichitsathian, B., 2004). The pH was adjusted to 7.0 ± 0.2 for bacterial culture enrichment. Mixed bacterial cells, normally, settle in the bottom, whereas the filamentous fungi and bacteria would remain in the suspension (Wichitsathian, B., 2004) that was removed from the system. However, many filamentous bacteria that cause sludge bulking have been classified (Jenkins et al., 1986; Lau et al., 1984a; Lau et al., 1984b and Richard, 1989), although newly isolated ones are occasionally reported. Jenkins et al. (1986), Metcalf and Eddy (2003); Grady et al. (1999) and Juang (2005) have proposed that the presence of certain filaments indicates the specific environmental conditions leading to activated sludge bulking. Examples include low DO, low F/M, low pH, increased concentration of sulfides, nutrient deficiency. These are insufficient conditions in sludge enrichment of bacterial system and floating sludge seems to be very low concentration during the experiment. Then, after eight hours of aeration, the biomass suspension was settled for 3 h. Subsequently, about 24 L of supernatant was removed and analyzed for COD concentration. A fresh UASB effluent of same volume (24 L) was added to the container for another batch. The MLSS concentrations of the mixture were measured at 2-3 days intervals before settling during the enrichment period.

Table 3.1 Operating conditions for fungal and bacterial culture enrichments

Operating condition	Fungal sludge	Bacterial sludge
COD (mg/L)	400 ± 100	400 ± 100
pH	4.0 ± 0.2	7.0 ± 0.2

MLSS (mg/L)	3,000	3,000
HRT (h)	12	12

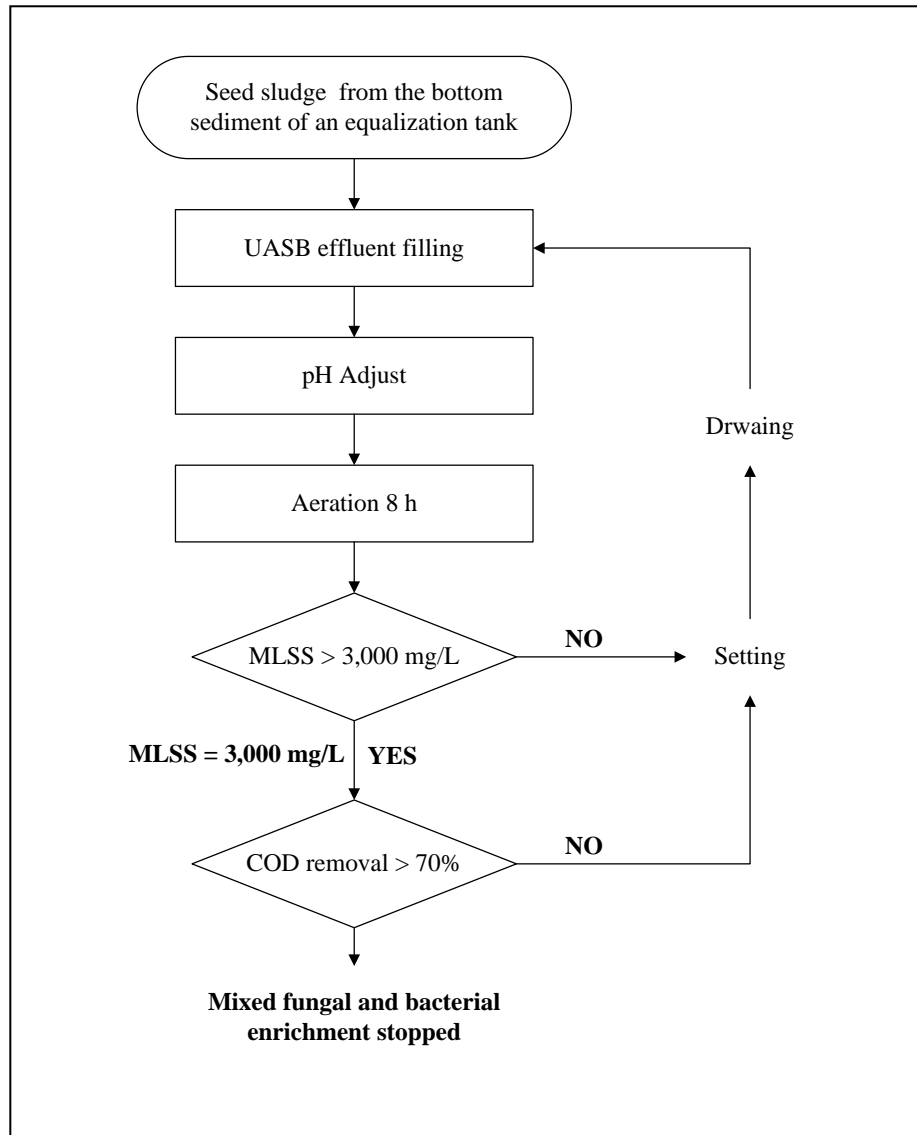


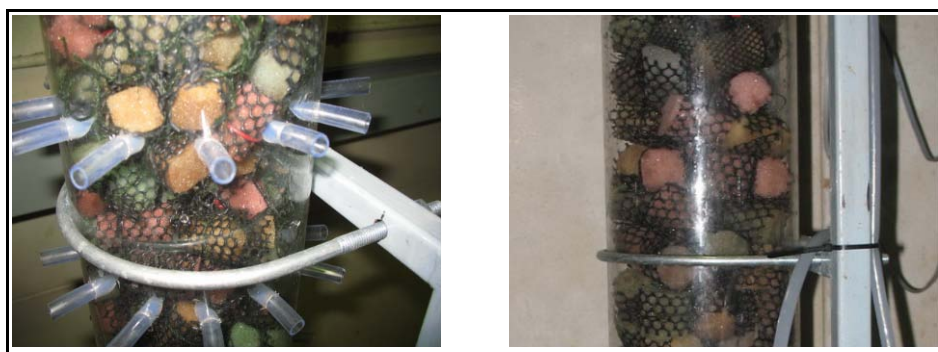
Figure 3.3 Mixed fungal and bacterial sludge enrichment processes

The enrichment process contained for 3 months until the fungal and bacterial biomass concentration reached to MLSS of above 3,000 mg/L and 70% COD removal was achieved.

The DHS experiments were started with pre-incubation by placing about 30 L volume of the sponge as the floating media into enriched seed sludge mixture for a week. The steps of fill-and-draw process were also used for the enrichment of sponges, i.e. replacing the enriched sludge and wastewater mixture daily during the 30 days period.

3.4 Experimental Setup of DHS System

The first design parameters were started with the criteria of trickling filter by [Grady et al. \(1999\)](#) for the reactor height but increasing organic surface loading to sufficient values for treating UASB effluent in tapioca starch industry following aerated biofilter design criteria ([Grady et al., 1999](#)). The schematic diagram of the experimental setup, consisting of a polyethylene tank of 100 L capacity with dimension: diameter (\emptyset)-410 mm and height (H)-800 mm for storage of the UASB effluent, and a DHS biofilter post-treatment unit as shown in Figure 3.4. The effluent from the UASB reactor was forwarded for polish-up to the aerobic DHS reactor used as a post treatment unit. The two DHS systems were made of acrylic columns, with internal diameter of 14 cm. The total height of the reactors was 430 cm. The sponges used were supported by polyethylene plastic material with fins. The DHS reactors consisted of four identical modules of column segments connected vertically, each segment being equipped with about 5.4 L of sponge randomly distributed. The dimensions of the polyurethane foam (sponge) were 20×20×20 mm for the first to third segments and 30×30×30 mm for the fourth segment as shown in Figure 3.5. The UASB effluent was fed by a peristaltic pump to the distributor located on the top of DHS systems and rotating at a speed of 9 rpm. The oxygen was naturally diffused through perforated plate windows located at different levels of the first, second and third segments of both BDHS and FDHS systems. Treated wastewater samples were collected from each segment of the systems.



(a) Segment 1-3

(b) Segment 4

Figure 3.5 The segment of two DHS systems and sponge media

Process performances of the systems were investigated during each run. Behavior of the two DHS systems in response to hydraulic loading rate (flow rate per unit volume of sponge) and organic loading rate were investigated. The experimental set-up and operating conditions for the three runs are shown in Figure 3.6 and Table 3.2.

Table 3.2 The operating conditions of two DHS systems during three runs

Operating conditions	RUN I	RUN II	RUN III
Flow rate (L/d)	75.0	25 (550 [*])	75 (475 [*])
HRT (h)	7.0	1.0	1.0
Downflow velocity (m/h)	0.2	1.5	1.5
Recirculation (L/d)	-	525	475

Remark: *inflow + recirculation

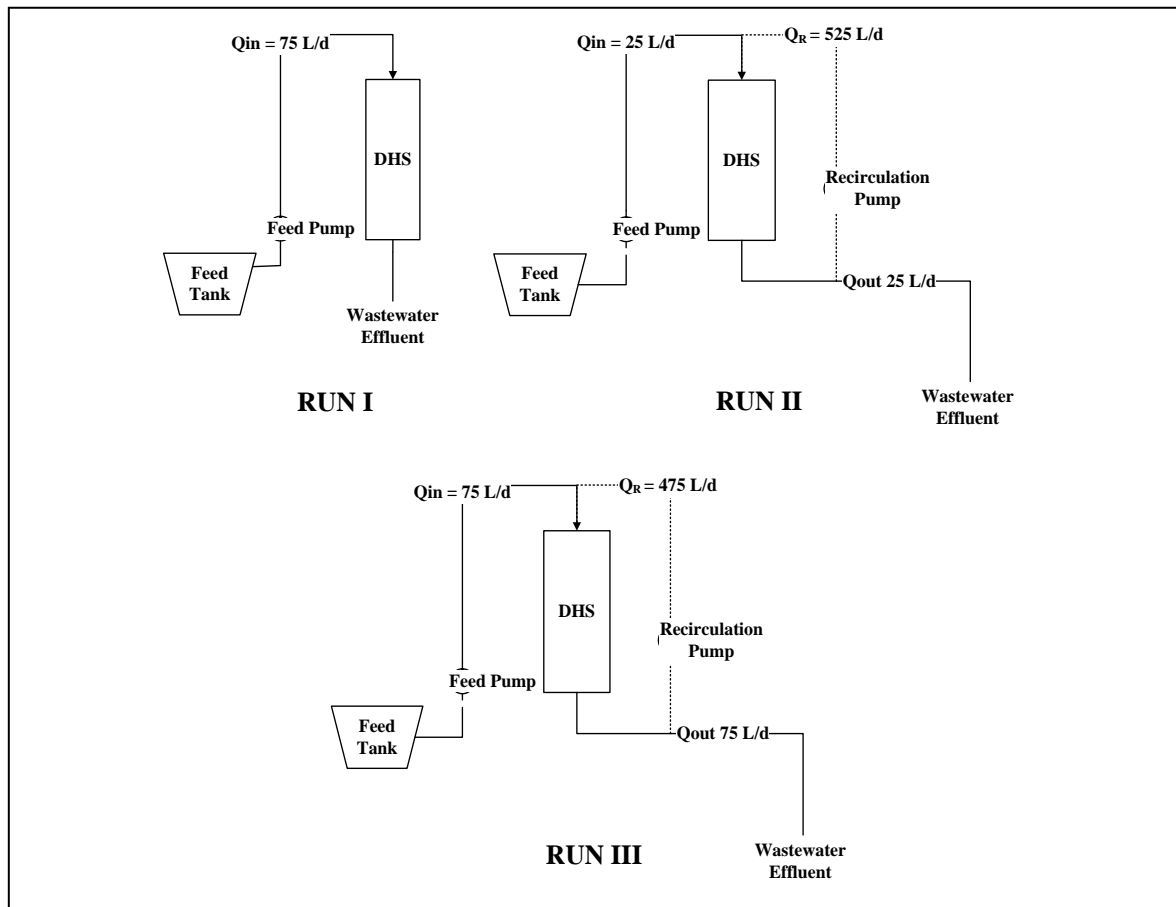


Figure 3.6 Experimental setups for RUN I, RUN II and RUN III

3.6 Biokinetic Coefficient Determination

Understanding the biodegradation kinetics of biofilms is essential for the rational optimization of biofilm reactor design and operation. However, the biokinetic parameters are particularly difficult to be measured because diffusional resistance within the biofilm would likely mask its true reaction kinetics. Respirometric technique, based on the determination of the respiration rate of microorganisms (oxygen uptake rate, OUR), has been commonly used to quantify microbial growth, associated substrate depletion, and product formation in activated sludge. Recently, several researchers have also determined

the OUR in biofilm reactors to quantify the biokinetic parameters in biofilm systems (Riefler et al., 1998; Carvallo et al., 2002; Plattes et al., 2007) and also applied in DHS system (Tawfik et al., 2006a; Tandurkar et al., 2006a and Tandurkar et al., 2006b). These studies have nonnegligible drawbacks, although these results can reflect heterogeneity of biofilms in that highly complex structures containing voids, connecting channels between these voids, and microbial clusters or layers with nonuniform spatial distribution of biofilm properties such as density, porosity, and the diffusivity mass transport limitations. However, a new approach to quantify spatial distribution of biofilm kinetic parameters by in situ determination of oxygen uptake rate (OUR) was studied by Zhou et al. (2009). This depends on oxygen concentration profiles, which are usually obtained by using a microelectrode technique. But it is only one research to study by this technique now.

The oxygen uptake rate (OUR) experiments were conducted to determine the biokinetic coefficients of aerobic heterotrophs in the sludge samples obtained from different DHS location heights (first, second, third and fourth segment). The harvested sponge with biomass was squeezed and centrifuged at 3000 rpm for 15 min and decant the supernatant. Dilute the sludge with phosphate buffer 10 mM, pH 7.0, homogenize and centrifuge, then decant again the supernatant. This step has been repeated 5.0 times. Before starting OUR experiments, both UASB effluent and the sludge were aerated for 45 min to ensure that no hydrogen sulfide and no external carbon source were present in the effluent of UASB reactor and the harvested sludge respectively (Tawfik et al., 2006a; Tandurkar et al., 2006a and Tandurkar et al., 2006b).

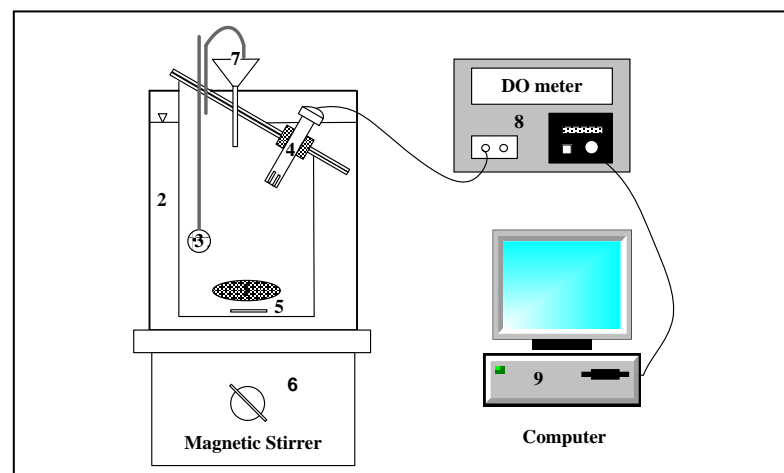
The initial MLVSS concentration, X_0 in the sludge samples of two DHS systems were brought to 400 mg/L by dilution for both runs. The biokinetic coefficients were determined using a closed 0.9 L batch respirometer, equipped with a recorder and a dissolved oxygen (DO) meter (YSI, model: 556 MPS). Constant temperature was

maintained by circulating water through a water jacket enclosing the reactor vessel. Figure 3.7 and Table 3.3 present the respirometer set up and operating conditions of the experiments. The S_0/X_0 ratio (initial substrate concentration/biomass concentration) that governs the quality of the batch respirometric tests was maintained in the range of 0.05-0.8.

The experimental procedures for OUR determination were summarized in Figure 3.8 with details below:

a) *Obtaining endogenous sludge:* The respirometer was filled with fresh sludge without substrate and aerated at least for 2 h.

b) *Suppressing nitrification:* NH_4Cl was with the concentration of 70 mg N-ammonium/L. [Dan, N. P. \(2001\)](#) and [Wichitsathian, B. \(2004\)](#) referred that if ammonia was presented in wastewater, organic oxidation and nitrification simultaneously occurred. At high enough ammonia concentration (70 mg/L), the OUR in nitrification process was constant during organic oxidation. When this ammonia dose was added to endogenous sludge, nitrification OUR was determined. Thus, OUR of organic oxidation was the difference between total OUR and the sum of endogenous OUR and nitrification OUR.



- | | | |
|-----------------------|------------------|-----------------------|
| (1) Respiration cells | (2) Water jacket | (3) Air diffuser |
| (4) DO probe | (5) Magnetic bar | (6) Magnetic stirrer |
| (7) Expansion funnel | (8) DO meter | (9) Computer recorder |

Figure 3.7 Experimental setup for the respirometric tests**Table 3.3** Operating conditions of the respirometric experiment of fungal and bacterial cultures (Wichitsathian, B., 2004)

Operating conditions	Fungal culture	Bacterial culture
Initial pH	4.0±0.2	7.5±0.2
Temperature (°C)	30±0.5	30±0.5
X ₀ (mgMLSS/L)	500	500
Substrate concentration, S ₀ (mgCOD/L)	5-50	5-50
S ₀ /X ₀ ratio (d ⁻¹)	0.01-0.10	0.01-0.10
Suppressing nitrification	-	⁷⁰ g N-ammonia/L ^(a)

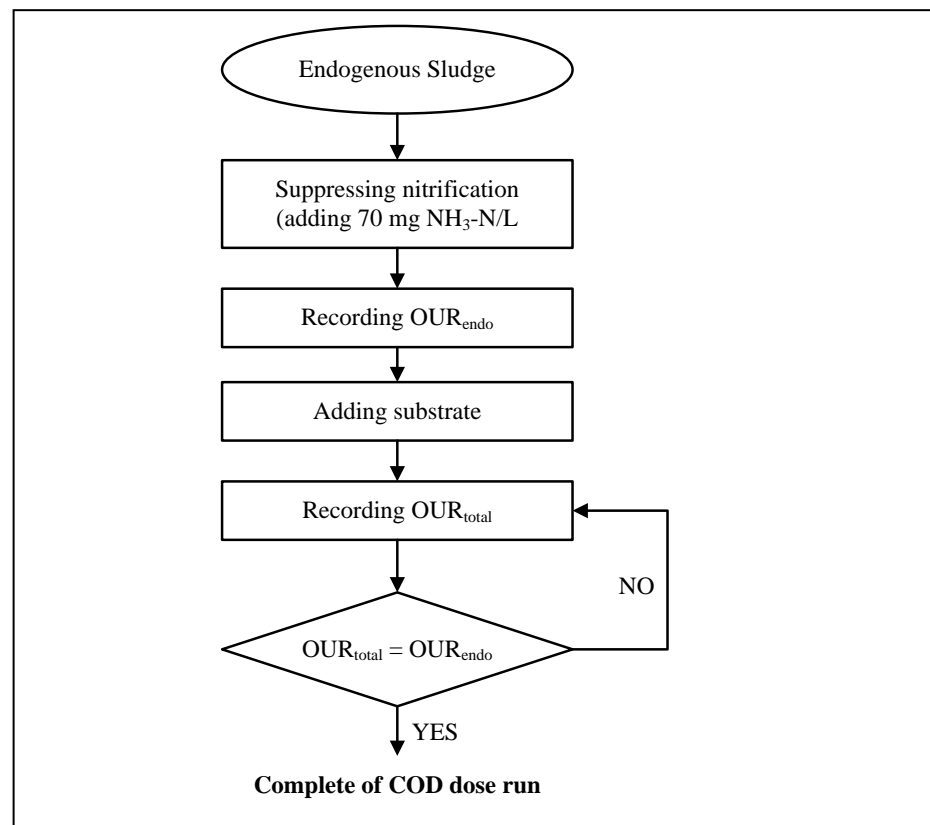


Figure 3.8 Biokinetics coefficients study processes

c) *Recording endogenous OUR:* After suppressing the nitrification process, the mixture was aerated at least half an hours before measuring endogenous OUR.

d) *Adding substrate:* An accurate amount of substrate was added to the respirometer and total OUR recorded by data logger. New re-aeration was necessary when the dissolved oxygen concentration dropped below 2 mg/L.

The results of the respirometric experiments provided values of the oxygen uptake rates (OUR) that were used for calculating maximum specific growth rates (μ_{\max}), substrate utilization rate (r_x), half-velocity constant (K_S) and sludge yield coefficient (Y) based on Monod kinetics by regression analysis (Wichitsathian, 2004; Dan, 2001 and Grady et al., 1999).

3.7 Investigation for Biodegradable COD Fractions

The carbonaceous material characterizations measured in terms of the COD parameter were subdivided into a number of fractions following Wentzel, et al. (1999) as shown in Figure 3.9. That is presented to quality four COD fractions—unbiodegradable soluble (USCOD) and particulate (UPCOD), readily (BSCOD) and slowly (BPCOD) biodegradable. Biodegradation fractions (BCOD) were calculated from the measured of the total COD (TCOD) and BOD 20 days with inhibited nitrification. The BOD values were calculated using negative pressure values from the OxiTop[®]-C measuring head (Boursier et al., 2005). The particle and colloidal were separated from soluble fractions by filtration method through a glass fiber filter (Whatman's GF/C).

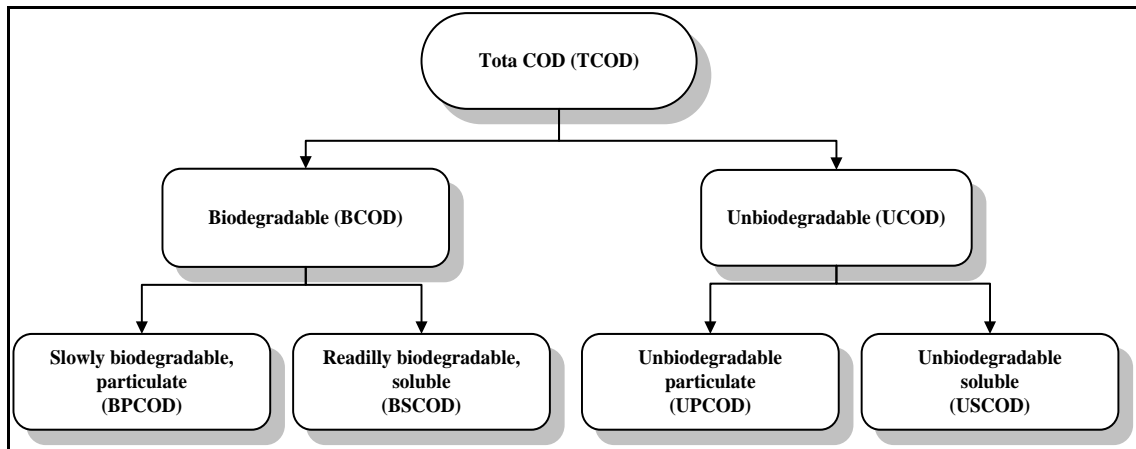


Figure 3.9 Division of COD fractions in two DHS systems

3.8 Material Balance Calculation Methods

The calculation methods of COD and nitrogen balances on two DHS systems were processed by following formula of [Barker and Dold \(1995\)](#). To perform a COD balance on two DHS systems, must be estimated the mass of COD in the influent and effluent, COD of wasted sludge, and amount of COD oxidized. The amount of COD mass balance can be noted by Equation 3.1.

$$M_{COD,inf} = M_{COD,eff} + M_{COD,oxid} + M_{loss} \quad (3.1)$$

Where: $M_{COD,inf}$ and $M_{COD,eff}$ is mass of TCOD in the influent and effluent, respectively (g/d); $M_{COD,oxid}$ is mass of TCOD oxidized through aerobic heterotroph utilization or oxygen utilization rate with deduction of oxygen required for nitrification (g/d); $M_{COD,denit}$ is a mass of nitrate denitrified per day multiplied by 2.86 that is the transfer of one electron equivalent requires the reduction of 1/4 mol of oxygen or 1/5 mol of nitrate during

denitrification process (g/d); $M_{COD,wasted}$ is mass of COD in wasted sludge of DHS effluent and $M_{COD,slu}$ mass of assimilated COD in sludge.

Based on nitrogen removal theory, nitrogen removal can be achieved by two principal processes, assimilation by microorganism and nitrification-denitrification. The amount of nitrogen mass balance was illustrated in the Equation 3.2.

$$M_{TKN,inf} + M_{NO_2-N,inf} + M_{NO_3-N,inf} = M_{TKN,eff} + M_{NO_2-N,eff} + M_{NO_3-N,eff} + M_{loss} - M_{N,slud} \quad (3.2)$$

Where: $M_{TKN,inf}$, $M_{NO_2-N,inf}$, $M_{NO_3-N,inf}$ are mass flow of TKN, nitrite and nitrate (g/d) in the influent, respectively; $M_{TKN,eff}$, $M_{NO_2-N,eff}$, $M_{NO_3-N,eff}$ are mass flow of TKN, nitrite and nitrate (g/d) in the effluent, respectively; $M_{N,ass}$ is nitrogen assimilation obtained by analyzing the amount of nitrogen accumulation in dry sludge (g/d); M_{denit} is the mass of nitrate denitrified per day which equals to the differences between the input and output nitrate and $M_{N,wasted}$ is mass of TKN in wasted sludge of DHS effluent.

3.9 Identifying Cultures

To investigate the predominant microorganisms in BDHS and FDHS sludge, they were cultured on medium of different mixtures the BDHS system used Trypti-caseine Soy Agar (TSA) medium with sterilized DHS influents and the FDHS system used Potato Dextrose Agar (PDA) medium with sterilized DHS influents. The predominant microorganisms were identified from their fast growing rate and in a considerable number. Subsequently, the purified dominant fungal and bacterial cultures were sent to National Center for Genetic Engineering and Biotechnology (BIOTEC), Thailand for genus identifications.

3.10 Sludge Characteristics

The variation in sludge characteristics were estimated in two DHS systems during three runs under different operational conditions on the sludge characteristics. Based on the system efficiencies and biofilm compositions were determined. The harvested sponges with biomass were squeezed. The obtained liquid was centrifuged at 3,000 rpm for 15 min and the supernatant was removed. The residual sludge was diluted with phosphate buffer of 10 mM, and pH of 7.0. Sludge was homogenized and centrifuged and then the supernatant was removed again. This step was repeated 5 times (Tandukar et al., 2005). Characteristics of the sludge after above steps, in terms of SS, VSS, and specific oxygen uptake rate (SOUR), as well as extracellular polymeric substances (EPS), active biomass and retained biomass concentrations were determined experimentally.

3.10.1 Microorganism Morphology

Microbial morphology in the two continuous reactors were determined by scanning electron microscopy (SEM) in JEOL, model JSM 6400, apparatus. For SEM preparation, harvested sponges were fixed for 4 h in 2% (v/v) glutaraldehyde, washed 3 times with 0.10M sodium cacodylate buffer, and dehydrated with T-butyl alcohol of increasing concentration (50, 70, 85, 95 and 100% v/v). Dehydrated sludge was dried with a freeze dryer, sputter-coated with gold at 20 mA in a high vacuum (2.8×10^{-6} Torr) and low temperature (-170°C) cryo-chamber for 90 seconds, and then viewed with SEM (Geng et al., 2004).

3.10.2 Extracellular Polymeric Substances (EPS)

The quantification of EPS in biomass was analyzed using thermal extraction method (Chang and Lee, 1998). A measured volume of sludge solid was centrifuged in order to subtract the soluble EPS at 3,200 rpm for 30 min from bound EPS. After collecting the soluble EPS, the remaining pellet was re-suspended with 0.9% NaCl solution before heating at 80°C for 1 h. The extracted solution was separated from the sludge solids by centrifugation at 3,200 rpm for 30 min. The obtained supernatant was the bound EPS. The quantity of bound EPS and soluble EPS were measured by measuring proteins and carbohydrates (Wichitsathian, B., 2004). Protein and carbohydrate, being the main components of EPS, were analyzed using Lowry method (Lowry et al., 1951) and phenolic sulfuric acid method (Dubois et al., 1956) with Bovine Serum Albumin (BSA) and glucose, respectively used as the standards.

3.10.3 Active biomass concentrations

The concentration of active biomass procedure was used in this study is referee of that by Zhang and Bishop (1994) with phospholipids analysis that consists of:

- 6 mL samples from homogenized bacterial suspensions for each biofilms was added into 150 mL screw cap bottles, while they used 50 mg of cells. Then, 20 mL of chloroform, 40 mL of methanol, and 10 mL of water was added to the samples (thus the ratio of chloroform: methanol: water was 1: 2: 0.8)

- 5 mL portions of the chloroform layer was transferred to clean COD test tube, while they transfer 100 µL portions to a 2 mL glass ampoule.

- 2.7 mL potassium persulfate was added;

- the sealed COD test tubes are heated in an oven at 103°C for 2 h;

- the phosphate release by digestion was determined by adding 0.6 mL ammonium molybdate; and

- The absorbance at 610 nm was then read using a diode array spectrophotometer. The concentration of phosphate was calculated by using a standard curve saved in diode array spectrophotometer.

In order to find the conversion factors from phospholipids concentration to active cells based on total volatile suspended solids (VSS). By measuring VSS and phospholipids content of these enrichment cultures, the conversion factors were obtained (Zhang and Bishop, 1994).

3.11 Analytical Methods

Table 3.4 illustrates the analytical methods of experimental study. Influent and effluent samples were analyzed following the Standard Methods for the examination of water and wastewater (APHA, 1998). The BOD values were obtained by using an OxiTop[®]-C measuring pressure head. Biodegradation rate was calculated from the measured BOD₂₀ values with inhibited nitrification and total COD (TCOD) (Reuschbach et al., 2003). Protein and carbohydrate, being the main components of EPS, were analyzed using Lowry method (Lowry et al., 1951) and phenolic sulfuric acid method (Dubois et al., 1956) with Bovine Serum Albumin (BSA) and glucose, respectively used as the standards.

Table 3.4 Parameters and analytical methods

Parameters	Methods	Equipments
pH	pH meter	pH meter
DO	DO meter	DO meter
COD	Dichromate reflux	Titration
BOD	OxiTop [®] -C	OxiTop [®] -C measuring pressure head/bottle
TKN	Marcro-Kjeldahl	Titration
NH ₃ -N	Nesslerization	Titration

MLSS	Dried at 103-105°C	Oven
MLVSS	Ignited at 550°C	Furnace
TOC	Combustion method	TOC analyzer
EPS	Thermal and centrifugal method	Centrifugal equipment
Proteins	Lowry	Spectrophotometer
Carbohydrates	Phenolic-sulfuric acid	Spectrophotometer
Microbial composition	Microscopic	Scanning electron microscopic

3.12 Application of the UMCCA Model for Biofilm Composition and Density in Two DHS Systems

Biofilm processes have been widely applied to the various fields of water and wastewater treatment technologies. Biofilm formation takes place by a variety of biological, chemical, and physical processes. During biofilm development, the large number of chemical and biological species that occur and interact simultaneously over a broad range of length and time scales can easily confuse human intuition. Mathematical models can help in deeper and broader understanding of a system by generating quantitative prediction from the descriptions of biofilm characteristics that have been turned into the rational form of a complete set of equations ([Piocioreanu et al., 2004](#)).

Biofilms are multiphase systems that consist of solids and a liquid phase in the void space between the solids. Most biofilms are spatially heterogeneous, characterized by complex assemblages of cell types and gradients of physical/chemical parameters. The spatial gradients of microbial species and density, the volume fraction of the water phase (porosity), and the tortuosity of biofilms have to change as the depth of the biofilm increases. These spatial distributions of biotic and abiotic components in turn affect the mass transfer mechanisms and diffusivities in biofilms ([Zhang and Bishop, 1994a, b](#)).

Because of the complexity of biofilms, the determination of diffusivities within the biofilm is extremely difficult. Up to now, the following three basic methods have been used to determine biofilm diffusivities: (a) the diffusion cell method; (b) the diffusion reaction model data fitting method; and (c) the concentration profiles data fitting method. The classical diffusion cell method depends on time course of concentration changes between two diffusion cells. It treats the biofilm as a black box, and does not take into consideration changes of density, porosity and pore structure within biofilm. Thus, it can only give average diffusion information over the total biofilm depth. The second method requires the accurate determination of kinetic parameters, which is usually done in a suspended microorganism system, a very labor intensive undertaking. The third method depends on concentration profiles, which are usually obtained by using a microelectrode technique (Zhang and Bishop, 1994b).

Along with increasing interests in biofilm processes, there have also been numerous efforts toward mathematical modeling of biofilms. In the early stage of biofilm modeling, a major issue was how to describe substrate dynamics including the mass transport of substrates and their microbial conversions which take place simultaneously within biofilms. These models usually assumed predefined biofilm thickness and homogeneous microbial density of the biofilm, not considering biofilm growth (Lee and Park, 2007).

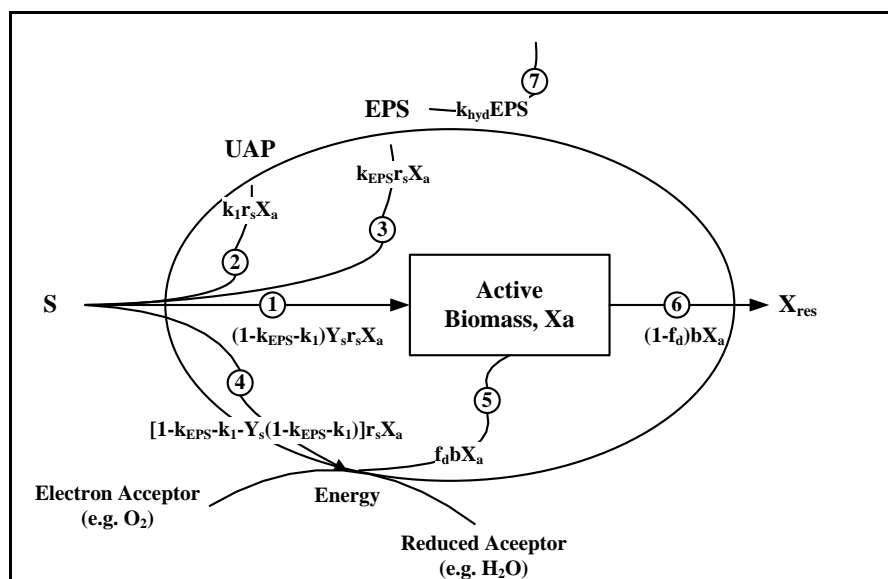
Study of biofilm growth is very important in the mathematical modeling of biofilms because it is closely related to microbial performance, which has an auto-catalytic effect on the substrate dynamics. Biofilm growth is an extremely complicated phenomenon where several fundamental sub-processes are involved. Microorganisms are subject to different environmental conditions depending on time and space of the biofilm, which would eventually lead to a non-homogeneous biofilm growth. Moreover, relocation of the biomass including all particulate components, such as active microorganisms (X_a), inert

residues (X_{res}), and extracellular polymeric substances (EPS), should be considered as the biomass exceeds a certain limit of space availability. Biomass attachment and detachment also remarkably contribute to overall biofilm growth (Lee and Park, 2007).

- **The unified multi-component cellular automaton (UMCCA) Model**

Definition

The unified multi-component cellular automaton (UMCCA) was developed by Laspidou and Rittmann (2002a, 2002b, 2003, 2004a, 2004b) aiming to quantify composite density of biofilm that shows relationships among three solid species – active cells (X_a), extracellular polymeric substances (EPS), and residual inert biomass (X_{res}), three soluble species – original substrate (S), utilization associated products (UAP), and biomass associated products (BAP), and electron acceptor, such as dissolved oxygen (DO) (Figures 3.10 and 3.11). The UMCCA model combines a discrete representation of the solid phase by cellular automaton (CA) with classical continuous methods for soluble components. The suitability of this combination for representing the structure of a heterogeneous biofilm has been demonstrated.



- | | |
|--|---|
| (1) Biomass synthesis | (4) Substrate respiration |
| (2) Substrate-utilization associated product (UAP) formation | (5) Endogenous biomass respiration |
| (3) Extracellular polymeric substance (EPS) formation | (6) Formation of inert biomass |
| | (7) Biomass association product (BAP) formation from EPS hydrolysis |

Figure 3.10 Schematic of electron flows dealing with original substrate and active biomass. Kinetic forms are shown for each flow. All flows are expressed in mg-COD/L-d ([Laspidou and Rittmann, 2002b](#))

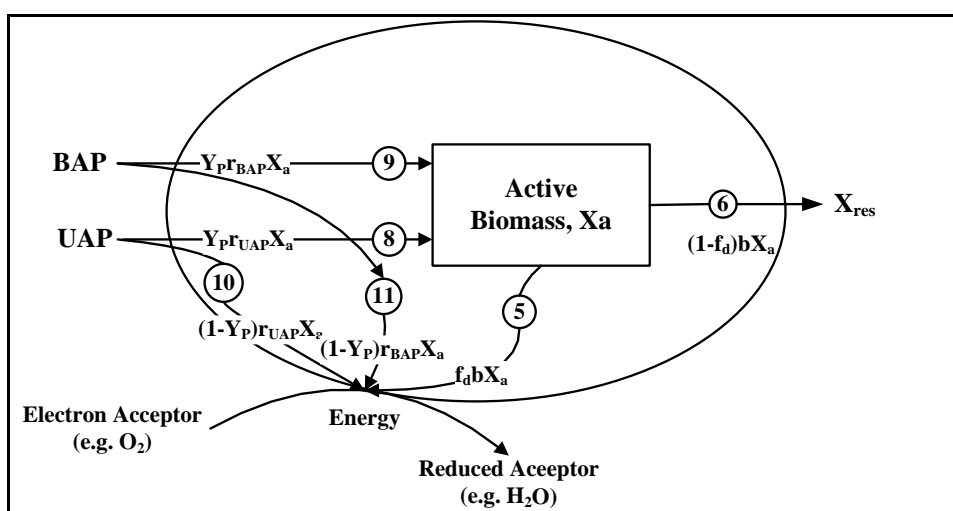
All mass in gCOD, L^3 is liters, and T is days. Subscript are S for organic substrate, P for UAP and BAP, EPS for EPS, and X for active biomass and residual biomass. where:

k_1	is UAP formation rate coefficient (M_P/M_S)	X_{res}	is residual inert biomass concentration (M_X/L^3)
k_{EPS}	is EPS formation rate coefficient (M_P/M_X)	Y_S	is true yield for substrate utilization (M_X/M_S)
k_{hyd}	is first-order hydrolysis rate coefficient (T^{-1})	Y_P	is true yield for soluble microbial product (SMP) utilization (M_X/M_P)
r_S	is specific substrate utilization rate (M_S/M_X-T)	f_d	is biodegradable fraction of active biomass (-)
S	is original substrate concentration (M_S/L^3)	b	is first-order endogenous decay rate coefficient (T^{-1})
X_a	is active biomass concentration (M_X/L^3)		

An advantage of this approach is that it can provide a fast and accurate model solution with readily available computing resources, such as high-capacity personal computers. The UMCCA model begins with a differential discrete cellular automaton (CA) approach similar to that used by [Picioreanu et al. \(1998a, 1998b\)](#). It computes properties that are associated with biofilm heterogeneity, such as biofilm density, porosity, and surface shape.

3.12.1 Computer Environment

The UMCCA model was programmed in Compaq Visual Fortran 6 and was executed on a personal computer that uses a standard, commercially available Pentium with 4 CPU, 2.8 GHz., with 1 GB of RAM.



- (1) Biomass synthesis by utilization of donor substrate UAP
- (2) Biomass synthesis by utilization of donor substrate BAP
- (3) Donor substrate UAP respiration
- (4) Donor substrate BAP respiration
- (5) Endogenous biomass respiration (same as Figure 5.1)
- (6) Formation of inert biomass from decay (same as Figure 5.1)

Figure 3.11 Schematic of electron flows for BAP and UAP utilization. Kinetic forms

are shown for each flow. All flows are expressed in COD/L-d

([Laspidou and Rittmann, 2002b](#))

where:

$$r_{\text{UAP}} \text{ is specific substrate utilization rate } \quad r_{\text{BAP}} \text{ is specific substrate utilization rate}$$

$$(M_{\text{P}}/M_{\text{X-T}}) \quad \quad \quad (M_{\text{P}}/M_{\text{X-T}})$$

3.12.2 System Definition

The physical space of the model is represented by a rectangular uniform grid with square compartments used to fill the 2D space. The model had $N_x = 150$ grid points across the x Cartesian direction (parallel to the substratum) and $N_z = 70$ square elements across the z direction (perpendicular to the substratum). The dimension of each square compartment is $d = 4 \mu\text{m}$, that is small enough to make it possible to have each compartment contain one microbial cell, as well as EPS and residual dead biomass. The entire domain is a biofilm cluster that is approximately twice as wide as it is long ([Laspidou and Rittmann, 2004a](#)).

3.12.3 Initial and Boundary Conditions

The initial conditions for all quantities are shown at the top of Figure 3.12. The grid starts saturating in original donor substrate and oxygen, while all other quantities except for active biomass are set at zero. A random seeding of half of the compartments adjacent to the substratum with biomass starts off the system with biomass. As biomass grows, it consumes substrate and produces UAP and BAP, which diffuse within and out of the biofilm. Biomass also produces EPS and residual dead biomass, which do not diffuse, but move according to the CA algorithm (Figure 3.13). An inexhaustible source of substrate is located at the upper boundary of the grid space, i.e. $S_{i_{\text{max}},j} = 1.0$ at all times, with $i_{\text{max}} = 70$. In other words, even if the substrate is consumed by the biofilm microorganisms, there is an infinite supply of substrate at the top of the grid, which diffuses down to the biofilm. The extent of the biofilm development, for example, is determined by

the balance between how fast the substrate diffuses down to the biofilm and how fast it is consumed by the microorganisms. The absolute concentration (dimensional domain) can vary with each model run. The zero-flux boundary condition is assumed for all soluble species at the substratum of the modeled space, i.e., $\left. \frac{\partial S}{\partial Z} \right|_{Z=0} = 0$ at that boundary. The same

is true for the two sides of the biofilm cluster, i.e., $\left. \frac{\partial S}{\partial X} \right|_{X=0} = 0$ and $\left. \frac{\partial S}{\partial X} \right|_{X=X_{\max}} = 0$. This

means that the substratum and the two sides of the system are completely impermeable to the substrate, while the top surface of the biofilm cluster is completely immersed in it.

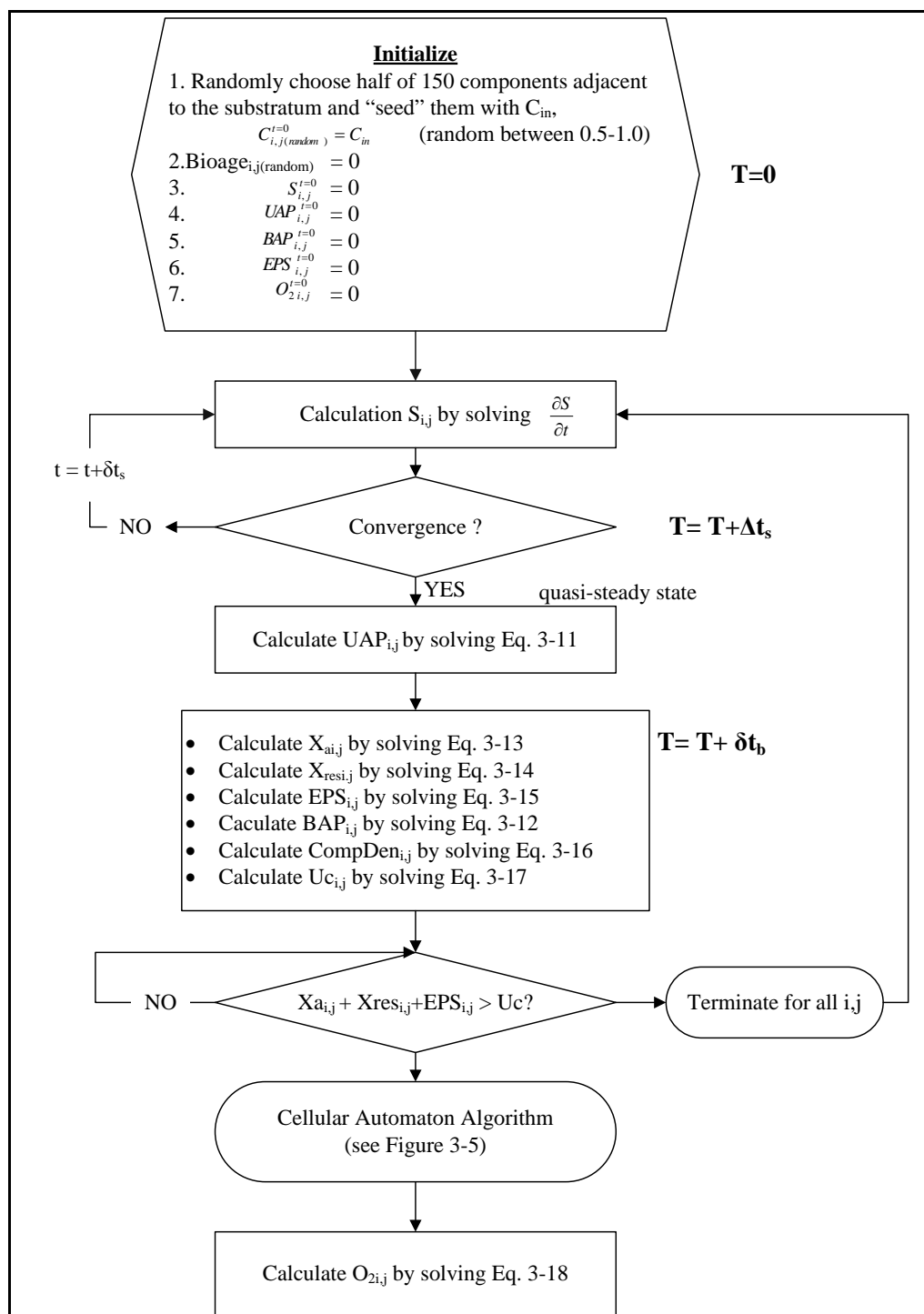


Figure 3.12 Flowchart of the solution strategy for the UMCCA model
(Laspidou and Rittman, 2004a).

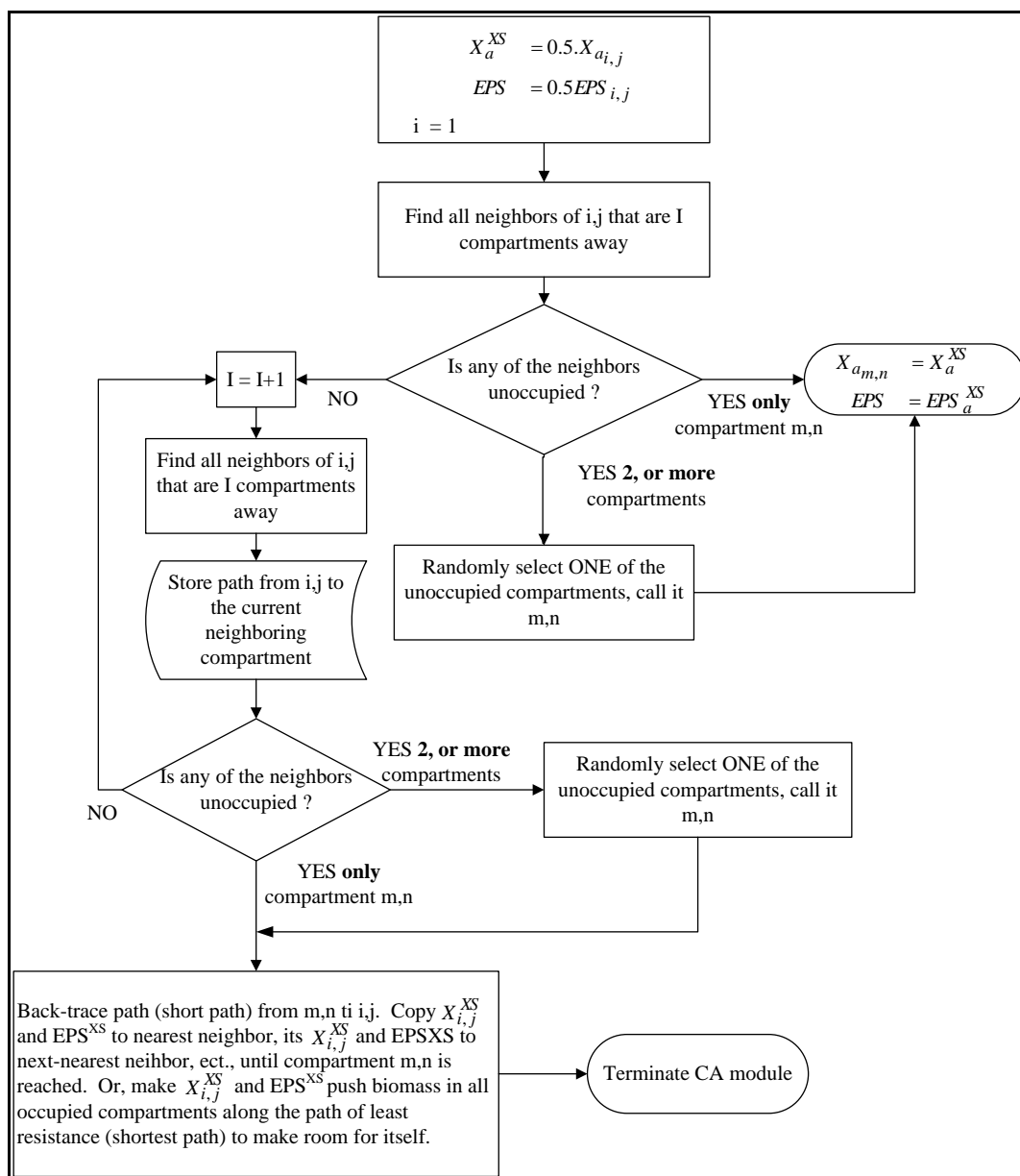


Figure 3.13 Flowchart of CA algorithm of the UMCCA model

(Lapidou and Rittman, 2004a).

3.12.4 Model Variables

The values of the variables the UMCCA model are listed in Tables 3.5 and 3.6 for FDHS and BDHS systems, respectively. The nomenclature lists are illustrated in Table 3.7. The unit system for the parameters used g-COD for all organic species, liters for volume, metres for distances, and days for time. This study chooses the UMCCA model parameter values based on the following criteria:

- The values for S_{max} , Y_s , b , K_s , q_s^A , f_d and $O_{2,max}$ took directly from the experimental study.

- The values for D_s , $x_{a,max}$, eps_{max} , Y_p , k_1 , k_{EPS} , k_{hyd} , K_{UAP} , q_{UAP}^A , K_{BAP} , and q_{BAP}^A directly from the literature. D_s and $x_{a,max}$ were taken from [Picioreanu et al. \(1998\)](#). eps_{max} was taken from [Kreft and Wimpenny \(2001\)](#), who quote a maximum EPS density as 75 g C/L. Assuming that a mole of EPS is similar to that of a cell ($C_5H_7O_2N$, as in [Rittmann and McCarty, 2001](#)), we can obtain eps_{max} , using the ratios of 60 g C per mole of EPS and 1.42 g COD_x per formula weight. The other variables are identical to the ones used in [Laspidou and Rittmann \(2002b\)](#), in which evaluated from the unified theory ([Laspidou and Rittmann, 2002a](#)) by comparing it with experimental data found in [Hsieh et al. \(1994\)](#).

- The value for b_{det} is typical for aerobic heterotrophs in environmental biotechnology ([Rittmann and McCarty, 2001](#)).

- Values for uap_{max} and bap_{max} are needed to have dimensionless concentrations of UAP and BAP. This study chose uap_{max} to be the same as S_{max} , since it

cannot exceed that maximum. Then chose a smaller value for bap_{max} , because BAP is usually smaller than UAP (Laspidou and Rittmann, 2004a).

Table 3.5 Parameter values for illustrating the trends of the UMCCA model
for FDHS system

Parameters	Units	Variable Values of FDHS system			
		Segment 1	Segment 2	Segment 3	Segment 4
D_S	m^2/day	1.38×10^{-4}	1.38×10^{-4}	1.38×10^{-4}	1.38×10^{-4}
S_{max}	mg_s/L	336.1	75.2	63.9	74.0
uap_{max}	$mgCOD_p/L$	336.1	75.2	63.9	74.0
bap_{max}	$mgCOD_p/L$	65.2	59.9	41.6	76.6
$x_{a,max}$	$mgCOD_x/L$	70	70	70	70
eps_{max}	$mgCOD_x/L$	200	200	200	200
$x_{res,max}$	$mgCOD_x/L$	220	220	220	220
$O_{2,max}$	$mg-O_2/L$	3.30	4.10	4.60	2.60
λ	$1/\mu m$	0.005	0.005	0.005	0.005
Y_S	mg_x/mg_s	0.63	0.63	0.63	0.63
Y_P	mg_x/mg_p	0.45	0.45	0.45	0.45
b	$1/day$	0.086	0.051	0.084	0.044
η	$1/h$	0.0315	0.0315	0.0315	0.0315
\hat{q}_S	$mgCOD_s/mgCOD_x-day$	3.40	1.60	1.20	1.60
K_S	$mgCOD_s/L$	92	100	52	80
f_D	-	1.5	1.2	1.4	1.5
b_{det}	$1/day$	0.15	0.15	0.15	0.15
k_I	$mgCOD_p/mgCOD_s$	0.05	0.05	0.05	0.05
k_{EPS}	$mgCOD_p/mgCOD_s$	0.18	0.18	0.18	0.18
k_{hyd}	$1/day$	0.17	0.17	0.17	0.17
\hat{q}_{UAP}	$mgCOD_p/mgCOD_s-day$	1.80	1.80	1.80	1.80

K_{UAP}	mgCOD _s /L	100	100	100	100
\hat{q}_{BAP}	mgCOD _s /mgCOD _s - day	0.1	0.1	0.1	0.1
K_{BAP}	mgCOD _s /L	85	85	85	85
B	-	0.9820	0.9820	0.9820	0.9820

Table 3.6 Parameter values for illustrating the trends of the UMCCA model
for BDHS system

Parameters	Units	Values of BDHS system			
		Segment 1	Segment 2	Segment 3	Segment 4
D_S	m ² /day	1.38×10 ⁻⁴	1.38×10 ⁻⁴	1.38×10 ⁻⁴	1.38×10 ⁻⁴
S_{max}	mg _s /L	336.1	240.1	156.5	136.2
$u_{ap,max}$	mgCOD _p /L	336.1	240.1	156.5	136.2
$b_{ap,max}$	mgCOD _p /L	29.3	22.2	30.6	26.3
$x_{a,max}$	mgCOD _x /L	70	70	70	70
eps_{max}	mgCOD _x /L	200	200	200	200
$x_{res,max}$	mgCOD _x /L	220	220	220	220
$O_{2,max}$	mg-O ₂ /L	0	1.06	2.60	3.20
λ	1/μm	0.005	0.005	0.005	0.005
Y_S	mg _x /mg _s	0.84	0.86	0.85	0.86
Y_P	mg _x /mg _p	0.45	0.45	0.45	0.45
b	1/day	0.199	0.098	0.082	0.093
η	1/h	0.0315	0.0315	0.0315	0.0315
\hat{q}_S	mgCOD _s /mgCOD _x - day	2.20	3.50	1.60	3.60
K_S	mgCOD _s /L	54.8	81.1	50.0	100.2
f_D	-	0.9	1.1	1.2	1.3
b_{det}	1/day	0.15	0.15	0.15	0.15
k_I	mgCOD _p /mgCOD _s	0.05	0.05	0.05	0.05
k_{EPS}	mgCOD _p /mgCOD _s	0.18	0.18	0.18	0.18
k_{hyd}	1/day	0.17	0.17	0.17	0.17

\hat{q}_{UAP}	mgCOD _p /mgCOD _s -day	1.8	1.8	1.8	1.8
K_{UAP}	mgCOD _s /L	100	100	100	100
\hat{q}_{BAP}	mgCOD _s /mgCOD _s -day	0.1	0.1	0.1	0.1
K_{BAP}	mgCOD _s /L	85	85	85	85
B	-	0.9820	0.9820	0.9820	0.9820

Table 3.7 Nomenclature for all components in the UMCCA model ([Laspidou and Rittmann, 2004a](#))

Nomenclature	Description	Nomenclature	Description
--------------	-------------	--------------	-------------

b	First-order endogenous decay rate coefficient (T^{-1})	Λ q_s	Maximum specific substrate utilization rate for original substrate [M_S/M_X-T]
B	Rate of secondary consolidation to total consolidation (-)	Λ q_{UAP}	Maximum specific UAP utilization rate [M_P/M_X-T]
BAP	Dimensionless concentration of BAP [-]	S	Dimensionless concentration of original donor substrate [-]
bap	Concentration of BAP concentration [M_P/L^3]	s	Concentration of original donor substrate [M_S/L^3]
bap _{max}	Maximum BAP concentration [M_P/L^3]	s_{max}	Maximum concentration of electron donor substrate [M_S/L^3]
b _{det}	Biofilm detachment coefficient [T^{-1}]	t_c	Consolidation time [T]
Bioage	“Age” of each biofilm compartment (T)	UAP	Dimensionless concentration of UAP [-]
CompDen	Composite density of biofilm [M_X/L^3]	uap	Concentration of UAP [M_P/L^3]
d	Dimension of each square grid space element [L]	uap _{max}	Maximum concentration of UAP [M_P/L^3]
D	Dimension donor substrate [-]	U_c	Consolidation ratio [-]
d_{max}	Maximum donor substrate concentration [M_D/L^3]	x	Biofilm width [L]
D_S	Diffusion coefficient [L^2/T]	X	Dimensionless biofilm width [-]
EPS	Dimensionless concentration of EPS [-]	X_a	Dimensionless density of active biomass [-]
eps	Concentration of EPS [M_P/L^3]	x_a	Active biomass density [M_X/L^3]
eps _{max}	Maximum EPS packing density [M_P/L^3]	$x_{a,max}$	Maximum active biomass packing density [M_X/L^3]
f_d	Biodegradable fraction of active biomass [-]	X_{res}	Dimensionless density of true residual inert biomass [-]
k_I	UAP formation rate coefficient [M_P/M_S]	x_{res}	Density of residual inert biomass packing density [M_X/L^3]
K_{BAP}	Half maximum rate concentration for BAP utilization [M_P/L_3]	$x_{res,max}$	Maximum residual inert biomass packing density [M_X/L^3]
K_D	Half maximum rate concentration for utilization	Y_p	True yield for SMP (UAP and BAP) utilization [M_X/M_P]
k_{ESP}	EPS formation coefficient [M_D/L^3]	Y_s	True yield for substrate utilization [M_X/M_S]
k_{hyd}	EPS formation coefficient [M_P/M_S]	z	Biofilm depth [L]
K_O	Half maximum rate concentration for O_2 consumption [M_O/L^3]	Z	Dimensionless biofilm depth [-]
K_S	Half maximum rate concentration for utilization of original substrate [M_S/L^3]	∂t_b	Time steps used for biomass growth [T]
K_{UAP}	Half maximum rate concentration for UAP utilization [M_P/L^3]	∂t_s	Time step usage for relaxation of S [T]
O_2	Oxygen concentration [M_{O_2}/L^3]	η	Creep constant [T^{-1}]
$O_{2,max}$	Maximum oxygen concentration [M_{O_2}/L^3]	λ	1 st order decay coefficient for dissolved oxygen in the biofilm [L^{-1}]
q_{BAP}	Maximum specific BAP utilization rate [M_P/M_X-T]	ρ_{BAP}	Utilization rate of BAP [T^{-1}]
q_D	Maximum specific substrate utilization rate for donor substrate [M_D/M_X-T]	ρ_D	Utilization rate of any donor
		ρ_S	Utilization rate of substrate [T^{-1}]
		ρ_{UAP}	Utilization rate of UAP [T^{-1}]

• The value of β , η and $x_{res,max}$ are unique to the UMCAA model, because they are new variables associated with biofilm consolidation. β and η were

developed in [Laspidou and Rittmann \(2002b, 2004a\)](#). The value for $x_{res,max}$ approaches the maximum packing density of biomass solids, because it includes the remains of the active cells, after their lysis when they have released their internal water.

In other words, unlike the active biomass that is mostly water, the residual dead biomass includes mostly the partially dehydrated remnants of the cells and all other mineral deposits that can achieve a maximum packing density; therefore, $x_{res,max}$ is higher than the other solid species.

3.12.5 Variables and Mass Balance Equations

The variables chosen to represent the status of each compartment are the dimensionless concentrations of the soluble organic species, densities of each of the solid species, and concentration of the electron acceptor, i.e., dissolved oxygen (O_2). Soluble organic species are the bacteria's limiting donor substrate (S) and two types of SMP, i.e., substrate utilization-associated products (UAP) and biomass-associated products (BAP). Solid species are the active biomass (X_a), EPS, and the inert biomass (X_{res}) produced by the decay/lysis of active biomass. For all species, dimensionless quantities are used to enhance the uniformity and stability of the algorithm, while time is not dimensionless ([Laspidou and Rittmann, 2004a](#)).

The mass balance equations used in the UMCCA model come directly from [Laspidou and Rittmann \(2004a\)](#), which quantified the unified theory presented in [Laspidou and Rittmann \(2002\)](#) were shown in Table 3.8 and nomenclature list illustrate in Table 3.7.

3.12.6 Solution Algorithm

The solution strategy follows [Laspidou and Rittmann \(2004a\)](#) directly and is illustrated in the flowchart in Figures 3.12 and 3.13. The model solution by a numerical method also follows the scheme presented by [Picioreanu et al. \(1998a\)](#) with a finite-difference discretization scheme that is then solved with the alternating-direction implicit

(ADI) method. Solution begins with initial conditions for all components in all compartments. For all compartments, $S_{i,j}=1.0$, indicating that the maximum substrate is initially available throughout the domain.

Table 3.8 Equation for all components in the UMCCA model

(Laspidou and Rittmann, 2004a)

Components	Equations	No.
Utilization rate of any donor substrate	$\rho_D = \frac{X_{a,\max}}{d_{\max}} q \left(\frac{D}{K_D/d_{\max} + D} \right) \left(\frac{O_2}{K_{O_2}/O_{2,\max} + O_2} \right) X_a$	(3.3)
Mass balance for original donor substrate	$\frac{\partial S}{\partial t} = \underbrace{\frac{D_s}{d^2} \left(\frac{\partial^2 S}{\partial X^2} + \frac{\partial^2 S}{\partial Z^2} \right)}_{\text{2-D diffusion}} - \underbrace{\rho_s}_{\text{utilization}}$	(3.4)
Mass balance for UAP	$\frac{\partial UAP}{\partial t} = \frac{D_s}{d^2} \left(\frac{\partial^2 UAP}{\partial X^2} + \frac{\partial^2 UAP}{\partial Z^2} \right) + \underbrace{\frac{S_{\max}}{uap_{\max}} k_1 \rho_s}_{\text{UAP formation}} - \underbrace{\rho_{UAP}}_{\text{UAP utilization}}$	(3.5)
Mass balance for BAP	$\frac{\partial BAP}{\partial t} = \frac{D_s}{d^2} \left(\frac{\partial^2 BAP}{\partial X^2} + \frac{\partial^2 BAP}{\partial Z^2} \right) + \underbrace{k_{hyd} EPS}_{\text{EPS formation}} - \underbrace{\rho_{BAP}}_{\text{BAP utilization}}$	(3.6)
Mass balance for active biomass (X_a)	$\frac{\partial X_a}{\partial t} = \underbrace{Y_s (1 - k_1 - k_{EPS}) \frac{S_{\max}}{x_{a,\max}} \rho_s}_{\text{synthesis from S}} + \underbrace{Y_p \frac{uap_{\max}}{x_{a,\max}} \rho_{UAP}}_{\text{synthesis from UAP}} + \underbrace{Y_p \frac{bap_{\max}}{x_{a,\max}} \rho_{BAP}}_{\text{synthesis from BAP}} - \underbrace{bX_a}_{\text{endogenous decay}} - \underbrace{b_{det} EPS}_{\text{detachment}}$	(3.7)
Mass balance for residual inert biomass (X_{res})	$\frac{\partial X_{res}}{\partial t} = \underbrace{b(1 - f_D) X_a}_{\text{formation of inert biomass}} - \underbrace{b_{det} X_{res}}_{\text{detachment}}$	(3.8)
Mass balance for EPS	$\frac{\partial EPS}{\partial t} = \underbrace{k_{EPS} \frac{S_{\max}}{eps_{\max}} \rho_s}_{\text{EPS formation}} - \underbrace{k_{hyd} EPS}_{\text{EPS hydrolysis}} - \underbrace{b_{det} EPS}_{\text{EPS detachment}}$	(3.9)
Definition of composite density	$CompDen^i = X_a^i x_{\max} + EPS^i eps_{\max} + X_{res}^i x_{res,\max}$	(3.10)
Definition of consolidation ratio	$U_c = 1 - \underbrace{0.9820}_{B [-]} \exp(-\underbrace{0.0315t}_{\eta [h^{-1}]})$	(3.11)
Profile for oxygen (O_2)	$O_2 = O_{2,\max} e^{-zZ}$	(3.12)

All other quantities, except for active biomass and oxygen are set to zero then randomly seeded with active biomass. Half of the compartments adjacent to the substratum (i.e., 35 out of 70) are randomly selected and inoculated with an amount of active biomass

that is randomly selected between 0.5 and 1.0 for each compartment. This inoculation simulates an initial random and patchy attachment of biomass across the substratum. All mass balance equations (Equations 3.3-3.12) are solved by using a strategy similar to described in [Lapidou and Rittmann \(2004a\)](#) and [Picioreanu et al. \(1998a\)](#) i.e., keeping the biomass density unchanged, while iterating until the substrate concentration field converges to a steady-state condition, and using a time step δt_s to solve the substrate field of about 1s and a time step for changes in biomass, δt_b of 1000s (Figures 3.12 and 3.13).

3.13 Dynamics of Biofilm Compositions and Density

In this study, a multi-component model—the Unified Multiple Component Cellular Automaton (UMCCA) model was used—that predicts quantitatively the biofilm’s heterogeneity for many components of a biofilm system: three solid species (active biomass, inert or dead biomass produced by dead and decay, and EPS) and three soluble components (soluble substrate and two type of soluble microbial products (SMP)). This model builds on the unified theory, which reconciles the apparently disparate findings about active and inert biomass, EPS, and SMP. The model presented here is the biofilm adaptation of the multi-component mathematical model that quantifies the unified theory ([Lapidou and Rittmann, 2004a](#)). The equations for all components of UMCCA model were summarized in Table 3.8. The flowchart for the solution of model equations carried out in Figure 3.12 and CA algorithm in Figure 3.13. Data prediction was real for as well as simulated conditions, including of low oxygen supply, higher detachment, and lower and higher substrate supply caused varying hydraulic loading rate and organic loading rate.

CHAPTER IV

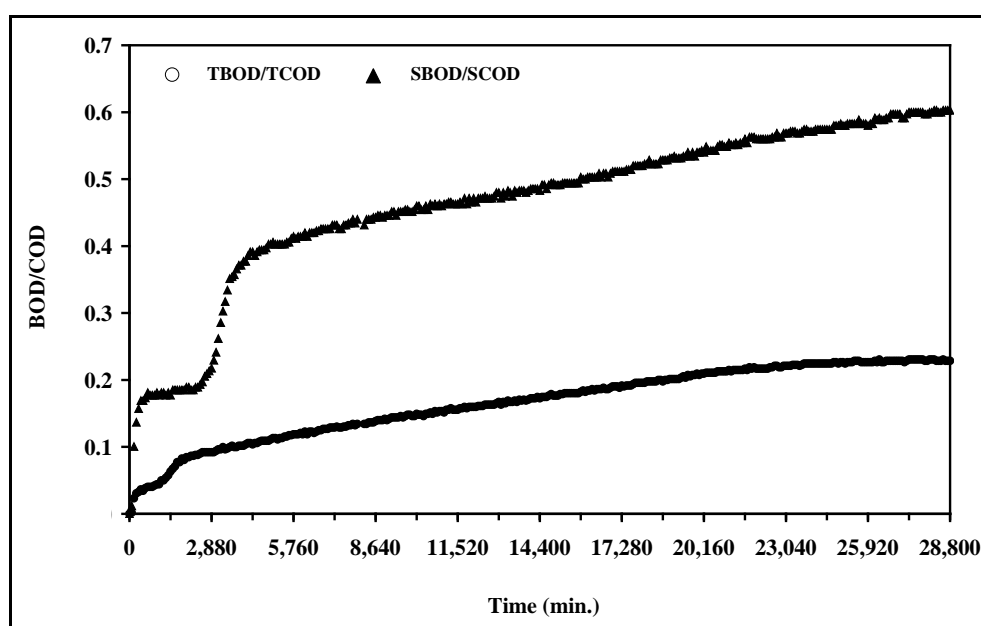
EXPERIMENTAL RESULTS AND DISCUSSION

4.1 UASB Effluent Characterizations

The initial wastewater characterization consisted of quantifying the solid, organic and nitrogen contents. The results are presented in Table 4.1. In order to find out the reason of poor removal efficiency of COD and nitrogen, the characteristics of influent and effluent were analyzed. The ratio of BOD/COD is often used as an index to evaluate biodegradability of wastewater. $BOD/COD > 0.45$ indicates that biodegradability is very good; $BOD/COD=0.45$, biodegradability is good; $BOD/COD = 0.2-0.3$, biodegradability is poor; $BOD/COD < 0.2$, biological treatment is unsuitable (Deng et al., 2006). Biodegradability of the wastewater could be continuously characterized by BOD/COD ratios during the period of 20 days as shown in Figure 4.1. The TBOD/TCOD ratios were found to be 0.13, 0.17, 0.22 and 0.23 on 5th, 10th, 15th and 20th days, respectively. The corresponding values were 0.41, 0.47, 0.53 and 0.60, respectively for soluble fractions. The results in Figure 4.1 indicated that the UASB effluent contained high amount of biologically resistant organics. These suggested that the residual COD of anaerobic effluent may be comprised of residual non-degraded substrate, intermediate volatile fatty acids (VFA) and soluble microbial products (SMP). In well operated systems only a small fraction of the effluent COD is usually due to VFAs, while SMP account for 85-100% of residual COD. These SMP may not be readily biodegradable, or may even be refractory, and comprise a wide variety of organic compounds distributed across a broad spectrum of molecular weight (MW) (Jarusutthirak, C. and Amy, G., 2007; Yun, M. E., 2007).

Table 4.1 The UASB effluent characteristics form tapioca starch industry

Parameters	Units	Concentrations
1. pH	-	6.5-7.8
2. TSS	mg/L	350-1,050
3. TCOD	mg/L	594-1,494
4. SCOD	mg/L	294-574
5. TBOD	mg/L	227-385
6. SBOD	mg/L	180-252
7. TKN	mg-N/L	85-267
8. NH_4^+ -N	mg-N/L	77-259
9. NO_3^- -N	mg-N/L	<0.1
10. NO_2^- -N	mg-N/L	<0.1
11. Total P	mg/L	5-10
12. TBOD/TCOD	-	0.29
13. SBOD/SCOD	-	0.50
14. TBOD/TKN	-	1.74

**Figure 4.1** Time profiles of BOD/COD ratio of UASB effluents

The effluents of UASB reactor still contained relatively high nitrogen nutrient contents based on the COD:N ratio which seems to be too high for heterotroph microorganisms utilization. Moreover, the UASB effluent characteristics suggest poor efficiency of denitrification process ($BOD/TKN < 2.5$ or $BOD/NH_3 < 4$ and $COD/TKN < 5$) (Grady et al., 1999)

4.2 Sludge Enrichment and Acclimatization

Prior to the DHS experimental study, it is necessary to acclimatize the organisms to the prevailing contaminants of the UASB effluent that having high COD and ammonia concentrations. After acclimatization of the culture to be used, a rich mixture of resistant UASB effluent degrading organisms could be obtained. The bacterial and fungal sludge enrichments were completely accomplishment when MLSS concentrations reached to 3,000 mg/L. The overall COD removal and biomass production during acclimatization processes as shown below:

4.2.1 COD Removal

In order to estimate organic removal rates, the COD profiles of acclimatized fungal and bacterial sludge batch were examined. The COD profiles were defined as the quantity of COD varies with times. The acclimatization was done step-wise until a COD removal approximately 70% could be achieved. The changes in the biomass concentration along with the F/M ratio and COD removal efficiencies were noticed. Acclimatization of fungal and bacterial cultures took about 60 days. The variation of COD removal efficiency and the F/M ratio of fungal and bacterial sludge are shown in Figure 4.2 and 4.3, respectively. In the final of this experiment, it was found to be the capability of fungal culture in COD removal efficiency was higher than bacterial sludge. These performances were reached to 75% and 70% of SCOD removed by fungal and bacterial sludge, respectively.

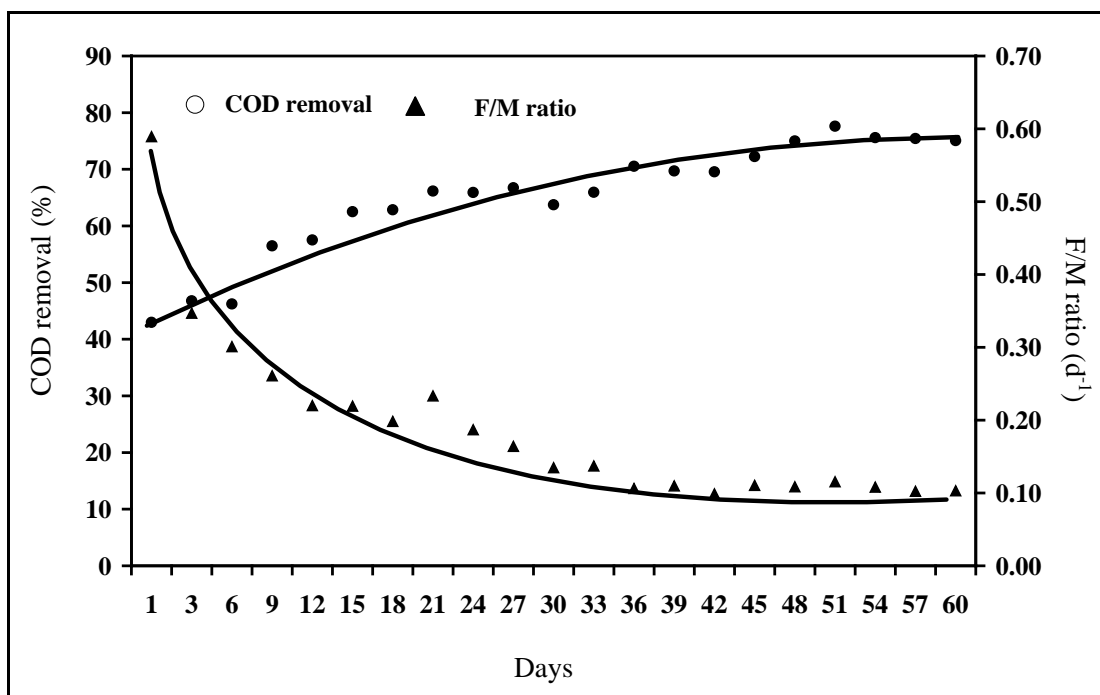


Figure 4.2 COD removal and F/M ratio profiles in fungal sludge

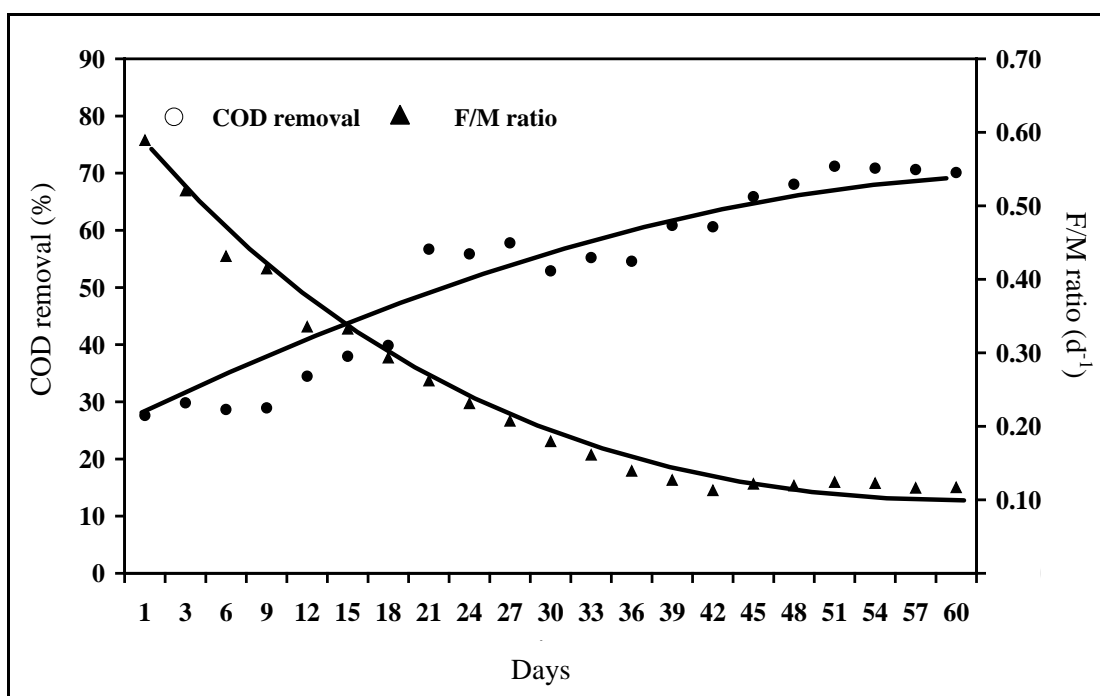


Figure 4.3 COD removal and F/M ratio profiles in bacterial sludge

This indicated that fungi culture could probably be more effective to treating organic contaminants in UASB effluent than the bacterial culture. However, as the results obtained are not sufficient to conclude that the fungi system has a better performance than the bacterial system, further investigation is necessary. The F/M ratios of fungal and bacterial systems were decreased from 0.59 to 0.10 kg COD/kg SS and 0.59 to 0.12 kg COD/kg SS-d, respectively. That seems to be the F/M ratios of fungal system were decreased faster than bacterial system. This suggested that the growth of the fungal culture was more prominence than the bacterial culture. Moreover, higher organic loading allows downsizing the treatment reactors, which improves the overall economy of the system. Thus, the fungi system could be the reason for the better efficiency of COD removal.

4.2.2 Biomass

The growth of biomass is important parameters for the biological wastewater treatment. Sufficient MLSS should be obtained in order to get a good COD removal efficiency. The change in the biomass for bacterial and fungal cultures was increased is illustrated in the Figure 4.4. The initial MLSS of the fungal and bacterial systems were about 1,500 mg/L. The final MLSS of fungal and bacterial mixed liquor after acclimatization were 9,012 and 7,954 mg/L, respectively. These values were 6 times of the initial MLSS concentration in fungal system which shown about 83% of biomass increasing. And in the bacterial system, the final MLSS was 5.3 times of initial biomass, which shown about of 81% in the biomass increasing.

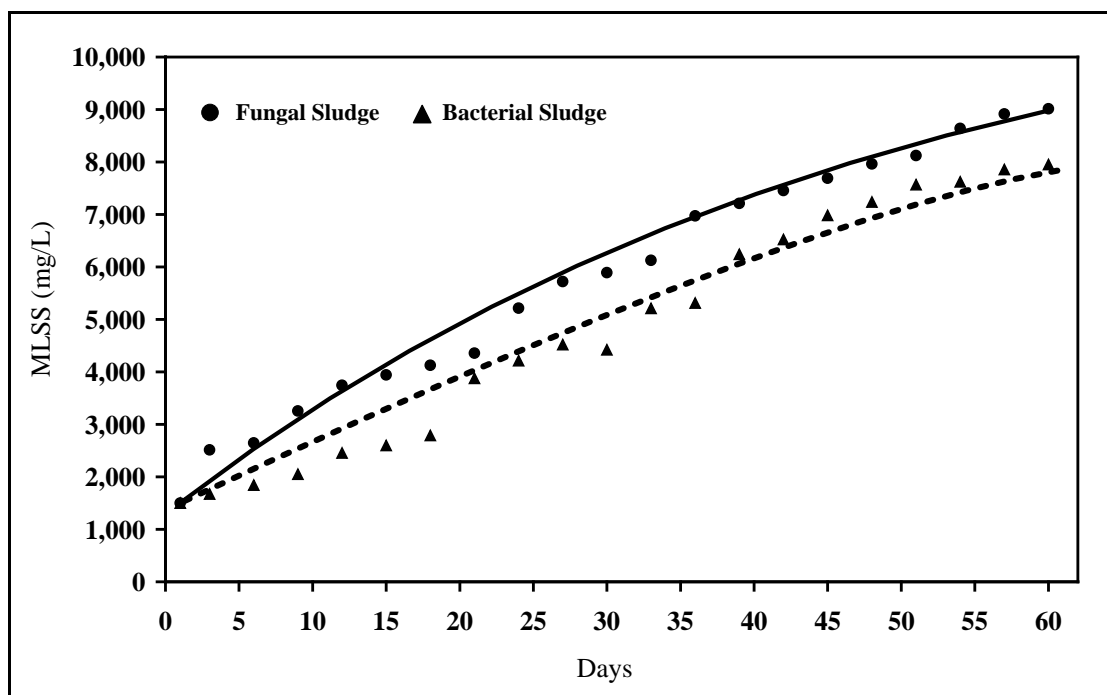


Figure 4.4 MLSS concentrations of two cultures during acclimatization processes

4.3 Sponge Media Characteristics

The physical characteristics of polyurethane foam media (sponge) are shown in Table 4.2. The sponge media has a high void space of about 90%, surface area $600 \text{ m}^2/\text{m}^3$ and pore size 0.7-1.0 mm (Figure 4.5). These could be better than physical properties of trickling filter media that recommended by [Metcalf and Eddy \(1991\)](#). It appeared to be an excellent colonization matrix for a biofilter. Pore size was one of most important parameter for microbiological and engineering requirements in high efficiency beds ([Nakamura et al., 1999](#); [Yang et al., 2004](#); [Quek et al., 2006](#)). The ideal filter medium is a material that has a high surface area per unit of volume, is low in cost, a high durability, and does not clog easily ([Metcalf and Eddy, 2003](#)). These could be the reason for used polyurethane sponge as filter media in DHS system.

Table 4.2 Physical characteristics of sponge media

Characteristics	Dimensions
1. Specific surface area (m^2/m^3)	600
2. Void ratio	0.9
3. Pore size (mm)	0.7-1.0
4. Density (kg/m^3)	2.5

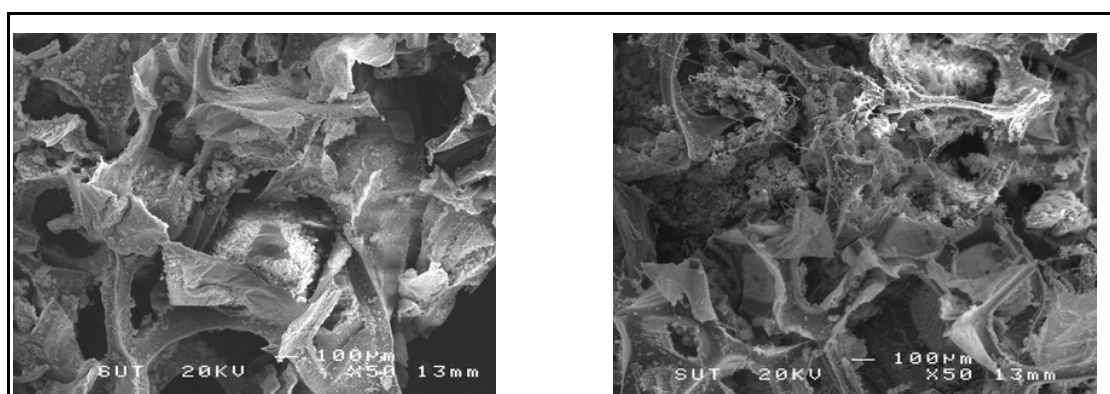
4.4 Immobilized Biomass Preparation

The steps of fill-and-draw process were also used for the enrichment of sponges, i.e. replacing the enriched sludge and wastewater mixture daily during the 30 days period. Bacterial and fungal sludge were used to degrade the UASB in the attached growth conditions like the moving bed biofilm reactors (MBBR). In order to two important criteria in the selection of microorganisms to be immobilized onto sponge media for biological wastewater treatment are ability to (i) immobilize on sponge media and (ii) carbonaceous material and nitrogen removal.

**Figure 4.5** The SEM photo of the sponge media

4.4.1 Immobilization of Microorganisms onto Sponge Media

The ability of fungal and bacterial biomass that was immobilized inside the sponge media with using UASB effluent as the substrate is shown in Figure 4.6. It is likely that the higher number of immobilized fungi than bacteria and was equally efficient on sponge surface. The efficient immobilization of fungal could also be due to the dispersed filaments (filamentous growth). Fungal culture also has potential application as immobilized cell systems which, because of their shape, may not require cross-linking or entrapment (Tung et al., 2004).



(a) Bacterial sludge

(b) Fungal sludge

Figure 4.6 SEM photos of microbes immobilized on sponge media

4.4.2 Retained Biomass and Treatment Efficiencies

As shown in Figure 4.7, the MLSS concentration inside of the sponge media in bacterial and fungal systems were increased to 13,400 mg/L and 25,600 mg/L of sponge volume, respectively, after starting the experiment for 30 days. The bacterial sludge has capability to COD and TKN removal efficiencies that were about 72% and 68%, respectively. Nitrogen was not removed in fungal system but high ability of organic degradation as about 92% of COD removal efficiency. After this stage, the two types of

harvested sponges were used as the filter media in fungal downflow hanging sponge (FDHS) and bacterial downflow hanging sponge (BDHS) systems, respectively.

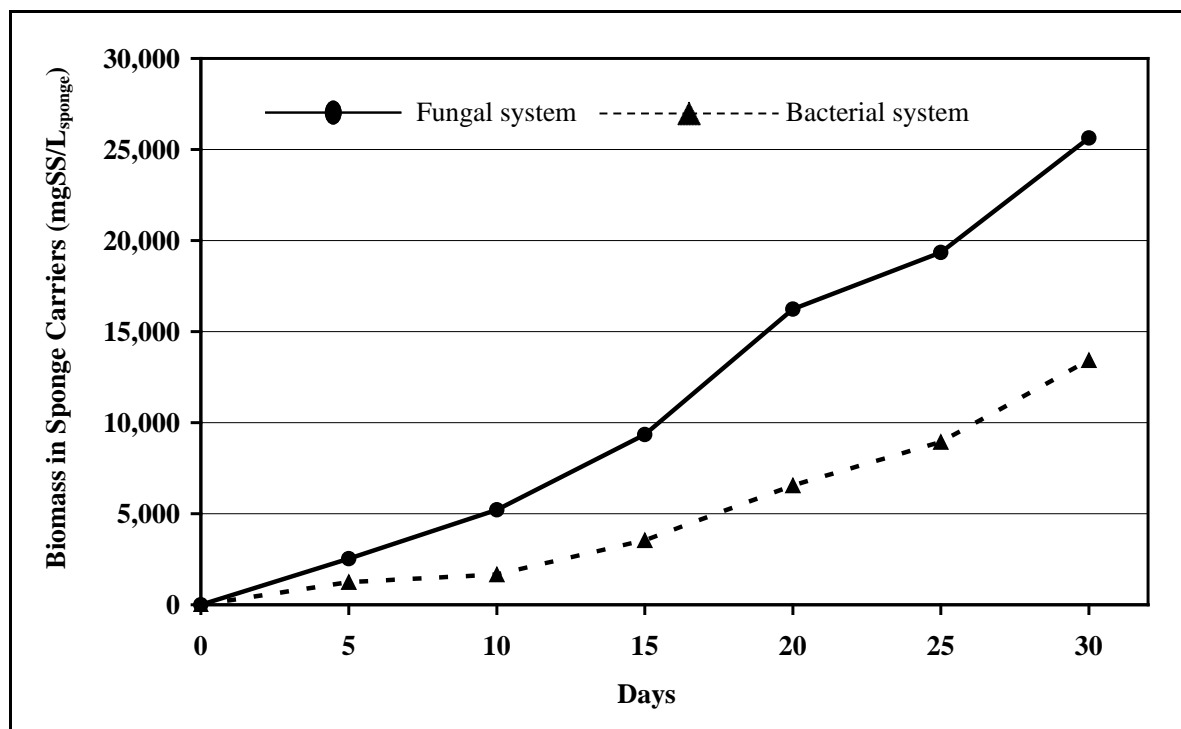


Figure 4.7 The profiles of retained biomass in sponge media

4.5 Tracer Study

At the onset of this research, a tracer study was carried out to evaluate the flow pattern in the experimental DHS system units. The NaCl solution was mixed with tap water (5 gNaCl/L) and fed into the DHS system. The effluents were observed of chloride concentrations. Tracer analysis for DHS system was performed different theoretical Hydraulic Retention Times (HRT) under clean sponge media (without biomass). The five inflow rates were used as 45, 75, 200, 300 and 550 L/d for fed NaCl solution to DHS systems. With Equations 4.1-4.5, data of tracer study were used to find out the dispersion number ($D/\mu\text{L}$) and actual HRT (Levenspiel, 1972) as results are shown in Table 4.3. And raw data of tracer study are given in Tables A.1-A.5 in Appendix A. Results shown the

percentage difference between the theoretical HRT (T_t : based on the sponge volume and flow rate) and the actual HRT (T_a : obtained from the tracer analysis) increased with the increase in flowrate. The fractions of dead volume in DHS system were determined with Equation 4.4 (Tandukar et al., 2006). Results shown the fractions of dead volume were decreased when increase inflow rate in DHS systems.

(i) Actual HRT (T_a)

$$T_a = \frac{\sum_{t=0}^t t_i C_i dt_i}{\sum_{t=0}^t C_i dt_i} \quad (4.1)$$

(ii) Variance (σ^2)

$$\sigma^2 = \frac{\sum_{t=0}^t t_i^2 C_i dt_i}{\sum_{t=0}^t C_i dt_i} - T_a^2 \quad (4.2)$$

(iii) Dispersion Number ($\frac{D}{uL} = d$)

$$\sigma_\theta^2 = \frac{\sigma^2}{T_a^2} = 2d + 8d^2 \quad (4.3)$$

(iv) Fraction of Dead Volume (f)

$$f = \frac{T_t - T_a}{T_t} \quad (4.4)$$

where: C is tracer concentration (mg/L); t is time (min) and T_t is theoretical HRT

Table 4.3 Actual HRT, dispersion numbers and fractions of dead volume of DHS system by tracer study

Flow rate (L/d)	Theoretical HRT (h)	Actual HRT (h)	Dispersion Number	Fractions of Dead Volume
45	11.52	3.94	0.077	0.66
75	6.91	3.94	0.077	0.43
200	2.59	1.25	0.105	0.52
300	1.73	1.27	0.077	0.27
550	0.94	0.89	0.105	0.05

Figure 4.8 shows the experimental outcome of tracer analysis. It seems to be the effluent of chloride concentrations increased with the time to reach peak values. After reaching the peak, chloride concentration decreased with time to low concentration approaching to steady values. The values of dispersion numbers indicated that the intermediate amount of dispersion according to the Levenspeil's classification as shown in Figure 4.9. The flow condition was characterized according to the following ranges; $D/\mu L = 0.002$, is small amount of dispersion; $D/\mu L = 0.0025$, is intermediate amount of dispersion; $D/\mu L = 0.2$, is large amount of dispersion; and $D/\mu L = \infty$, is mixed flow condition (large dispersion). The dispersion number, determine by Equation 4.3 were in range of 0.077-0.105. This value showed intermediate amount of flow dispersion in the DHS system unit. In view of the dispersion number ($D/\mu L$) the all flow characteristics could be classified as approaching plug flow pattern.

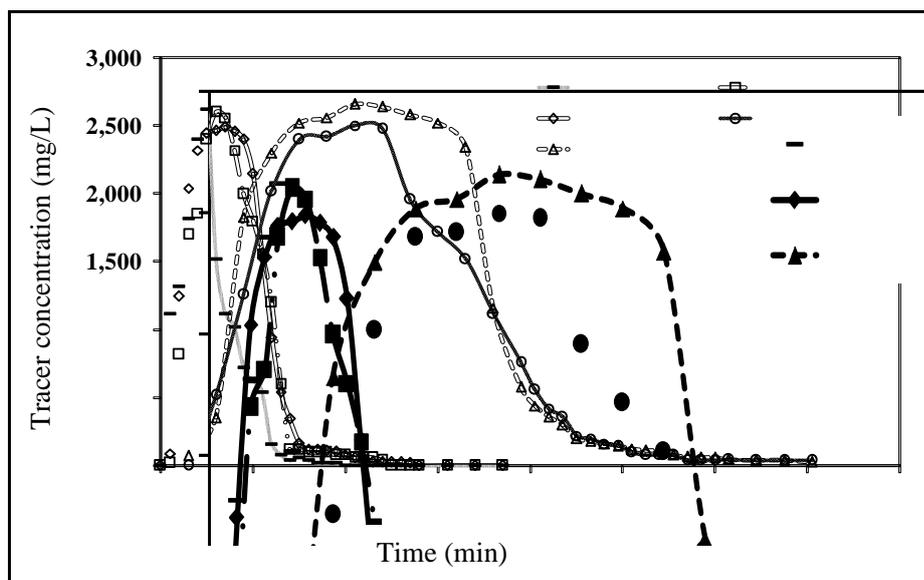


Figure 4.8 The variation curve of tracer concentrations in relation to elapsed times

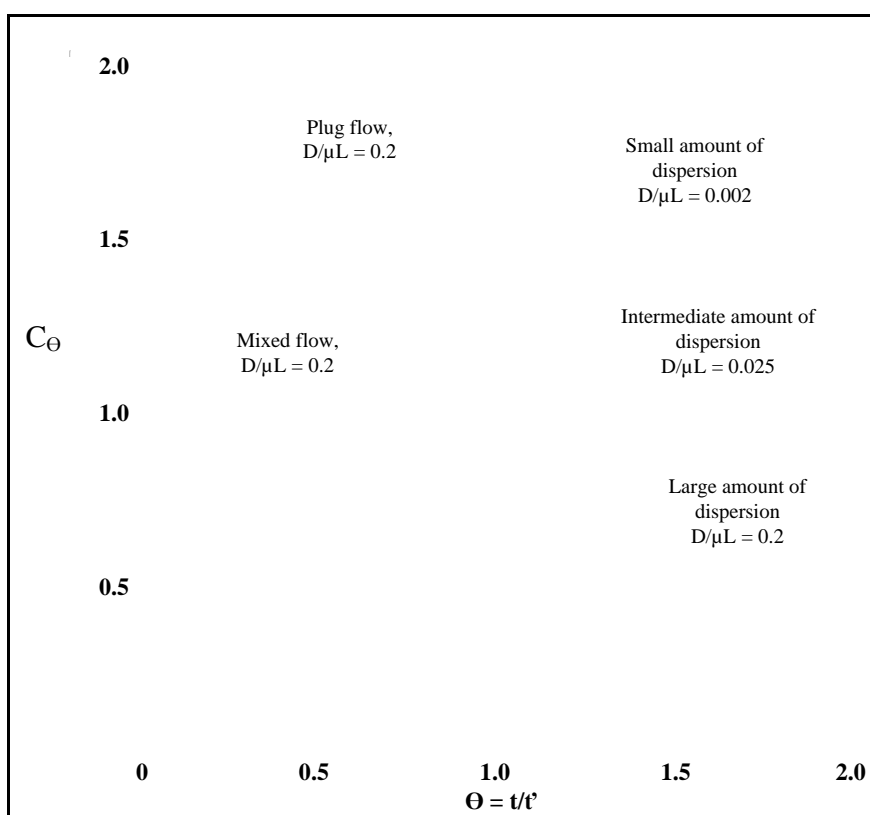


Figure 4.9 C-curve of simulation dispersion in closed vessels (Levenspeil, 1972)

4.6 DHS Treatment Efficiency

In order to examine the suitable treatment methods for UASB effluent from tapioca starch industry. The main role of the post treatment is to complete the removal of organic, as well as constituents little affected by the anaerobic treatment, such as nitrogen nutrient. In this study was focus on removal efficiencies and several operating parameters. The evaluated parameters were included of DO, SS, COD, BOD and nitrogen species as details below:

4.6.1 Dissolved Oxygen (DO) Profiles

DO profiles of the two DHS systems during 3 runs are shown in Table 4.4. DO concentration was very low in UASB effluent. But as the wastewater passed through DHS, the DO concentration increased steadily attaining the values of about 5.0 mg/L in the system. The fate of wastewater in the DHS is such that, it first flows into a sponge unit, comes out of it, comes in contact with air and then again penetrates the next sponge unit. As the wastewater comes in contact with air, the air gets diffused into it, thus increasing the DO concentrations gradually in each segment. This repeated phenomena maintains DO in the wastewater almost to the level that whereby satisfy the demand of aerobes residing in DHS system. By virtue of this, there is no need for aeration in the system. In RUN I, DO concentrations were very low in the first and second segments of BDHS system. This suggests that oxygen utilization of bacteria was higher than fungi. There is more evidence from typical stoichiometry of aerobic respiration of bacteria and fungi using glucose as the substrate (Equations 4.5 and 4.6). That shows bacteria consumed oxygen higher than fungi. Moreover, DHS clearly demonstrated the advantage of needlessness of external aeration for RUN II and RUN III operating conditions because of the DO concentration in recirculation flows.

Aerobic respiration of fungi (Berry, 1998):



Aerobic respiration of bacteria (Supawech, S. and Vorawichit, M., 1990):



Table 4.4 Average dissolved oxygen concentration in segment effluent of FDHS and BDHS system

RUN	Segment effluents							
	Segment 1		Segment 2		Segment 3		Segment 4	
	FDHS	BDHS	FDHS	BDHS	FDHS	BDHS	FDHS	BDHS
RUN I	3.27	0.18	4.12	0.63	4.56	2.64	2.55	3.23
RUN II	3.44	3.72	5.08	3.60	4.92	5.16	3.76	3.56
RUN III	3.08	2.7	4.26	3.24	5.14	3.48	3.8	3.32

Remark: Number of samples and standard deviation are shown in Appendix H

4.6.2 pH

The influent wastewater was adjusted pH to 4.0 ± 0.2 and 7.0 ± 0.2 for FDHS and BDHS systems, respectively during three experimental runs. The average pH values of two DHS system effluent are shown in Table 4.5 and raw data in Appendix H. Results of pH effluents were in range of 4.0-5.0 and 7.0-8.0 for FDHS and BDHS systems, respectively. The pH values along two DHS height seem to be regularity. This was encouraging the growth of fungi and bacteria in FDHS and BDHS systems, respectively.

Table 4.5 Average process performance of BDHS and FDHS systems during three runs

Parameters	RUN I				RUN II				RUN III			
	Effluent (mg/L)		Efficiency (%)		Effluent (mg/L)		Efficiency (%)		Effluent (mg/L)		Efficiency (%)	
	FDHS	BDHS	FDHS	BDHS	FDHS	BDHS	FDHS	BDHS	FDHS	BDHS	FDHS	BDHS
pH	4.7	7.8	-	-	4.8	7.8	-	-	4.8	7.9	-	-
TSS (mg/L)	65	195	91	72	70	77	90	89	82	164	88	76
VSS (mg/L)	61	183	-	-	66	69	-	-	79	139	-	-
TCOD (mg/L)	306	634	76	50	229	236	85	85	260	486	77	56
SCOD (mg/L)	222	201	50	54	102	111	72	76	119	162	74	64
TBOD (mg/L)	56	60	83	82	21	27	95	94	25	117	95	77
SBOD (mg/L)	34	35	85	84	16	21	92	90	18	25	93	90
Total N (mg-N/L)	178	62	-	68	197	78	-	59	191	78	-	56
NH ₄ -N (mg-N/L)	170	35	-	79	180	62	-	63	184	62	-	63
NO ₂ -N (mg-N/L)	<0.1	7.8	-	-	<0.1	0.4	-	-	<0.1	0.2	-	-
NO ₃ -N (mg-N/L)	<0.1	8.4	-	-	<0.1	7.3	-	-	<0.1	7.4	-	-

Remark: “—” the data cannot calculate the removal efficiency; “<0.1” the concentration is lower than detection limit of the analytical method

4.6.3 TSS Removal

The average influent and effluent TSS concentrations during the three experimental runs are presented in Table 4.1 and 4.5, respectively. Raw data and standard deviation are shown in Appendix H. High TSS removal efficiencies of FDHS systems were about 91%, 90% and 88% during RUN I, RUN II and RUN III, respectively. In BDHS system, the TSS removal efficiency was lower than FDHS system with amount of 72%, 89% and 76% in RUN I, RUN II and RUN III, respectively. In DHS system, TSS concentrations were mainly removed by retained on sponge media and degraded (Tawfik et al., 2006a). However, TSS concentrations in the effluent of two DHS systems were higher during RUN II and RUN III. The biomass sloughing is one cause of TSS concentration in biofilter effluent. It is known that the shear force of water flow amplifies as hydraulic loading increases. This may lead the disruption of the retained sludge inside the sponge DHS, finally raising the value of SS in the effluent (Tandukar et al., 2006a). Also high value organic loading rate (OLR) increased the retained biomass in sponge that can be washed out of the system.

4.6.4 Organic Matter Removal

In order to estimate organic removal rate, the SCOD profiles of DHS influent and effluent were examined. The results of this experiment during three runs (522 days) are shown in Figure 4.11 and 4.12 for FDHS and BDHS systems, respectively. The fluctuation SCOD influents were in range of 179-647 mg/L. The SCOD effluent concentrations were fluctuate with the influent concentrations in three runs of BDHS system. However, in FDHS system, the SCOD effluents quite are steady in RUN II and RUN III. Time profiles of total and soluble BOD (SBOD) of raw UASB effluent and DHS effluents as well as TBOD/TCOD ratios of the two systems are presented in Figure 4.13 for each run.

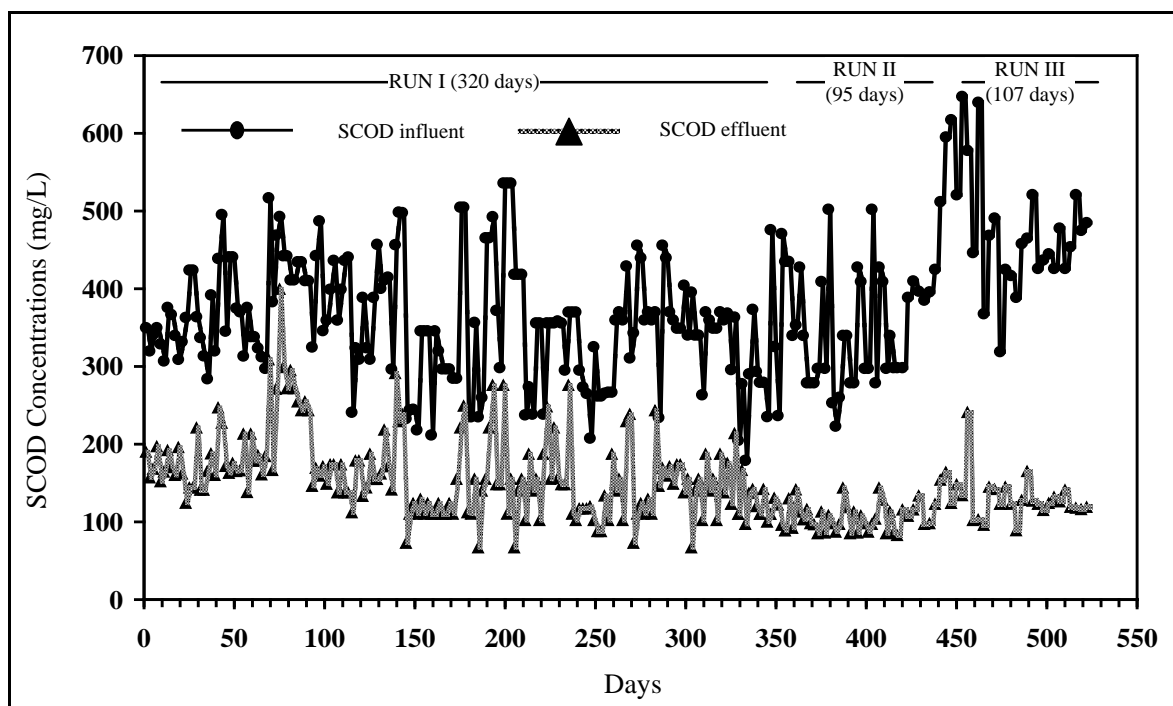


Figure 4.11 SCOD removal profiles of FDHS system during three runs

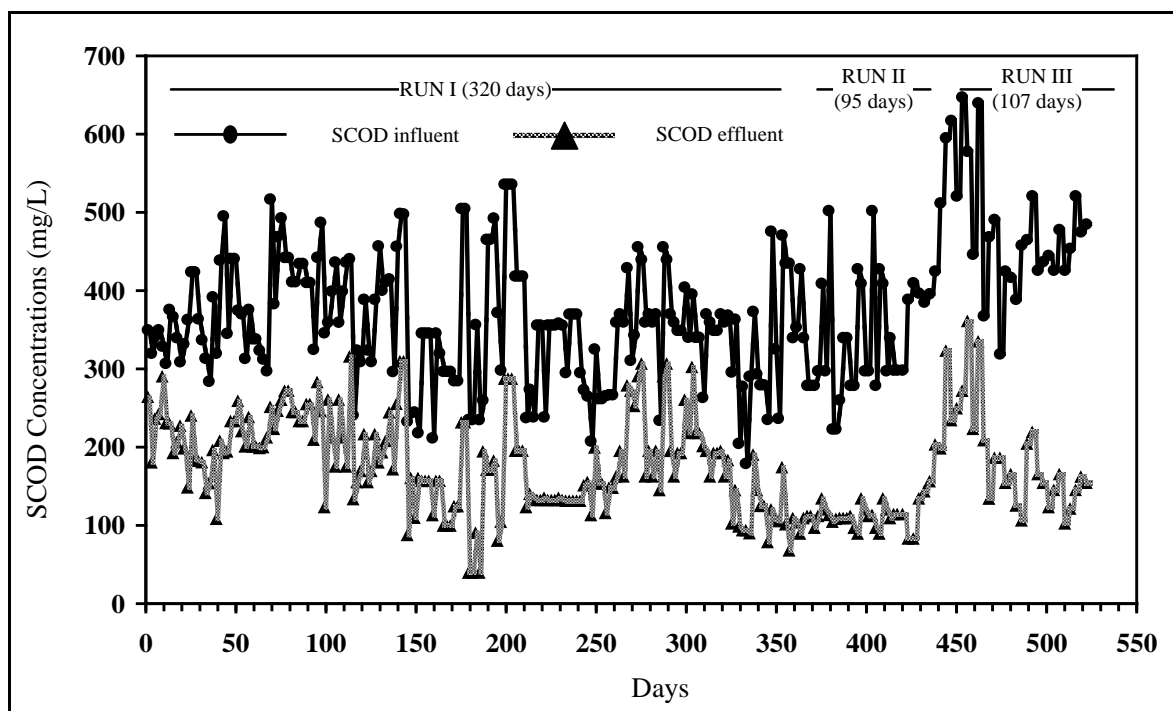


Figure 4.12 SCOD removal profiles of BDHS system during three runs

The overall process performance of the two DHS systems during the whole experimental period are shown in Table 4.5. During three runs, the low BOD/COD ratios in BDHS and FDHS effluents, as shown in Figure 4.13, indicate the presence of refractory substances which were either slowly biodegradable organic materials or non-biodegradable materials.

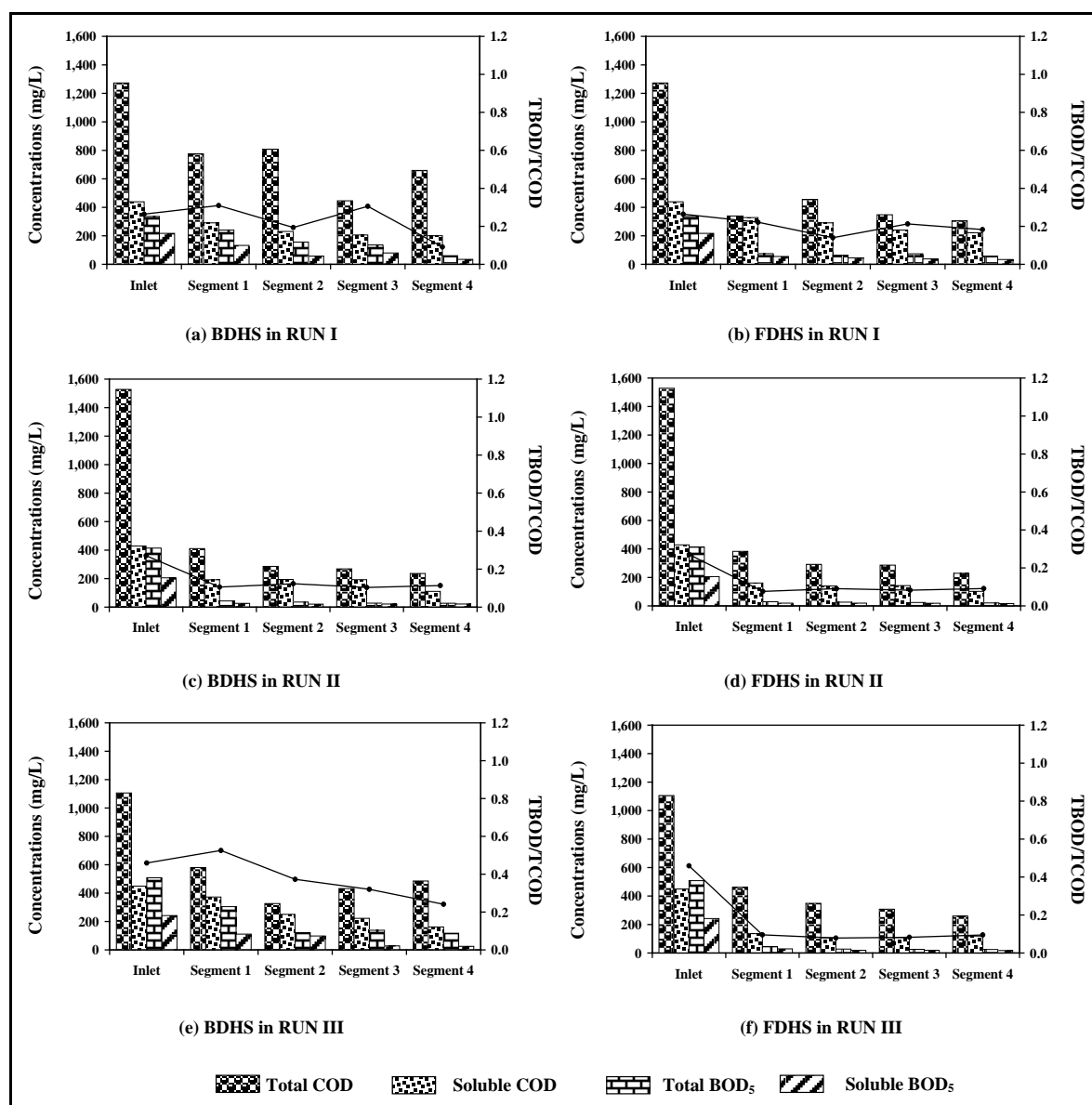


Figure 4.13 Organic removal profiles in two DHS systems during three runs

In RUN I, two random types of DHS systems operated in parallel for 320 days. The organic loading rate (OLR) in inflows of DHS systems were about $1.0 \text{ kgTBOD/m}^3\text{-d}$

(Table 4.6). The results in Table 4.5 showed that the DHS systems achieved high organic removal. The overall TBOD removal efficiency reached about 82-83% in both BDHS and FDHS systems.

The results presented in Figure 4.13 show that during the RUN I, most of TBOD were removed in the first segment of FDHS (about 70% of TBOD₅ removed). But the BOD was removed gradually in all 4 segments of BDHS system. This can be explained by the fact that the most coarse and soluble organic matter were adsorbed and degraded in the first segment of FDHS system. And this also indicated the potential advantage of fungi over bacteria in terms of rate of organics removed. High organic loading may enable downsizing of reactors and better rate of acclimation allows for early start-up and rapid recovery from shock, both of that being desirable from the practical stand point. Several researches recommended that fungi have a wide range of enzymes, and are capable of metabolizing complex mixtures of organic compounds such as particulate matters and dead cells (Tripathi et al., 2007; Thanh and Simard, 1973; Mannan et al., 2005; Tung et al., 2004; Guest et al., 2002)

In RUN II, two DHS systems operated in parallel for 95 days. In this run, OLR in two DHS system decreased to 0.86-1.01 kgTBOD/m³_{sponge-d}, but the HLR was increased from 6.1 m³/m³_{sponge-d} to 25.6 m³/m³_{sponge-d} (Table 4.6). Organic removal improved with the efficiencies for TBOD reaching up to 96% and 94% in FDHS and BDHS, respectively (Table 4.6). Most of TBOD was removed in the 1st segment of both systems. This was probably due to the recirculation of DHS effluents and thus more effective for dissolved oxygen (DO) transfer to the wastewater due to increased flow velocity. Tandurkar et al. (2006a) also reported that dissolution of air into the wastewater was further enhanced by increased down-flow velocity, providing more oxygen to aerobic organisms residing inside the sponge. In addition, higher flow rate also increased the penetration of wastewater deep into the sponge material, facilitating better substrate distribution.

Table 4.6 Organic and nitrogen loading profiles along the four segments during three runs

Parameters	Segment 1		Segment 2		Segment 3		Segment 4		Overall	
	FDHS	BDHS	FDHS	BDHS	FDHS	BDHS	FDHS	BDHS	FDHS	BDHS
Run I										
OLR (kgTBOD ₅ /m ³ _{sponge} -d)	4.25	4.25	1.04	3.33	0.89	2.18	1.03	1.89	1.06	1.06
NLR (kg-N/m ³ -d)	2.44	2.44	2.47	2.02	1.92	1.60	1.93	1.39	0.61	0.61
ALR (kg-N/m ³ -d)	2.33	2.33	2.39	1.82	2.71	1.17	2.53	0.79	0.58	0.58
Run II										
OLR (kgTBOD ₅ /m ³ _{sponge} -d)	3.46	4.04	2.75	4.68	2.75	3.56	2.34	0.86	0.86	1.01
NLR (kg-N/m ³ -d)	19.87	8.40	21.08	9.67	21.49	8.76	20.27	4.99	4.99	2.10
ALR (kg-N/m ³ -d)	18.27	6.71	19.05	7.74	20.17	6.93	18.54	4.57	4.57	1.70
Run III										
OLR (kgTBOD ₅ /m ³ _{sponge} -d)	6.45	15.54	4.52	31.0	2.79	12.41	2.59	14.10	1.61	3.63
NLR (kg-N/m ³ -d)	19.25	9.97	19.86	10.98	19.15	9.31	20.47	9.11	4.81	2.49
ALR (kg-N/m ³ -d)	18.52	7.79	18.84	8.65	18.13	7.23	19.56	6.62	4.63	1.95

Remark: Organic and nitrogen loading profiles along the four segments during RUN I calculated by actual HRT values

In RUN III, two DHS systems operated in parallel for 105 days. In this run, OLR in FDHS and BDHS systems were about 1.60 kgTBOD/m³-d and 3.63 kgTBOD/m³-d, respectively. The difference OLR of two systems was causing of the remained TBOD in BDHS system is higher than FDHS system. And it comes to the BDHS system with recirculation flow During RUN III. The HLR in DHS remained the same as in RUN II, 25.6 m³/m³_{Sponge}-d. Organic removal improved with the efficiencies for TBOD about 95% in FDHS system but decreased to 77% in BDHS system (Table 4.5). Most of TBOD was removed in the 1st segment of FDHS systems. But in this run, it was the lowest TBOD removal efficiency for BDHS system. These caused of biomass sloughing is one cause of TSS concentration in biofilter effluent under high value HLR and OLR conditions.

4.6.5 Nitrogen Removal

During RUN I, two DHS systems received total nitrogen loading (NLR) 1.06 kg-N/m³-d, which includes 1.02 kg-N/m³-d of ammonia nitrogen loading (AUR) as shown in Table 4.6. Nitrogen was not removed in FDHS system during three runs. However, it was reduced in BDHS via nitrification and denitrification. During RUN I, the concentrations of total nitrogen, ammonia, nitrite and nitrate in the effluent of BDHS system were 62, 35, 7 and 8 mg/L, respectively, amounting to 68% of total nitrogen removal efficiency as shown in Figure 4.14. Nitrification in BDHS took place in second, third and fourth segments shown by the appearance of nitrogen oxides. Results also indicated that nitrification was limited in the first segment of BDHS system at high organic contents. The ammonia oxidizer populations at high loading rate compete with heterotrophs for space and oxygen. The ammonia oxidation activities appeared to be slightly higher than nitrite oxidation activities, accounting for the observation that nitrite was present in the effluents.

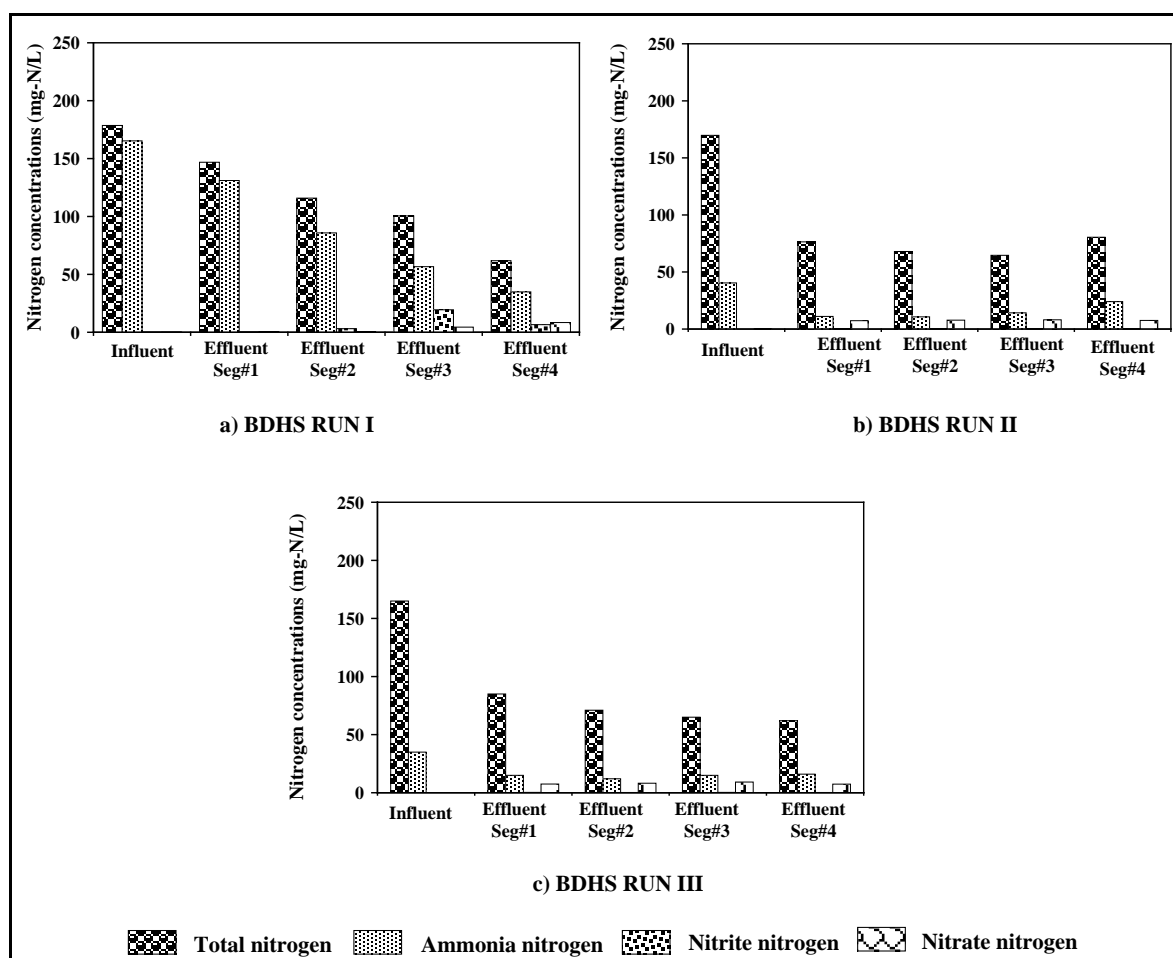


Figure 4.14 Nitrogen profiles of BDHS systems in two runs

In RUN II, two DHS systems received total nitrogen loading rate (NLR) of about $2.10 \text{ kg-N/m}^3\text{-d}$ and $4.99 \text{ kg-N/m}^3\text{-d}$ of BDHS and FDHS systems, respectively. This included $1.70 \text{ kg-N/m}^3\text{-d}$ and $4.57 \text{ kg-N/m}^3\text{-d}$ of ammonia nitrogen for BDHS and FDHS systems, respectively. Under such conditions, oxygen was not limiting in BDHS because recirculation wastewater enhanced dissolved oxygen concentration. However, due to increased NLR, the nitrogen removal efficiencies decreased to 59% and 63% for total nitrogen and ammonia nitrogen, respectively. It is a known fact that the shear force of water flow amplifies as hydraulic loading increases. This may lead to the disruption of the retained sludge inside the sponge of DHS, finally raising the value of SS in the effluents. [Tawfik et al. \(2002\)](#) also observed deterioration in the nitrogen removal in RBC during

hydraulic shock load. It was explained that the contact time between the nitrifiers and substrate was very short.

In RUN III, two DHS systems received total nitrogen loading rate (NLR) of about 9.97 kg-N/m³-d and 19.25 kg-N/m³-d of BDHS and FDHS systems, respectively. This included 7.79 kg-N/m³-d and 18.52 kg-N/m³-d of ammonia nitrogen for BDHS and FDHS systems, respectively. During this run, the concentrations of total nitrogen, ammonia, nitrite and nitrate in the effluent of BDHS system were 85, 62, 0.2 and 7.4 mg/L, respectively, amounting to 56% and 63% of total nitrogen and ammonia nitrogen removal efficiencies, respectively.

The nitrification under high influent organic concentrations was found in the BDHS. This is in contrast with the results of [Chae et al. \(2004\)](#) according to which, the presence of organic matter in aerobic system, that promotes the growth of heterotrophs, inhibits ammonia oxidation. The result of present study was very interesting as it meant that the attached nitrifiers in the sponge media were quite resistant to organic shocks. However, nitrifying bacteria are strict aerobes that are they can only nitrify in the presence of dissolved oxygen. Therefore, at DO concentration <0.5 mg/L, little, if any, nitrification occurs ([Geradi, 2002](#)). The influent BOD/TKN ratios of BDHS during both runs were about 1.7 (Table 4). This was much less than the recommend BOD₅/TKN ratio of about 20 which promotes the growth of aerobic heterotrophs. Probably, the nitrogen removal in BDHS system was caused by aerobic denitrification and/or denitrification occurring in the anoxic biomass ([Mechdar et al., 1997](#)). [Araki et al. \(1999\)](#) suggested that the internal part of the sponge maintains anoxic environment where denitrification prevails, whereas up to the depth of approximately 0.75 cm from the surface of the sponge, aerobic environment prevails. Nitrifiers in this region convert ammonium nitrogen in to oxide forms, which are then transferred to the anoxic zone where they are denitrified. In this way, DHS allows both nitrification and denitrification to take place within a single system ([Tandukar et al.,](#)

2006a). In addition, even though from the wastewater characteristics in each segment of BDHS reactors, efficiency of denitrification process is usually considered poor at BOD/TKN <2.5. Also, Grady et al. (1999) suggested that in order to ensure successful ammonia removal in the nitrification process, an external carbon source would be necessary. However, few past studies reported high endogenous respiration of DHS sludge suggesting that the sludge accumulation was in near balance with the degradation of sludge in reactor itself. And it was also being utilized as a carbon source during denitrification (Tandukar et al., 2006a). When high amounts of organic matter are present in a biofilter, the fast growing heterotrophic bacteria will 'out-space' the slow growing nitrifiers from the aerobic zone in the biofilm as they compete for oxygen and space.

4.6.6 Effect of Recirculation on DHS Efficiencies

The term recirculation refers to the return of DHS effluents. That purposes to couple the effect of hydraulic and organic loading rates on two DHS efficiencies. The effect of recirculation flows on the DHS efficiencies was investigated during three runs. Hydraulic loading rate (HLR) of RUN I to two DHS systems were $3.5 \text{ m}^3/\text{m}^3_{\text{sponge-d}}$ at 7.0 h HRT, which increased to $25.6 \text{ m}^3/\text{m}^3_{\text{sponge-d}}$ (HRT 1 h) during RUN II and RUN III. Organic loading rate (OLR) of RUN I and RUN II were in the same OLR ranges about 0.86-1.06 kgTBOD/ $\text{m}^3\text{-d}$ by recirculation as shown in Table 4.5. Figure 4.15 shows the effect of recirculation on BOD removal efficiencies of FDHS and BDHS systems were increased in RUN II. This indicated that the organic removal of two DHS systems were almost unaffected by increased hydraulic loading. This can explain by microbial utilization of macromolecules involves several steps, including transport to the cell and binding to hydrolytic enzymes; macromolecule hydrolysis in to sizes of compounds able to be transported across the cell membrane; and metabolism of components for either energy (catabolism) or cell growth (anabolism). Confer and Logan (1991) suggested that fluid shear can increase macromolecule uptake by suspended bacteria in trickling filter. And this

confirmed by [Confer and Logan \(1998\)](#) study that found the majority of protein and polysaccharide hydrolytic activity in trickling filter effluent was associated with suspended cells. Although it is likely that substantially higher hydrolytic activity would be produced by biofilm itself than was produced by the sloughed and recycled cells present in trickling filter effluent. “And this obtained by the other research suggest that the present results can be generalized to other macromolecules and colloidal substrates in wastewater treatment plants, indicating that successively smaller compounds will be produced from degradation by cell-associated hydrolytic enzymes” ([Confer and Logan, 1991](#)). Based on these results, FDHS system had high capable of hydrolytic activity and it produced low excess sludge with high organic removal rate. These suggested that the sludge accumulation was near balance with the degradation of sludge in the reactor itself. However, TBOD effluent from BDHS system during RUN III was higher than RUN I and RUN II. Because of both highest OLR and HLR values were operated in RUN III. That was presence of sufficient high heterotroph organism population at high loading rate.

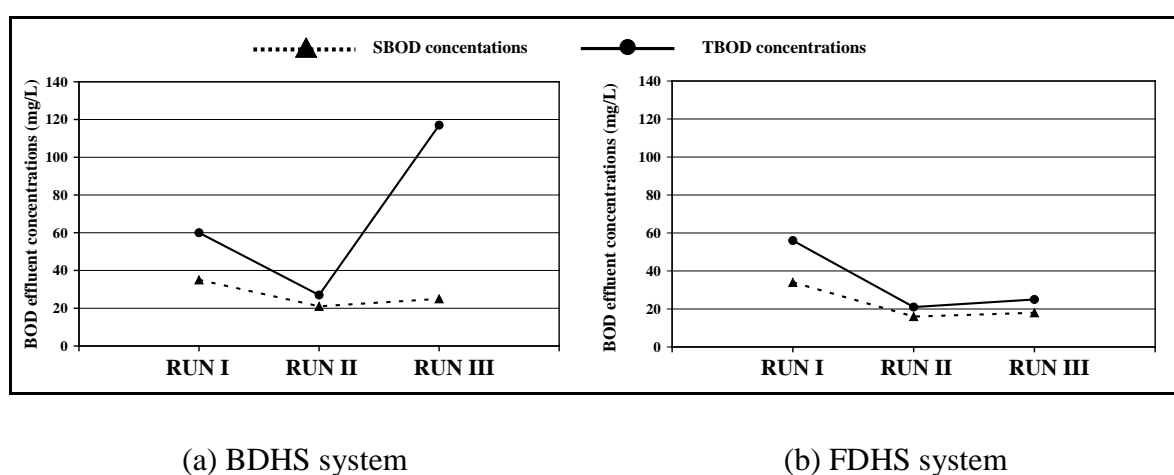


Figure 4.15 Effect of recirculation flows on organic removal of two DHS systems

Furthermore, results obtained also verified that BDHS system can exhibit substantial tolerance against about four fold organic (RUN II and RUN III) and seven fold hydraulic (RUN I and RUN II) increased loading. HLR was affected on nitrogen removal as decreased about 9% of total nitrogen removal but unaffected of increasing OLR. [Tawfik et al \(2002\)](#) and [Tandurkar et al. \(2006\)](#) explained by contact time between the nitrifiers and substrate was very short and high hydraulic loading lead to the disruption of the retained sludge inside the sponge of BDHS system, finally raising the value of SS in the effluent.

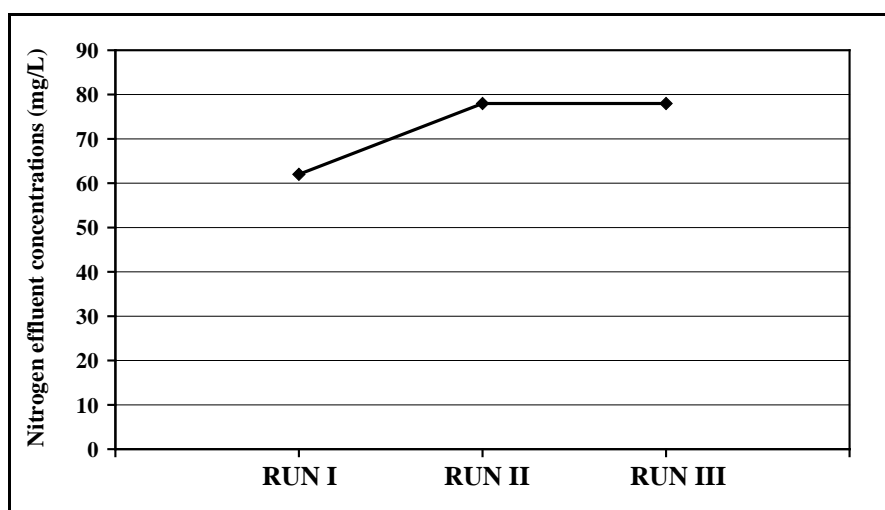


Figure 4.16 Effect of recirculation flows on nitrogen removal of BDHS system

Recirculation treated effluent to the two DHS systems dilutes the influent wastewater entering the DHS system. Since the BOD removal process is first order (i.e., the rate of removal of BOD is affected by the initial concentration of BOD), recirculation helps distribute the loading evenly through the depth of the filter. It also helps to manage the diurnal variation in loading while maintaining a minimum wetting rate throughout the day. In general, higher recirculation ratios (recirculation flow rate: influent flow rate) the better the effluent quality, at least to the point where the hydraulic retention time in the filter bed becomes too short.

4.7 COD Fractions and Organic Biodegradation

The average fraction of influent and effluent of two DHS systems during three runs were obtained with division in Figure 3.8 as results shown in Figure 4.17. In RUN I, most BSCOD fractions were removed in the first segment of the two DHS segments. And the slowly biodegradation or BPCOD fractions increased in effluent of BDHS system in segment 1 and 4 of BDHS system. This caused of high accumulated biomass in these segments then it became to BPCOD fraction in the DHS effluent by sloughed biomass. And it also found that the BPCOD in BDHS effluent was higher than FDHS system in every segment. In general, a biofilter as concept of trickling filter performs optimally at increasing or stable waste loads (up to the designed maximum load). When the feed load in the system is reduced, part of the filter may be detached. The filter sheds part of its biofilm and the detached biofilm particles add to the SS concentration in the water. Since they generally have a size below 40 μm , they are difficult to remove (Eding et al., 2006). The process of biofilter detachment is not yet fully understood. Biofilm parameters, which were used to clarify the process of biofilm detachment, are dry density, wet density, the content of the extra cellular biopolymer (ECP), increased gas content in maturing biofilm and shear stress (Ohashi and Harada, 1994). Further research is required to in biofilter filters. As a consequence of UPCOD variations, the slowly biodegradable fraction (BPCOD) was strongly variable for the four segment of BDHS effluent. This reveals that the hydrolysis rate by bacteria more slowly than fungi. Thus it led to strong limiting process in substrate biodegradation in denitrification process in BDHS system. In contrast, the FDHS system achieved an almost complete removal of BPCOD fraction in the final effluent. And this also indicated the potential advantage of fungi over bacteria in terms of organic removal rate. From several studies, fungi had a wide range of enzyme, and were capable of metabolizing complex mixtures of organic compounds such as particulate matters and dead cells (Jin et al., 2002; Orgaz et al., 2006; Tripathi et al., 2007).

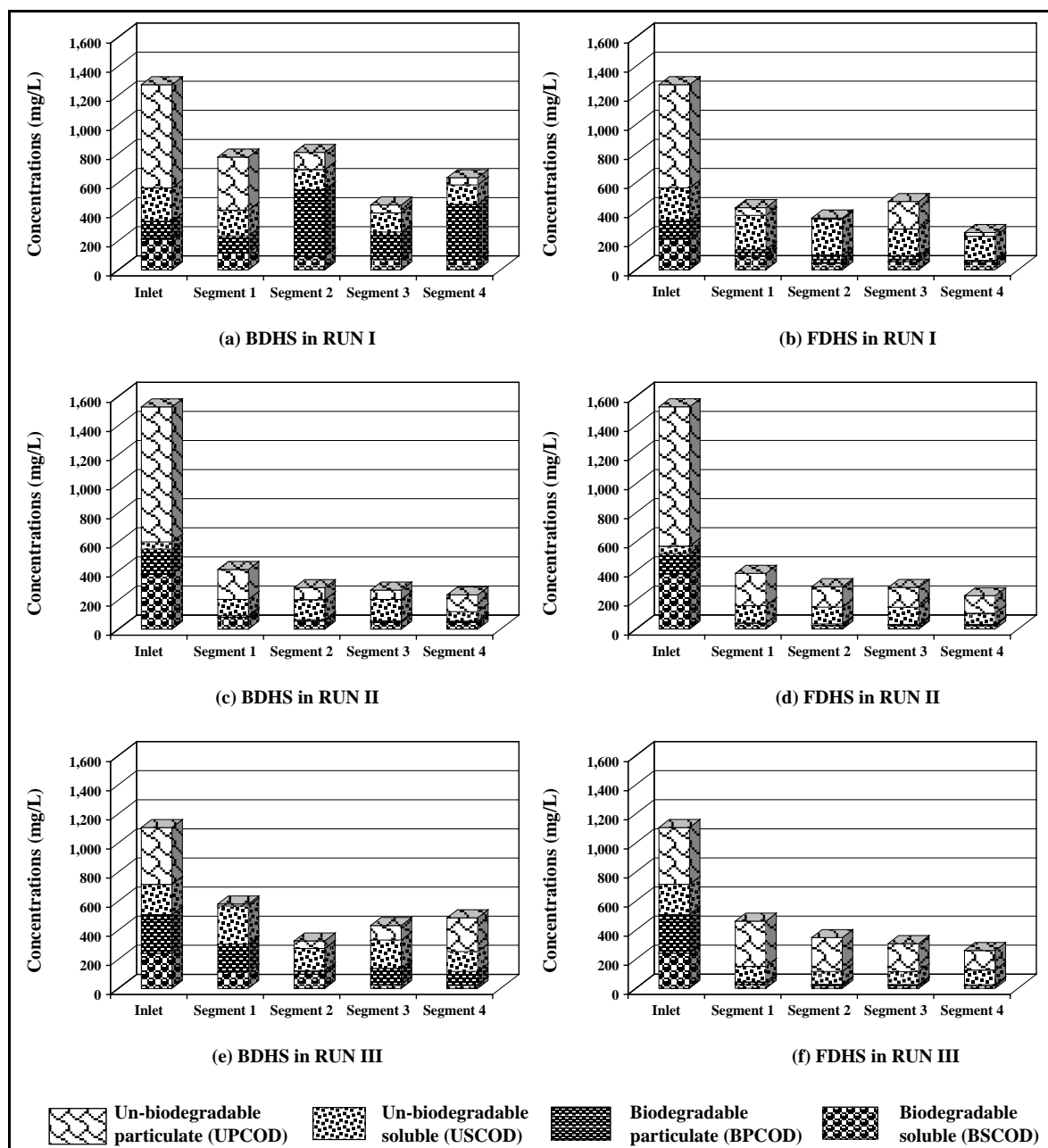


Figure 4.17 The carbonaceous material characterizations of two DHS systems

In RUN II, the average COD fractions of BDHS effluent were about 115.4 mg/L, 65.6 mg/L, 10 mg/L and 45 mg/L of UPCOD, USCOD, BPCOD and BSCOD, respectively. Those were same ranges of FDHS system as about 120.1 mg/L, 76.9 mg/L, 7 mg/L and 25 mg/L, respectively. Most of particulate fractions (UPCOD and BPCOD) were decreased in segment 1 of two DHS systems. This can be explained by particulate matters were retained

on sponge media and degraded in segment 1 during RUN II. This is a recommended recirculation method of increasing the BOD removal efficiency. The main finding of [Confer and Logan \(1998\)](#) study, that hydrolysis occurs primarily in contact with cells in suspended culture and in contact with biofilms in fixed-film systems, makes good sense for two main reasons. First, hydrolytic enzymes released into bulk solution are soluble proteins that could become microbial substrate. Second, and perhaps more important, any hydrolytic enzymes released into bulk solution by cells could be quickly washed out of the reactor and would need to be continuously replenished, a process that would be energetically unfavorable to cells.

In RUN III, the average COD fractions of BDHS effluent were about 232.4 mg/L, 136.2 mg/L, 91.6 mg/L and 25.4 mg/L of UPCOD, USCOD, BPCOD and BSCOD, respectively. And FDHS system were about 133.8 mg/L, 101.1 mg/L, 7 mg/L and 17.7 mg/L, respectively. Particulate fractions of BDHS effluent were being higher than FDHS effluent. It was likely that fungi substantially higher hydrolytic activity than bacteria.

4.8 Mass Balances

As consequence, the two DHS systems achieve simultaneous removal of organic matter and nutrients. Current understanding of biological wastewater treatment system behavior has developed from observations on operating systems. Mass balances provide one way of checking the data. Surprisingly this is seldom done, most likely because gathering the data to conduct these balances may necessitate additional sampling and monitoring of the experimental system, beyond the regarded as necessary for addressing a particulate research problem. Also, in certain cases it may not be feasible to gather the required data; for example, on a full-scale plant with dynamic influent loading ([Barker and Dold, 1995](#)). Two balances be applied to experimental data are for chemical oxygen demand (COD) and nitrogen (N) during RUN I. In addition the results of mass balance

calculations can also be used to investigate process behavior, leading to improved understanding of underlying mechanisms.

4.8.1 COD and Nitrogen Assimilation in Sludge

Based on theory of metabolism, microorganisms require nutrients such as organic matter and nitrogen to assimilate into cell components. The ratios of COD/VSS (f_{CV}) and TKN/VSS (f_N) of sludge in two DHS systems were analyzed in four identical modules of column segments. The amount of COD and nitrogen for microbial synthesis were calculated from Equations 4.7 and 4.8, respectively.

$$M_{\text{COD,ass}} = f_{\text{CV}} \times Y \times M_{\text{COD}_{\text{removed}}} \quad (4.7)$$

$$M_{\text{N,ass}} = f_{\text{N}} \times Y \times M_{\text{COD}_{\text{removed}}} \quad (4.8)$$

Table 4.7 illustrates the mass flow of COD and nitrogen were used in microbial assimilation. The COD used in microbial assimilation decreased according to the levels of the height of the DHS reactors in both systems. This became the amount of influent COD in the upper segments was higher than in the lower ones. And in general, higher contents of organic in the system resulted in higher heterotroph organism population. Moreover, the content of the organic and nitrogen assimilated in FDHS sludge is higher than in BDHS sludge in every segments except in segment 1 having lower contents. This indicated that the organic nitrogen utilization rate of fungi was higher than bacteria.

Table 4.7 Mass flows of COD and nitrogen assimilation in cells

DHS profiles/ Parameters	FDHS system				BDHS system			
	Segment 1	Segment 2	Segment 3	Segment 4	Segment 1	Segment 2	Segment 3	Segment 4
Sludge yield*	0.63	0.63	0.63	0.63	0.84	0.86	0.88	0.86
f_N	0.07	0.42	0.18	0.18	0.11	0.19	0.21	0.10
f_{COD}	1.54	1.20	1.38	1.38	0.88	1.08	1.20	1.31
Assimilated mass flows:								
$M_{COD,ass}$ (g/d)	29.5	19.5	3.5	0.7	15.7	17.9	2.2	-15.6
$M_{N,ass}$ (g/d)	0.3	0.7	0.4	0.1	1.0	0.7	0.3	0
Assimilated ratio (M_{ass}/M_{inf}):								
$M_{COD,ass}$ (%)	37.7	41.6	15.5	3.9	20.1	37.4	10.0	-86.7
$M_{N,ass}$ (%)	2.3	6.7	3.8	1.0	7.5	6.7	2.9	0.3
COD:N	100:4.2	100:35.0	100:12.8	100:7.9	100:12.8	100:17.3	100:17.3	100:7.5

Remark: Sludge yield in unit of mgVSS/mgCOD_{removed}

4.8.2 COD and Nitrogen Mass Balances

Two balances applied to experimental data were chemical oxygen demand (COD) and nitrogen (N). Results of COD and nitrogen mass balances in two DHS systems are shown in Tables 4.8 and 4.9. The highest COD removed was found in segment 1 of FDHS system which included the electron transferred from the organic material to electron acceptor (COD oxidized) about 11.6 g/d and COD loss 18.9 g/d. And COD loss in segment 4 of two DHS systems were to be in deficit because oxygen utilization (COD oxidized) is higher than $M_{COD,removed}$. This indicated the sludge was utilized as a carbon sources during endogenous respiration in two DHS systems. Moreover, the result of two mass balances studies indicated that there was a possibility in eliminating COD in BDHS system due to aerobic heterotroph consumption and denitrification processes. Although, nitrogen removal did not occur in overall FDHS system but nitrogen loss was found in segment 1, 2 and 3. This caused by the nitrogen assimilation in sludge and the metabolism by facultative microorganism in anoxic zone as more detail in Table 4.7.

Table 4.8 Total COD mass balance in two DHS systems

DHS profiles	FDHS (g/d)					BDHS (g/d)				
	M_{inf}	M_{eff}	$M_{removed}$	M_{oxid}	M_{loss}	M_{inf}	M_{eff}	M_{rem}^b	M_{oxid}	M_{loss}
Segment 1	78.3	47.8	30.5	11.6	18.9	78.3	57.0	21.3	4.7	16.6
Segment 2	47.8	21.9	25.9	0.9	25.0	57.0	37.7	19.3	3.4	15.9
Segment 3	21.9	18.0	3.9	1.8	2.1	37.7	35.6	2.2	1.8	0.4
Segment 4	18.0	17.3	0.8	3.3	-2.6	35.6	49.4	-13.9	6.1	-19.9

Table 4.9 Nitrogen mass balance in two DHS systems

DHS profiles	FDHS (g/d)								BDHS (g/d)							
	Nitrogen influent			Nitrogen effluent			Sludge TKN	TN loss	Nitrogen influent			Nitrogen effluent			Sludge TKN	TN loss
	TKN	NO ₃ ⁻	NO ₂ ⁻	TKN	NO ₃ ⁻	NO ₂ ⁻			TKN	NO ₃ ⁻	NO ₂ ⁻	TKN	NO ₃ ⁻	NO ₂ ⁻		
Segment 1	13.2	0	0	10.4	0	0	0.3	3.1	13.2	0	0	11.0	0	0	1.0	3.1
Segment 2	10.4	0	0	10.4	0	0	0.7	0.7	11.0	0	0	8.7	0	0.2	0.7	2.8
Segment 3	10.4	0	0	9.8	0	0	0.4	1.0	8.7	0	0.2	7.5	0.3	1.5	0.3	0
Segment 4	9.8	0	0	13.4	0	0	0.1	-3.5	7.5	0.3	1.5	4.7	0.6	0.5	0	3.5

4.8.3 Denitrification Potential in DHS Systems

Biological nitrogen removal of an UASB effluent without substrate addition is possible if the wastewater contains enough biodegradable organics to denitrify all its nitrifiable nitrogen content. The denitrification potential is often expressed with the ratio TCOD/TKN or TCOD/NH₄-N instead of TBOD/TKN or TBOD/NH₄-N. Results indicated that some organic nitrogen was generally in particulate form, thus becoming inert organic polymers and probably not nitrifiable (Table 4.10). The stoichiometric requirement for denitrification is theoretically 2.86 gO₂/gN. Therefore, it can be concluded that BDHS system can be denitrified, whereas most of the BDHS segment system will need an external carbon source to achieve complete denitrification. However, the result of COD and N balances in BDHS system showed potential of denitrification in segment 1, 2 and 4. Thus, sludge was also being utilized as a carbon source during denitrification in BDHS system.

Table 4.10 Denitrification potential of two DHS systems

Runs	TBOD/NH ₄ -N of FDHS Influent (gO ₂ /gN)				TBOD/NH ₄ -N BDHS of Influent (gO ₂ /gN)			
	Seg. 1	Seg. 2	Seg. 3	Seg. 4	Seg. 1	Seg. 2	Seg. 3	Seg. 4
RUN I	2.03	0.44	0.33	0.41	2.03	1.83	1.82	2.40
RUN II	2.43	0.16	0.13	0.13	2.43	0.57	0.52	0.43
RUN II	3.08	0.24	0.15	0.13	3.08	3.60	1.63	0.47

4.9 Biokinetic Parameters

Values of biokinetic coefficients of aerobic heterotrophs during RUN I shown in Table 4.11 indicated that substrate utilization rate (r_x) and maximum specific growth rate (μ_{max}) were higher in the first segment of fungal culture in FDHS, which explained the highest BOD removal in this segment.

Table 4.11 Biokinetic coefficients of FDHS and BDHS sludge during RUN I

Biokinetic parameters	Segment 1		Segment 2		Segment 3		Segment 4	
	BDHS	FDHS	BDHS	FDHS	BDHS	FDHS	BDHS	FDHS
μ_{\max} (d^{-1})	2.20	3.40	3.50	1.60	1.60	1.20	3.60	1.60
r_x (mgCOD/mgVSS-h)	0.11	0.21	0.16	0.10	0.09	0.09	0.15	0.10
Y (mgVSS/mgCOD)	0.84	0.63	0.86	0.63	0.85	0.63	0.86	0.63
k_d (d^{-1})	0.199	0.086	0.198	0.051	0.182	0.184	0.193	0.044
K_S (mg/L)	54.8	92	81.1	100	50.0	52	100.2	80
$\mu_{\max}/Y.K_S \times 10^{-3}$ (L/mg-h)	1.99	2.35	2.09	1.12	1.57	1.53	1.74	1.30

The r_x and μ_{\max} decreased in the lower segments caused by limiting organic content as shown in the organic content profiles in Table 4.6. This was different in case of bacterial cultures in BDHS. The r_x and μ_{\max} values were highest in second and fourth segments. The organic biodegradation rate of bacteria was less than fungi in the first segment. And the most of suspended solids were adsorbed and inhibited organic removal in the first segment of BDHS. Additionally, estimation of $\mu_{\max}/Y.K_S$ is used as a measure for comparing the biodegradation kinetics, as suggested by [Grady et al. \(1999\)](#), indicating the highest biodegradation of organics in the first segment of fungal sludge (FDHS). Results of biokinetics experiments show that a fungi-based DHS have the higher potential for organic removal than BDHS treating the UASB effluent of tapioca starch wastewater. Moreover, it can also be observed that the yield (Y) of the fungal culture is lower than that of the bacterial culture. This indicates that lower excess sludge would be produced from the fungal system compared to the bacterial system for the same substrate quantity, thus having the advantage of less sludge handling.

4.10 Dominant Culture in DHS Sludge

From the identification, it appeared that *nitrosomonas* and *nitrobacter* were dominant cultures in segment 2, 3 and 4 of the BDHS biomass. Cell concentrations of both nitrifying bacteria were in good agreement with the magnitudes of ammonia-oxidizing and nitrite-oxidizing activities evaluated from those segments. The three dominant fungal genera in FDHS system were included of *Trichoderma*, *Aspergillus* and *Candida*. As presented by several researchers, these fungi had a wide range of enzymes, and were capable of metabolizing complex mixtures of organic compounds such as particulate matters and dead cells (Tripathi et al., 2007). Moreover, simple operating control condition can be operated by adjusting the pH to 4.0 ± 0.2 and 7.0 ± 0.2 for FDHS and BDHS systems, respectively. Under such condition, fungi and bacteria were the dominant cultures of FDHS and BDHS systems, respectively for treating UASB effluent in tapioca starch industry. The photos of dominant cultures are showed in Figures 4.18 and 4.19.

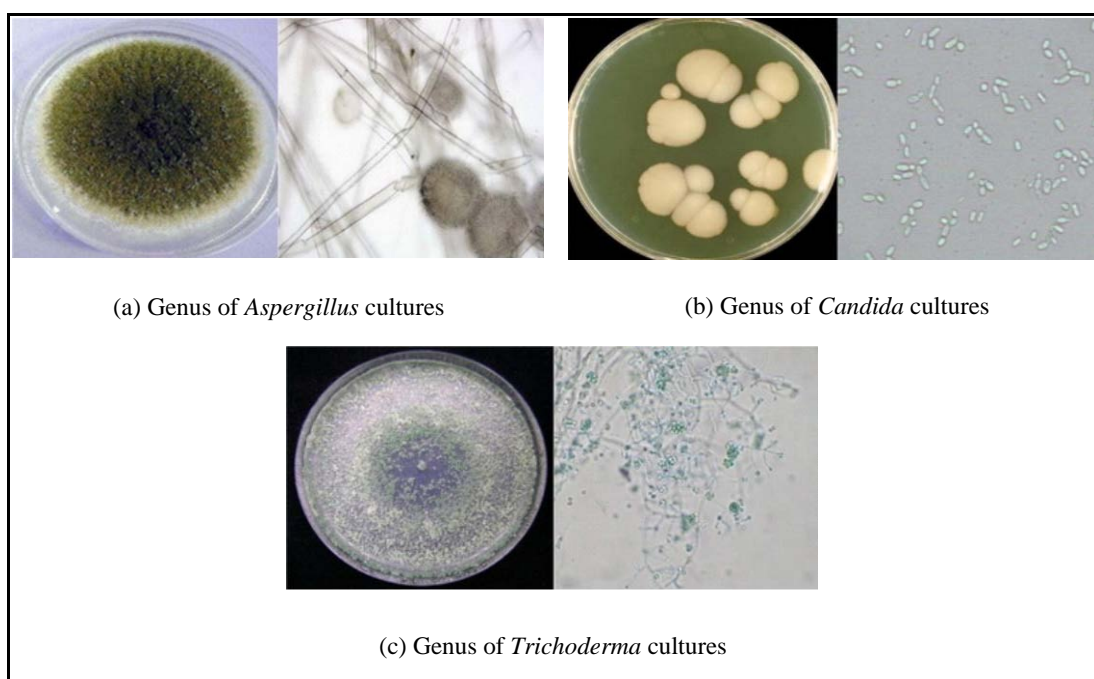


Figure 4.18 Dominant cultures in FDHS sludge

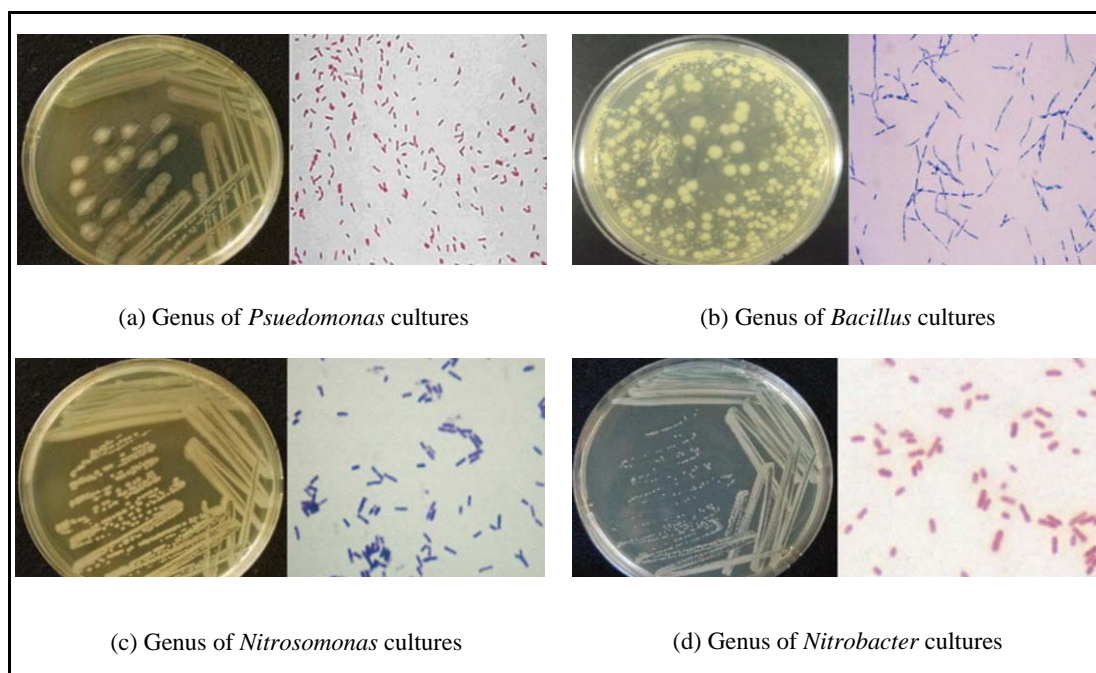


Figure 4.19 Dominant cultures in BDHS sludge

4.11 Sludge Characteristics

Table 4.12 shows the comprehensive results of sludge composition study. In Table 4.12, the data concerning TS, TVS, EPS and lipid phosphate concentrations are direct measurements.

4.11.1 Retained Sludge

The good performance of organic removal in two runs can be attributed to a large amount of retained biomass in sponge media of FDHS and BDHS systems. The values are 5-20 times higher than that of activated sludge system and trickling filter treating domestic sewage (Tandukar et al., 2006a). The characteristics of sponge biomass along two DHS systems height were determined (Table 4.12). Little differences were found in total solids and volatile solids accumulated in the various segments of the FDHS reactor. In steady state, the concentration of retained sludge in FDHS and BDHS systems remained almost constant suggesting that the degradation of old biomass nearly balanced the accumulation of fresh one.

Table 4.12 Retained sludge concentrations in sponge media of two DHS systems

DHS profiles/ Retained sludge		Segment 1		Segment 2		Segment 3		Segment 4		Average	
		FDHS	BDHS	FDHS	BDHS	FDHS	BDHS	FDHS	BDHS	FDHS	BDHS
RUN I	MLVSS (g/L)	75.6	30.3	12.1	21.4	28.8	20.0	41.9	50.4	39.6	30.5
	MLVSS/MLSS	0.97	0.76	0.95	0.72	0.92	0.66	0.94	0.85	0.95	0.75
RUN II	MLVSS (g/L)	50.9	20.0	12.3	18.5	25.8	15.5	35.6	30.2	31.2	21.1
	MLVSS/MLSS	0.93	0.76	0.97	0.71	0.97	0.68	0.94	0.89	0.95	0.76
RUN III	MLVSS (g/L)	55.4	25.5	13.4	19.4	27.2	18.3	38.5	42.5	33.6	26.4
	MLVSS/MLSS	0.94	0.77	0.95	0.75	0.96	0.67	0.96	0.85	0.95	0.76

The MLVSS/MLSS ratio of sludge was also measured; it was found that the bacterial sludge (MLVSS/MLSS: 0.66-0.89) had a lower degradability compared to that of the fungal sludge (MLVSS/MLSS: 0.92-0.97). In a previously (Tandukar et al., 2006a) on bacterial DHS system treating domestic sewage, the MLVSS/MLSS was also found to be lower about 0.66-0.75. This suggested that the ratios fungal sludge has higher degradability compared to BDHS sludge.

4.11.2 Viable Cell Concentrations

Based on phospholipid analysis, the ratios of viable cells to total biomass of all fungal and bacterial sludge were in range of 56-89% and 35-82%, respectively. That seems to be fungal sludge contained active biomass in sludge higher than bacterial sludge. The ratios of viable cells to total biomass decreased during DHS height decrease.

4.11.3 Extracellular Polymeric Substances (EPS)

The extracellular polymeric substances (EPS) production is a general property of microorganisms in natural environments and occurs in bacteria, algae, yeast, and fungi. They are construction materials for microbial aggregates such as biofilm, floc, and sludge. However, EPS is inert biofilm composition and can also act as a diffusion barrier to nutrients and cellular products (Allison, 1998; Lapidou and Rittmann, 2002). EPS in fungal and bacterial sludge were measured in two DHS systems. Figure 4.20 and Table 4.13 summarize the variation in bound and soluble EPS of BDHS and FDHS sludge. The bound EPS corresponds to polymeric substance adhered together with each other and microorganisms. The soluble EPS indicate the microbial products which have been produced by the microorganisms and suspended in mixed liquor in a soluble form.

Several studies have suggested a major disadvantage of trickle-bed bioreactors and so causing the limiting use of them for biological wastewater treatment. This is attributed to the progressive simultaneous biological clogging and physical plugging phenomena induced by the formation of an excessive amount of biomass and the retention

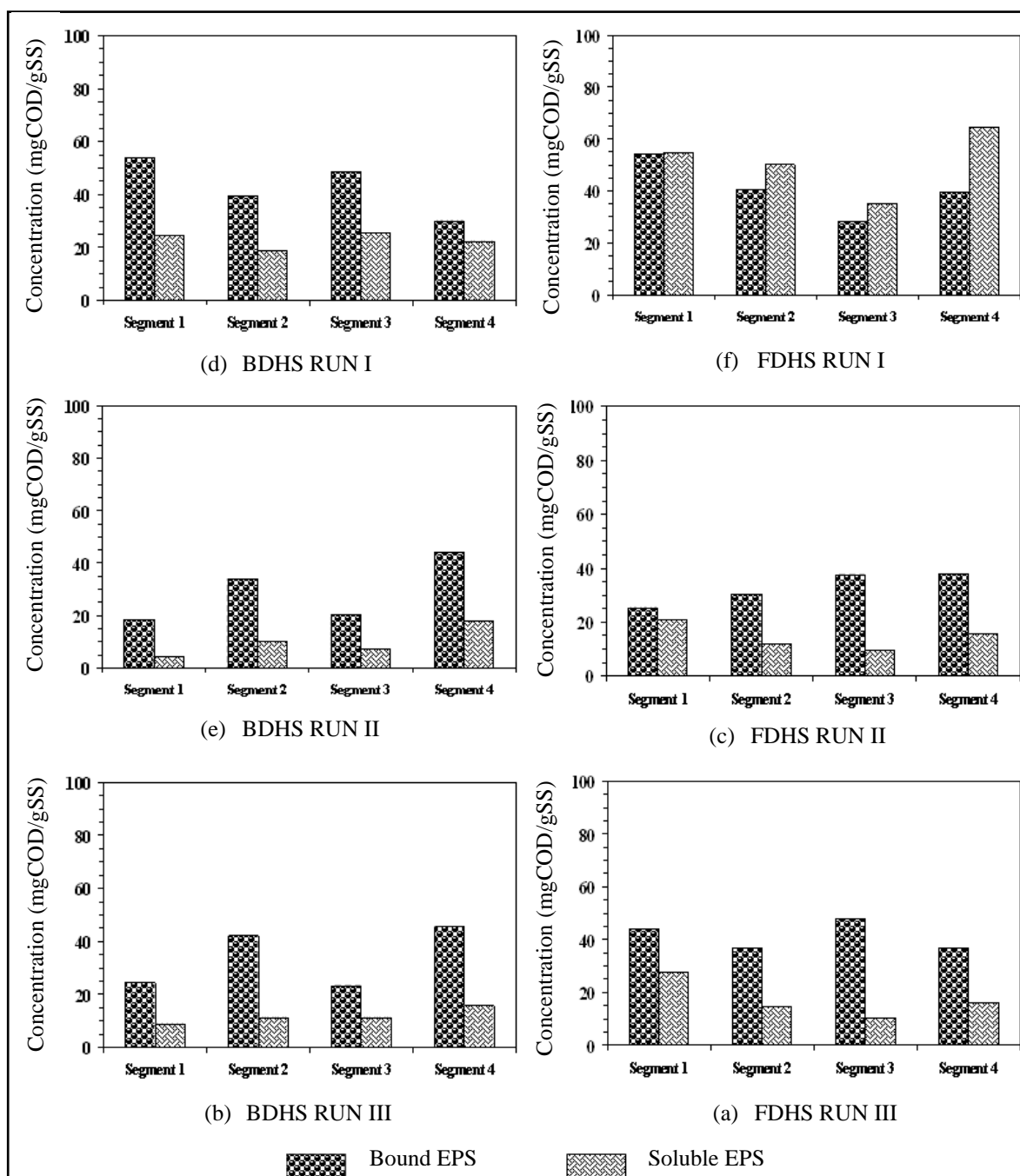


Figure 4.20 Extracellular polymeric substances (EPS) concentrations in two DHS systems

Table 4.13 Retained sludge, Extracellular polymeric substances (EPS), viable cell and dead concentrations of two DHS sludge

DHS profiles/ Sludge compositions		Segment 1		Segment 2		Segment 3		Segment 4	
		FDHS	BDHS	FDHS	BDHS	FDHS	BDHS	FDHS	BDHS
RUN I	EPS (mgCOD _{EPS} /gCOD _{SS})	47.4	58.7	33.3	39.0	22.5	48.7	32.4	26.0
	Viable cells (mgCOD _{cell} /gCOD _{SS})	848.9	792.4	735.3	732.0	656.6	607.1	632.2	469.2
	Dead cells (mgCOD _{dead-cell} /gCOD _{SS})	103.7	148.9	231.4	229.0	320.9	344.2	335.4	232.1
RUN II	EPS (mgCOD _{EPS} /gCOD _{SS})	21.0	20.6	25.0	35.4	29.2	20.1	29.7	41.3
	Viable cells (mgCOD _{cell} /gCOD _{SS})	897.0	821.8	752.8	674.0	639.9	498.8	562.4	358.9
	Dead cells (mgCOD _{dead-cell} /gCOD _{SS})	82.0	157.6	222.2	290.6	330.9	481.1	408.0	599.9
RUN III	EPS (mgCOD _{EPS} /gCOD _{SS})	41.1	26.9	30.8	41.1	37.7	22.4	28.6	38.5
	Viable cells (mgCOD _{cell} /gCOD _{SS})	878.4	803.8	762.6	596.6	676.4	367.4	572.6	388.7
	Dead cells (mgCOD _{dead-cell} /gCOD _{SS})	80.5	169.3	206.5	362.2	285.9	610.2	398.8	572.7

of inert suspended fine particles and EPS (Iluita and Larachi, 2005; Thullner et al., 2004). Results of a study Thullner et al. (2004) reported that porous media samples showed that only 5% of the total organic carbon was present as bacterial biomass, whereas the remaining 95% were attributed to EPS. The total volume of the bacterial cells remained below 0.01% of the pore space even in the vicinity of the injection port. Therefore, the observed clogging effects were assumed to be mainly caused by EPS. This is one of the causes of filter clogging in BDHS system as found during the first experimental run.

Experimental results of BDHS sludge show that the two highest bound EPS concentrations were found to be in the first and third segments which had two lowest biomass growth rates. This suggests that the highly bound EPS accumulated in the sludge may have the negative effect on the bacteria consumption rate. In case of fungal sludge (FDHS), higher amount of bound EPS were accumulated in biofilms than bacterial sludge. Highest values of bound EPS concentrations and specific growth rate were found to be in the first segment of FDHS. Evidence from experiment suggests that the relationship of EPS-production rate with substrate consumption rate seems to depend on the kind of microorganisms involved and system conditions. Furthermore, it can be observed that the sludge respiration rate in second, third and fourth segments of FDHS systems were under low OLR or limiting carbon source in influent wastewater. This suggests that fungi are more capable to consume soluble EPS as the carbon source (Belén et al. 2006).

4.11.4 Dead Cell Fractions

In this study, dead cells fractions can include the residues of dead cells, captured suspended solids, and inorganic precipitates as results shown in Table 4.12. Based on the calculation, the ratios of dead cells to total biomass of all fungal and bacterial sludge were in range of 8-40.8% and 14-61%, respectively. That seems to be bacterial sludge contained dead biomass fraction in sludge is higher concentration than fungal sludge. The ratios of dead cells to total biomass increased during DHS height decrease.

4.11.5 Sludge Retention Time (SRT)

The sludge of two DHS systems were calculated according to the following Equation 4.9 as results were showed in Table 4.14.

$$\text{SRT} = \frac{XV}{X_R Q_W + (Q - Q_W) X_e} \quad (4.9)$$

Where, V is sponge volume of DHS system, Q_w is wasted sludge flow rate of recirculation line (L/d), Q_e is volumetric flow rate of effluent wastewater (L/d), X is VSS concentration in harvested sponge (mg/L), X_e is VSS concentration in wasted sludge (mg/L), X_R is concentration of VSS in wasted sludge in recirculation line (mg/L).

Table 4.14 Sludge retention time of two DHS systems

System/Operating Conditions	SRT (days)		
	RUN I	RUN II	RUN III
FDHS	187	204	61
BDHS	48	132	27

In general, the organic and nitrogen removal increases with the increase sludge age. Those results shown that higher organic removal performance of FDHS system can be attributed longer SRT than BDHS system. However, two DHS systems were possibility due to the long sludge age or longer SRT in RUN I, which was calculated to be 187 days of FDHS system and 48 days of BDHS system considering the sludge input, retained biomass, its degradation and yield. The value of FDHS system in RUN I was more than double that of extended aeration system, which ranges from 20-40 days (Metcalf and Eddy, 2003).

4.11.6 Sludge Morphology

The morphological and structural characteristics of two DHS sludge were investigated using scanning electronic microscopy (SEM) are shown in Figures 4.21 and 4.22. The retained sludge was consisting mainly small granules in sponge pore and biofilm formation on sponge surface. Results suggested that bacterial sludge exhibited a denser and more compact structure than fungi with a variety of morphotypes, embedded in extracellular polymeric substances, dominated. Mycelial granules consisting of fungi and filamentous microorganisms formed the loose filamentous granular and biofilm that presence the sufficient high in substrate and oxygen mass transport. Fungal culture has potential application as immobilized cell systems, because of their shape, may not require cross-linking or entrapment (Tung et al., 2004). However, bacteria can be formed filamentous structure but SEM photos show a little filamentous microorganism in BDHS sludge. This may cause of insufficient conditions in BDHS system not suitable to promote filamentous bacterial growth.

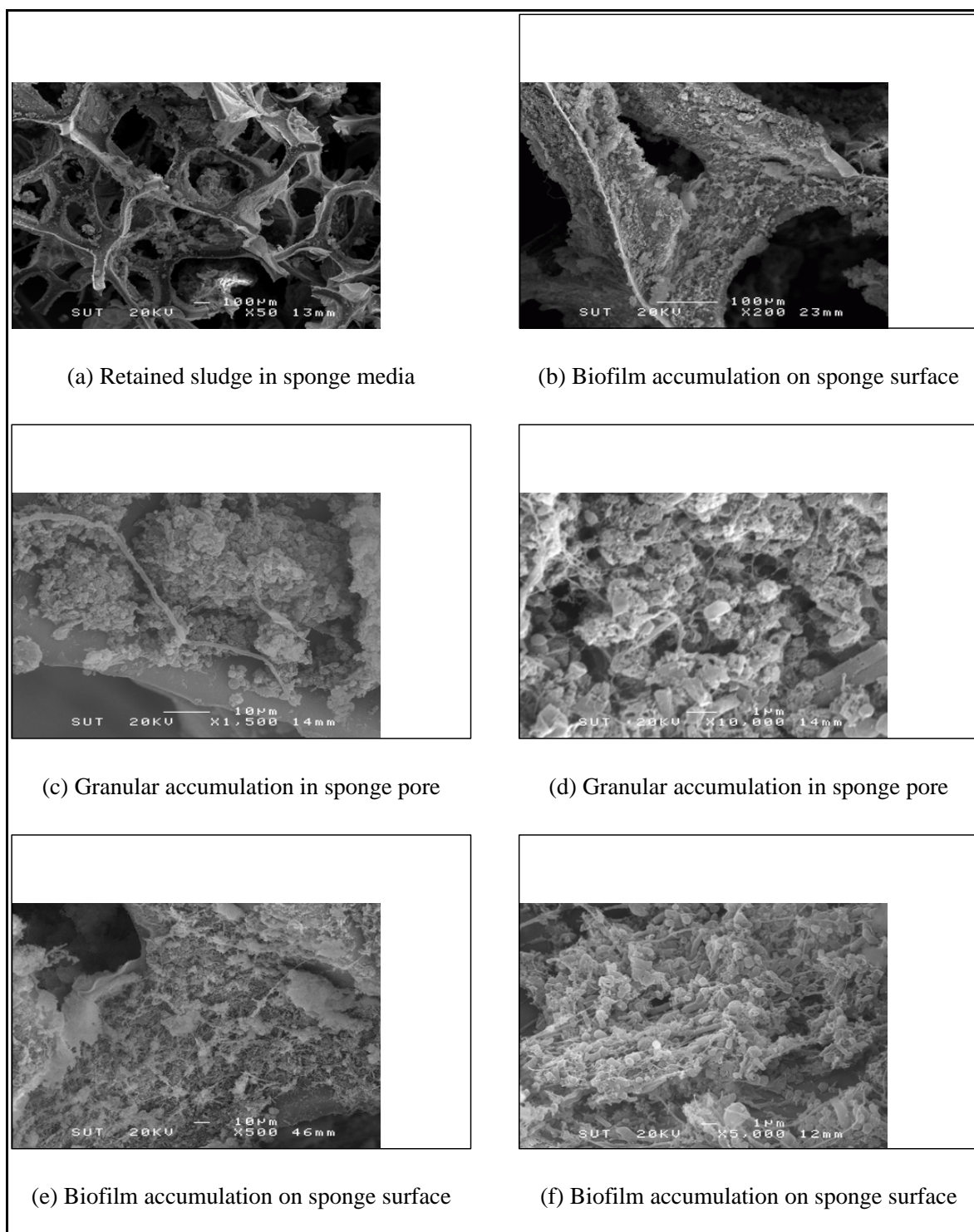


Figure 4.21 Sludge Morphology of BDHS System by SEM Photos

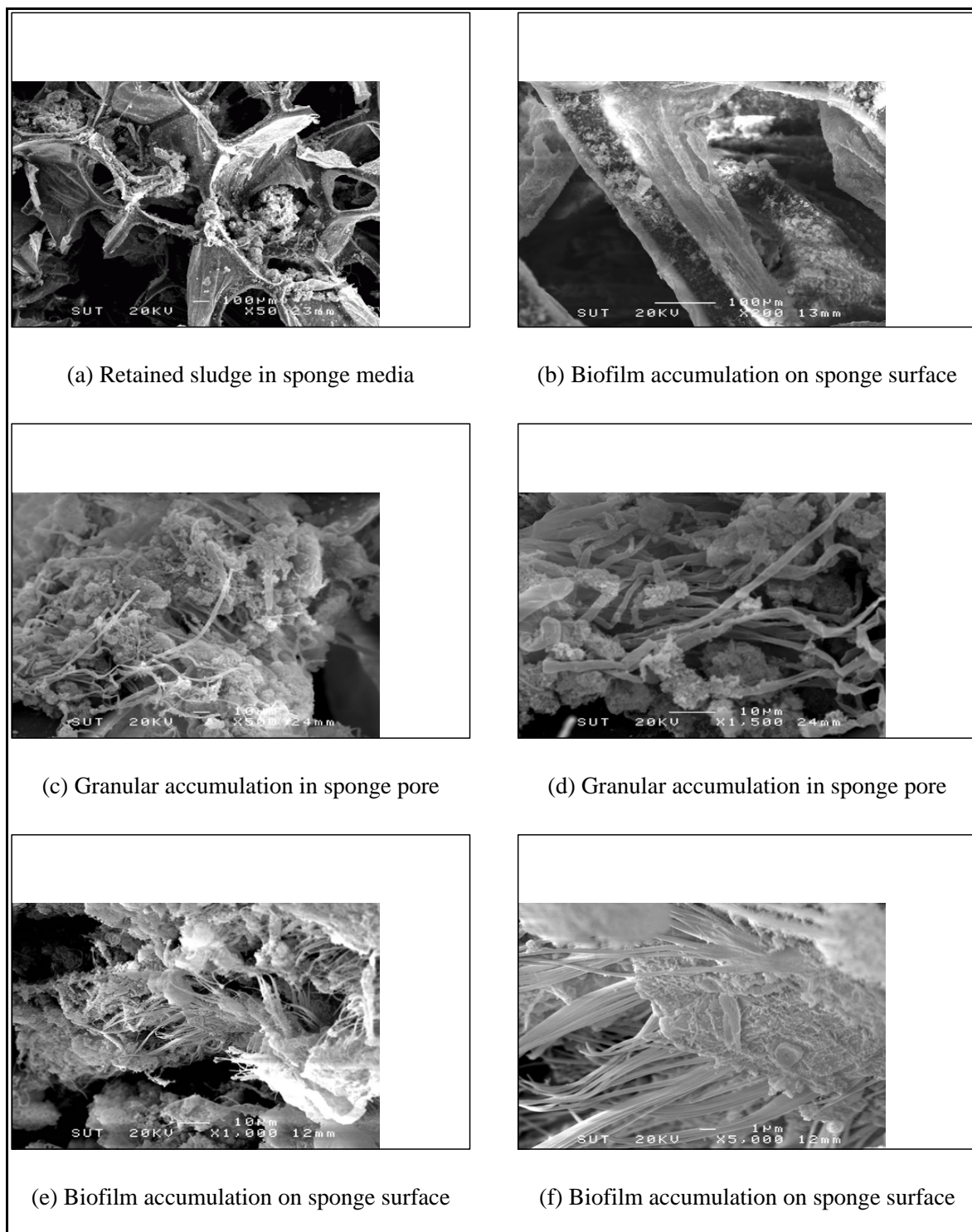


Figure 4.22 Sludge Morphology of FDHS System by SEM Photos

4.12 Effect of Extracellular Polymeric Substances (EPS) on Effluent

Organic Matter Concentrations

Effluent from biological wastewater treatment contains complex and heterogeneous soluble organic compounds. The so-called effluent organic matter (EfOM) is composed of refractory compounds, residual degradable substrate, intermediates, end products, complex organic compounds, and soluble microbial products (SMP). The SMP are organic compounds that are biologically derived from substrate metabolism during biomass growth (utilization associated products, UAP) and that are released from cell lysis during biomass decay (biomass-associated products, BAP). The SMP are found to be the majority of soluble organic matter in wastewater effluent. The characteristics of EfOM and/or SMP from different wastewater treatment plants vary due to differences in treatment processes and their operational conditions. Several process parameters influence the production and properties of SMP, leading to the different quantities and qualities of EfOM. Formation of SMP was found to increase during stress conditions, e.g., hydraulic shock loads, low pH, nutrient deficiency, and presence of toxic compounds, etc. With an increase of feed strength, the SMP–UAP concentration increased, whereas the SMP–BAP concentration decreased. However, the SMP–UAP was more biodegradable than the SMP–BAP, therefore, the accumulation of the SMP–BAP was expected in most biological treatment systems ([Jarusutthirak, C. and Amy, G., 2007](#)).

As EPS are microbial mass produced, which are not active cells, they represent a diversion of electrons and carbon that could otherwise be invested in cells yield and growth rate. Hence ignoring EPS formation could lead to a general overestimation of true cellular growth rate. Moreover, both soluble microbial products (SMP) and the soluble component of EPS may contribute to the residual soluble COD causing the lower effluent quality. Macromolecular compounds such as protein and carbohydrate can comprise a significant

portion of dissolved organic carbon in the DHS effluents (about 60-70% of effluent COD; details shown in Table 4.15). Several researchers found that the chemical components of SMP consisted mainly of proteins, polysaccharides, and organic colloids, and that the SMP and EPS were identical (Wichitsathian, B., 2004; Jarusutthiruk, C., and Amy, G., 2007; Yan, M. E., et al., 2007). The presence and characteristics of effluent organic matter and/or SMP in wastewater effluent are of great interest with respect to discharge quality and the efficiency of advanced treatment facilities.

Table 4.15 Soluble EPS concentrations in the DHS effluents

DHS Effluents	Soluble EPS (mgCOD/L)					
	RUN I		RUN II		RUN III	
	BDHS	FDHS	BDHS	FDHS	BDHS	FDHS
Segment 1	132.8	199.8	53.0	119.9	169.7	165.4
Segment 2	126.0	187.3	50.9	107.8	179.2	145.3
Segment 3	123.0	175.5	56.6	98.6	189.1	140.2
Segment 4	121.6	170.2	55.2	93.7	136.4	146.3

4.13 Effect of Treatment Loading on Sludge Compositions

Experience over the years with biofilms and other microbial processes have suggested that many physical, biological and chemical factors affect the structure to various extents. The hydrodynamic shear, mass transfer, detachment, substratum texture and particulate matter are among the physical forces whereas substrate concentration, physico-chemical environment, type of substrate and nutrients are some of the chemical factors reported to influence biofilm structure. The investigation into the influence of each of these parameters on biofilm structure is straightforward; however, the biological parameters (physiology of cells, microbial population and EPS) remain intermingled with the above and present a formidable problem. Conceptual and mathematical modeling attempts have

been made to describe the influence of some of the factors on biofilm structure. However, very little experimental evidence is available as to how each of the factors sighted; influence the structure due to the difficulty in developing appropriate methodologies for studying each independent event.

In this study, the effect of substrate and hydraulic loading on biofilm composition/structure were investigated by analyzed the concentrations of viable or active cells, EPS and dead cells during three runs as results shown in Figure 4.23. The inert or dead cells of BDHS sludge increased in every segment with organic and hydraulic loading rate increase (RUN II, RUN III) with caused of decreasing in viable cell fractions. Sludge composition fractions were not different in FDHS system during three runs. However, viable cells were decreased gradually in all 4 segments of BDHS and FDHS systems. This caused of low substrate concentrations in lower FDHS and BDHS height. Moreover, hydrodynamic strength is one of the key parameters that influence microbial adhesion (Busscher and van der Mei, 2006) and biofilm formation (Liu and Tay, 2002; Wa'she et al., 2004). A wide literature is available on the influence of hydrodynamic conditions on the physical structure of the biofilms; high shear forces usually result in thinner, denser and stronger biofilms (Kwok et al., 1998; Liu and Tay, 2002; Laspidou and Rittmann, 2004a).

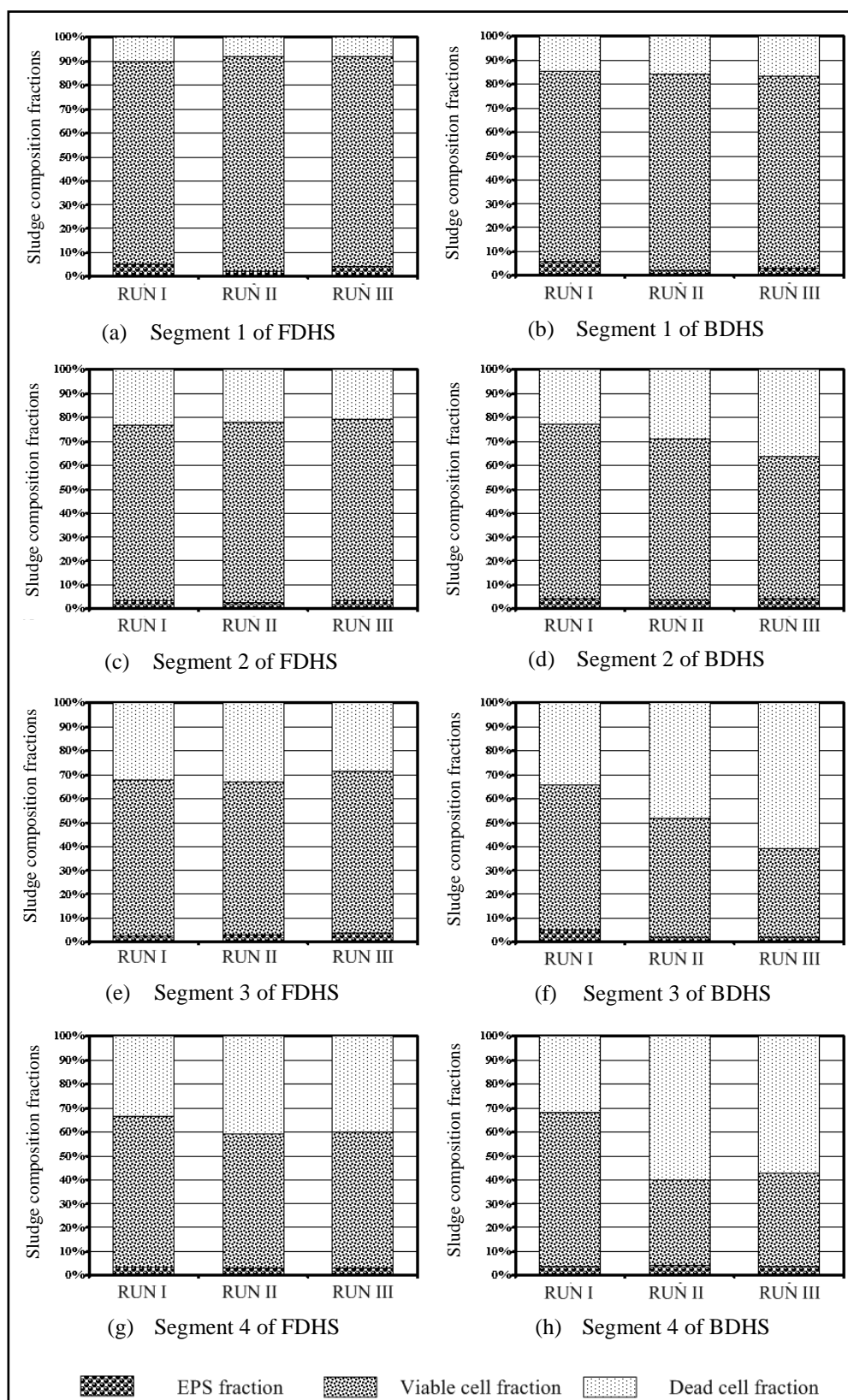


Figure 4.23 The fractions of two DHS sludge compositions

However, little is known about the effect of shear stress on the microbial composition of biofilms. Recent works showed that hydrodynamic conditions influence the composition and diversity of freshwater biofilm communities (Rickard et al., 2004; Besemer et al., 2007). Also, Rochex et al. (2008) recommended shear stress affects the composition biofilm of bacterial communities. High shear stress decreases biofilm diversity which confirms the effect of shear on biofilm diversity in another environment (simulated industrial conditions). The dynamics of biofilm communities also change in relation to shear stress. Our results suggest that shear stress would slow down biofilm maturation and tend to maintain a young biofilm. Furthermore, biofilm growth rate was positively influenced by substrate loading. It was demonstrated that biofilm internal microstructure is affected by substrate loading rate with increasingly high substrate concentrations producing increasingly compact biofilms with lower porosity. Specific activities were found to decrease with increasing cell age and biofilm compactness. Slowly growing biofilms having porous structures were found to have higher specific activities, which exemplifies the importance of microstructure for mass transport. The spatial competition between nitrifiers and heterotrophs is one of the limiting criteria for stable nitrification. The ammonia oxidizer spatial organization is strongly related to the structure of the biofilms. They were exclusively found close to the top surface in dense biofilms and close to the pores in porous biofilms. The higher ammonium concentrations seem to select for the faster growing ammonia oxidizer strains. The above findings provide clear experimental evidence concerning the influence of substrate loading on biofilm structure and function (Wijeyekoon et al., 2004). Furthermore, the same sponge media was used during three experimental runs via flushing reactor by tap water about 12 h with inflow rate 550 L/d to remove some of the retained sludge before starting the new runs. This seems to be effect on the sludge compositions and its density during RUN II and RUN III. High values of dead cell fraction were accumulated in DHS sludge this promised the higher biofilm

density during the start up period of RUN II and RUN III. However, at steady state conditions, the overall process performance of two DHS systems were rather constant. This can explained by inert biomass was degraded or washed out of the system by hydraulic shear strength during the initial of startup period. Moreover, the sludge composition was balance at the steady state condition. Few past studies reported endogenous respiration of DHS sludge suggesting that the sludge accumulation was in near balance with degradation of sludge in reactor itself (Tandukar et al., 2006a; Tawfik et al., 2006a)

4.14 Problems and Limitation of DHS Systems

4.14.1 The development of predators

The development of predators (e.g. worms, filter flies etc.) has caused serve problems in BDHS system in sustaining organic and nitrogen removal. Won et al. (2004) observed that fly larvae rapidly spread throughout the biofilter reactor and biomass was rapidly removed from the packing, initially at a rate of 13.1 kg wet weight/m³-day and increasing up to 70-140 kg/m³-day of reactor. In that case, the wet biomass content in the reactor was reduced from 455 to 28 kg/m³ of reactor in 16 days with 80% of biomass reduction occurring in 2-4 days. An aspect of biofilm control in BDHS system concerns prevention of and the control of predators. The key to controlling the level of nuisance organisms is finding a condition toxic to the target nuisance organism that either no effect upon or is only temporarily inhibiting to organic and nitrogen removal of BDHS system. This study used substances toxic to eukaryotic organisms (Cypermethrin) to control biofilm predators (Parker et al., 1997; Grant et al., 2002). However, it's not observed the predator aspect in FDHS system. This can be explained by a study of Prakash et al. (2008) showed that the toxicity of fungal spore on earthworms which included of 14 different species

belonging to the genera, *Aspergillus*, *Chaetomium*, *Cladosporium*, *Cunninghamella*, *Fusarium*, *Mucor*, *Penicillium* and *Rhizopus*.

4.14.2 Filter clogging

Several physico-chemical and biological phenomena can be involved in the clogging. The evolution of the head loss of biofilter process is mostly caused by the accumulation of solids and the growth of biomass. For high filtration rates, the inert particles and the biofilm detached from the support are distributed deep in filter, hence accelerating the clogging (Bihan and Lessard, 2000). During whole experimental study, filter clogging aspect was observed in RUN I of BDHS system. We control this phenomenon by hydraulic flushing (tap water) with inflow rate 550 L/d every 30 days of operating period.

4.15 Operating Cost Analysis

In comparison of overall performance of FDHS and BDHS systems, the operating cost analysis of two DHS systems was evaluated. Chemical using for pH adjusts is only one main operating cost of BDHS and FDHS systems that results are illustrated in Table 4.16. The activated sludge process (ASP) has long been a main in the world of wastewater treatment especially in industrialized or developed countries through it is complex and expensive system. Stare et al. (2007) was study on the operating cost of IWA activated sludge model No. 1 (ASM1) with inflow rate 300 m³/d (Table 4.17). Results of this past study suggested that requirement of aeration and production of huge amount of excess sludge is two main drawbacks of ASP in spite of its superior performance. Likewise, cost for sludge handling in ASP constitutes up to 40% of the total operating cost.

Table 4.16 The operating cost of BDHS and FDHS treatment systems

Treatment systems	Chemicals requirements (kg/m ³ wastewater)		Chemicals cost per unit (Baht/kg)		Sponge cost (Baht/m ³)	Sponge replacement cost @ every 5 years (Baht/m ³ wastewater)	Operating cost (Baht/m ³ wastewater)
	NaOH	H ₂ SO ₄	NaOH	H ₂ SO ₄			
BDHS	0.19	-	15	-	400	6.30×10 ⁻⁵	2.85
FDHS	-	1.05	-	12	400	6.30×10 ⁻⁵	12.60

Table 4.17 The operating cost of IWA activated sludge model No. 1 (ASM1) was operated with inflow rate 300 m³/d (Stare et al., 2007)

	Cost (€d)	Cost* (Baht/d)	Cost (Baht/m ³)
Aeration costs	576	30,528	101.8
Sludge disposal costs	1,258	66,674	222.2
Carbon costs	264	13,992	46.6
Effluent fines	976	51,728	172.4
Total operating costs	3,074	162,922	543.1

Remark: * Based on average exchange rate on February 2010 (1 €= 53 Baht)

However, regarding operation and maintenance of the reactors, ASP is labor-intensive and demands regular and skilled operation and maintenance to ensure proper functioning of moderately complex equipment.

This result seems UASB-DHS system could be a better option as it has very less mechanical and electrical appurtenances and thus less threatened by power outages. Moreover, since it is a simple system, it does not demand highly skilled personnel for its operation and maintenance, which is one of constrains in developing countries.

CHAPTER V

MATHEMATICAL MODELING OF BIOFILM COMPOSITION AND DENSITY DYNAMICS

5.1 Application of the UMCCA Model for Biofilm Composition and Density in two DHS Systems

5.1.1 Simulated Dynamics of Biofilm Compositions

In this study applied a mechanistic, multiple component model – the UMCCA model for the quantitative simulation of the biofilm's heterogeneity through many components related to a biofilm system: three solid species [active biomass (X_a); inert or dead biomass (X_{res}) and extracellular polysaccharides (EPS)], and three soluble components [soluble organic donor substrate (S) and two types of soluble microbial products (UAP and BAP)]. Simulation results by using the UMCCA model showed how the six components varied, on average, along the depth of biofilm for segments 1-4 of FDHS and BDHS systems as shown in Figures 5.1-5.6. Each graph (Figures 5.1-5.6) of the model shows 70 data points, one for the average of every row of the grid, and error bars show the two standard deviations one above and one below the mean. The simulated data are shown in Appendix G (Table G.3-G.8). All variables on the abscissa (Y-axis) are dimensionless, while the ordinate (X-axis) represents the biofilm depth and ranges from 0 to 280 μm , corresponding to termination time or biofilm age (*Bioage*) for each segment of BDHS and FDHS systems as illustrated in Table 5.1.

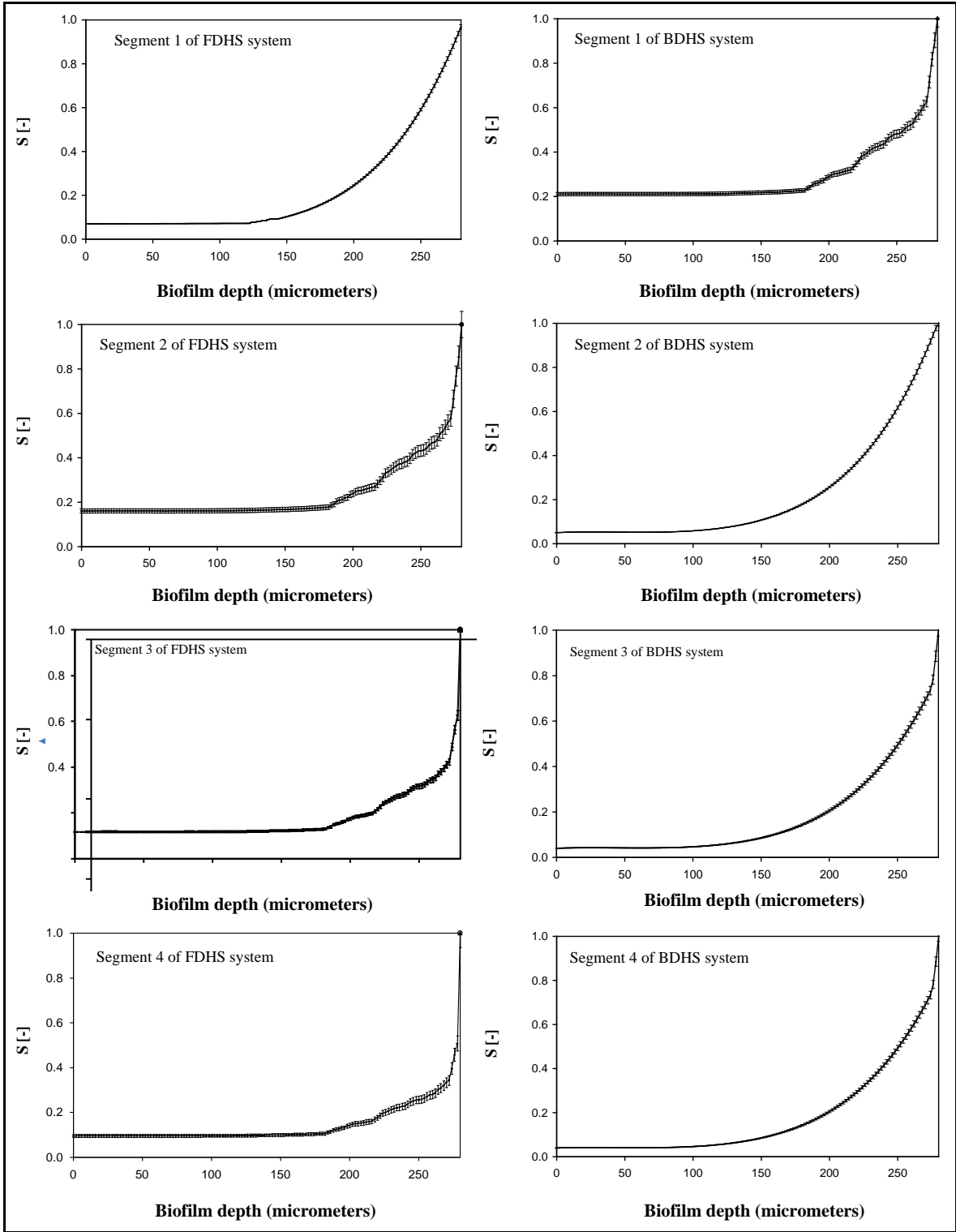


Figure 5.1 Simulated soluble organic donor substrate (S) profiles along the biofilm depth in four segments of FDHS and BDHS systems

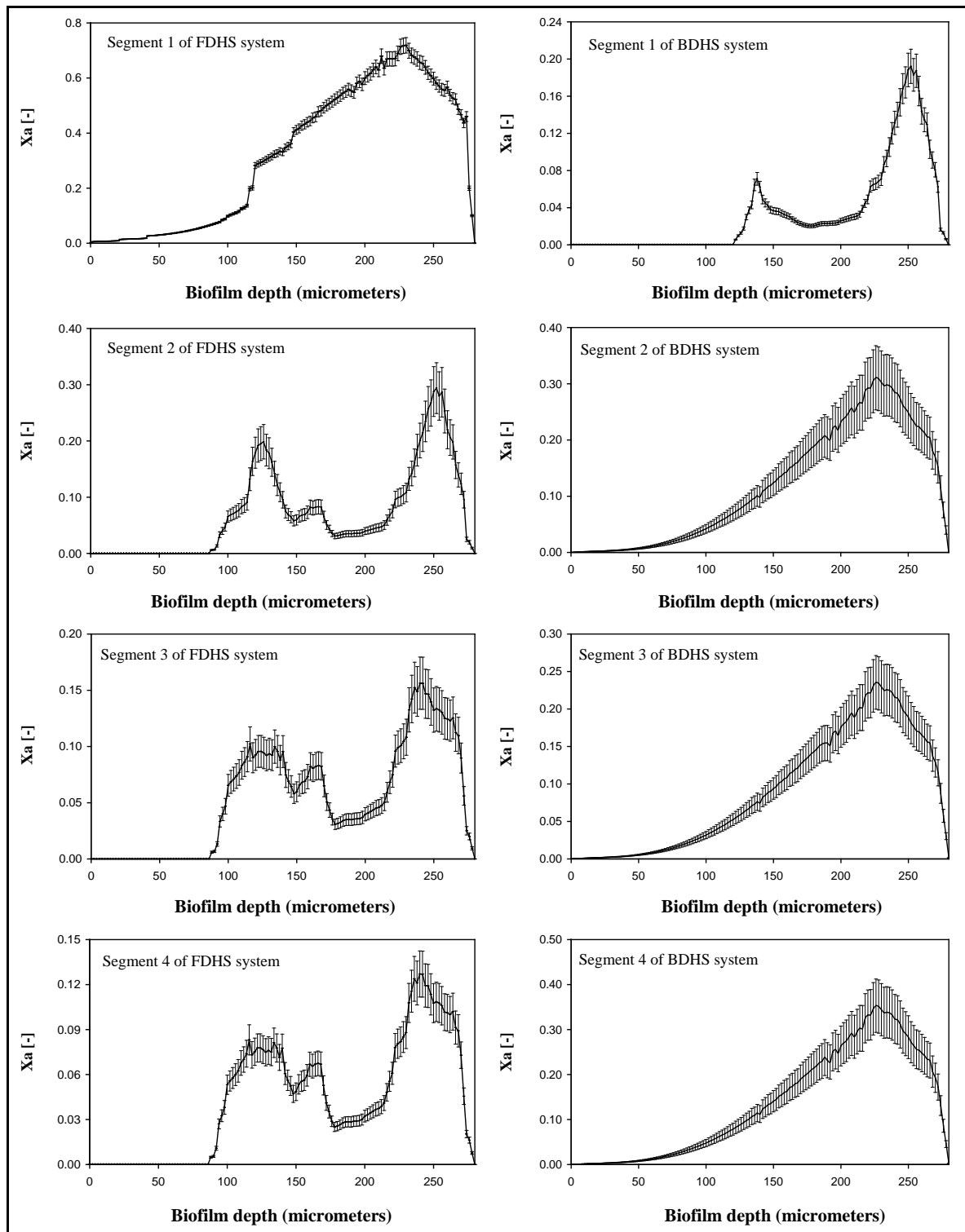


Figure 5.2 Simulated active biomass (X_a) profiles along the biofilm depth in four segments of FDHS and BDHS systems

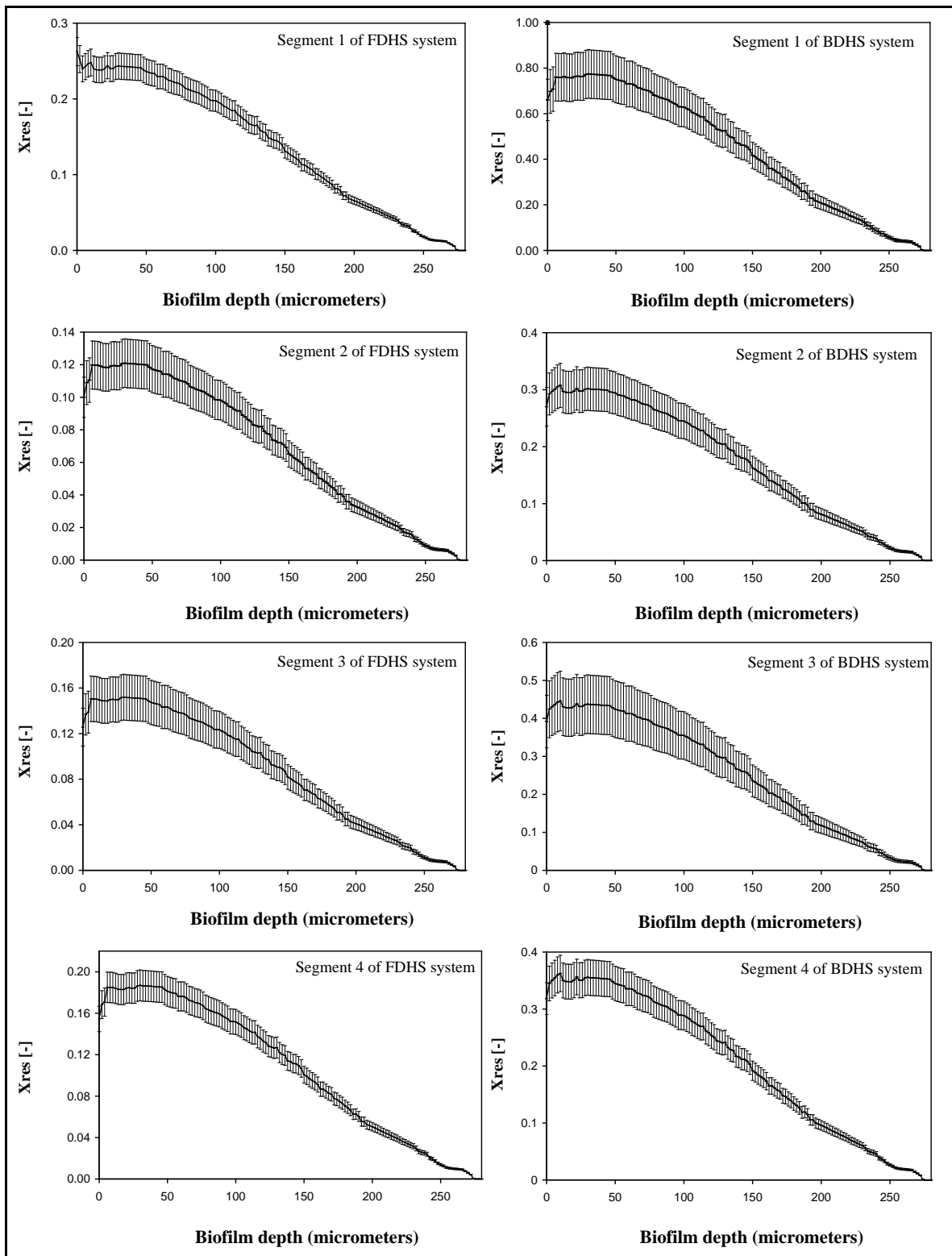


Figure 5.3 Simulated residual or inert biomass (X_{res}) profiles along the biofilm depth in four segments of FDHS and BDHS systems

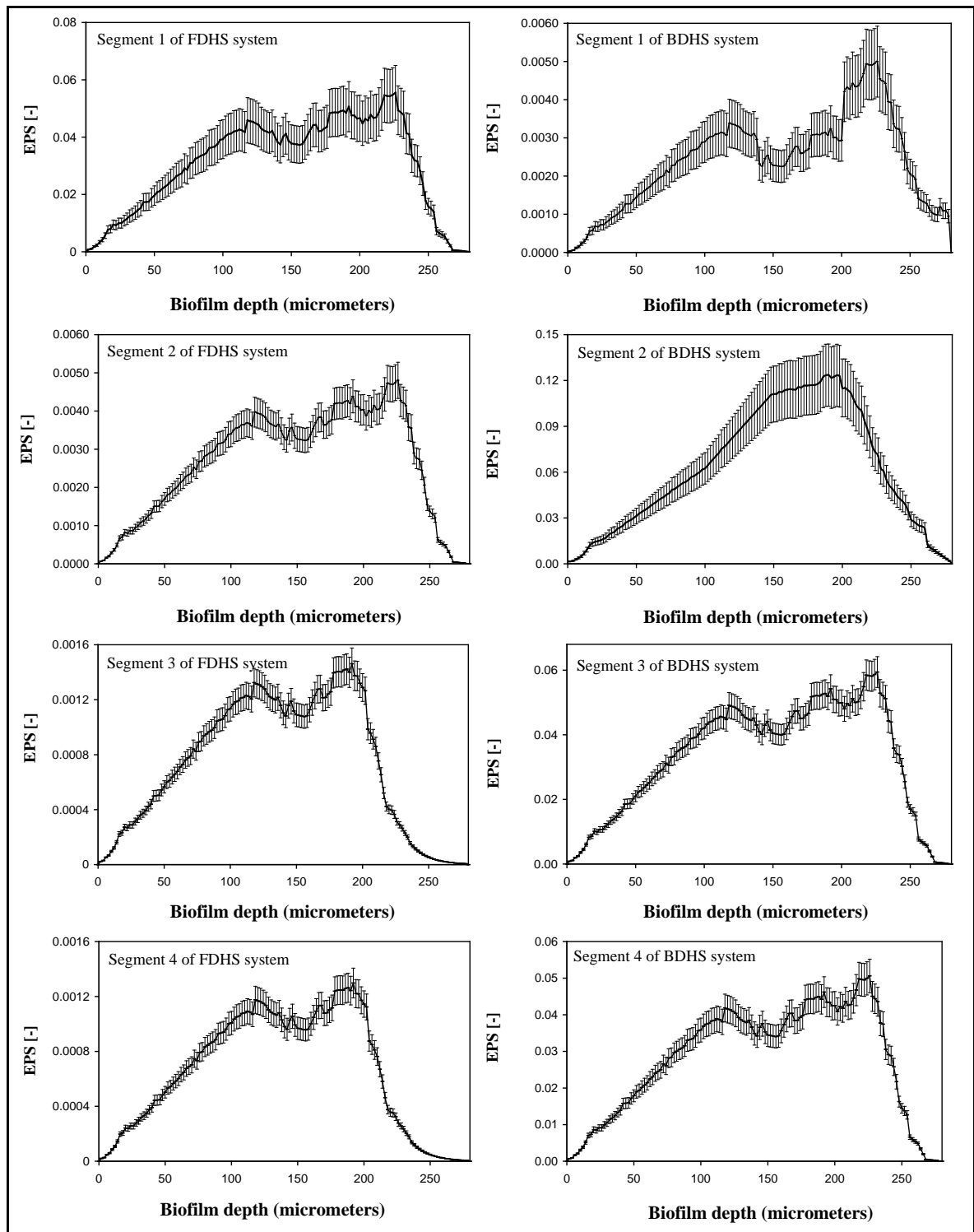


Figure 5.4 Simulated extracellular polymeric substances (*EPS*) profiles along the biofilm depth in four segments of FDHS and BDHS systems

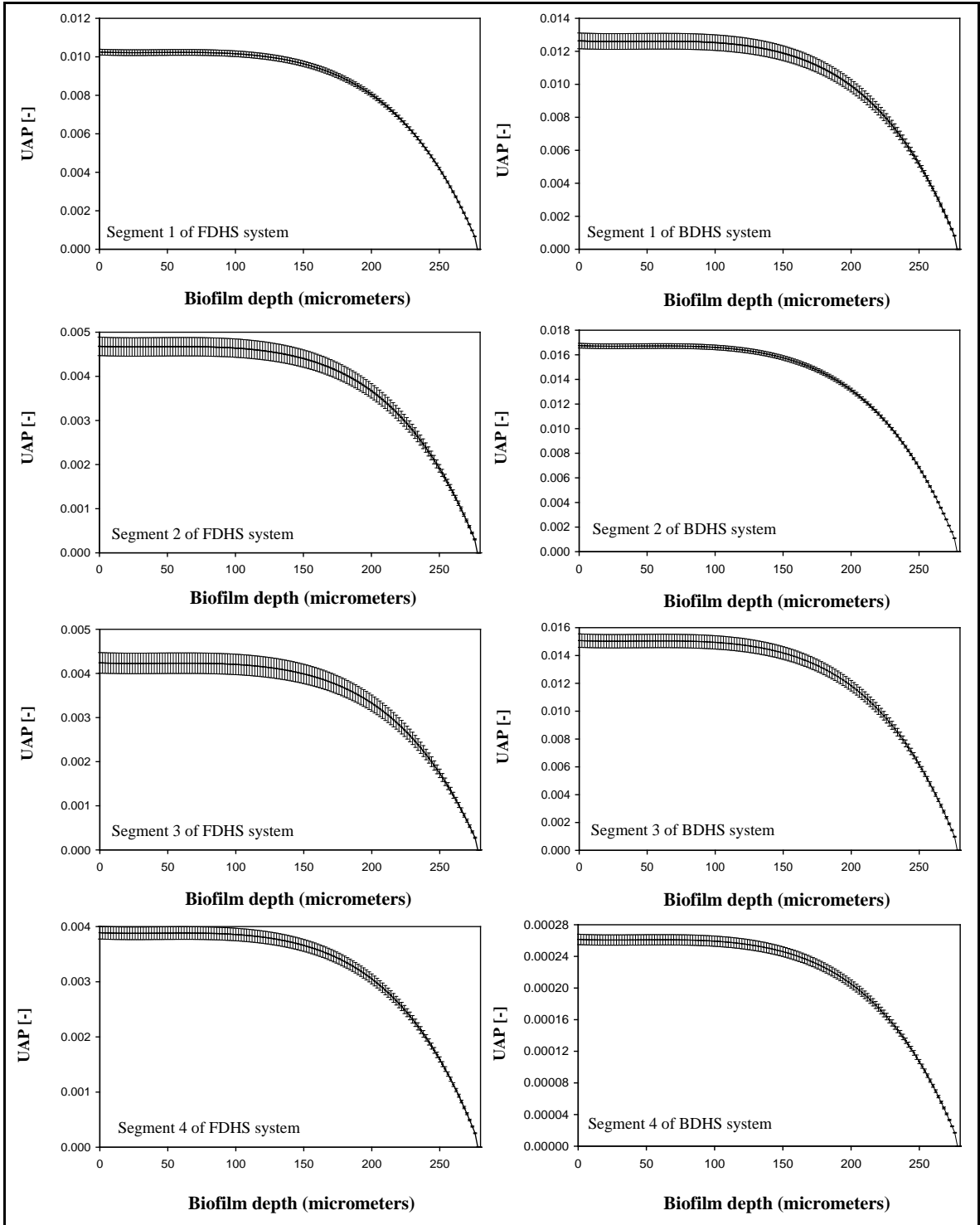


Figure 5.5 Simulated utilization-associated product (*UAP*) profiles along the biofilm depth in four segments of FDHS and BDHS systems

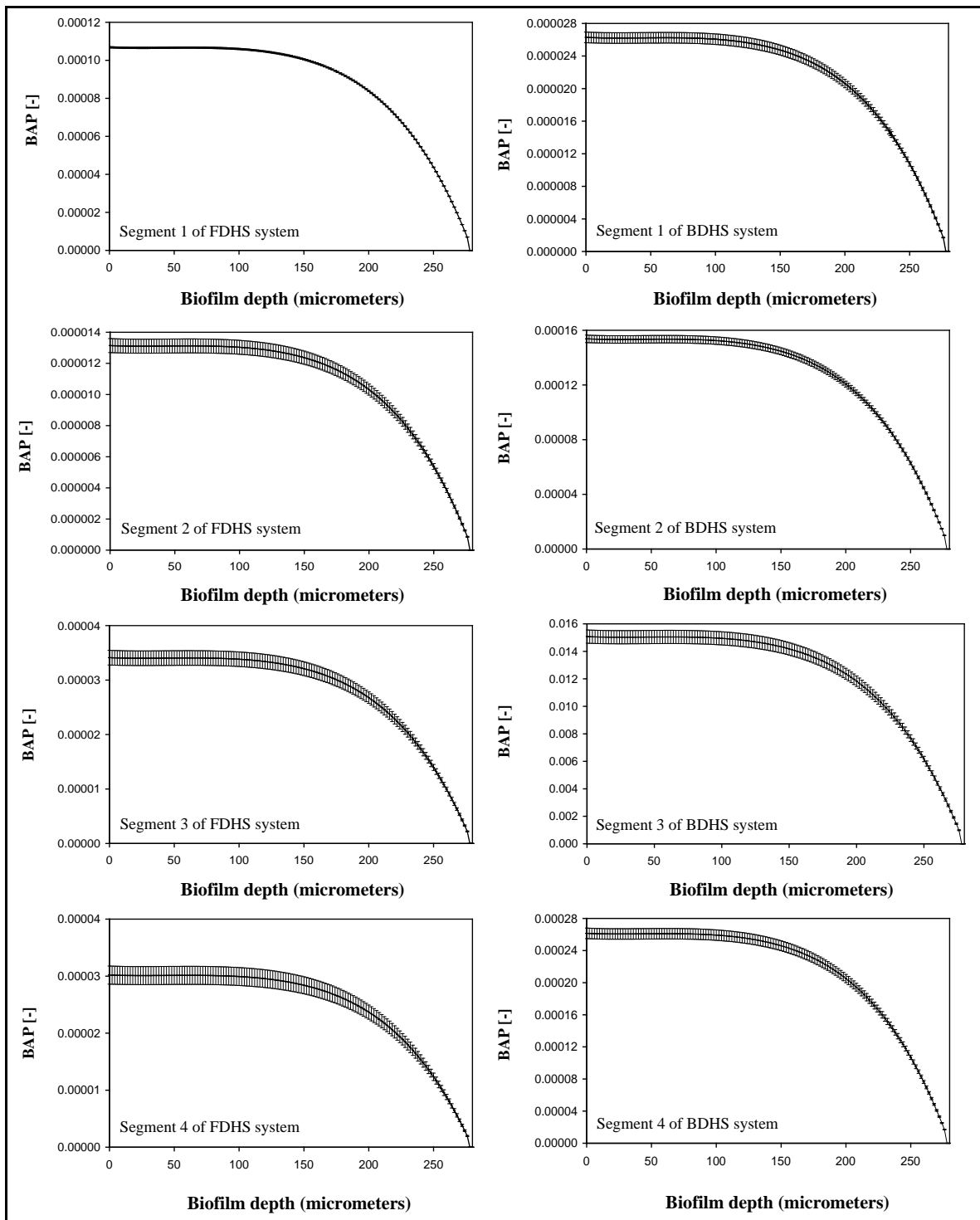


Figure 5.6 Simulated biomass-associated product (*BAP*) profiles along the biofilm in four segments of FDHS and BDHS systems

Table 5.1 The run termination time (*Bioage*) sufficient in 280 μm of the biofilm depth

DHS Profiles	<i>Bioages</i> (days)	
	FDHS	BDHS
Segment 1	45	245
Segment 2	180	65
Segment 3	180	145
Segment 4	180	105

The simulation run termination time of segments 2 to 4 of FDHS system and segments 1, 3 and 4 of BDHS system were much longer than for the segments 1 and 2 of FDHS and BDHS system, respectively. This could possibly be explained by the fact that active biomass and EPS growth were slowed down significantly due to the low substrate or oxygen concentrations.

(i) **Simulated Organic Donor Substrate (*S*) Profiles along Biofilm Depth**

The substrate mass balance (Equation 3.4) was solved for all locations follow the solution algorithm (Figures 3.9 and 3.10) to define the substrate field at time $T+\delta t_b$; while the biomass field was kept constant. This computation was then repeated until the substrate concentration converged to steady state. This was done using a strategy similar to that described in [Lapidou and Rittmann \(2004\)](#), i.e. keeping the biomass density unchanged, while iterating until the substrate concentration field converged to a steady-state condition, and using a time step δt_s of about 1s to solve the substrate field, and a time step δt_b of 1000s to incorporate changes in biomass. The substrate field solution by a numerical method was also applied that followed the scheme presented by [Picioreanu et al. \(1998\)](#) and [Lapidou \(2003\)](#) with a finite-difference discretization scheme that was then solved with the alternating-direction implicit (ADI) method.

Results showed that the substrate concentration decreased with distance from the top surface of the biofilms (Figure 5.1). The substrate concentrations within each row stayed relatively constant, so the concentration was determined almost totally by distance from the substratum, not by lateral position. The error bars were very small, signifying the small variability (low σ) of substrate concentration within each row. On the other hand, column variability was high (high σ), for every column (Tables G.1-G.8). Thus, lateral diffusion in the biofilm was sufficient to “level out” the substrate concentration, despite differences in utilization rate due to different densities of active biomass.

When compared for each segment of two DHS systems, organic donor substrate concentration appeared to have much greater variability substrate concentrations for segments 2 and 4 of FDHS system, and segment 1 of BDHS system. Of high significance is the fact that the variability of original substrate was greater for biofilm depths, higher than 150-200 μm , where most of the growth was concentrated in one mushroom cluster as explained in detail in Section 2.15. This non-uniform pattern for substrate explains why the large clusters preferentially developed in biofilm. Once a new cluster develops above the top of the other clusters, it is exposed to a higher substrate concentration than the other clusters, and this gave it a growth-rate advantage. This cluster effect was not present in segment 1 and 3 of FDHS system and segment 2, 3 and 4 of BDHS system, because S_{max} was sufficiently greater than K_s so that the biomass growth rate was not sensitive to differences in S_{max} (Table 5.2) (Laspidou and Rittmann, 2004a; Picioreanu et al., 1998a). However, S_{max} even if was also greater than K_s in segment 1 of BDHS system the dissolved oxygen concentration in wastewater was about zero (Section 4.6.1). The lower dissolved-oxygen concentration caused a slower growth rate and, hence, a longer time to have some biomass in each compartment. Laspidou and Rittmann (2004b) suggested that, under low dissolved oxygen conditions (bottom row of biofilm had 0.49 mg DO/L), cavities form at the base of an old biofilm. Hence, the integrity of the base of the

biofilm is compromised when low dissolved-oxygen concentration leads to a biofilm with cavities at its base. Such loss of biofilm integrity in its base can be extended to possibly provide an explanation for biofilm sloughing, a phenomenon not well understood so far.

Table 5.2 Comparison of S_{\max} and K_s values

DHS profiles	FDHS system		BDHS system	
	S_{\max}	K_s	S_{\max}	K_s
Segment 1	336	92	336	55
Segment 2	75	100	240	81
Segment 3	64	52	157	50
Segment 4	74	80	136	100

(ii) Simulated Biomass Species (X_a , EPS, X_{res}) Profiles along Biofilm

Depth

Mathematical modeling was used in this study to quantify the relationships among three solid species – active or viable cells, EPS, and residual inert biomass following Equations 3.7, 3.8 and 3.9, respectively. Active biomass decays in two ways. Part of the active biomass is oxidized by endogenous respiration (path 5 in Figure 3.9) to yield energy for maintenance. The rate is proportional to the biodegradable fraction of the active biomass (f_d), the endogenous-decay coefficient (b ; T^{-1}), and the active biomass concentration (X_a). Acceptor is consumed at the same rate. Biomass decay produces residual inert biomass (X_{res}) in proportion to the rate of endogenous decay (path 6 in Figure 3.9) and the fraction of the active biomass that is not biodegradable ($1-f_d$). EPS dissolution/hydrolysis produces BAP (path 7 in Figure 3.9), with a rate proportional to EPS and with k_{hyd} being the first-order rate coefficient (T^{-1}). As discussed in [Laspidou and Rittmann \(2002a\)](#), hydrolysis of EPS is the only source of BAP. Overall, active biomass was very low in the bottom rows of the biofilm column, peaks just above the middle rows,

and drops down to lower values in the top rows (Figure 5.2). In the bottom rows, active biomass was close to zero, because the termination time (*bioages*) was long enough for all the initially synthesized active biomass to decay almost completely and turn to residual inert biomass (X_{res}), which was relatively high. Thus, X_{res} had its highest concentration below the point where the active biomass peaks (Figure 5.3). The top of the biofilm also had a low concentration of active biomass, but for the opposite reason: the biofilm was very young and had not had enough time to synthesize and consolidate biomass that completely fills in the top compartments; thus, the active biomass and the inert biomass were close to zero at the top. Although the average active biomass concentration was low in the top and bottom rows, the variability (error bars) was high only in the top rows. This was true because, in the top rows, even if some compartments were relatively full, most were almost completely unoccupied, resulting in a low mean value with a high standard deviation. In the bottom rows, the mean value was close to zero, because most compartments had active-biomass concentrations close to zero, due to extensive decay; thus the standard deviation was close to zero as well.

All EPS concentrations trends were similar to active biomass, thus the values were lower than active biomass throughout the biofilm depth (Figure 5.4). The biofilm was “old”, near the bottom of the biofilm, and EPS had decayed to *BAP*. EPS was at a low concentration in the top layers, since its formation depended on the presence of active biomass, which was very sparse at the top of the biofilm. EPS showed small-scale heterogeneity similar to that of active biomass. The standard deviation by row was low in the bottom rows and got higher for the top rows, where many of the compartments were nearly unoccupied.

Due to the lower substrate and oxygen concentration throughout much of the biofilm, active biomass and EPS were lower throughout the biofilm for lower oxygen and S_{max} cases (segment 1 of BDHS system and segment 2, 3 and 4 of FDHS system).

Active biomass and EPS dip at about the 150 μm biofilm depth, because almost all biomass at was in one “mushroom”-shaped cluster. The large cluster had little active biomass (and EPS) at that depth, because its active biomass was much closer to its top surface. The very top of the mushroom cluster was fluffy, being irregular with small X_a , EPS, and X_{res} . Residual inert biomass was very high in the bottom rows, since the biofilm in the bottom rows was very old and, hence, fully consolidated (i.e. $U_c = 1$). The plateau from about 150 to 200 μm occurred with the transition to all the biomass being in the one mushroom-like cluster above 150 μm .

(iii) Simulated Soluble Microbial Products Profiles along Biofilm Depth

The first type of soluble microbial products (SMP) is utilization-associated products (UAP), which are produced as a direct result of substrate utilization. The formation kinetics of UAP was presented in Equation 3.5. The second category is biomass-associated products (BAP), and they are formed from biomass, presumably as part of decay. The BAP rate is expressed by Equation 3.6. In addition to S , the other two soluble substrates are UAP and BAP, UAP is formed directly during substrate utilization, consumed by active biomass as an electron-donor substrate, and diffuse out of the biofilm through the top surface. Like S , UAP had little heterogeneity across their rows (very small average σ by row, shown in Tables G.3-G.8, and small error bars in Figure 5.5). The UAP concentration was lower throughout the biofilm depth. Moreover, due to the BAP was formed from the hydrolysis of EPS. The BAP concentration was stable, since active biomass was low there and unable to consume BAP.

Like UAP, the BAP concentration declined toward the top surface because of its consumption by active biomass and diffusion to the bulk liquid above the biofilm. The BAP concentrations also had little heterogeneity across the rows (Figure 5.6). UAP concentrations were higher for high S_{max} case (segment 1 of FDHS system and segment 2-4 of BDHS system) than for the other cases. This could have happened because,

although UAP formation was lower due to the lower substrate utilization rate, UAP utilization was also lower due to the lower active biomass. So, UAP became relatively more important when S_{max} was lower. BAP were lower too because their parent compounds—EPS—were also lower.

5.1.2 Biofilm Composite Density Simulation

The UMCCA model was used to compute the composite density of the solid components for every compartment following Equation 3.10. Figures 5.7 and 5.8 are shown the simulated composite density of FDHS and BDHS systems, respectively. The top, where the biofilm was young and irregular, had small composite densities, since all three solid species had low values. With little of any type of biomass and an irregular surface, the top of the biofilm took on a “fluffy” nature. The highest composite density, near the middle of the biofilm, was the result of active biomass, EPS, and inert biomass having significant densities together. The highest composite density did not correspond to the location that has high active biomass. The highest density was somewhat deeper in the biofilm, where inert biomass had time to accumulate. The bottom part of the biofilm had high composite density, composed almost totally of inert biomass. The composite density showed small-scale heterogeneity. Its average standard deviation by row (as a percentage) was among those of EPS, X_a , and X_{res} , while the standard deviation by column was lower than the other solid species (Table G.3-G.8), since combining all 3 solid species (X_a , EPS, and X_{res}) “evens out” their differences. Results showed that average biofilm densities of FDHS system were about 43.8, 20.4, 22.7 and 26.3 gCOD/L for segment 1 to 4, respectively (Table 5.3). The average values in BDHS system were about 99, 58.2, 67.2 and 59.2 gCOD/L for segment 1 to 4, respectively (Table 5.3).

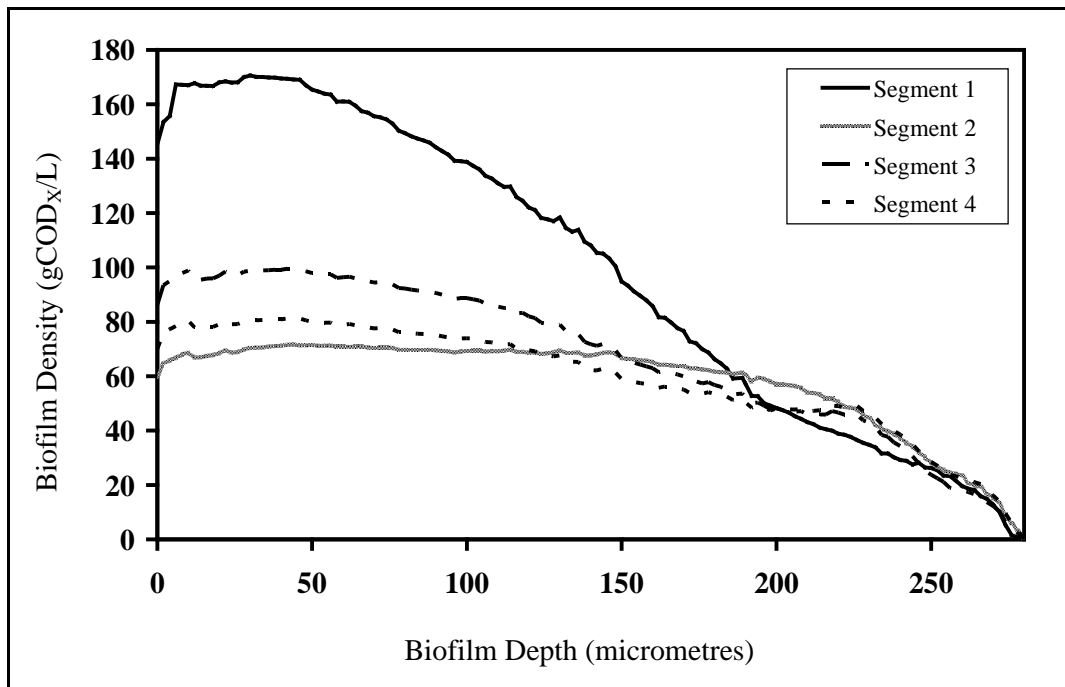


Figure 5.7 Simulated composite densities along the biofilm depth of BDHS system

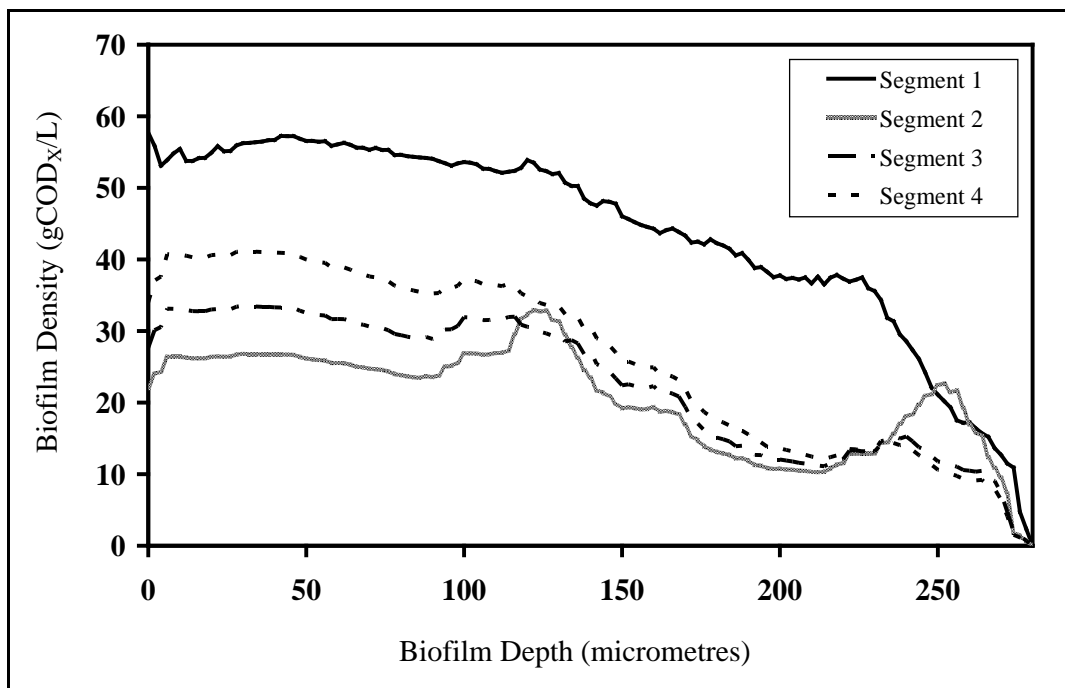


Figure 5.8 Simulated composite densities along the biofilm depth of FDHS system

Table 5.3 Simulated average composite biofilm density in each segment of FDHS and BDHS systems

Parameters	Average composite biofilm densities (gCOD/L)							
	Segment 1		Segment 2		Segment 3		Segment 4	
	FDHS	BDHS	FDHS	BDHS	FDHS	BDHS	FDHS	BDHS
Average	43.80	99.05	20.44	58.19	22.69	67.24	26.33	59.19
S.D.	13.82	55.95	7.24	17.56	9.34	28.27	12.45	20.14

All results indicated that BDHS biofilms were denser than FDHS biofilms. This can be explained by the biomass decay rates (k_d) of FDHS system which were lower than BDHS system. For segment 1, BDHS system had the highest density under low dissolved oxygen concentrations (the value about zero), in such condition active biomass and EPS growth might have slowed down significantly due to the low dissolved oxygen concentration. This simulation run terminated in 245 days, which is much longer than the other runs (Table 5.1) because active biomass and EPS growth were slowed down significantly due to the low oxygen concentration. As a result, the biofilm grew very slowly, while accumulation of residual dead biomass proceeded even in the absence of oxygen, making the biofilm aged and dense.

Simulations with low substrate concentration near and below K_s or lower dissolved-oxygen concentration, promote the formation of the cluster-and-channel structure. Then, once a new cluster developed above the top of the other clusters, it was exposed to a higher substrate concentration than the other clusters, and this gave it a growth-rate advantage. Low substrate or/and dissolved oxygen concentration also slowed the biofilm's growth rate, while accumulation of residual dead biomass proceeds even in this conditions, making biofilm aged, dense, and almost composition was inert. A high specific detachment rate also favored the cluster-and-channel structure and maintains relatively open channels

near the substratum. The high surface-detachment rate accentuated the growth-rate benefit for a protruding cluster. It also kept the biofilm less dense overall, but with a lower proportion of residual inert biomass. Consolidation showed two dramatic trends. First, it makes the biofilm denser overall, and this slowed its vertical expansion rate. Second, consolidation increased the local heterogeneity in all biomass types ([Lapidou and Rittmann, 2004b](#)).

5.1 Influence of Biofilm Density on Mass Transport

Mass transport in biofilms is influenced by the biofilm structure which in turn is influenced by the local availability of substrate. A quantitative understanding of how biofilm structure is linked to mass transport is essential for understanding of biofilms. Solute transport in biofilms is the result of diffusion in the denser aggregates and potentially convective transport within pores and water channels. Diffusion has been shown to dominate mass transport in many biofilm systems ([Horn and Morgenroth, 2006](#)). Moreover, biofilm density and depth are the main design parameters used to evaluate substrate consumption rate in a biofilm. The density of the biofilm increases the reaction rate in the biofilm, meanwhile it limits the diffusion substrate transfer due to the decreased effective diffusion coefficient. Therefore, substrate consumption rate must yield a maximum as a function of biofilm density, whereas the rate controlling step changes from reaction to diffusion. When the biofilm thickness increases, the total reaction volume of the microorganisms increases accordingly and, in turn, the substrate consumption rate of the biofilm increases. However, due to diffusion limitations, an inactive core layer of microorganisms develops with the increasing biofilm thickness and an active portion of the biofilm will be solely responsible for the consumption ([Şeker et al, 1995](#)).

5.1.1 Relative Diffusivity (f_D)

Biofilms are mainly composed of water and the macro scale diffusion coefficient for the biofilm (D_F) is often related to the diffusion coefficient in pure water (D_W) as $D_F = f_D D_W$ where f_D is relative diffusivity. A number of reviews on diffusion in biofilms have summarized the available data (Fan et al., 1990, Hinson and Kocher, 1996, Stewart, 1998). A key motivation of such literature reviews are to identify a relationship between parameters characterizing the biofilm or solute properties and the macro scale diffusion coefficient so that relative diffusivity (f_D) can be predicted. Based on their experimental results evaluating diffusion of phenol in particle fixed biofilms and data from the literatures, Fan et al. (1990) and Horn and Morgenroth (2006) provided an empirical relationship between f_D and the biofilm density (ρ) as follows (Equation 5.1):

$$f_D = 1 - \frac{0.43\rho^{0.92}}{11.19 + 0.27\rho^{0.99}} \quad (5.1)$$

Profiles of f_D along the biofilm depth were obtained for both of FDHS and BDHS systems by Equation 5.1 as shown in Figures 5.9 and 5.10. The average f_D values are illustrated in Table 5.4. Results showed that the f_D values had opposite trends of density. The top, where the biofilm was young and irregular, had high f_D values which were the cause of small composite density. Also f_D values of all segments of FDHS system were higher than BDHS system.

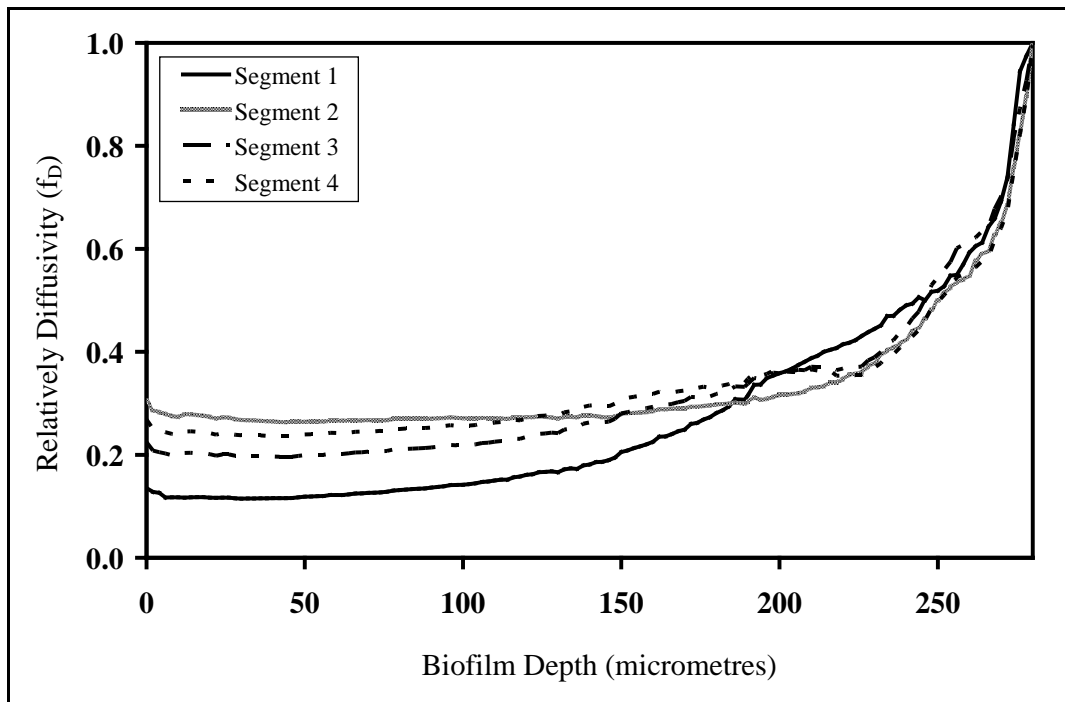


Figure 5.9 Simulated relative diffusivity (f_D) along the biofilm depth of BDHS system

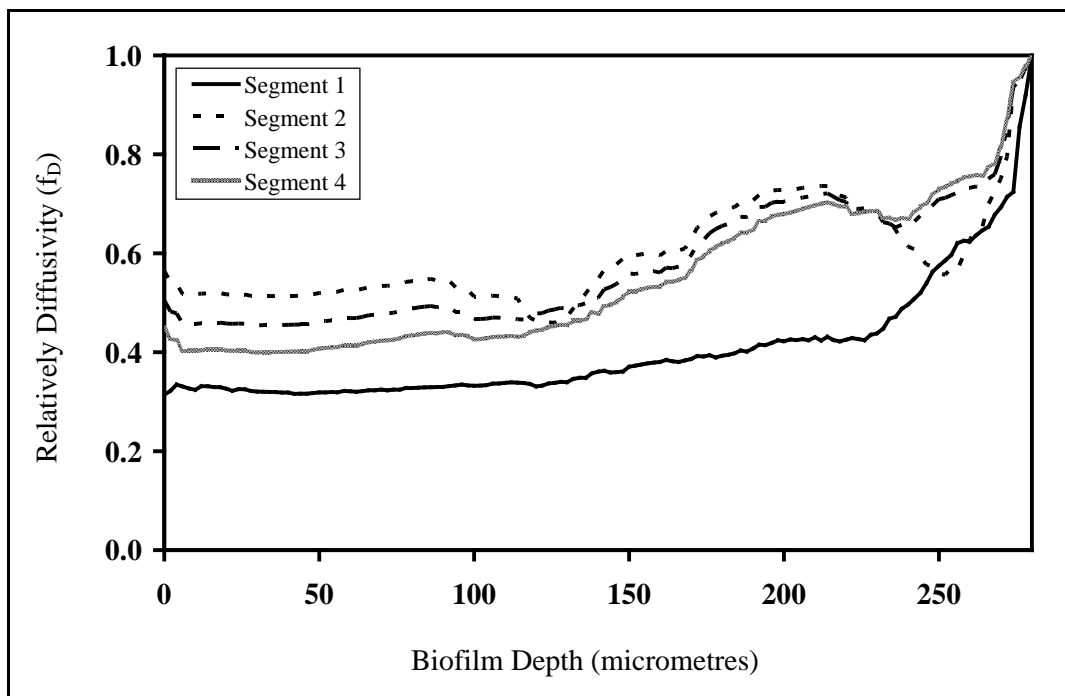


Figure 5.10 Simulated relative diffusivity (f_D) along the biofilm depth of FDHS system

Table 5.4 Simulated average relative diffusivity (f_D) in each segment of FDHS and BDHS systems

Parameters	f_D							
	Segment 1		Segment 2		Segment 3		Segment 4	
	FDHS	BDHS	FDHS	BDHS	FDHS	BDHS	FDHS	BDHS
Average f_D	0.405	0.275	0.596	0.336	0.577	0.321	0.548	0.335
S.D.	0.123	0.195	0.104	0.130	0.126	0.160	0.147	0.132

As shown in Figures 5.9 and 5.10, simulation values of f_D were plotted as a function of biofilm depth. It can be seen that, for the biofilms tested in this study, there was correlation between biofilm depth and f_D . Similar results of Zhang et al. (1998) reported a dependence of f_D on the biofilm depth, and that biofilms were grown on substratum with an electron donor and acceptor diffusing into the biofilm through the substratum and the bulk phase, respectively. Zhang et al. (1998) observed that a correlation between depth and f_D could be due to culturing of the biofilm on such a substratum or due to an indirect effect where the internal biofilm structure (e.g., density, porosity, tortuosity) is, in turn, correlated with the biofilm depth. However, this study assumed that the f_D depended on the biofilm density and its compositions. The results showed that the f_D for each segment of two DHS systems decreased with biofilm thickness due to the amount of biomass. Meanwhile, the f_D decreased with an enhanced biofilm density up to a critical values of about 80 g/L (or equal to 96 gCOD/L with 1.2 gCOD/gSS as conversion factor), and then started to decrease due to the dominating effect of diffusion (Şeker et al., 1995). Moreover, Şeker et al. (1995) recommended this density value (96 gCOD/L) limit substrate consumption rate in biofilms. However, fungal biofilm densities for all segments were lower than the critical value; that means there was no limitation of biofilm diffusion in FDHS system within 250 μm of biofilm depth (maximum biofilm density of FDHS system was 57.7 gCOD/L). But for the

BDHS system, the biofilm diffusion was limited in segment 1 and 4 where critical depth were about 130 μm and 180 μm , respectively.

5.2 Biofilm Porosity by Simulation

Recently, several experimental methods have been developed for a more direct quantification of biofilm structure rather than characterizing biofilm structure based on density. For example, specific staining combined with confocal laser scanning microscopy (CLSM) and digital image analysis can provide three dimensional representations of the different constituents within the biofilm matrix (Heydorn et al., 2000). Parameters, such as porosity or the maximum and average diffusion distance could then be correlated with the factor f_D . Zhang and Bishop (1994b) correlated diffusion in a biofilm with the biofilm porosity (ε_f) and tortuosity (τ) and proposed the following Equation 5.2:

$$f_D = \frac{\varepsilon_f}{\tau^2} \quad (5.2)$$

Equation 5.2 can be further simplified by approximating the tortuosity as the inverse of the porosity (Zhang and Bishop, 1994b) resulting in

$$f_D = \varepsilon_f^3 \quad (5.3)$$

To be able to use Equation 5.3 by using results from this study, the biofilm porosity was approximated from the measured biofilm density. The results of simulated porosities along the biofilm depth are illustrated in Figures 5.11 and 5.12 for BDHS and FDHS systems, respectively.

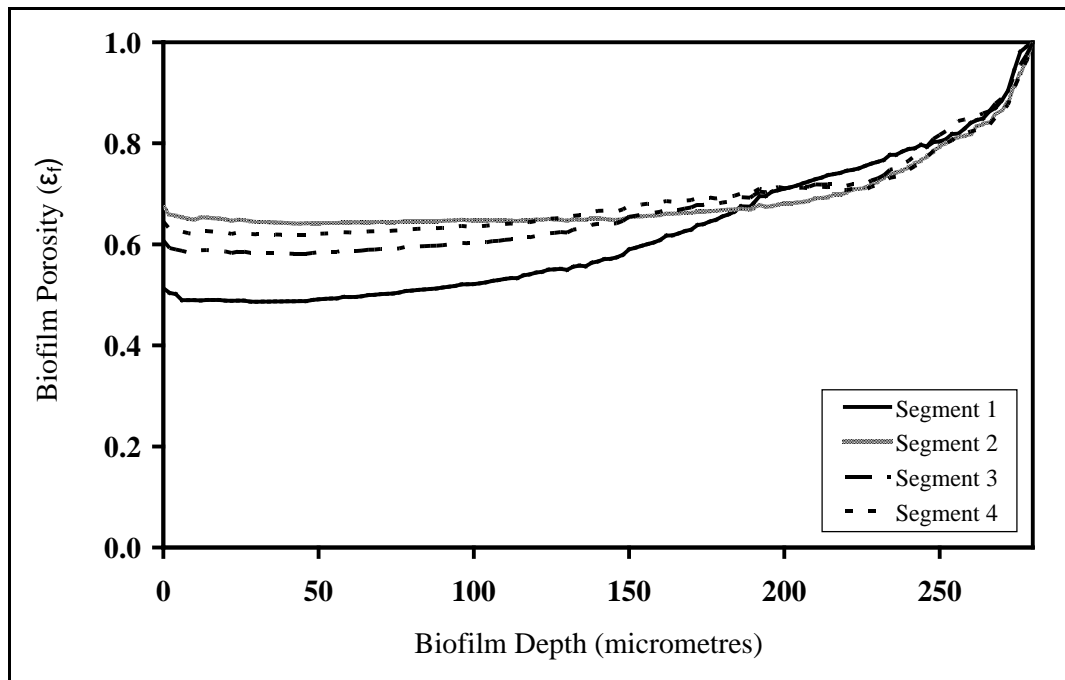


Figure 5.11 Simulated biofilm porosity of BDHS system along the biofilm depth

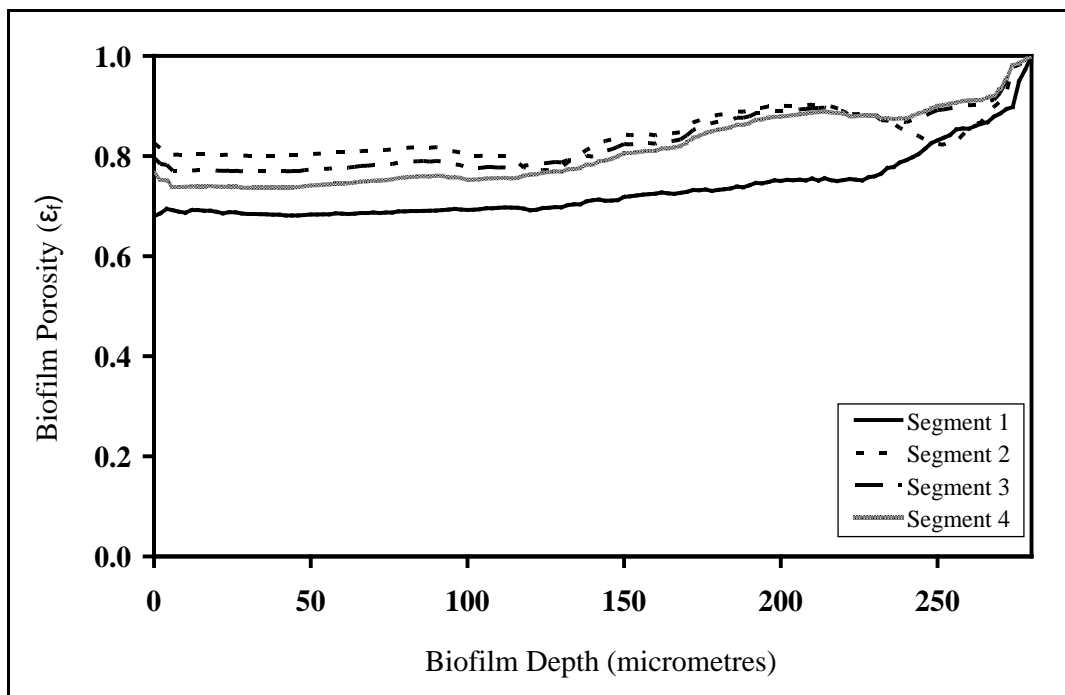


Figure 5.12 Simulated biofilm porosity of FDHS system along the biofilm depth

And the average value porosity values of two DHS biofilms are shown in Table 5.5. Results show that porosity decreased along the biofilm depth while the density was increased. The biofilm porosities changed from 100% to 51% and 100% to 67% in the top biofilm layer of BDHS and FDHS systems, respectively. This shows that biofilm porosities for almost all segments of FDHS system were higher than BDHS system.

Table 5.5 Simulated average porosities (ϵ_f) in each segment of FDHS and BDHS systems

Parameters	ϵ_f							
	Segment 1		Segment 2		Segment 3		Segment 4	
	FDHS	BDHS	FDHS	BDHS	FDHS	BDHS	FDHS	BDHS
Average f_D	0.73	0.62	0.84	0.69	0.83	0.67	0.81	0.69
S.D.	0.06	0.13	0.04	0.07	0.06	0.10	0.07	0.08

Moreover, the results showed that the biofilm became denser and porosity decreased along the biofilm depth. Simulated trends were observed past studies, by the [Zhang and Bishop \(1994\)](#); [Roger et al. \(1996\)](#); [Zhang and Bishop \(2001\)](#) and [Laspidou and Rittmann \(2004b\)](#). The biofilm porosity is a parameter to describe the internal mass transfer efficiency. Several researchers suggested that high biofilm cavity provide an explanation for biofilm sloughing ([Rittmann and McCarty, 2001](#); [Zhang and Bishop, 2001](#); [Horn and Morgenroth, 2006](#) and [Laspidou and Rittmann, 2004b](#)). However, the experimental results showed that the value of SS effluent in FDHS system was lower than BDHS system (Section 4.6.2). This can explained by most of fungi were filamentous structure that provides greater aggregate and adhesion that act in same manner as the EPS matrix ([Guest and Smith, 2002](#)).

5.3 Model Validation

Validity of the UMCCA model application was carried out by comparing the simulated results with the experimental data from two previous studies: [Bishop et al. \(1995\)](#) and [Zhang and Bishop \(2001\)](#) and simulated data of [Laspidou and Rittmann \(2004b\)](#).

5.3.1 Comparison of the UMCCA Model Results with [Laspidou and Rittmann \(2004b\)](#) Study

For the validation of the algorithm to solve the equations of UMCCA model, the simulated program was run with the initial conditions of [Laspidou and Rittmann \(2004b\)](#). In this part, we present the results at the end of simulation run for six variables: S, UAP, BAP, X_a , X_{res} and EPS by using standard parameter values for UMCCA model (standard case). For standard case, the elapsed time was 24.5 days (*bioages*). Figure 5.13 shows how the six parameters of biofilm components varied on average along the depth of the biofilm that appear to be similar to the trends of [Laspidou and Rittmann \(2004b\)](#) study, in Figure 5.14. Table 5.6 illustrates the comparison range values (lowest and highest) for the whole biofilm and total average, or the average of all values in every biofilm compartment. The experiment was evaluated by computing the average values and standard deviations for each row and each column. As a measure of heterogeneity, Table 5.10 presents the standard deviations (σ) of the row and column averages. Since some average values are much smaller than others, we also present the values of σ as percentages of the mean value, which makes the standard deviations directly comparable.

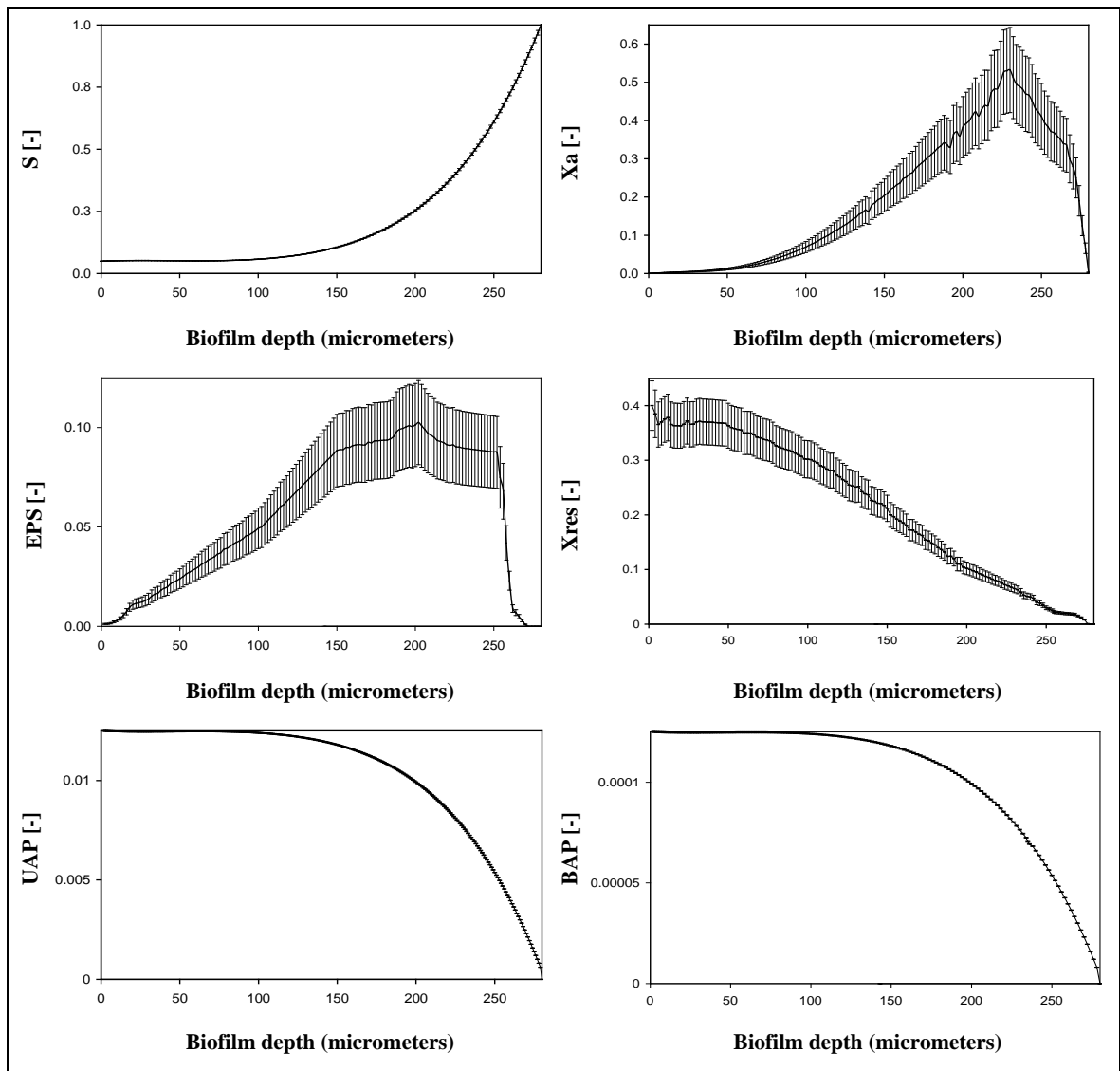


Figure 5.13 Simulated profiles of six biofilm components along the biofilm depth using parameter values of the UMCCA model presented in this study (termination time = 24.5 days)

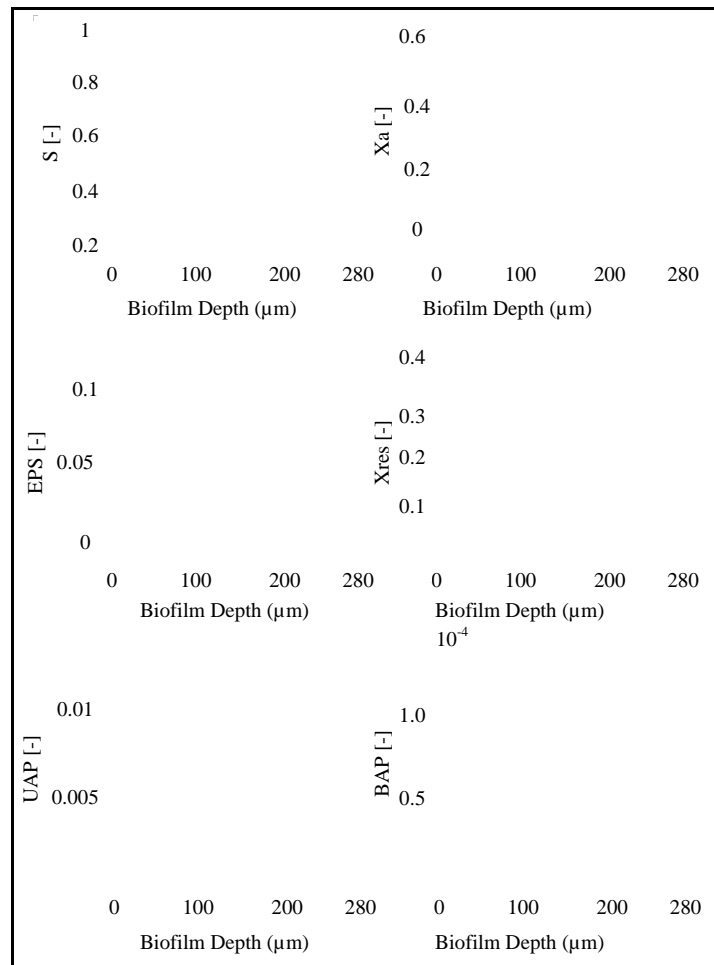


Figure 5.14 Simulated profiles of six biofilm components along the biofilm depth by [Lapidou and Rittmann \(2004b\)](#) study (termination time=24.5 days)

Table 5.6 The comparison of the variables range for whole biofilm depth and the average values from the model output with [Laspidou and Rittmann \(2004b\)](#) results

Variables	Range of values		Total average		Average σ by row		% of average value by row		Average σ by column		% of average value by column	
	A	B	A	B	A	B	A	B	A	B	A	B
S	0.1890-1	0.1972-1	0.3479	0.3629	0.0034	0.0035	0.98	0.96	0.2130	0.2312	61.2	63.7
X_a	0-0.7537	0-0.6386	0.2430	0.1983	0.0508	0.0414	20.9	20.8	0.2125	0.1553	87.4	78.3
X_{res}	0-0.4887	0-0.4488	0.2299	0.2111	0.0260	0.0239	11.3	10.3	0.1322	0.1165	57.5	55.2
EPS	0-0.1553	0-0.1236	0.0652	0.0519	0.0134	0.0107	20.6	16.4	0.0402	0.0345	61.7	67.2
UAP	0-0.0131	0-0.0124	0.0109	0.0103	1.85×10^{-5}	1.74×10^{-5}	0.17	0.16	0.0034	3.32×10^{-3}	31.2	32.3
BAP	$0-1.3 \times 10^{-4}$	$0-1.3 \times 10^{-4}$	9.94×10^{-5}	9.89×10^{-5}	2.50×10^{-7}	2.48×10^{-7}	0.25	0.25	3.85×10^{-5}	3.83×10^{-3}	38.7	38.9
CompDen (gCOD _x /L)	0-131.4	0-124.6	80.6	76.4	11.42	10.82	14.2	14.1	23.54	23.8	29.2	31.2

Remark: A is output data from the application of [Laspidou and Rittmann \(2004b\)](#) study (termination time = 24.5 days)

B is output data of our program following the application of [Laspidou and Rittmann \(2004\)](#), (termination time = 24.5 days)

5.4.2 Comparison of the Simulated Biofilm Compositions and Density with some Previous Studies

Bishop et al. (1995) and Zhang and Bishop (2001) used laboratory-scale rotating drum biofilm reactors with the working volumes of 954 mL to develop their biofilms. The outer cylinder of each reactor had removable strips wrapped with polyolefin shrink film, offering a surface for the growth of biofilms that could be sampled easily. Influent COD concentrations were 350 and 700 mg/L. The effluent COD concentrations were usually higher than 30 mg/L, with bulk DO in the range of 0.5–2.0 mg/L. They used a microtome to slice the biofilm into layer samples with a thickness of 10–20 μm . This enabled them to measure the density of the biofilm for different distances from the substratum. The results represented by the model with the experimental data of Bishop et al. (1995) can be compared by computing the average composite density in layers of different distances from the substratum. Also, simulated dynamics of biofilm components (S and X_a) were compared with the experimental study of Zhang and Bishop (2001). Since the biofilms assayed by Zhang and Bishop (2001) were much thicker than the ones included in this modeling study here, they surely had an anaerobic sub-layer through much of the bottom of the biofilm. This anaerobic sub-layer supported the metabolism and accumulation of fermenting bacteria, something that the UMCCA model does not include. Therefore, we cannot directly compare the viable biomass values in this study with those of Zhang and Bishop (2001). However, Laspidou and Rittmann (2004b) suggested the UMCCA model can be describes the trends of biofilm components that included anaerobic sub-layer (Zhang and Bishop, 1994a). To simulate the experimental conditions, the UMCCA model was ran by using the set of parameters in Table 5.7. The microbial kinetic parameters, also used in the case of Laspidou and Rittmann (2004a), are appropriate, since they are typical values of heterotrophic biofilms. Three variables differ from the standard case. The bulk substrate concentrations S_{max} and $O_{2,max}$ were reduced to 30 mg COD_s/L and

2.0 mg DO/L, respectively, to match the experimental conditions in [Bishop et al. \(1995\)](#) and [Zhang and Bishop \(2001\)](#). The decay rate (b) was set at 0.2/day, a value typical for aerobic heterotrophs in environmental biotechnology ([Rittmann and McCarty, 2001](#)).

Table 5.7 Parameters values used in the UMCCA model to simulate the experiments of [Bishop et al. \(1995\)](#) and [Zhang and Bishop \(2001\)](#)

Parameters	Values	Parameters	Values
D_s	$1.38 \times 10^{-4} \text{ m}^2/\text{day}$	\hat{q}_s	28.5 mgCOD _s /L-day
S_{max}	350 mg _s /L	K_S	20 mgCOD _s /L
uap_{max}	500 mgCOD _p /L	\hat{q}_{uap}	1.8 mgCOD _p /mgCOD _x -day
bap_{max}	50 mgCOD _p /L	K_{UAP}	100 mgCOD _p /L
$x_{a,max}$	70 gCOD _x /L	\hat{q}_{bap}	0.1 mgCOD _p /mgCOD _x -day
eps_{max}	200 gCOD _x /L	K_{BAP}	85 mgCOD _p /L
$x_{res,max}$	220 gCOD _x /L	k_I	0.05 mgCOD _p /mgCOD _s
$O_{2,max}$	2.0 mgO ₂ /L	k_{EPS}	0.18 mgCOD _p /mgCOD _s
Y_s	0.34 mg _x /mg _s	k_{hyd}	0.17/day
Y_p	0.45 mg _x /mg _p	λ	0.005/m
b	0.2/day	η	0.0315/h
b_{det}	0.15/day	B	0.9820
f_d	0.8		

(i) Substrate (S)

[Zhang and Bishop \(2001\)](#) was study on the spatial distribution of the soluble COD (SCOD) concentration along the biofilm depth. A layered biofilm sample was well mixed by applying the washing and stripping steps, was steamed in an autoclave at 80°C under 1 bar pressure for 10 min and then centrifuged while still hot at 8,000g for 10 min. Result shows simulated S are similar trend that observed for the SCOD profile throughout the biofilm depth by [Zhang and Bishop \(2001\)](#) that illustrate in Figure 5.15. The

variance of simulated S and experimental data of [Zhang and Bishop \(2001\)](#) was statistically compared as details in Table 5.8.

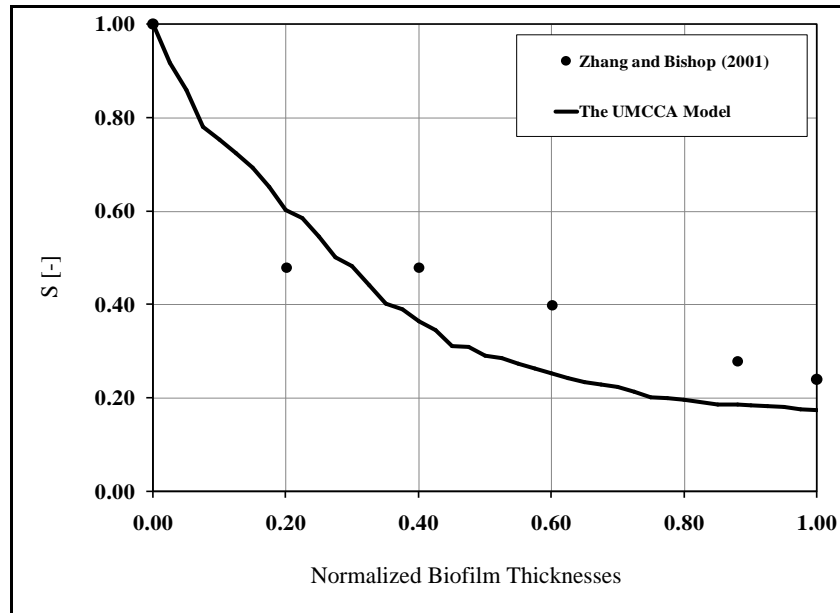


Figure 5.15 Modeling results for SCOD profile throughout the biofilm depth and experimental data of [Zhang and Bishop \(2001\)](#) for the 1,420 μm of thickness layer

From statistical analysis (independent samples t test), it was found the variance of two groups, simulated and the experimental study of [Zhang and Bishop \(2001\)](#) was equal. Therefore, the UMCCA model can be used to predict the trend of SCOD profile throughout the biofilm depth.

Table 5.8 The group statistics and independent samples t test of simulated and experimental data of [Zhang and Bishop \(2001\)](#)
for original substrate

Group Statistics

Study Cases	N	Mean	Std. Deviation	Std. Error Mean
S Zhang and Bishop (2001)	6	0.48000	0.273642	0.111714
The UMCCA Model	46	0.37266	0.232307	0.034252

Independent Sample

	Levene's Test for Equality of Variances		t-test for Equality of Mean						
	F	Sig.	T	df	Sig. (2-tailed)	Mean Difference	Std. Error Difference	95% Confidence Interval of the Difference	
								Lower	Upper
S Equal variances assumed	0.076	0.784	1.044	50	0.301	0.107340	0.102770	-0.099080	0.313759
Equal variances not assumed			0.919	5.978	0.394	0.107340	0.116847	-0.178825	0.393505

(ii) Active Biomass (X_a)

Zhang and Bishop (2001) presented data on the active biomass concentration throughout the biofilm depth. To find the viable biomass within the biofilm, they measured lipid phosphate concentrations within the biofilm using phospholipids as a predictor of viable biomass. Lipid phosphate can occur inside living cells, this study interpret that the “viable” biomass measured by Zhang and Bishop (2001) is most like active biomass in the UMCCA model. The trends of the UMCCA model describes for active biomass are similar to those observed for “viable” biomass by Zhang and Bishop (2001) that illustrate in Figure 5.16. The average active biomass of simulated and experimental data of Zhang and Bishop (2001) was statistically compared as details in Table 5.9. From statistical analysis (independent samples t test), it was found the variance of two groups, simulated and the experimental study of Zhang and Bishop (2001) was equal.

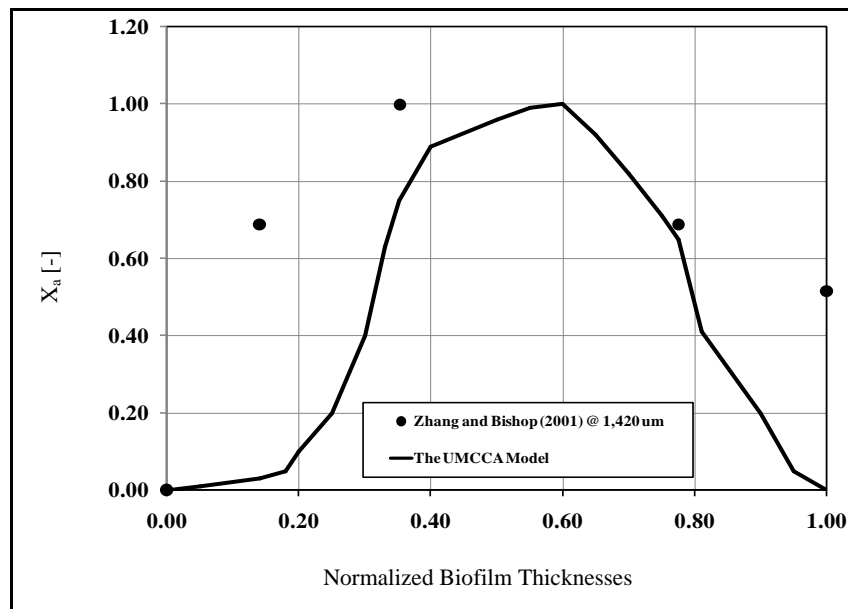


Figure 5.16 Modeling results for active biomass profile throughout the biofilm depth and experimental data of Zhang and Bishop (2001) for the 1,420 μm of thickness layer

Table 5.9 The group statistics and independent samples t test of simulated and experimental data of [Zhang and Bishop \(2001\)](#) for active biomass

Group Statistics

Study Cases		N	Mean	Std. Deviation	Std. Error Mean
X _a	Zhang and Bishop (2001)	5	.5800	.36763	.16441
	The UMCCA Model	21	.4652	.38583	.08420

Independent Sample

	Levene's Test for Equality of Variances		t-test for Equality of Mean						
	F	Sig.	t	df	Sig. (2-tailed)	Mean Difference	Std. Error Difference	95% Confidence Interval of the Difference	
								Lower	Upper
X _a Equal variances assumed	1.343	.258	.602	24	.553	.11476	.19052	-.27844	.50797
Equal variances not assumed			.621	6.287	.556	.11476	.18471	-.33226	.56179

Therefore, the UMCCA model can be used to predict the trend of active biomass throughout the biofilm depth.

(iii) Composite Density

In his section, the UMCCA model was solved for the set parameters shown in Table 5.7. This solution is used to evaluate how well the model can describe experimental results (Bishop et al., 1995) and illustrate the dynamics of biofilm density along the biofilm depth using the micro slice technique. The average composite density values produced by the UMCCA model match the trends of the measured density distribution very well (Figures 5.17 and Figure 5.18). The first set of data (●) (Bishop et al., 1995) was obtained from biofilms of thicknesses between 52 and 130 μm , and the experimental values follow the model outputs for the thicknesses in that range (64 and 96 μm).

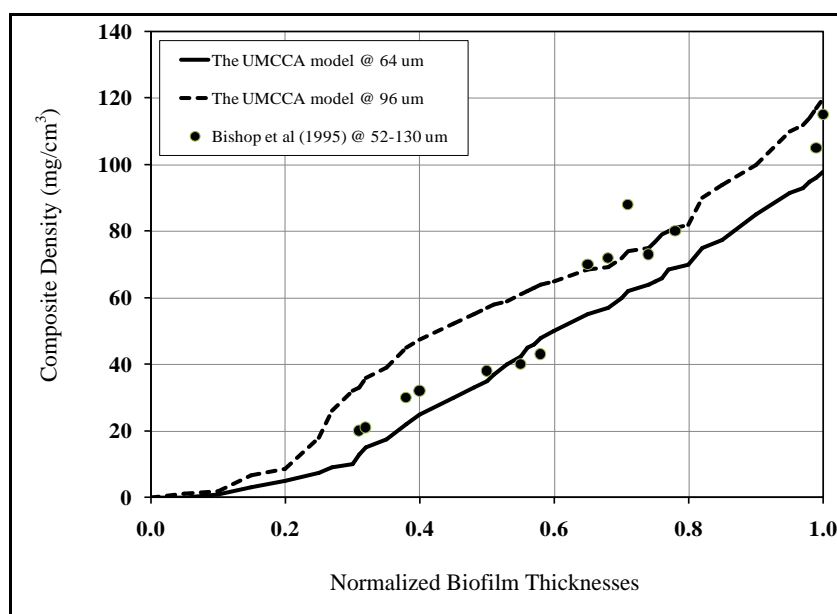


Figure 5.17 Modeling results for composite density and experimental data of Bishop et al. (1995) for the 52-130 μm of thickness layer

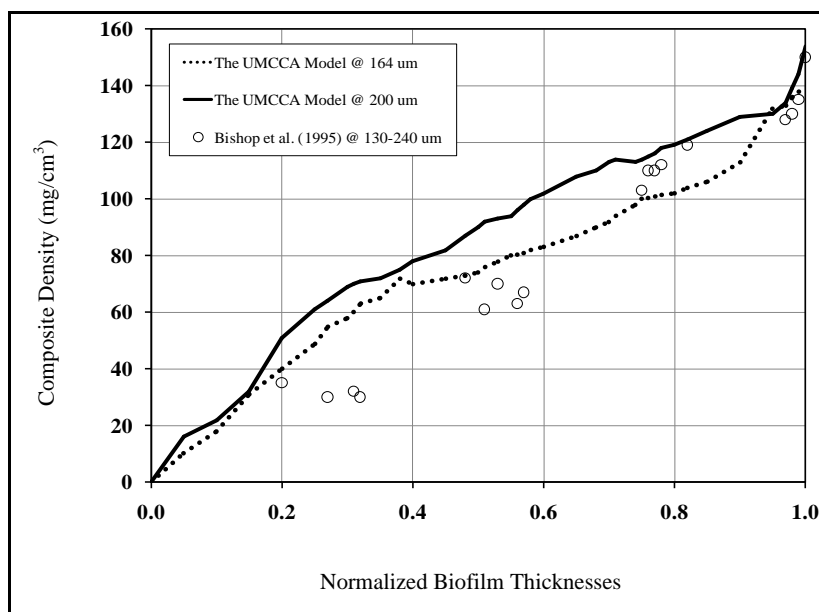


Figure 5.18 Modeling results composite density and experimental data of [Bishop et al. \(1995\)](#) for the 130-240 μm of thickness layer

The other data set (O), which was obtained with biofilms 130–240 μm thick, lies above the first data set and matches well to the modeling results for 164 μm and 200 μm . The modeling curve for the highest thickness (280 μm) lies above the second data set, as we would expect, since that thickness is outside the data range.

For all curves and data sets, average biofilm densities in the bottom layers are 5–10 times higher than those in the top layers. This happens because the bottom layers have a biofilm that is much “older” than the ones in the top. A large bioage leads to the bottom layers having a consolidation ratio (U_c) much larger than the younger top layers, and, as a result, being packed more densely. In addition, the bottom layers have more time to accumulate inert biomass, with a higher maximum density, which also contributes to the higher composite density near the substratum. The top layers, which are “young” biofilms, have a small consolidation factor, are mostly active biomass and EPS, and remain loosely packed and fluffy. The average biofilm density of simulated and experimental data of

[Bishop et al. \(1995\)](#) was statistically compared as details in Tables 5.10 and 5.11. From statistical analysis (ANOVA), it was found the average biofilm density in the study of [Bishop et al. \(1995\)](#) with respect to simulated density were not different for all experimental data in case of the thicknesses in range of 64-96 μm and 130-240 μm . Therefore, the UMCCA model can be used to predict the density in biofilm wastewater treatment.

5.5 Summary

The aims of mathematical modeling of biofilm composition and density dynamics study were to (i) investigated the spatial distribution of biofilm components throughout the biofilm depth, (ii) to computed a “composite density” or the density that includes active biomass (X_a), inert biomass (X_{res}) and extracellular polymeric substance (EPS) using Unified Multiple Component Cellular Automotan (UMCCA) model and (iii) evaluated the biofilm mass transport through its density provide an empirical relationship between relative diffusivity (f_D) and biofilm density (ρ) and approximated the porosity that correlated with the factor f_D ([Horn and Morgenroth, 2006](#)).

5.5.1 The UMCCA Model

All outputs of the UMCCA model showed five general trends. First, the concentration profiles for the two soluble microbial products are opposite the profile for original substrate, since they are produced in the biofilm and must diffuse out the top surface. Second, the top of the biofilm is dominated by active biomass and EPS, while the bottom is dominated by residual inert biomass. Within the top layers, active biomass has a much higher concentration than EPS. Third, the top of all biofilms is quite “fluffy,” since the newly synthesized biomass has not had time to fill in the top compartments and consolidate. Fourth, the peak of the composite density does not correspond to the peak of active biomass.

Table 5.10 Statistical analysis of biofilm density through the model validation within the biofilm thickness 52-130 μm (Bishop et al., 1995)

ANOVA

Source	Sum of Squares	df	Mean Square	F	Sig.
Between Group	2173.823	2	1086.912	1.375	.265
Within Group	30839.926	39	790.767		
Total	33013.750	41			

Multiple Comparisons

Dependent Variable: Density

LSD

(I) Case Study	(J) Case Study	Mean Difference (I-J)	Std. Error	Sig.	95% Confidence Interval	
					Lower Bound	Upper Bound
Bishop experimental	Model Output @ 64 μm	8.964	10.629	.404	-12.53	30.46
	Model Output @ 96 μm	-8.657	10.629	.420	-30.16	12.84
Model Output @ 64 μm	Bishop experimental	-8.964	10.629	.404	-30.46	12.53
	Model Output @ 96 μm	-17.621	10.629	.105	-39.12	3.88
Model Output @ 96 μm	Bishop experimental	8.657	10.629	.420	-12.84	30.16
	Model Output @ 64 μm	17.621	10.629	.105	-3.88	39.12

Table 5.11 Statistical analysis of biofilm density through the model validation within the biofilm thickness 130-240 μm (Bishop et al., 1995)

ANOVA

Source	Sum of Squares	df	Mean Square	F	Sig.
Between Group	3038.559	2	1519.279	1.315	.278
Within Group	55467.088	48	1155.564		
Total	58505.647	50			

Multiple Comparisons

Dependent Variable: Density

LSD

(I) Case Study	(J) Case Study	Mean Difference (I-J)	Std. Error	Sig.	95% Confidence Interval	
					Lower Bound	Upper Bound
Bishop experimental	Model Output @ 164 μm	-6.97059	11.65971	.553	-30.4140	16.4728
	Model Output @ 200 μm	-18.70588	11.65971	.115	-42.1493	4.7375
Model Output @ 164 μm	Bishop experimental	6.97059	6.97059	.553	-16.4728	30.4140
	Model Output @ 200 μm	-11.73529	11.65971	.319	-35.1787	11.7081
Model Output @ 200 μm	Bishop experimental	18.70588	11.65971	.115	-4.7375	42.1493
	Model Output @ 164 μm	11.73529	11.65971	.319	-11.7081	35.1787

Finally, the biomass concentration has considerable local heterogeneity in the vertical and later a direction, even when the soluble species have generally flat profiles that vary only in the vertical direction.

All results indicated that BDHS biofilms were denser than FDHS biofilms. This can be explained by the biomass decay rates (k_d) of FHDS system which were lower than BDHS system. For segment 1, BDHS system had the highest density under low dissolved oxygen concentrations (the value about zero), in such condition active biomass and EPS growth might have slowed down significantly due to the low dissolved oxygen concentration. As a result, the biofilm grew very slowly, while accumulation of residual dead biomass proceeded even in the absence of oxygen, making the biofilm aged and dense. And, in condition of the substrate concentration was near and below K_s or lower dissolved-oxygen concentration promotes the formation of the cluster-and-channel structure in two DHS biofilms. A high specific detachment rate also favors the cluster-and-channel structure and maintains relatively open channels near the substratum. The high surface-detachment rate accentuates the growth-rate benefit for a protruding cluster. It also keeps the biofilm less dense overall, but with a lower proportion of residual inert biomass.

5.5.2 Mass Transport Approach

Mass transport in biofilms is influenced by the biofilm structure which in turn is influenced by the local availability of substrate. Solute transport in biofilms is the result of diffusion in the denser aggregates and potentially convective transport within pores and water channels. Diffusivity has been shown to dominate mass transport in many biofilm systems (Horn and Morgenroth, 2006). Moreover, biofilm density and depth are the main design parameters used to evaluate substrate consumption rate in a biofilm.

(i) Relative Diffusivity (f_D)

Results shown the f_D values are opposite trends of density. The top, where the biofilm was young and irregular, had high f_D values that causes of small

composite density. Also f_D values of all segments of FDHS system were higher than BDHS system. This study would consider the f_D that depends on the biofilm density and its compositions. The results show that the f_D for each segment of two DHS systems decreased with biofilm depth due to the amount of biomass.

(ii) Biofilm Porosity (ϵ)

Results show porosity decrease along the biofilm depth or the density was increased. The biofilm porosities change from 100% to 51% and 100% to 67% in the top biofilm layer of BDHS and FDHS systems, respectively. These show most of all biofilm porosities of FDHS system are higher than BDHS system. Moreover, the results show that the biofilm becomes denser and porosity was decrease along the biofilm depth. Although, the biofilm porosity is a parameter to describes the internal mass transfer efficiency. Several researchers suggested that high biofilm cavity provide an explanation for biofilm sloughing.

CHAPTER VI

CONCLUSIONS AND RECOMMENDATIONS

6.1 Conclusions

This study investigated both of fungal and bacterial downflow hanging sponge systems as a post treatment of UASB effluent of a tapioca starch wastewater by experimental study and mathematical modeling for evaluated the on biofilm composition and density dynamics.

6.1.1 Experimental Results

The overall experimental results show two DHS systems viable and economic treatment method as it ensures low investment and running costs, operational simplicity. Cost is reduced as there was no need for aeration, cutting down the expenses associated with aerating device, their operation, maintenance or replacement. Various aspects of the bacterial downflow hanging sponge (BDHS) and fungal downflow hanging sponge (FDHS) systems had been elaborated in this study were considered into five parts namely, (1) treatment efficiencies and suitable operating conditions; (2) treatment mechanisms; (3) biokinetic parameters and (4) sludge characteristics.

(1) Treatment Efficiencies and Suitable Operating Conditions

- The dissolved oxygen (DO) concentration increased steadily attaining the values of about 5.0 mg/L in the system. Two DHS systems clearly demonstrated the advantage of needlessness of external aeration for RUN II and RUN III operating conditions because of the DO concentration in recirculation flows. However, In RUN I, DO concentrations were low in the first and second segments of BDHS system. This suggests that oxygen utilization of bacteria was higher than fungi.

- High TSS removal efficiencies of FDHS systems were about 91%, 90% and 88% during RUN I, RUN II and RUN III, respectively. In BDHS system, the TSS removal efficiency was lower than FDHS system with amount of 72%, 89% and 76% in RUN I, RUN II and RUN III, respectively.

- The overall organic removal performance of the two DHS systems during the whole experimental period. In RUN I, the organic loading rate (OLR) in inflows of DHS systems were in the range of 1.0-1.1 kgTBOD/m³-d which results of the overall TBOD removal efficiency reached about 82-83% in both BDHS and FDHS systems. The most of TBOD were removed in the first segment of FDHS system (about 70% of TBOD₅ removed). But the BOD was removed gradually in all 4 segments of BDHS system. In RUN II, OLR in DHS remained the same as in RUN I, but the hydraulic loading rate (HLR) was increased from 3.5 m³/m³_{sponge}-d to 25.6 m³/m³_{sponge}-d. Organic removal improved with the efficiencies for TBOD reaching up to 96% and 94% in FDHS and BDHS systems, respectively. And in RUN III, two DHS systems operated with OLR in FDHS and BDHS systems were about 1.60 kgTBOD/m³-d and 3.63 kgTBOD/m³-d, respectively. The difference OLR of two systems was causing of the remained TBOD in BDHS effluent was higher than FDHS system. The HLR in two DHS systems remained the same as in RUN II. Organic removal improved with the efficiencies for TBOD about 95% and 77% in FDHS and BDHS systems, respectively.

- Nitrogen was not removed in FDHS system during three runs. BDHS system received total nitrogen loading rate (NLR) about 0.61, 2.1 and 9.97 kg-N/m³-d during RUN I, RUN II and RUN III, respectively. Under these conditions, the total nitrogen removal efficiencies were about 68%, 59% and 56%, respectively. The nitrogen removal decreased during RUN II and RUN III that shear force of water flow amplifies as

HLR increases. This may lead to the disruption of the retained sludge inside the sponge of DHS, finally raising the value of SS in the effluents.

(2) Treatment Mechanisms

- Results of biodegradation determination showed that the inert fraction of organic matter has an impact on BDHS system removal efficiencies. It also found that the BPCOD in BDHS effluent was higher than FDHS system in every segment. Thus it led to strong limiting process in substrate biodegradation by aerobic heterotrophs and denitrifying bacteria in BDHS system. However, the FDHS system achieved an almost complete removal of BPCOD fraction in the final effluent. This indicated the potential advantage of fungi over bacteria in terms of organic removal rate.

- The results of COD and nitrogen mass balances indicated that the highest COD removed was found in segment 1 of FDHS system which included the electron transferred from the organic material to electron acceptor (COD oxidized) about 11.6 g/d and COD loss, 18.9 g/d. And COD loss in segment 4 of two DHS systems were to be in deficit because oxygen utilization (COD oxidized) was higher than mass flow of COD removal ($M_{COD,inf} - M_{COD,eff}$). This caused of the sludge was utilized as a carbon sources during endogenous respiration in two DHS systems.

- The identification dominant cultures in two DHS systems appeared that *nitrosomonas* and *nitrobacter* were dominant cultures in segment 2, 3 and 4 of the BDHS biomass. Cell concentrations of both nitrifying bacteria were in good agreement with the magnitudes of ammonia-oxidizing and nitrite-oxidizing activities evaluated from those segments. The three dominant fungal genuses in FDHS system were included of *Trichoderma*, *Aspergillus* and *Candida*. As presented by several researchers, these fungal genuses had a wide range of enzymes, and were capable of metabolizing complex mixtures of organic compounds such as particulate matters and dead cells.

(3) Biokinetic Parameters

Results of biokinetic parameters showed that the fungi-based DHS system had the higher potential for organic removal than BDHS system treating the UASB effluent of tapioca starch wastewater. Moreover, it can also be observed that the yield (Y) of the fungal culture is lower than that of the bacterial culture. This indicates that lower excess sludge would be produced from the fungal system compared to the bacterial system for the same substrate quantity, thus having the advantage of less sludge handling.

(4) Sludge Characteristics

The good performance of organic removal in two runs can be attributed to a large amount of retained biomass in sponge media of FDHS and BDHS systems. The values are 5-20 times higher than that of activated sludge system and trickling filter treating domestic sewage. However, the FDHS achieved higher removal rate than bacteria. This can explain by the higher ratios of viable cells to total biomass of all fungal sludge than bacterial sludge. Moreover, the results suggested that the highly bound EPS accumulated in the sludge may have the negative effect on the bacteria consumption rate but fungal sludge (FDHS) that seems to be no effects.

6.1.2 Mathematical Modeling of Biofilm Compositions and Density Dynamics

Application of the Unified Multi-component cellular automaton (UMCCA) model for quantitative simulation of the biofilm's composite density for three biofilm components: active bacteria, inert or dead biomass, and extracellular polymeric substances. The model also described the concentrations of three soluble organic components (soluble substrate and two types of soluble microbial products). All simulated results of the UMCCA model were shown in five trends.

(1) The concentration profiles for the two soluble microbial products are opposite the profile, for original substrate, since they were produced in the biofilm and must diffuse out the top surface.

(2) The top of the biofilm was dominated by active biomass and EPS, while the bottom was dominated by residual inert biomass. Within the top layers, active biomass had a much higher concentration than EPS.

(3) The top of all biofilms was quite “fluffy,” since the newly synthesized biomass has not had time to fill in the top compartments and consolidate.

(4) The peak of the composite density did not correspond to the peak of active biomass.

(5) Finally, the biomass concentration had considerable local heterogeneity in the vertical and later a direction, even when the soluble species have generally flat profiles that vary only in the vertical direction.

Moreover, all simulated results indicated that BDHS biofilms were denser than FDHS biofilms. This can be explained by the biomass decay rates (k_d) of FHDS system which were lower than BDHS system. The relative diffusivity (f_D) values were opposite trends of density. The top, where the biofilm was young and irregular, had high f_D values that causes of small composite density. Also f_D values of all segments of FDHS system were higher than BDHS system. Furthermore, results show porosity decrease belong the biofilm depth or the density was increased.

6.2 Recommendations

Based on the literatures and results of this study obtained, several recommendations for further research are suggested as follow:

6.2.1 The experimental results suggested that FDHS system had high capable in TSS and organic removal but not effective to remove nitrogen. However, BDHS system is effective in nitrification process but most of the BDHS segment system will need an external carbon source to completed denitrification. In order to achieve sufficiently organic and nitrogen removal efficiency in tapioca starch wastewater that completed with long biomass retention time, high organic and hydraulic loading rate operation, high process stability, oxygen requirement and low production of waste sludge. Thus, it is strongly recommended to apply DHS system in treating tapioca starch wastewater by using UASB reactor and two post treatments of FDHS and BDHS systems, respectively, the schematic diagram was showed in Figure 6.1. FDHS system offers an attractive process for remove organic contents. They are capable of metabolizing complex mixtures of organic compounds such as particulate matters and dead cells. Filamentous fungi formed the loose biofilm that presented sufficient high substrate and oxygen mass transport. However, nitrogen concentration still high contained in FDHS effluents. Thus, BDHS system should be applied to polish up the nitrogen nutrient before discharge to receiving water. In addition, most of BDHS segment system will need an external carbon source to achieve complete denitrification and establishment of a cost-efficient treatment system. Raw tapioca starch wastewater is too high COD/N ratio that suitable for used to improve carbon source in inflows of BDHS system.

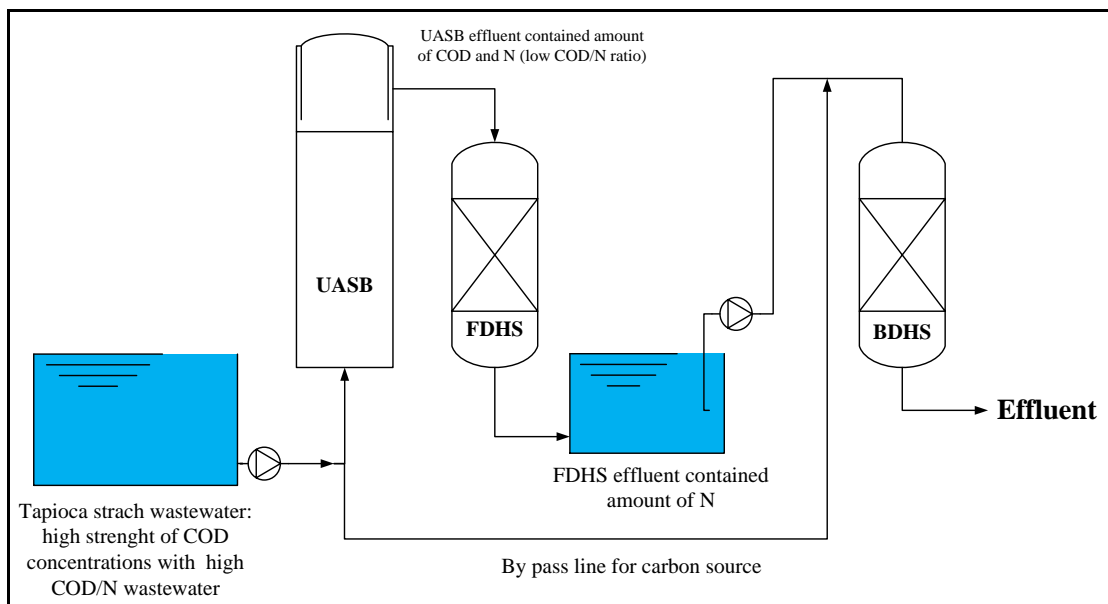


Figure 6.1 The schematic diagram of recommendation of two DHS systems for tapioca starch industry

6.2.2 Several literatures suggested that bacterial and fungal sludge have capable for treating acute and chronic heavy metal stress (Section 2.9.5). The results from such studies might provide information on quantitative toxicity evaluation of the heavy metals for both fungal and bacterial treatment systems. The mechanisms of heavy metal removal by fungal and bacterial sludge may also be investigated.

6.2.3 The application of fungal downflow hanging sponge (DHS) system treatment for high strength hazardous organic wastewater may be a feasible biological approach such as toxic or chemical wastes, pesticides, herbicides, phenolic derivatives, aromatic compounds, cyanide, and tannery wastewater.

6.2.4 The dynamic phenomenon investigation of specific activities of carbon, ammonia and nitrite oxidizers along the two DHS heights with the function of the C/N ratio in wastewater entering the biofilter.

REFERENCES

- Ahmadi, M., Vahabzadeh, F., Bonakdarpour, B. and Mehranian, M. (2006). Empirical modeling loofa-immobilized *Phanerochaete chrysosporium*. **Process Biochemistry**. 41: 1148-1154.
- Alam, M. Z., Fakhru-Razi, A., Abd-Aziz, S. and Molla, A. H. (2003). Optimization of compatible mixed cultures for liquid state bioconversion of municipal wastewater sludge. **Water, Air, and Soil Pollution**. 149: 113-126.
- Amatya, P. L. (1996). **Anaerobic Treatment of Tapioca Starch Industry Wastewater by Bench Scale Upflow Anaerobic Sludge Blanket (UASB) Reactor**. Master thesis. Asian Institute of Technology. Bangkok, Thailand.
- Agrawal, L., Ohashi, Y., Mochida, E., Okui, H., Ueki, Y., Harada, H. and Ohashi, A. (1997). Treatment of raw sewage in a temperature climate using a UASB reactor and the hanging sponge cubes process. **Water Sci. and Technol.** 36(6-7): 433-440.
- Annachatre A. P. and Amatya P. L. (2000). UASB Treatment of Tapioca Starch Wastewater. **J. Envi. Eng.** 126(12): 1149-1152.
- Annachatre A. P. and Amornkaew A. (2001). Upflow Anaerobic Sludge Blanket Treatment of Starch Wastewater Containing Cyanide. **Water Environmental Research**. 73(5): 622-632.
- APHA, AWWA, WEF. (2003). **Standard Methods for the Examination of Water and Wastewater**. 20th (ed). Washington, DC, USA.
- Araki, N., Ohashi, A., Mechadar, I. and Harada, H. (1999). Behaviors of nitrifiers in a novel biofilm reactor employing hanging sponge cubs as attachment site. **Water Sci. and Technol.** 39(7): 23-31.

- Barker, P. S. and Dold, P. L. (1995). COD and nitrogen mass balances in activated sludge systems. **Water Research**. 29(2): 633-643.
- Barana A. C. and Cereda M. P. (2000). Cassava Wastewater (Manipureira) Treatment Using a Two-phase Anaerobic Biodigestor. **Ciênc Technol Aliment** [Online]. 20(2). Available: <http://www.scielo.br/scielo.php>.
- Berry, D. R. (1998). Product and primary metabolism pathway. **Physiology of Industrial Fungi**. Backwell Scientific Publications. London, UK.
- Besemer, K., Singer, G., Limberger, R., Chlup, A.-K., Hochedlinger, G., Hödl, I., Baranyi, C., Battin, T.J. (2007). Biophysical controls on community succession in stream biofilms. **Appl. Environ. Microbiol.** 73 (15): 4966–4974.
- Blánquez, P., Caminal, G., Sarrá, M. and Vicent, T. (2007). The effect of HRT the decolorisation of the Grey Lanaset G textile dye by *Trametes versicolor*. **Chemical Engineering Journal**. 126: 163-169.
- Bihan, Y. and Lessard, P. (2000). Monitoring biofilter clogging: biochemical characteristics of the biomass. **Water Research**. 34(17): 4284-4294.
- Bishop, P. L., Zhang, T. C., Fu, Y. C. (1995). Effect of biofilm structure, microbial distribution and mass transport on biodegradation processes. **Water Sci. Technol.** 31(1): 143-152.
- Boursier, H., Beline, F. and Paul, E. (2005). Piggery wastewater characterization for biological nitrogen removal process design. **Bioresource Technology**. 96: 351-358.
- Brauer, H. (1991). Growth of fungi and bacteria in the reciprocating jet bioreactor. **Bioprocess Engineering**. 6: 1-15.
- Busscher, H.J., van der Mei, H.C. (2006). Microbial adhesion in flow displacement systems. **Clin. Microbiol. Rev.** 19 (1): 127–141.

- Carvalho, L., Carrera, J. and Chamy, R. (2002). Nitrifying activity monitoring and kinetic parameters determination in a biofilm airlift reactor by respirometry. **Biotechnol. Lett.** 24: 2063–2066.
- Cech J. S., Chudoba J. and Grau P. (1984). Determination of kinetic constants of activated sludge microorganisms. **Water. Sci. Tech.** 17: 259-272.
- Chaiprasert, C., et.al. (2003). **Thai Biogas Plants High Rate Anaerobic Fixed Film Technology for Agroindustrial Wastewater.** The Award Contest of Best Program on New and Renewable Sources of Energy (Off-Grid) in Year 2003. Research and development cluster unit of waste utilization and management laboratory. King Mongkut's University of Technology Thonburi (KMUTT). Bangkok, Thailand.
- Chang, I.S., and Lee, C.H. (1998). Membrane filtration characteristics in membrane coupled activated sludge system-the effect of physiological states of activated sludge on membrane fouling. **Desalination.** 120: 221-233.
- Chang, I., Gilbert, E. S., Eliashberg, N. and Keasling¹, J. D. (2003). A three-dimensional, stochastic simulation of biofilm growth and transport-related factors that affect structure. **Microbiology.** 149: 2859-2871.
- Chavalparit, O. and Ongwandee, M. (2009). Clean technology for the tapioca starch industry in Thailand. **Journal of Cleaner Production.** 17(2): 105-110.
- Chea, K.J., Yim, S.K. and Choi, K. H. (2004). Application of a sponge media (BioCube) process for upgrading and expansion of existing caprolactam wastewater treatment plant for nitrogen removal. **International Conference on Wastewater Treatment for Nutrient Removal and Reuse 2004.** Phatumthanee, Thailand: Asian Institute of Technology.
- Chernicharo, C. A. L. (2006). Post-treatment options for the anaerobic treatment of domestic wastewater. **Environmental Science and Bio/Technology.** 5:73–92.

- Chuang, H., Ohashi, A., Imachi, H, Tandukar, M, Harada, H. (2007). Effective partial nitrification to nitrite by down-flow hanging sponge reactor under limited oxygen condition. **Water Research**. 41: 295-302.
- Chernicharo, C. A. L. and Nasciimento, M. C. P. (2001). Fesibility of a pilot-scale UASB/tricking filter system for domestic sewage treatment. **Water Sci. and Technol**. 44(4): 221-228.
- Confer, D. R. and Logan, B. E. (1991). Increased bacterial uptake of marcromolecular substrates with fluid shear. **Applied and Environmental Microbiology**. 57(11): 3093-3100.
- Confer, D. R. and Logan, B. E. (1998). Location of protein and polysaccharide hydrolytic activity in suspended and biofilm wastewater cultures. **Water Research**. 32(1): 31-38.
- Coulibaly, L., Gourène, G. and Agathos, N. S. (2003). Utilization of fungi for biotreatment of raw wastewaters A Review. **African Journal Biotechnology**. 2(12): 620-630.
- Dan, N.P. (2001). **Biological Treatment of High Salinity Wastewater using Yeast and Bacterial System**. Ph. D. thesis, Asian Institute of Technology. Pathumthani, Thailand.
- Dan, N. P., Visvanathan, C., Biswadeep Basu. (2003). Comparative evaluation of yeast and bacterial treatment of high salinity wastewater based on biokinetic coefficients. **Bioresource Technology**. 87: 51-56.
- Deng, W., Zheng, P. and Chen, Z. (2006). Anaerobic digestion and post-treatment of swine wastewater using IC–SBR process with bypass of raw wastewater. **Process of Biochemistry**. 41: 965-969.

- Dhouib, A., Aloui, F., Hamad, N. and Sayadi, S. (2006). Pilot-plant treatment of olive mill wastewater by *Phanerochaete chrysosporium* coupled to anaerobic digestion and ultrafiltration. **Process Biochemistry**. 41: 159-167.
- Dubois, M., Gilles, K. A., Hamilton, J. K., Rebers R. A. and Smith, F. (1956). Colorimetric method for the determination of sugars and related substances. **Analytical Chemistry**. 28(3): 350-356.
- Eberl, H., Morgenroth, E., Noguera, D., Picioreanu, C., Rittmann, B., Loosdrecht, M. and Wanner, O. (2006). **Mathematical Modeling of Biofilms**. Scientific and Technical Report No. 18. IWA Publishing. Hove, UK.
- Eding, E. H., Kamstra, A. J., Verreth, A. J., Huisman, E. A., and Klapwijk, A. (2006). Design and operation of nitrifying trickling filters in recirculating aquaculture: A review. **Aquacultural Engineering**. 34: 234-260.
- Elmaleh S., Defrance M.B., Ghommidh C. and Navarro J.M. (1996). Technical note: Acidogenic effluents treatment in a yeast reactor. **Water Research**. 30(10): 2526-2529.
- Ekama G. A., Dold P. L. and Marais G. V. R. (1986). Procedures for determining influent COD fractions and the maximum specific growth rate of heterotrophs in activated sludge systems. **Water Sci. Tech**. 18 (6): 91-114.
- Eusébio, A. et. al. (2007). Characterization of the microbial communities in jet-loop (JACTO) reactors during aerobic olive oil wastewater treatment. **International Biodeterioration & Biodegradation**. 59: 226-233.
- Falih, A. M. K., and Wainwright, M. (1995). Nitrification in vitro by a range of filamentous fungi and yeasts. **Lett. Appl. Microbiol**. 21: 18–19.

- Fakhru'l-Razi, A. and Molla, A. H. (2007). Enhancement of bioseparation and dewaterability of domestic wastewater sludge by fungal treated dewatered sludge. **J. Hazardous Material.** 147(1-2): 350-356.
- Fan, L-S., Leyva-Romos, R., Wisecarver, K. D. and Zehner, B. J. (1990). Diffusion of phenol through a biofilm grown on activated carbon particles in a draft-tube three phase fluidized bed bioreactor. **Biotechnology and Bioengineering.** 35: 279-286.
- Fu, Y. and Viraraghavan, T. (2001). Fungal decolorization of dye wastewater: a review. **Bioresource Technology.** 79. 251-262.
- Gao, D., Wen, X., Zeng, Y. and Qian, Y. (2006). Decolourization of a textile-reactive dye with *Phanerochaete chrysosporium* incubated in different ways under non-sterile conditions. **Water Practice & Technology.** 11(3):
- Geng, A. L., Lim, A. E., Soh, E. W., Zhao, B. and Leck, T. S. (2004). **Physiological and Proteomic Analysis of EPS Production and Biofilm Formation for Phenol Degrading Bacterium.** Teylor & Francis Group. ISBN 90 5809 653 X. London. pp195-198.
- Geradi, M. H. (2002). Dissolved Oxygen. **Nitrification and denitrification in the activated sludge process.** Jonh Weiley & Sons, Inc., Publication, New York, pp103-108.
- Grady Jr C. P. L., Daigger, T. G., and Lim H. C. (1999). **Biological Wastewater Treatment.** Marcel Dekker Inc. New York, USA.
- Grant, R. J., Daneill, T. J. and Betts, W. B. (2002). Isolation and identification of synthetic pyretroid-degrading bacteris. **J. App. Micro.** 92: 534-540.
- Gonçalves, R. F., de Araújo, V. L. and Bof, V. S. (1999). Combining upflow anaerobic sludge blanket (UASB) reactors and submerged aerated biofilters for secondary domestic wastewater treatment. **Water Sci. and Technol.** 40(8): 71-79.

- Guest R. K. and Smith (2002). A potential new role for fungi in a wastewater MBR biological nitrogen reduction system. **J. Environ. Sci.** 1: 433-437.
- Hai, F. I., Yamamoto, K. and Fukushi, K. (2006). Development of a submerged membrane fungi reactor for textile wastewater treatment. **Desalination.** 192: 315-322.
- Hein, P. G., Oanh, L. T. K., Viet, N. T. and Lettingga, G. (1999). Closed Wastewater System in the Tapioca Industry in Vietnam. **Water Sci and Technol.** 39(5): 89-96.
- Heydom, A., Nielson, A. T., Hentzer, M., Stenberg, C., Givskov, M., Ersböll, B. K., and Molin, S. (2000). Quantification of biofilm structure by the novel computer program COMSTAT. **Microbiology.** 146: 2395-2407.
- Hinson, R. K., Kocher, W. M. (1996). Model for effective diffusivities in aerobic biofilms. **Journal of Environmental Engineering.** 122(11): 1023-1030.
- Hirsch, P., Overrein, L., and Alexander, M. (1961). Formation of nitrite and nitrate by actinomycetes and fungi. **J. Bacteriol.** 82: 442-448.
- Horn, H. and Morgenroth, E. (2006). Transport of oxygen, sodium chloride, and sodium nitrate in biofilms. **Chemical Engineering Science.** 61: 1347-1356.
- Hwang, S., Lin, C., Chen, I., Chen, J., Liu, L. and Dodds, W. K. (2004). Removal of multiple nitrogenous wastes by *Aspergillus niger* in a continuous fixed-slab reactor. **Bioresource Technology.** 93: 131-138.
- Jackson J. V. and Edwards V. H. (1975). Kinetics of substrate inhibition of exponential yeast growth. **Biotechnol. Bioeng.** 17: 943-983.
- Jarusutthirak, C. and Amy, G. (2007). Understanding soluble microbial products (SMP) as a component of effluent organic matter (EfOM). (2007). **Water Research.** 41: 2787-2793.

- Jasti, N., Khanal, S. K., Anthony, L. P. and Leeuwen, J. (2006). Fungal treatment of corn processing wastewater in an attached growth system. **Water Practice & Technology**. 1(3): 1-8.
- Jin, B., Leeuwen, H. J., Patel, B., Doelle, H. W. and Yu, Q. (1999). Production of fungal protein and glucoamylase by *Rhizopus oligosporus* from starch processing wastewater. **Process Biochemistry**. 34: 59-65.
- Juang, D. (2005). Effects of synthetic polymer on the filamentous bacteria in activated sludge. **Bioresource Technology**. 96(1): 31-40.
- Karim, M. I. A., and Sistrunk, W. A. (1984). Efficiency of selected strains of fungi in reducing chemical reducing chemical oxygen demand in wastewater from steam-peeled potatoes. **Journal of Food Processing and Preservation**. 8: 211-218.
- Kurakov, A. V., and Popov, A. I. (1996). Nitrifying activity and phytotoxicity of microscopic soil fungi. **Eurasian Soil Sci**. 28: 73–84.
- Kwok, W.K., Picioreanu, C., Ong, S.L., van Loosdrecht, M.C.M., Ng, W.J., Heijnen, J.J. (1998). Influence of biomass production and detachment forces on biofilm structures in a biofilm airlift suspension reactor. **Biotechnol. Bioeng**. 58 (4): 400–407.
- Lapidou, C. Y. and Rittmann, B. E. (2002a). A unified theory for extracellular polymeric substances, soluble microbial products, and active and inert biomass. **Water Research**. 36: 2711–2720.
- Lapidou, C. Y. and Rittmann, B. E. (2002b). Non-steady state modeling of extracellular polymeric substances, soluble microbial products, and active and inert biomass. **Water Research**. 36: 1983–1992.

- Lapidou, C. Y. (2003). **Modeling Heterogeneous Biofilms Including Active Biomass, Inert and Extracellular Polymeric Substances**. Ph. D. thesis. **Northwestern University**. Evanston, Illinois, USA.
- Lapidou, C. Y. and Rittmann, B. E. (2004a). Modeling the development of biofilm density including active bacteria, inert biomass, and extracellular polymeric substances. **Water Research**. 38: 3349–3361.
- Lapidou, C. Y. and Rittmann, B. E. (2004b). Evaluating trends in biofilm density using the UMCCA model. **Water Research**. 38: 3362–3372.
- Lee, M. W. and Park, J. M. (2007). One-dimensional mixed-culture biofilm model considering different space occupancies of particulate components. **Water Research**. 41: 4317-7328.
- Levenspiel, O. (1972). **Chemical Reaction Engineering**. 2nd edition. John Wiley & Sons. Canada.
- Lettinga, G., and Hulshoff Pol, L. W. (1991). UASB process design, operation and economy. **Water Sci and Technol**. 24: 87-107.
- Loosdrecht, M. C. M., Heijnen, J. J., Eberl, H., Kreft, J. and Picioreanu, C. (2002). **Mathematical Modelling of Biofilm Structures**. Antonie van Leeuwenhoek. 81: 245-256, Kluwer Academic Publishers. Netherlands
- Lowry, O. H., Rosebrough, N. J., Farr, A. L. and Randall, R. J. (1951). Protein measurement with the Folin-Phenol reagents. **J. Biol. Chem**. 193: 265–275.
- Liu, Y., Tay, J.-H. (2002). The essential role of hydrodynamic shear force in the formation of biofilm and granular sludge. **Water Res**. 36 (7): 1653–1665.
- Machdar, I., Harada, H., Ohashi, A., Sekiguchi, Y., Okui, H. and Ueki, K. (1997). A novel & cost effective sewage treatment system consisting of UASB pre treatment and

- aerobic post treatment units for developing countries. **Water Sci. and Technol.** 36(12): 189-197.
- Machdar, I., Sekiguchi, Y., Sumino, H. and Harada, H. (2000). Combination of a UASB reactor and a curtain DHS reactor as cost effective sewage treatment system for developing countries. **Water Sci. and Technol.** 42(3): 83-89.
- Mai, H. N. P., Duong, H. T., Trang, T. T. T., and Viet, N. T. (2004). Sustainable treatment of tapioca processing wastewater in South Vietnam. **International Conference on Wastewater Treatment for Nutrient Removal and Reuse**. Asian Institute of Technology, Vol. 2. Bangkok: Thailand.
- Mannan, S., Fakhru'l-Razi, A. and Alam, M. Z. (2005). Use of fungi improve bioconversion of activated sludge. **Water Research.** 39: 2935-2943.
- Metcalf & Eddy Inc. (2003). **Wastewater Engineering**. Tchobanoglous and Burton (eds.). McGraw-Hill, Inc., New York, USA.
- Molla, A. H., Fakhru'l-Razi, A., Abd-Aziz, S., Hanafi, M. M., Roychoudhury, P. K., Alam, M. Z. (2002). A potential resource for bioconversion of domestic wastewater sludge. **Bioresource Technology.** 85: 263–272
- Nakamura, Y., Sungusia, M. G., Sawada, T. and Kuwahara, M. (1999). Lignin-Degrading enzyme production by *Bjerkandera adusta* immobilized on polyurethane foam. **J. of Biosci. and Bioeng.** 88(1): 41-47.
- Ohashi, A., Harada, H. (1994). Adhesion strength of biofilm developed in an attached growth reactor. **Water Sci. Technol.** 29(10–11): 281–288.
- Ohashi, K., Hiroyuki, I., Harada, H. (2006). Anaerobic/Aerobic Treatment of Actual Dye Wastewater Using System Combining UASB and DHS Reactors. **J. Japan Society on Water Environment** [Online]. 29(10): 613-620. Available: <http://sciencelinks.jp/j-east/article/200622/000020062206A09>

21183.php

- Oliveira, M.A. Reis, E. and Nozaki, J. (1999). Biological treatment of wastewater from the cassava meal industry. **Environmental Research**. 85: 177-183.
- O’Nill, C., Hawkes, F. R., Hawkes, D. L., Lourenço, N. D. Pinheiro, H. M. and Delée, W. (1999). Colour in textile effluent-sources, measurement, discharge consents and simulation: a reviews. **J. Chem. Technol. Biotechnol**. 74: 1009-1018.
- Parker, D. S., Jacobs, T. Bower, E., Stowe, D. W. and Faemer, G. (1997). Maximizing trickling filter nitrification rates through biofilm control: Research review and full scale application. **Wat. Sci. Tech**. 36(1): 255-262.
- Plattes, M., Fiorelli, D., Gille, S., Girard, C., Henry, E., Minette, F., O’Nagy, O. and Schosseler, P. M. (2007). Modelling and dynamic simulation of a moving bed bioreactor using respirometry for the estimation of kinetic parameters. **Biochem. Eng. J**. 33. 253–259.
- Pizarro, G. E., Teixeira, J., Sepúlveda, M. and Noguera, D. R. (2005). Bitwise implementation of a two-dimensional cellular automata biofilm model. **J. Computing in Civil Engineering**. 19(3): 258-268.
- Picioreanu, C., Loosdrecht, M. C. M. and Heijnen, J. J. (1998a). A new combined differential-discrete cellular automaton for growth in gel beads. **Biotechnology and Bioengineering**. 57(6): 718-731.
- Picioreanu, C., van Loosdrecht, M. C. M. and Heijnen, J. J. (1998b). Mathematical modeling of biofilm structure with a hybrid differential-discrete cellular automaton approach. **Biotechnology and Bioengineering**. 58(1): 101-116.
- Polprasert C. and Chatsangthai S. (1989). Sulfide Production during Anaerobic Lagoon Treatment of Tapioca Wastewater. **Environmental International**. 14: 563-567.

- Pontes, P. P, Chernicharo, C. A. L, Frade, E. C. and Porto M. T. R. (2003). Performance evaluation of an UASB reactor used for combined treatment of domestic sewage and excess aerobic sludge from a trickling filter. **Water Sci. Technol.** 48(6): 227–234
- Quek, E., Ting, Y. and Tan, H. M. (2006). *Rhodococcus sp.* F92 immobilized on polyurethane foam shows ability to degrade various petroleum products. **Bioresource Technology.** 97: 32–38.
- Radwan, K. H. and Ramanujam, T. K. (1996). Organic reduction of tapioca wastewater using modified RBC. **Bioprocess Engineering.** 14: 125-129.
- Reampim, J. (2002). **Kinetics of Tapioca Starch Wastewater Treatment Using Anaerobic Contact Process with Steel Plates.** M. S. thesis (ISBN 974-533-167-8). Suranaree University of Technology. Nakhon Ratchasima, Thailand.
- Reuschenbach, P., Pagga, U. and Strotmann, U. (2003). A critical comparison of respirometric biodegradation tests based on OECD 301 and related methods. **Wat. Res.** 37(7): 1571-1582.
- Rickard, A.H., McBain, A.J., Stead, A.T., Gilbert, P., 2004. Shear rate moderates community diversity in freshwater biofilms. **Appl. Environ. Microbiol.** 70 (12): 7426–7435.
- Riefler, R. G., Ahlfeld, D. P. and Smets, B. F. (1998). Respirometric assay for biofilm kinetics estimation: parameter identifiability and retrievability. **Biotechnol. Bioeng.** 57(1): 35–45.
- Rittmann, B. E. and McCarty, P. L. (2001). **Environmental Biotechnology: Principles and Applications.** McGraw-Hill. New York. USA.

- Rochex, A., Godon, J., Bernet, N. and Escudié, R. (2008). Role of shear stress on composition, diversity and dynamics of biofilm bacterial communities. **Water Res.** 42: 4915-4922.
- Roh, S., Chum, Y. N., Nah, J., Shin, H. and Kim, S. (2006). Wastewater treatment by anaerobic digestion coupled with membrane processing. **J. Ind. Eng. Chem.** 12(3): 489-493.
- Rukvichitkul, T. (2002). **Treatment of Tapioca Starch Wastewater Using Anaerobic Attached Growth Pond.** M. S. thesis (ISBN 974-533-164-3). Suranaree University of Technology. Bangkok, Thailand.
- Seejuhn, R. (2002). **Waste Audit in a Tapioca Starch Milk Processing Factory.** M. S. thesis. Asian Institute of Technology. Pathunthani, Thailand.
- Şeker, Ş., Beyenal, H. and Tanyolac, A. (1995). The effects of biofilm thickness on biofilm density and substrate consumption rate in a differential fluidized bed biofilm reactor (DFBBR). **Journal of Biotechnology.** 41:39-47.
- Shoun, H., and Tanimoto, T. (1991). Denitrification by the fungus *Fusarium oxysporum* and involvement of cytochrome P-450 in the respiratory nitrite reduction. **J. Biol. Chem.** 266: 11078–11082.
- Stare, A., Vrečko, D., Hvala, N. and Strmčnik, S. (2007). Comparison of control strategies for nitrogen removal in an activated sludge process in terms of operating costs: A simulation study. *Water Research.* 41(9): 2004-2014.
- Stewart, P. S., (1998). A review of experimental measurements of effective diffusive permeability and effective diffusion coefficients in biofilms. *Biotechnology and Bioengineering.* 59(3): 261-272.
- Supawech, S. and Vorawichit, M. (1990). **Basic Bacteriology.** Siriyod Publication. Bangkok, Thailand.

- Tandukar, M., Uemura, S., Machdar, I., Ohashi, A. and Harada, H. (2005). A low cost municipal sewage treatment system with a combination of UASB and the “forth generation” downflow hanging sponge reactors. **Water Sci. and Technol.** 52(1-2): 323-329.
- Tandukar, M., Mechdar, I., Uemura, S., Ohashi, A. and Harada, H. (2006a). Potential of a novel sewage treatment system for developing countries: long term evaluation. **J. Environ. Eng.** 32(2): 166-172.
- Tandukar, M., Uemura, S., Ohashi, A. and Harada, H. (2006b). Combining UASB and the “fourth generation” down-flow hanging sponge reactor for municipal wastewater treatment. **Wat. Sci. Tech.** 53(3): 209-218.
- Tawfik, A. Machdar, I., Uemura, S., Ohashi, A. and Harada, H. (2006a). Sewage treatment in a combined upflow anaerobic sludge blanket (UASB)–DHS system. **Biochemical Engineering J.** 26: 210-219.
- Tawfik, A., El-Gohary, F., Ohashi, A. and Harada, H. (2006b). The influence of physical-chemical and biological factors on the removal a fecal coliform through down-flow hanging sponge (DHS) system treating UASB reactor effluent. **Water Research.** 40: 1877-1883.
- Thanh, N. C. and Simard, R. E. (1973). Biological treatment of domestic sewage by fungi. **Mycopathologia et Mycologia Applicata.** 51(2-3): 223-232.
- Tripathi, A. K., Harsh, N. S. K. and Gupta, N. (2007). Fungal treatment of industrial effluent: a mini review. **Life Science Journal.** 4(2): 78-81.
- Thullner, M., Schroth, M. H., Zeyer, J. and Kinzelbach, W. (2004). Modeling of microbial growth experiment with bio-clogging in two-dimensional saturated porous media flow field. **J. Contaminant Hydrology.** 70(1-2): 37-62.

- Torres, P. and Foresti, E. (2001). Domestic sewage treatment in a pilot system composed of UASB and SBR reactors. **Water Sci. and Technol.** 44(4): 247-253.
- Tung, T. Q., Miyata, N. and Iwahori, K. (2004). Growth of *Aspergillus oryzae* during treatment of cassava starch processing wastewater with high content of suspended solids. **Journal of Bioscience and Bioengineering.** 97(5): 329-335.
- von-Sperling, M., Freire, V. H. and de Lemon-Chernicharo, C. A. (2001). Performance evaluation of UASB-activated sludge system treating municipal wastewater. **Water Sci. and Technol.** 43(11): 323-328.
- Vanrolleghem P. A., Spanjers H., Petersen B., Ginestet P. and Takacs, I. (1999). Estimating (combinations of) activated sludge model No.1 parameters and components by respirometry. **Water Sci. Tech.** 39 (1): 195-214.
- Vogelaar, J. C. T., Klapwijk, B., Temmink, H., van Lier, J. B. (2003). Kinetic comparisons of mesophilic and thermophilic aerobic biomass. **J. Microbiol. Biotechnol.** 30: 81–88.
- Washe, S., Horn, H., Hempel, D.C., 2004. Influence of growth conditions on biofilm development and mass transfer at the bulk/biofilm interface. **Water Res.** 36 (19): 4775–4784.
- Wentzel, M., Mbewe, A., Lakay, M. and Ekama, G. (1999). Batch test for characterization of the carbonaceous materials in municipal wastewater. **Water SA.** 25(2): 327-335.
- Wichitsathian, B. (2004). **Application of Membrane Bioreactor System for Landfill Leachate Treatment.** Ph.D. thesis. Asian Institute of Technology. Pathumthani, Thailand.

- Wijeyekoon, S., Mino, T., Satoh, H. and Matsuo, T. (2004). Effects of substrate loading rate on biofilm structure. **Water Res.** 38: 2479-2488.
- Won, Y., Lee, T., Wu, Y. G. and Deshusses, M.R. (2004). An environmentally friendly methods controlling biomass in biotrickling filter for air pollution control. **J. Ind. Eng. Chem.** 10(1): 60-65.
- Uemara, S., Takahashi, K., Takaishi, A., Machdar, I., Ohashi, A. and Harada, H. (2002). Removal of indigenous coliphages and fecal coliforms by a novel sewage treatment system consisting of UASB and DHS units. **Water Sci. and Technol.** 46(1): 303-309.
- Vanrolleghem P. A., Spanjers H., Petersen B., Ginestet P. and Takacs, I. (1999). Estimating (combinations of) activated sludge model No.1 parameters and components by respirometry. **Water Sci. Tech.** 39 (1): 195-214.
- Vigneswaran, S., Ngo, H. H., Harada, H., Moon, H. and Aim, R. B. (2003). **Hanging sponge aerobic bioreactor and membrane-adsorption hybrid system: a novel two stage system in wastewater reuse** [Online]. Available: http://64.233.179.104/search?q=cache:kQCkbVm6t3wJ:www.uts.edu.au/research/docs/2002_UTS.pdf+Downflow+hanging+sponge&hl=th&gl=th&ct=clnk&cd=6.
- Yan, S., Subramanian, B., Surampalli, R. Y., Narasiah, S. and Tyagi, R. D. (2007). Isolation, characterization, and identification of bacteria from activated sludge and sludge and soluble microbial products in wastewater treatment systems. **Practice Periodical of Hazardous, Toxic, and Radioactive Waste Management.** 11(4): 240-258.
- Yang, Y., Tada, C., Tsukahara, K. and Sawayama, S. (2004). Methanogenic community and performance of fixed- and fluidized-bed reactors with reticular polyurethane form with different pore sizes. **Material Science and Engineering.** 24: 803-813.

- Yun, M. E., Yeon, K. M., Park, J. S., Lee, C. H., Chun, J. and Lim, D. J. (2006). Characterization of biofilm structure and its effect on membrane permeability in MBR for dye wastewater treatment. **Water Research**. 40(1): 45-52.
- Zhang, T. C. and Bishop, P. L. (1994a). Density porosity and pore structure of biofilms. **Water Research**. 28(11): 2267-2277.
- Zhang, T. C. and Bishop, P. L. (1994b). Evaluation tortuosity factors and effective diffusivities in biofilms. **Water Research**. 59: 80-89.
- Zhang, S-F, Splendiani, A., Freitas dos Santos, L. M. and Livingston, A. G. (1988). Determination of pollutant diffusion coefficients in naturally formed biofilms using a single tube extractive membrane bioreactor. **Biotechnology and Bioengineering**. 59: 80-89.
- Zhang, X. and Bishop, P. L. (2001). Spatial distribution of extracellular polymeric substances in biofilms. **J. Envi. Eng.** 127(9): 850-856.

APPENDIX A

EXPERIMENTAL DATA OF TRACER STUDY

Table A.1 The experimental data of tracer study at HRT = 0.9 h

Time (min)	mL of AgNO ₃ 0.141 N	C (mgCl/L)	dt _i	$C_i = C/C_0$	t _i C _i	t _i C _i dt _i	C _i dt _i	t _i ² C _i	t _i ² C _i dt _i
0	0.0	0.0	0	0.0	0.0	0.0	0.0	0.0	0.0
10	6.0	1119.7	10	0.4	4.0	40.3	4.0	40.3	402.9
20	7.0	1319.6	10	0.5	9.5	95.0	4.7	189.9	1899.4
30	9.5	1819.4	10	0.7	19.6	196.4	6.5	589.2	5892.4
40	12.4	2399.3	10	0.9	34.5	345.3	8.6	1381.4	13813.6
50	13.5	2619.2	10	0.9	47.1	471.2	9.4	2356.2	23562.3
60	8.0	1519.5	10	0.5	32.8	328.1	5.5	1968.4	19684.4
70	6.0	1119.7	10	0.4	28.2	282.0	4.0	1974.2	19742.0
80	5.5	1019.7	10	0.4	29.4	293.5	3.7	2348.3	23483.2
90	4.0	719.8	10	0.3	23.3	233.1	2.6	2097.9	20979.5
100	3.5	619.8	10	0.2	22.3	223.0	2.2	2230.3	22303.3
110	3.1	539.8	10	0.2	21.4	213.7	1.9	2350.5	23504.8
120	1.2	160.0	10	0.1	6.9	69.1	0.6	828.8	8288.2
130	0.8	80.0	10	0.0	3.7	37.4	0.3	486.4	4863.6
140	0.6	40.0	10	0.0	2.0	20.1	0.1	282.0	2820.3
150	0.7	60.0	10	0.0	3.2	32.4	0.2	485.6	4856.4
160	0.6	40.0	10	0.0	2.3	23.0	0.1	368.4	3683.6
170	0.5	20.0	10	0.0	1.2	12.2	0.1	207.9	2079.2
180	0.5	20.0	10	0.0	1.3	13.0	0.1	233.1	2331.1
190	0.5	20.0	10	0.0	1.4	13.7	0.1	259.7	2597.3
200	0.4	0.0	10	0.0	0.0	0.0	0.0	0.0	0.0
210	0.4	0.0	10	0.0	0.0	0.0	0.0	0.0	0.0
220	0.4	0.0	10	0.0	0.0	0.0	0.0	0.0	0.0
230	0.4	0.0	10	0.0	0.0	0.0	0.0	0.0	0.0
240	0.4	0.0	10	0.0	0.0	0.0	0.0	0.0	0.0
250	0.4	0.0	10	0.0	0.0	0.0	0.0	0.0	0.0
260	0.4	0.0	10	0.0	0.0	0.0	0.0	0.0	0.0
270	0.4	0.0	10	0.0	0.0	0.0	0.0	0.0	0.0
280	0.4	0.0	10	0.0	0.0	0.0	0.0	0.0	0.0
310	0.4	0.0	30	0.0	0.0	0.0	0.0	0.0	0.0
340	0.4	0.0	30	0.0	0.0	0.0	0.0	0.0	0.0
370	0.4	0.0	30	0.0	0.0	0.0	0.0	0.0	0.0
Total				5.5	294.3	2942.6	54.9	20,678.7	20,6787.3

Table A.2 The experimental data of tracer study at HRT = 1.7 h

Time (min)	mL of AgNO ₃ 0.141 N	C (mgCl ⁻ /L)	dt _i	$C_i = C/C_0$	t _i C _i	t _i C _i dt _i	C _i dt _i	t _i ² C _i	t _i ² C _i dt _i
0.0	0.0	0.0	0.0	0.0	0.0	0.0	0.0	0.0	0.0
10.0	0.5	20.0	10.0	0.0	0.1	0.7	0.1	0.7	7.2
20.0	4.5	819.7	10.0	0.3	5.9	59.0	2.9	118.0	1179.9
30.0	8.9	1699.5	10.0	0.6	18.3	183.5	6.1	550.4	5503.9
40.0	9.7	1859.4	10.0	0.7	26.8	267.6	6.7	1070.6	10705.6
50.0	12.4	2399.3	10.0	0.9	43.2	431.7	8.6	2158.4	21583.8
60.0	13.4	2599.2	10.0	0.9	56.1	561.2	9.4	3367.1	33670.7
70.0	13.2	2559.2	10.0	0.9	64.5	644.6	9.2	4512.5	45124.5
80.0	12.0	2319.3	10.0	0.8	66.8	667.7	8.3	5341.3	53412.7
90.0	10.4	1999.4	10.0	0.7	64.8	647.5	7.2	5827.6	58276.3
100.0	9.4	1799.4	10.0	0.6	64.8	647.5	6.5	6475.1	64751.4
110.0	8.2	1559.5	10.0	0.6	61.7	617.3	5.6	6790.3	67902.7
120.0	6.4	1199.6	10.0	0.4	51.8	518.0	4.3	6216.1	62161.4
130.0	3.4	599.8	10.0	0.2	28.1	280.6	2.2	3647.7	36476.6
140.0	1.0	120.0	10.0	0.0	6.0	60.4	0.4	846.1	8460.9
150.0	1.0	120.0	10.0	0.0	6.5	64.8	0.4	971.3	9712.7
160.0	0.9	100.0	10.0	0.0	5.8	57.6	0.4	920.9	9209.1
170.0	0.9	100.0	10.0	0.0	6.1	61.2	0.4	1039.6	10396.2
180.0	0.9	100.0	10.0	0.0	6.5	64.8	0.4	1165.5	11655.3
190.0	0.8	80.0	10.0	0.0	5.5	54.7	0.3	1038.9	10389.0
200.0	0.8	80.0	10.0	0.0	5.8	57.6	0.3	1151.1	11511.4
210.0	0.7	60.0	10.0	0.0	4.5	45.3	0.2	951.8	9518.5
220.0	0.7	60.0	10.0	0.0	4.7	47.5	0.2	1044.7	10446.6
230.0	0.7	60.0	10.0	0.0	5.0	49.6	0.2	1141.8	11417.8
240.0	0.6	40.0	10.0	0.0	3.5	34.5	0.1	828.8	8288.2
250.0	0.4	0.0	10.0	0.0	0.0	0.0	0.0	0.0	0.0
260.0	0.4	0.0	10.0	0.0	0.0	0.0	0.0	0.0	0.0
270.0	0.4	0.0	10.0	0.0	0.0	0.0	0.0	0.0	0.0
280.0	0.4	0.0	10.0	0.0	0.0	0.0	0.0	0.0	0.0
310.0	0.4	0.0	30.0	0.0	0.0	0.0	0.0	0.0	0.0
340.0	0.4	0.0	30.0	0.0	0.0	0.0	0.0	0.0	0.0
370.0	0.4	0.0	30.0	0.0	0.0	0.0	0.0	0.0	0.0
Total				8.0	612.5	6124.8	80.4	57,176.2	57,1762.2

Table A.3 The experimental data of tracer study at HRT = 2.6 h

Time (min)	mL of AgNO ₃ 0.141 N	C (mgCl ⁻ /L)	dt _i	$C_i = C/C_0$	t _i C _i	t _i C _i dt _i	C _i dt _i	t _i ² C _i	t _i ² C _i dt _i
0	0.0	0.0	0.0	0.0	0.0	0.0	0.0	0.0	0.0
10	0.9	90.0	10.0	0.0	0.3	3.2	0.3	3.2	32.4
20	6.6	1245.6	10.0	0.4	9.0	89.6	4.5	179.3	1792.9
30	10.6	2039.4	10.0	0.7	22.0	220.2	7.3	660.5	6604.6
40	12.0	2319.3	10.0	0.8	33.4	333.8	8.3	1335.3	13353.2
50	12.6	2445.2	10.0	0.9	44.0	439.9	8.8	2199.7	21997.5
60	12.7	2465.2	10.0	0.9	53.2	532.3	8.9	3193.5	31935.4
70	12.9	2489.2	10.0	0.9	62.7	627.0	9.0	4389.1	43890.7
80	12.7	2459.2	10.0	0.9	70.8	707.9	8.8	5663.6	56635.9
90	12.4	2399.3	10.0	0.9	77.7	777.0	8.6	6993.2	69931.5
100	11.1	2147.3	10.0	0.8	77.3	772.7	7.7	7727.0	77270.0
110	8.2	1565.5	10.0	0.6	62.0	619.7	5.6	6816.4	68163.8
120	5.1	943.7	10.0	0.3	40.8	407.5	3.4	4890.0	48900.3
130	3.1	541.8	10.0	0.2	25.3	253.5	1.9	3295.1	32950.6
140	2.1	345.9	10.0	0.1	17.4	174.3	1.2	2439.5	24395.5
150	1.2	165.9	10.0	0.1	9.0	89.6	0.6	1343.6	13435.9
160	1.0	120.0	10.0	0.0	6.9	69.1	0.4	1105.1	11050.9
170	1.0	118.0	10.0	0.0	7.2	72.2	0.4	1226.8	12267.5
180	1.0	112.0	10.0	0.0	7.3	72.5	0.4	1305.4	13053.9
190	0.9	108.0	10.0	0.0	7.4	73.8	0.4	1402.5	14025.2
200	0.8	84.0	10.0	0.0	6.0	60.4	0.3	1208.7	12086.9
210	0.7	60.0	10.0	0.0	4.5	45.3	0.2	951.8	9518.5
220	0.7	52.0	10.0	0.0	4.1	41.2	0.2	905.4	9053.7
230	0.6	30.0	10.0	0.0	2.5	24.8	0.1	570.9	5708.9
240	0.6	30.0	10.0	0.0	2.6	25.9	0.1	621.6	6216.1
250	0.6	30.0	10.0	0.0	2.7	27.0	0.1	674.5	6744.9
260	0.6	30.0	10.0	0.0	2.8	28.1	0.1	729.5	7295.3
270	0.5	20.0	10.0	0.0	1.9	19.4	0.1	524.5	5244.9
280	0.4	0.0	10.0	0.0	0.0	0.0	0.0	0.0	0.0
310	0.4	0.0	30.0	0.0	0.0	0.0	0.0	0.0	0.0
340	0.4	0.0	30.0	0.0	0.0	0.0	0.0	0.0	0.0
370	0.4	0.0	30.0	0.0	0.0	0.0	0.0	0.0	0.0
Total				8.8	660.8	6607.9	88.0	62355.7	623556.9

Table A.4 The experimental data of tracer study at HRT = 6.9 h

Time (min)	mL of AgNO ₃ 0.141 N	C (mgCl/L)	dt _i	$C_i = C/C_0$	t _i C _i	t _i C _i dt _i	C _i dt _i	t _i ² C _i	t _i ² C _i dt _i
0.0	0.0	0.0	0.0	0.0	0.0	0.0	0.0	0.0	0.0
30.0	0.4	0.0	30.0	0.0	0.0	0.0	0.0	0.0	0.0
60.0	3.0	519.8	30.0	0.2	10.9	327.3	5.5	654.6	19,637.1
90.0	6.7	1,259.6	30.0	0.4	39.7	1,189.6	13.2	3,568.7	107,060.2
120.0	10.5	2,019.4	30.0	0.7	84.8	2,542.8	21.2	10,171.0	305,131.0
150.0	12.4	2,399.3	30.0	0.8	125.9	3,776.4	25.2	18,881.9	566,456.0
180.0	12.5	2,419.2	30.0	0.8	152.3	4,569.4	25.4	27,416.5	822,494.2
210.0	12.9	2,499.2	30.0	0.9	183.6	5,507.2	26.2	38,550.5	1,156,514.4
240.0	12.8	2,479.2	30.0	0.9	208.1	6,243.6	26.0	49,948.8	1,498,465.0
270.0	10.2	1,959.4	30.0	0.7	185.0	5,551.3	20.6	49,961.4	1,498,842.7
300.0	9.0	1,719.5	30.0	0.6	180.4	5,412.8	18.0	54,128.0	1,623,840.6
330.0	8.0	1,519.5	30.0	0.5	175.4	5,261.7	15.9	57,879.2	1,736,376.6
360.0	6.0	1,119.7	30.0	0.4	141.0	4,229.5	11.7	50,754.5	1,522,633.8
390.0	4.2	759.8	30.0	0.3	103.6	3,109.2	8.0	40,419.8	1,212,593.5
405.0	3.2	559.8	15.0	0.2	79.3	1,189.6	2.9	32,118.1	481,770.9
420.0	2.5	419.9	15.0	0.1	61.7	925.2	2.2	25,905.9	388,588.8
435.0	2.2	359.9	15.0	0.1	54.8	821.4	1.9	23,819.5	357,292.1
450.0	1.5	219.9	15.0	0.1	34.6	519.3	1.2	15,577.5	233,663.1
465.0	1.4	199.9	15.0	0.1	32.5	487.8	1.0	15,121.2	226,818.4
480.0	1.2	160.0	15.0	0.1	26.9	402.8	0.8	12,890.0	193,350.3
495.0	1.1	146.0	15.0	0.1	25.3	379.1	0.8	12,508.8	187,631.5
510.0	0.9	100.0	15.0	0.0	17.8	267.5	0.5	9,094.8	136,421.5
525.0	0.8	80.0	15.0	0.0	14.7	220.3	0.4	7,710.1	115,651.4
540.0	0.8	80.0	15.0	0.0	15.1	226.6	0.4	8,157.0	122,354.5
555.0	0.8	80.0	15.0	0.0	15.5	232.9	0.4	8,616.4	129,246.4
570.0	0.6	40.0	15.0	0.0	8.0	119.6	0.2	4,544.2	68,163.5
585.0	0.6	40.0	15.0	0.0	8.2	122.7	0.2	4,786.6	71,798.3
600.0	0.6	40.0	15.0	0.0	8.4	125.9	0.2	5,035.2	75,527.5
615.0	0.6	46.0	15.0	0.0	9.9	148.4	0.2	6,083.6	91,253.7
645.0	0.6	40.0	30.0	0.0	9.0	270.6	0.4	5,818.8	174,562.9
675.0	0.6	40.0	30.0	0.0	9.4	283.2	0.4	6,372.6	191,178.9
705.0	0.6	40.0	30.0	0.0	9.9	295.8	0.4	6,951.7	208,550.2
Total				8.1	2,031.6	54,759.3	231.7	613,446.7	15,523,869.2

Table A.5 The experimental data of tracer study at HRT = 11.5 h

Time (min)	mL of AgNO ₃ 0.141 N	C (mgCl/L)	dt _i	$C_i = C/C_0$	t _i C _i	t _i C _i dt _i	C _i dt _i	t _i ² C _i	t _i ² C _i dt _i
0	0.0	-80.0	0.0	0.0	0.0	0.0	0.0	0.0	0.0
30	0.8	72.0	30.0	0.0	0.8	22.7	0.8	22.7	679.7
60	2.2	353.9	30.0	0.1	7.4	222.8	3.7	445.6	13,368.4
90	9.5	1,825.4	30.0	0.6	57.5	1,723.9	19.2	5171.7	15,5152.3
120	11.9	2,299.3	30.0	0.8	96.5	2,895.2	24.1	11,580.9	34,7426.4
150	13.0	2,519.2	30.0	0.9	132.2	3,965.2	26.4	19,826.0	59,4778.8
180	13.2	2,559.2	30.0	0.9	161.1	4,833.8	26.9	29,002.5	870,076.5
210	13.7	2,659.2	30.0	0.9	195.3	5,859.7	27.9	41,017.7	1,230,531.3
240	13.6	2,639.2	30.0	0.9	221.5	6,646.4	27.7	53,171.3	1,595,140.2
270	13.3	2,579.2	30.0	0.9	243.6	7,307.3	27.1	65,765.5	1,972,966.4
300	13.0	2,519.2	30.0	0.9	264.3	7,930.4	26.4	79,303.8	2,379,115.3
330	12.1	2,339.3	30.0	0.8	270.0	8,100.3	24.5	89,103.5	2,673,106.0
360	6.2	1,159.6	30.0	0.4	146.0	4,380.6	12.2	52,567.1	1577013.6
390	3.3	579.8	30.0	0.2	79.1	2,372.8	6.1	30,846.7	925,400.3
405	2.6	439.9	15.0	0.2	62.3	934.7	2.3	25,235.6	378,534.2
420	2.2	359.9	15.0	0.1	52.9	793.0	1.9	22,205.1	333,076.1
435	1.9	299.9	15.0	0.1	45.6	684.5	1.6	19,849.6	297743.5
450	1.4	199.9	15.0	0.1	31.5	472.0	1.0	14,161.4	212,421.0
465	1.3	179.9	15.0	0.1	29.3	439.0	0.9	13,609.1	204,136.6
480	1.2	160.0	15.0	0.1	26.9	402.8	0.8	12,890.0	193,350.3
495	1.1	146.0	15.0	0.1	25.3	379.1	0.8	12,508.8	187,631.5
510	1.0	120.0	15.0	0.0	21.4	321.0	0.6	10,913.7	163,705.8
525	1.0	114.0	15.0	0.0	20.9	313.9	0.6	10,986.9	164,803.3
540	1.0	114.0	15.0	0.0	21.5	322.9	0.6	11,623.7	174,355.2
555	0.8	80.0	15.0	0.0	15.5	232.9	0.4	8,616.4	129,246.4
570	0.7	66.0	15.0	0.0	13.2	197.3	0.3	7,498.0	112,469.8
585	0.7	60.0	15.0	0.0	12.3	184.1	0.3	7,179.8	107,697.5
600	0.7	60.0	15.0	0.0	12.6	188.8	0.3	7,552.7	113,291.2
615	0.6	46.0	15.0	0.0	9.9	148.4	0.2	6,083.6	91,253.7
645	0.6	40.0	30.0	0.0	9.0	270.6	0.4	5,818.8	174,562.9
675	0.6	40.0	30.0	0.0	9.4	283.2	0.4	6,372.6	191,178.9
705	0.5	26.0	30.0	0.0	6.4	192.3	0.3	4,518.6	135,557.6
Total				9.3	2,301.2	63,021.5	266.9	68,5449.6	17,699,770.8

APPENDIX B

EXPERIMENTAL DATA OF ORGANIC REMOVAL EFFICIENCY

Table B.1 SCOD removal efficiencies monitoring of two DHS systems during all experimental study

DATE	Influent (mg/L)	SCOD Effluent			
		FDHS		BDHS	
		SCOD (mg/L)	% COD removal	SCOD (mg/L)	% COD removal
23 Sep 07	350.0	190.0	45.7	264.0	24.6
25 Sep 07	320.0	157.0	50.9	180.0	43.8
27 Sep 07	341.0	168.0	50.7	236.0	30.8
29 Sep 07	350.0	197.0	43.7	242.0	30.9
1 Oct 07	329.0	152.0	53.8	290.0	11.9
3 Oct 07	307.0	164.5	46.4	230.4	25.0
5 Oct 07	376.0	192.0	48.9	230.0	38.8
7 Oct 07	367.0	170.0	53.7	192.0	47.7
9 Oct 07	340.0	160.0	52.9	206.0	39.4
11 Oct 07	309.0	196.0	36.6	227.0	26.5
13 Oct 07	332.0	162.0	51.2	198.0	40.4
15 Oct 07	363.0	124.3	65.8	148.0	59.2
17 Oct 07	424.0	144.0	66.0	240.0	43.4
19 Oct 07	424.0	144.0	66.0	184.0	56.6
21 Oct 07	364.0	221.0	39.3	182.0	50.0
23 Oct 07	337.1	141.1	58.1	180.3	46.5
25 Oct 07	313.6	141.0	55.0	141.1	55.0
27 Oct 07	284.2	165.1	41.9	153.6	46.0
29 Oct 07	392.0	187.8	52.1	196.0	50.0
31 Oct 07	320.0	160.0	50.0	108.0	66.3
2 Nov 07	439.0	247.0	43.7	207.8	52.7
4 Nov 07	495.4	227.2	54.1	192.0	61.2
6 Nov 07	345.4	171.6	50.3	194.0	43.8
8 Nov 07	441.1	162.8	63.1	232.8	47.2
10 Nov 07	441.1	175.5	60.2	232.8	47.2
12 Nov 07	375.1	165.0	56.0	258.7	31.0
14 Nov 07	370.3	165.9	55.2	219.9	40.6
16 Nov 07	313.3	213.1	32.0	200.5	36.0
18 Nov 07	376.0	138.0	63.3	238.1	36.7
20 Nov 07	338.4	213.1	37.0	200.5	40.7
22 Nov 07	338.4	178.1	47.4	200.5	40.7
24 Nov 07	323.7	185.6	42.7	198.4	38.7
26 Nov 07	312.5	160.8	48.5	199.6	36.1

Table B.1 SCOD removal efficiencies monitoring of two DHS systems during all experimental study (Continued)

DATE	Influent (mg/L)	SCOD Effluent			
		FDHS		BDHS	
		SCOD (mg/L)	% COD removal	SCOD (mg/L)	% COD removal
28 Nov 07	297.6	184.4	38.0	212.0	28.8
30 Nov 07	517.0	308.8	40.3	251.0	51.5
2 Dec 07	383.2	166.4	56.6	223.0	41.8
4 Dec 07	469.0	271.0	42.2	246.0	47.5
6 Dec 07	493.0	399.6	18.9	260.0	47.3
8 Dec 07	442.3	298.8	32.4	271.6	38.6
10 Dec 07	442.3	271.6	38.6	271.6	38.6
12 Dec 07	411.3	294.9	28.3	244.4	40.6
14 Dec 07	411.3	271.6	34.0	244.4	40.6
16 Dec 07	434.6	254.6	41.4	232.8	46.4
18 Dec 07	434.6	243.2	44.0	232.8	46.4
20 Dec 07	410.4	254.6	38.0	254.6	38.0
22 Dec 07	410.4	243.2	40.7	254.6	38.0
24 Dec 07	325.0	146.0	55.1	209.0	35.7
26 Dec 07	442.7	169.2	61.8	282.7	36.1
28 Dec 07	487.3	159.2	67.3	245.5	49.6
31 Dec 07	346.0	171.1	50.5	122.8	64.5
2 Jan 08	359.6	148.8	58.6	260.4	27.6
4 Jan 08	399.3	173.6	56.5	212.0	46.9
6 Jan 08	436.5	173.6	60.2	174.8	60.0
8 Jan 08	359.6	137.6	61.7	260.4	27.6
10 Jan 08	399.3	173.6	56.5	212.0	46.9
12 Jan 08	436.5	137.6	68.5	174.8	60.0
14 Jan 08	440.8	137.6	68.8	315.4	28.4
16 Jan 08	241.0	112.0	53.5	133.2	44.7
18 Jan 08	324.0	178.6	44.9	154.8	52.2
20 Jan 08	309.2	178.6	42.2	169.2	45.3
22 Jan 08	388.8	133.2	65.7	216.0	44.4
24 Jan 08	324.0	144.0	55.6	154.8	52.2
26 Jan 08	309.2	187.2	39.5	169.2	45.3
28 Jan 08	388.8	154.8	60.2	216.0	44.4
30 Jan 08	457.2	154.8	66.1	180.0	60.6
1 Feb 08	400.4	162.0	59.5	192.9	51.8

Table B.1 SCOD removal efficiencies monitoring of two DHS systems during all experimental study (Continued)

DATE	Influent (mg/L)	SCOD Effluent			
		FDHS		BDHS	
		SCOD (mg/L)	% COD removal	SCOD (mg/L)	% COD removal
3 Feb 08	411.3	218.4	46.9	207.5	49.6
5 Feb 08	415.0	171.1	58.8	243.9	41.2
7 Feb 08	296.6	141.2	52.4	171.1	42.3
9 Feb 08	456.7	291.2	36.2	254.8	44.2
11 Feb 08	498.7	229.3	54.0	309.4	38.0
13 Feb 08	498.0	238.5	52.1	309.4	37.9
15 Feb 08	232.9	72.8	68.7	87.4	62.5
17 Feb 08	243.9	110.2	54.8	160.2	34.3
19 Feb 08	245.0	123.8	49.5	109.2	55.4
21 Feb 08	218.4	110.2	49.5	160.2	26.6
23 Feb 08	345.8	129.3	62.6	156.5	54.7
25 Feb 08	345.8	110.2	68.1	156.5	54.7
27 Feb 08	345.8	123.8	64.2	156.5	54.7
29 Feb 08	211.9	110.2	48.0	112.8	46.8
2 Mar 08	345.8	110.2	68.1	156.5	54.7
4 Mar 08	320.1	123.8	61.3	156.5	51.1
6 Mar 08	296.9	110.2	62.9	99.4	66.5
8 Mar 08	296.9	110.2	62.9	99.4	66.5
10 Mar 08	296.9	123.8	58.3	99.4	66.5
12 Mar 08	284.7	110.2	61.3	124.0	56.4
14 Mar 08	284.7	155.2	45.5	124.0	56.4
16 Mar 08	505.0	221.2	56.2	231.4	54.2
18 Mar 08	505.0	249.2	50.7	231.4	54.2
20 Mar 08	235.1	112.0	52.4	39.2	83.3
22 Mar 08	235.1	110.2	53.1	39.2	83.3
24 Mar 08	356.8	155.2	56.5	90.2	74.7
26 Mar 08	235.1	67.0	71.5	39.2	83.3
28 Mar 08	260.0	140.0	46.2	194.0	25.4
30 Mar 08	465.6	155.2	66.7	170.7	63.3
1 Apr 08	465.6	221.2	52.5	170.7	63.3
3 Apr 08	492.8	276.0	44.0	182.4	63.0
5 Apr 08	372.0	148.0	60.2	80.0	78.5
7 Apr 08	298.5	148.0	50.4	104.0	65.2

Table B.1 SCOD removal efficiencies monitoring of two DHS systems during all experimental study (Continued)

DATE	Influent (mg/L)	SCOD Effluent			
		FDHS		BDHS	
		SCOD (mg/L)	% COD removal	SCOD (mg/L)	% COD removal
9 Apr 08	536.0	276.0	48.5	287.1	46.4
11 Apr 08	536.0	110.2	79.4	287.1	46.4
13 Apr 08	536.0	155.2	71.0	287.1	46.4
15 Apr 08	418.5	67.0	84.0	195.0	53.4
17 Apr 08	418.5	140.0	66.5	195.0	53.4
19 Apr 08	418.5	155.2	62.9	195.0	53.4
21 Apr 08	237.7	102.0	57.1	123.0	48.3
23 Apr 08	273.9	187.4	31.6	140.0	48.9
25 Apr 08	238.5	140.0	41.3	135.0	43.4
27 Apr 08	356.0	155.2	56.4	132.0	62.9
29 Apr 08	356.0	102.0	71.3	132.0	62.9
1 May 08	238.5	187.4	21.4	135.0	43.4
3 May 08	356.0	248.3	30.3	132.0	62.9
5 May 08	356.0	155.2	56.4	132.0	62.9
7 May 08	356.0	221.2	37.9	132.0	62.9
9 May 08	358.5	156.0	56.5	135.0	62.3
11 May 08	356.0	148.0	58.4	132.0	62.9
13 May 08	295.3	148.0	49.9	131.0	55.6
15 May 08	370.1	276.0	25.4	131.0	64.6
17 May 08	370.1	110.2	70.2	131.0	64.6
19 May 08	370.1	102.0	72.4	131.0	64.6
21 May 08	295.3	116.9	60.4	131.0	55.6
23 May 08	273.4	116.9	57.2	150.7	44.9
25 May 08	265.2	116.9	55.9	154.9	41.6
27 May 08	207.7	119.7	42.4	112.6	45.8
29 May 08	325.5	102.0	68.7	199.0	38.9
31 May 08	262.0	87.7	66.5	153.0	41.6
2 Jun 08	262.0	87.7	66.5	153.0	41.6
4 Jun 08	265.6	133.6	49.7	115.5	56.5
6 Jun 08	266.8	102.0	61.8	147.6	44.7
8 Jun 08	266.8	187.4	29.8	147.6	44.7
10 Jun 08	359.9	140.0	61.1	162.2	54.9
12 Jun 08	370.2	155.2	58.1	194.7	47.4

Table B.1 SCOD removal efficiencies monitoring of two DHS systems during all experimental study (Continued)

DATE	Influent (mg/L)	SCOD Effluent			
		FDHS		BDHS	
		SCOD (mg/L)	% COD removal	SCOD (mg/L)	% COD removal
14 Jun 08	359.9	102.0	71.7	162.2	54.9
16 Jun 08	429.2	229.3	46.6	278.4	35.1
18 Jun 08	310.8	238.5	23.3	271.6	12.6
20 Jun 08	343.4	72.8	78.8	252.2	26.6
22 Jun 08	456.0	110.2	75.8	290.3	36.3
24 Jun 08	440.0	123.8	71.9	306.4	30.4
26 Jun 08	359.9	110.2	69.4	162.2	54.9
28 Jun 08	370.2	129.3	65.1	194.7	47.4
30 Jun 08	359.9	110.2	69.4	162.2	54.9
2 Jul 08	370.2	243.2	34.3	194.7	47.4
4 Jul 08	234.3	146.0	37.7	144.6	38.3
6 Jul 08	456.0	169.2	62.9	290.3	36.3
8 Jul 08	440.0	159.2	63.8	306.4	30.4
10 Jul 08	370.2	171.1	53.8	194.7	47.4
12 Jul 08	359.9	148.8	58.7	162.2	54.9
14 Jul 08	349.2	173.6	50.3	192.0	45.0
16 Jul 08	349.2	173.6	50.3	192.0	45.0
18 Jul 08	404.5	137.6	66.0	260.0	35.7
20 Jul 08	340.4	155.2	54.4	217.6	36.1
22 Jul 08	395.6	67.0	83.1	302.1	23.6
24 Jul 08	30.4	140.0	58.9	217.6	36.1
26 Jul 08	340.4	155.2	54.4	217.6	36.1
28 Jul 08	263.4	102.0	61.3	201.0	23.7
30 Jul 08	370.2	187.4	49.4	194.7	47.4
1 Aug 08	359.9	140.0	61.1	162.2	54.9
3 Aug 08	349.2	155.2	55.6	192.0	45.0
5 Aug 08	349.2	102.0	70.8	192.0	45.0
7 Aug 08	370.2	187.4	49.4	194.7	47.4
9 Aug 08	359.9	137.6	61.8	162.2	54.9
11 Aug 08	368.7	175.4	52.4	183.0	50.4
13 Aug 08	296.0	123.0	58.4	102.0	65.5
15 Aug 08	363.5	213.8	41.2	144.6	60.2
17 Aug 08	204.8	110.0	46.3	98.2	52.1

Table B.1 SCOD removal efficiencies monitoring of two DHS systems during all experimental study (Continued)

DATE	Influent (mg/L)	SCOD Effluent			
		FDHS		BDHS	
		SCOD (mg/L)	% COD removal	SCOD (mg/L)	% COD removal
19 Aug 08	277.8	166.4	40.1	93.4	66.4
21 Aug 08	179.2	97.0	45.9	93.4	47.9
23 Aug 08	290.5	136.9	52.9	89.6	69.2
25 Aug 08	373.5	142.0	62.0	190.0	49.1
27 Aug 08	293.7	120.0	59.1	145.0	50.6
29 Aug 08	279.5	110.0	60.6	124.6	55.4
31 Aug 08	279.5	142.0	49.2	124.6	55.4
2 Sep 08	235.3	100.0	57.5	78.1	66.8
4 Sep 08	476.0	110.0	76.9	120.0	74.8
6 Sep 08	325.6	130.6	59.9	107.0	67.1
8 Sep 08	236.8	122.0	48.5	105.0	55.7
10 Sep 08	471.0	96.0	79.6	173.9	63.1
12 Sep 08	435.2	88.7	79.6	100.9	76.8
14 Sep 08	435.2	130.0	70.1	67.5	84.5
16 Sep 08	340.0	92.0	72.9	108.8	68.0
18 Sep 08	353.6	141.4	60.0	103.4	70.8
20 Sep 08	427.8	113.0	73.6	89.2	79.1
22 Sep 08	340.0	103.0	69.7	108.8	68.0
24 Sep 08	279.0	116.0	58.4	111.6	60.0
26 Sep 08	279.0	98.0	64.9	111.6	60.0
28 Sep 08	279.0	96.7	65.3	96.7	65.3
30 Sep 08	297.6	85.0	71.4	111.6	62.5
2 Oct 08	409.2	113.0	72.4	134.0	67.3
4 Oct 08	297.6	86.0	71.1	120.0	59.7
6 Oct 08	502.2	108.3	78.4	113.0	77.5
8 Oct 08	253.2	98.0	61.3	104.2	53.3
10 Oct 08	223.2	87.0	61.0	108.0	51.6
12 Oct 08	260.4	97.0	62.7	109.0	58.1
14 Oct 08	340.0	143.8	57.7	108.8	68.0
16 Oct 08	340.0	118.6	65.1	108.8	68.0
18 Oct 08	279.0	85.0	69.5	111.6	60.0
20 Oct 08	279.0	113.0	59.5	96.7	65.3
22 Oct 08	427.8	86.0	79.9	89.2	79.1
24 Oct 08	409.2	108.0	73.6	134.0	67.3

Table B.1 SCOD removal efficiencies monitoring of two DHS systems during all experimental study (Continued)

DATE	Influent (mg/L)	SCOD Effluent			
		FDHS		BDHS	
		SCOD (mg/L)	% COD removal	SCOD (mg/L)	% COD removal
26 Oct 08	297.6	98.0	67.1	120.0	59.7
28 Oct 08	297.6	87.0	70.8	111.6	62.5
30 Oct 08	502.2	97.0	80.7	113.0	77.5
1 Nov 08	279.0	103.8	62.8	96.7	65.3
3 Nov 08	427.8	143.8	66.4	89.2	79.1
5 Nov 08	409.2	128.2	68.7	134.0	67.3
7 Nov 08	297.6	85.0	71.4	120.0	59.7
9 Nov 08	340.0	113.0	66.8	108.8	68.0
11 Nov 08	298.4	86.0	71.2	114.0	61.8
13 Nov 08	298.4	82.7	72.3	114.0	61.8
16 Nov 08	298.4	115.7	61.2	114.0	61.8
19 Nov 08	389.0	107.5	72.4	82.7	78.7
22 Nov 08	410.0	115.7	71.8	82.7	79.8
25 Nov 08	396.8	133.6	66.3	134.0	66.2
28 Nov 08	385.2	97.0	74.8	143.0	62.9
1 Dec 08	396.0	98.0	75.3	156.0	60.6
4 Dec 08	425.0	123.0	71.1	203.0	52.2
7 Dec 08	512.0	154.0	69.9	198.0	61.3
10 Dec 08	595.2	164.0	72.4	323.0	45.7
13 Dec 08	617.5	124.0	79.9	234.0	62.1
16 Dec 08	520.8	148.0	71.6	249.2	52.2
19 Dec 08	647.3	134.0	79.3	271.6	58.0
22 Dec 08	578.0	241.0	58.3	360.8	37.6
25 Dec 08	446.4	102.0	77.2	223.0	50.0
28 Dec 08	639.8	103.0	83.9	334.8	47.7
31 Dec 08	367.8	96.0	73.9	208.3	43.4
3 Jan 09	468.7	145.0	69.1	133.9	71.4
6 Jan 09	491.0	142.0	71.1	186.0	62.1
9 Jan 09	319.0	123.0	61.4	186.0	41.7
12 Jan 09	425.0	145.0	65.9	154.0	63.8
15 Jan 09	417.0	123.0	70.5	165.0	60.4
18 Jan 09	389.0	89.0	77.1	125.0	67.9
21 Jan 09	458.0	128.0	72.1	106.0	76.9

Table B.1 SCOD removal efficiencies monitoring of two DHS systems during all experimental study (Continued)

DATE	Influent (mg/L)	SCOD Effluent			
		FDHS		BDHS	
		SCOD (mg/L)	% COD removal	SCOD (mg/L)	% COD removal
24 Jan 09	465.0	165.0	64.5	204.0	56.1
27 Jan 09	521.0	127.0	75.6	219.0	58.0
30 Jan 09	426.0	123.0	71.1	165.0	61.3
2 Feb 09	437.0	115.0	73.7	154.0	64.8
5 Feb 09	445.0	124.0	72.1	123.0	72.4
8 Feb 09	426.0	132.0	69.0	145.0	66.0
11 Feb 09	478.0	126.0	73.6	165.0	65.5
14 Feb 09	426.0	141.0	66.9	102.0	76.1
17 Feb 09	454.0	119.0	73.8	121.0	73.3
20 Feb 09	521.0	118.0	77.4	145.0	72.2
23 Feb 09	475.0	116.0	75.6	162.0	65.9
26 Feb 09	485.0	119.0	75.5	154.0	68.2

Table B.2 Experimental results of TCOD, TBOD, SCOD and SBOD concentrations of two DHS influents (RUN I)

DHS profiles	DATE	BDHS						FDHS					
		TCOD (mg/L)	SCOD (mg/L)	TBOD (mg/L)	SBOD (mg/L)	A*	B*	TCOD (mg/L)	SCOD (mg/L)	TBOD (mg/L)	SBOD (mg/L)	A*	B*
Inlet	10 Dec 08	729.4	442.3	330.0	193.8	0.45	0.44	729.4	442.3	330.0	193.8	0.45	0.44
	23 Feb 08	1,106.6	436.8	416.0	234.0	0.38	0.54	1,106.6	436.8	416.0	234.0	0.38	0.54
	4 Mar 08	538.7	254.8	280.0	180.0	0.52	0.71	538.7	254.8	280.0	180.0	0.52	0.71
	18 Mar 08	1,685.0	605.0	308.0	257.0	0.18	0.42	1,685.0	605.0	308.0	257.0	0.18	0.42
	7 Jun 08	754.0	432.0	397.0	211.0	0.53	0.49	754.0	432.0	397.0	211.0	0.53	0.49
	30 May 08	1,830.0	297.0	230.0	170.0	0.13	0.57	1,830.0	297.0	230.0	170.0	0.13	0.57
	7 Jul 08	1,285.0	537.0	340.0	215.0	0.26	0.40	1,285.0	537.0	340.0	215.0	0.26	0.40
	8 Jul 08	1,343.0	521.5	350.0	230.0	0.26	0.44	1,343.0	521.5	350.0	230.0	0.26	0.44
	9 Jul 08	1,567.0	366.1	340.0	250.0	0.22	0.68	1,567.0	366.1	340.0	250.0	0.22	0.68
	10 Jul 08	1,890.0	497.0	370.0	230.0	0.20	0.46	1,890.0	497.0	370.0	230.0	0.20	0.46
AVE		1,272.9	439.0	336.1	217.1	0.3	0.5	1,272.9	439.0	336.1	217.1	0.3	0.5
SD		481.2	108.9	54.5	28.8	0.1	0.1	481.2	108.9	54.5	28.8	0.1	0.1

Remark: A = TBOD/TCOD, B=SBOD/SBOD

Table B.3 Experimental results of TCOD, TBOD, SCOD and SBOD concentrations in segment 1 effluent of two DHS systems (RUN I)

DHS profiles	DATE	BDHS						FDHS					
		TCOD (mg/L)	SCOD (mg/L)	TBOD (mg/L)	SBOD (mg/L)	A*	B*	TCOD (mg/L)	SCOD (mg/L)	TBOD (mg/L)	SBOD (mg/L)	A*	B*
Segment 1	10 Dec 08	541.4	399.6	225.1	159.1	0.42	0.40	342.0	415.2	83.0	32.0	0.24	0.08
	23 Feb 08	786.2	254.8	298.0	116.0	0.38	0.46	655.2	269.0	60.0	50.0	0.09	0.19
	4 Mar 08	385.8	207.5	230.0	113.0	0.60	0.54	364.0	207.5	90.0	45.0	0.25	0.22
	18 Mar 08	795.0	284.0	224.0	131.0	0.28	0.46	450.0	397.0	87.0	67.0	0.19	0.17
	7 Jun 08	398.0	97.2	135.0	50.6	0.34	0.52	340.0	162.0	67.5	45.0	0.20	0.28
	30 May 08	1,651.0	257.0	245.0	180.0	0.15	0.70	340.0	257.0	56.0	68.0	0.16	0.26
	7 Jul 08	865.0	413.0	267.0	132.0	0.31	0.32	265.0	467.7	86.0	56.0	0.32	0.12
	8 Jul 08	765.0	451.6	256.0	145.0	0.33	0.32	450.0	505.3	76.0	47.0	0.17	0.09
	9 Jul 08	780.0	262.1	245.0	156.0	0.31	0.60	387.0	353.6	78.0	65.0	0.20	0.18
	10 Jul 08	789.0	282.9	276.0	143.0	0.35	0.51	399.0	249.6	68.0	77.0	0.17	0.31
AVE		775.6	291.0	240.1	132.6	0.31	0.46	399.2	328.4	75.2	55.2	0.19	0.17
SD		353.5	105.6	43.8	35.2			105.6	115.8	11.8	13.8		

Remark: A = TBOD/TCOD, B=SBOD/SBOD

Table B.4 Experimental results of TCOD, TBOD, SCOD and SBOD concentrations in segment 2 effluent of two DHS systems (RUN I)

DHS profiles	DATE	BDHS						FDHS					
		TCOD (mg/L)	SCOD (mg/L)	TBOD (mg/L)	SBOD (mg/L)	A*	B*	TCOD (mg/L)	SCOD (mg/L)	TBOD (mg/L)	SBOD (mg/L)	A*	B*
Segment 2	10 Dec 08	451.2	349.2	196.4	89.0	0.44	0.25	579.0	388.0	50.0	35.0	0.09	0.09
	23 Feb 08	567.8	193.0	154.0	69.0	0.27	0.36	582.4	256.5	43.0	30.0	0.07	0.12
	4 Mar 08	990.0	145.6	143.0	45.0	0.14	0.31	458.6	265.7	34.0	45.0	0.07	0.17
	18 Mar 08	676.0	178.0	134.0	52.0	0.20	0.29	557.0	231.0	35.0	65.0	0.06	0.28
	7 Jun 08	1,204.0	55.1	234.0	22.5	0.19	0.41	356.0	184.7	42.2	35.0	0.12	0.19
	30 May 08	894.0	222.0	127.0	67.0	0.14	0.30	344.0	208.0	67.0	50.0	0.19	0.24
	7 Jul 08	980.0	397.8	145.0	54.0	0.15	0.14	450.0	376.3	87.0	49.0	0.19	0.13
	8 Jul 08	750.0	344.1	134.0	45.0	0.18	0.13	356.0	467.7	98.0	45.0	0.28	0.10
	9 Jul 08	670.0	228.8	154.0	67.0	0.23	0.29	445.0	303.7	88.0	54.0	0.20	0.18
	10 Jul 08	890.0	193.4	144.0	66.0	0.16	0.34	427.0	235.0	95.0	45.0	0.22	0.19
AVE		807.3	230.7	156.5	57.7	0.19	0.25	455.5	291.7	63.9	45.3	0.14	0.16
SD		225.7	104.7	33.3	18.1			91.2	91.2	26.0	10.3		

Remark: A = TBOD/TCOD, B=SBOD/SBOD

Table B.5 Experimental results of TCOD, TBOD, SCOD and SBOD concentrations in segment 3 effluent of two DHS systems (RUN I)

DHS profiles	DATE	BDHS						FDHS					
		TCOD (mg/L)	SCOD (mg/L)	TBOD (mg/L)	SBOD (mg/L)	A*	B*	TCOD (mg/L)	SCOD (mg/L)	TBOD (mg/L)	SBOD (mg/L)	A*	B*
Segment 3	10 Dec 08	376.0	310.4	144.4	123.7	0.38	0.40	451.2	399.6	80.0	40.0	0.18	0.10
	23 Feb 08	313.0	182.0	99.0	77.0	0.32	0.42	509.6	229.3	85.0	36.0	0.17	0.16
	4 Mar 08	231.0	83.7	123.0	112.0	0.53	1.34	269.4	163.8	78.0	54.0	0.29	0.33
	18 Mar 08	534.0	249.0	134.0	57.0	0.25	0.23	581.0	207.0	79.0	38.0	0.14	0.18
	7 Jun 08	786.0	48.6	194.0	22.5	0.25	0.46	469.0	178.2	39.4	19.7	0.08	0.11
	30 May 08	708.0	191.0	123.0	65.0	0.17	0.34	206.0	142.0	69.0	36.0	0.33	0.25
	7 Jul 08	480.0	306.4	145.0	77.0	0.30	0.25	250.0	376.3	79.0	47.0	0.32	0.12
	8 Jul 08	342.0	306.4	132.0	98.0	0.39	0.32	235.0	290.3	76.0	44.0	0.32	0.15
	9 Jul 08	456.0	194.7	112.0	89.0	0.25	0.46	243.0	182.2	78.0	34.0	0.32	0.19
	10 Jul 08	234.0	190.9	156.0	78.0	0.67	0.41	267.0	232.1	77.0	32.0	0.29	0.14
AVE		446.0	206.3	136.2	79.9	0.31	0.39	348.1	240.1	74.0	38.1	0.21	0.16
SD		200.7	110.3	57.9	39.8			138.2	88.5	12.8	9.3		

Remark: A = TBOD/TCOD, B=SBOD/SBOD

Table B.6 Experimental results of TCOD, TBOD, SCOD and SBOD concentrations in segment 4 effluent of two DHS systems (RUN I)

DHS profiles	DATE	BDHS						FDHS					
		TCOD (mg/L)	SCOD (mg/L)	TBOD (mg/L)	SBOD (mg/L)	A*	B*	TCOD (mg/L)	SCOD (mg/L)	TBOD (mg/L)	SBOD (mg/L)	A*	B*
Segment 4	10 Dec 08	278.2	271.6	60.0	50.0	0.22	0.18	353.4	298.8	40.0	32.0	0.11	0.11
	23 Feb 08	1,092.0	156.5	50.0	45.0	0.05	0.29	509.6	229.3	62.0	30.0	0.12	0.13
	4 Mar 08	240.2	156.5	45.0	67.0	0.19	0.43	342.2	192.9	50.0	40.0	0.15	
	18 Mar 08	676.0	231.0	65.0	36.0	0.10	0.16	391.0	249.0	45.0	60.0	0.12	0.24
	7 Jun 08	1,095.4	45.6	30.9	16.9	0.03	0.37	256.0	204.0	30.9	25.3	0.12	0.12
	30 May 08	571.0	199.0	67.0	32.0	0.12	0.16	206.0	102.0	67.0	32.0	0.33	0.31
	7 Jul 08	567.0	290.3	45.0	19.0	0.08	0.07	232.0	267.0	68.0	33.0	0.29	0.12
	8 Jul 08	398.0	306.4	75.0	24.0	0.19	0.08	234.0	306.4	85.0	27.0	0.36	0.09
	9 Jul 08	654.0	162.2	87.0	32.0	0.13	0.20	256.0	215.9	45.0	29.0	0.18	0.13
	10 Jul 08	765.0	194.7	78.0	27.0	0.10	0.14	277.0	153.5	67.0	28.0	0.24	0.18
AVE		633.7	201.4	60.3	34.9	0.10	0.17	305.7	221.9	56.0	33.6	0.18	0.15
SD		295.9	77.9	17.5	15.4			93.5	63.4	16.4	10.1		

Remark: A = TBOD/TCOD, B=SBOD/SBOD

Table B.7 Experimental results of TCOD, TBOD, SCOD and SBOD concentrations of two DHS influents (RUN II)

DHS profiles	DATE	BDHS						FDHS					
		TCOD (mg/L)	SCOD (mg/L)	TBOD ₅ (mg/L)	SBOD ₅ (mg/L)	A*	B*	TCOD (mg/L)	SCOD (mg/L)	TBOD ₅ (mg/L)	SBOD ₅ (mg/L)	A*	B*
Inlet	2 Sep 08	1,358.0	420.0	410.0	165.0	0.30	0.39	1,358.0	420.0	410.0	165.0	0.30	0.39
	3 Sep 08	1,657.0	416.0	396.0	175.0	0.24	0.42	1,657.0	416.0	396.0	175.0	0.24	0.42
	11 Sep 08	1,537.0	465.0	430.0	259.0	0.28	0.56	1,537.0	465.0	430.0	259.0	0.28	0.56
	15 Sep 08	1,442.0	445.0	425.0	210.0	0.29	0.47	1,442.0	445.0	425.0	210.0	0.29	0.47
	20 Sep 08	1,647.0	398.0	410.0	220.0	0.25	0.55	1,647.0	398.0	410.0	220.0	0.25	0.55
AVE		1,528.2	428.8	414.2	205.8	0.27	0.48	1,528.2	428.8	414.2	205.8	0.27	0.48
SD		129.6	26.3	13.5	37.6	0.03	0.07	129.6	26.3	13.5	37.6	0.03	0.07

Remark: A = TBOD/TCOD, B=SBOD/SBOD

Table B.8 Experimental results of TCOD, TBOD, SCOD and SBOD concentrations in segment 1 effluent of two DHS systems (RUN II)

DHS profiles	DATE	BDHS						FDHS					
		TCOD (mg/L)	SCOD (mg/L)	TBOD ₅ (mg/L)	SBOD ₅ (mg/L)	A*	B*	TCOD (mg/L)	SCOD (mg/L)	TBOD ₅ (mg/L)	SBOD ₅ (mg/L)	A*	B*
Segment 1	2 Sep 08	448.8	220.0	52.0	32.0	0.12	0.15	364.0	198.0	25.0	20.0	0.07	0.10
	3 Sep 08	544.0	182.0	49.0	25.0	0.09	0.14	320.0	142.1	32.0	19.2	0.10	0.14
	11 Sep 08	380.0	186.0	42.2	28.0	0.11	0.15	432.0	133.8	33.8	19.5	0.08	0.15
	15 Sep 08	325.0	175.0	39.0	23.0	0.12	0.13	432.0	174.0	28.0	16.0	0.06	0.09
	20 Sep 08	354.0	195.0	35.0	24.0	0.10	0.12	368.0	156.0	27.0	21.0	0.07	0.13
AVE		410.4	191.6	43.4	26.4	0.11	0.14	383.2	160.8	29.2	19.1	0.08	0.12
SD		87.6	17.4	7.0	3.6	0.01	0.01	48.4	25.8	3.6	1.9	0.01	0.02

Remark: A = TBOD/TCOD, B=SBOD/SBOD

Table B.9 Experimental results of TCOD, TBOD, SCOD and SBOD concentrations in segment 2 effluent of two DHS systems (RUN II)

DHS profiles	DATE	BDHS						FDHS					
		TCOD (mg/L)	SCOD (mg/L)	TBOD ₅ (mg/L)	SBOD ₅ (mg/L)	A*	B*	TCOD (mg/L)	SCOD (mg/L)	TBOD ₅ (mg/L)	SBOD ₅ (mg/L)	A*	B*
Segment 2	2 Sep 08	336.0	256.0	32.0	21.0	0.10	0.08	320.0	102.0	22.0	18.0	0.07	0.18
	3 Sep 08	230.0	185.0	40.2	19.0	0.17	0.10	297.0	149.0	29.0	19.0	0.10	0.13
	11 Sep 08	310.0	175.0	36.6	22.5	0.12	0.13	275.0	113.1	28.1	19.6	0.10	0.17
	15 Sep 08	257.0	165.0	32.0	21.0	0.12	0.13	310.0	182.4	28.1	19.6	0.09	0.11
	20 Sep 08	295.0	187.0	35.0	22.0	0.12	0.12	254.0	156.0	25.0	19.6	0.10	0.13
AVE		285.6	193.6	35.2	21.1	0.13	0.11	291.2	140.5	26.4	19.2	0.09	0.14
SD		42.2	36.0	3.4	1.3	0.03	0.02	26.8	32.8	2.9	0.7	0.01	0.03

Remark: A = TBOD/TCOD, B=SBOD/SBOD

Table B.10 Experimental results of TCOD, TBOD, SCOD and SBOD concentrations in segment 3 effluent of two DHS systems (RUN II)

DHS profiles	DATE	BDHS						FDHS					
		TCOD (mg/L)	SCOD (mg/L)	TBOD ₅ (mg/L)	SBOD ₅ (mg/L)	A*	B*	TCOD (mg/L)	SCOD (mg/L)	TBOD ₅ (mg/L)	SBOD ₅ (mg/L)	A*	B*
Segment 3	2 Sep 08	408.0	210.0	32.0	25.0	0.08	0.12	321.0	120.0	25.0	19.7	0.08	0.16
	3 Sep 08	236.0	220.0	32.0	30.0	0.14	0.14	310.0	177.6	20.0	19.3	0.06	0.11
	11 Sep 08	210.0	189.0	28.1	19.5	0.13	0.10	235.0	81.5	25.3	18.0	0.11	0.22
	15 Sep 08	234.0	179.0	23.0	15.0	0.10	0.08	289.0	170.2	23.0	19.0	0.08	0.11
	20 Sep 08	256.0	165.0	24.0	17.0	0.09	0.10	275.0	164.0	25.0	17.0	0.09	0.10
AVE		268.8	192.6	27.8	21.3	0.11	0.11	286.0	142.7	23.7	18.6	0.08	0.14
SD		79.5	22.4	4.3	6.1	0.03	0.02	33.7	40.9	2.2	1.1	0.02	0.05

Remark: A = TBOD/TCOD, B=SBOD/SBOD

Table B.11 Experimental results of TCOD, TBOD, SCOD and SBOD concentrations in segment 4 effluent of two DHS systems (RUN II)

DHS profiles	DATE	BDHS						FDHS					
		TCOD (mg/L)	SCOD (mg/L)	TBOD ₅ (mg/L)	SBOD ₅ (mg/L)	A*	B*	TCOD (mg/L)	SCOD (mg/L)	TBOD ₅ (mg/L)	SBOD ₅ (mg/L)	A*	B*
Segment 4	2 Sep 08	225.0	118.0	27.0	23.0	0.12	0.19	265.0	98.0	20.0	17.0	0.08	0.17
	3 Sep 08	223.0	114.0	25.0	24.0	0.11	0.21	256.0	101.0	19.4	16.0	0.08	0.16
	11 Sep 08	267.0	95.0	28.0	22.0	0.10	0.23	178.0	93.6	23.4	16.5	0.13	0.18
	15 Sep 08	245.0	114.0	27.0	19.0	0.11	0.17	232.0	122.0	23.0	17.0	0.10	0.14
	20 Sep 08	221.0	112.0	27.0	19.0	0.12	0.17	214.0	95.0	19.0	15.0	0.09	0.16
AVE		236.2	110.6	26.8	21.4	0.11	0.19	229.0	101.9	21.0	16.3	0.09	0.16
SD		19.7	9.0	1.1	2.3	0.01	0.03	34.9	11.6	2.1	0.8	0.02	0.01

Remark: A = TBOD/TCOD, B=SBOD/SBOD

Table B.12 Experimental results of TCOD, TBOD, SCOD and SBOD concentrations of two DHS influents (RUN III)

DHS profiles	DATE	BDHS						FDHS					
		TCOD (mg/L)	SCOD (mg/L)	TBOD ₅ (mg/L)	SBOD ₅ (mg/L)	A*	B*	TCOD (mg/L)	SCOD (mg/L)	TBOD ₅ (mg/L)	SBOD ₅ (mg/L)	A*	B*
Inlet	12 Jan 09	1,421.0	541.0	541.0	297.0	0.38	0.55	1,421.0	541.0	541.0	297.0	0.38	0.55
	15 Jan 09	954.0	421.0	457.0	234.0	0.48	0.56	954.0	421.0	457.0	234.0	0.48	0.56
	25 Feb 09	754.0	365.0	386.0	168.0	0.51	0.46	754.0	365.0	386.0	168.0	0.51	0.46
	15 Mar 09	1,141.0	485.0	534.0	256.0	0.47	0.53	1,141.0	485.0	534.0	256.0	0.47	0.53
	17 Mar 09	1,259.0	435.0	621.0	254.0	0.49	0.58	1,259.0	435.0	621.0	254.0	0.49	0.58
AVE		1,105.8	449.4	507.8	241.8	0.47	0.54	1,105.8	449.4	507.8	241.8	0.47	0.54
SD		260.2	66.7	89.5	47.2	0.05	0.05	260.2	66.7	89.5	47.2	0.05	0.05

Remark: A = TBOD/TCOD, B=SBOD/SBOD

Table B.13 Experimental results of TCOD, TBOD, SCOD and SBOD concentrations in segment 1 effluent of two DHS systems (RUN III)

DHS profiles	DATE	BDHS						FDHS					
		TCOD (mg/L)	SCOD (mg/L)	TBOD ₅ (mg/L)	SBOD ₅ (mg/L)	A*	B*	TCOD (mg/L)	SCOD (mg/L)	TBOD ₅ (mg/L)	SBOD ₅ (mg/L)	A*	B*
Segment 1	12 Jan 09	745.0	425.0	325.0	132.0	0.44	0.31	650.0	112.0	52.0	32.0	0.08	0.29
	15 Jan 09	525.0	321.0	315.0	103.0	0.60	0.32	418.0	154.0	42.0	25.0	0.10	0.16
	25 Feb 09	421.0	312.0	298.0	98.0	0.71	0.31	398.0	132.0	45.0	34.0	0.11	0.26
	15 Mar 09	589.0	410.0	330.0	120.0	0.56	0.29	417.0	147.0	52.0	29.0	0.12	0.20
	17 Mar 09	621.0	394.0	256.0	104.0	0.41	0.26	425.0	132.0	30.0	25.0	0.07	0.19
AVE		580.2	372.4	304.8	111.4	0.54	0.30	461.6	135.4	44.2	29.0	0.10	0.22
SD		119.7	52.3	29.9	14.2	0.12	0.02	105.8	16.2	9.1	4.1	0.02	0.05

Remark: A = TBOD/TCOD, B=SBOD/SBOD

Table B.14 Experimental results of TCOD, TBOD, SCOD and SBOD concentrations in segment 2 effluent of two DHS systems (RUN III)

DHS profiles	DATE	BDHS						FDHS					
		TCOD (mg/L)	SCOD (mg/L)	TBOD ₅ (mg/L)	SBOD ₅ (mg/L)	A*	B*	TCOD (mg/L)	SCOD (mg/L)	TBOD ₅ (mg/L)	SBOD ₅ (mg/L)	A*	B*
Segment 2	12 Jan 09	350.0	287.0	134.0	99.0	0.38	0.34	450.0	102.0	22.0	18.0	0.05	0.18
	15 Jan 09	325.0	241.0	119.0	82.0	0.37	0.34	360.0	92.0	29.0	19.0	0.08	0.21
	25 Feb 09	312.0	169.0	108.0	95.0	0.35	0.56	325.0	113.1	28.1	19.6	0.09	0.17
	15 Mar 09	351.0	269.0	127.0	102.0	0.36	0.38	310.0	125.0	28.1	19.6	0.09	0.16
	17 Mar 09	294.0	287.0	121.0	110.0	0.41	0.38	298.0	103.0	30.0	18.0	0.10	0.17
AVE		326.4	250.6	121.8	97.6	0.37	0.40	348.6	107.0	27.4	18.8	0.08	0.18
SD		24.6	49.3	9.7	10.3	0.02	0.09	61.3	12.5	3.1	0.8	0.02	0.02

Remark: A = TBOD/TCOD, B=SBOD/SBOD

Table B.15 Experimental results of TCOD, TBOD, SCOD and SBOD concentrations in segment 3 effluent of two DHS systems (RUN III)

DHS profiles	DATE	BDHS						FDHS					
		TCOD (mg/L)	SCOD (mg/L)	TBOD ₅ (mg/L)	SBOD ₅ (mg/L)	A*	B*	TCOD (mg/L)	SCOD (mg/L)	TBOD ₅ (mg/L)	SBOD ₅ (mg/L)	A*	B*
Segment 3	12 Jan 09	569.0	256.0	165.0	25.0	0.29	0.10	359.0	109.0	25.0	19.7	0.07	0.18
	15 Jan 09	457.0	248.0	108.0	30.0	0.24	0.12	310.0	104.0	20.0	19.3	0.06	0.19
	25 Feb 09	362.0	198.0	145.0	27.0	0.40	0.14	286.0	98.0	25.3	18.0	0.09	0.18
	15 Mar 09	378.0	196.0	165.0	29.0	0.44	0.15	289.0	154.0	23.0	19.0	0.08	0.12
	17 Mar 09	396.0	213.0	109.0	28.0	0.28	0.13	294.0	75.0	34.0	19.0	0.12	0.25
AVE		432.4	222.2	138.4	27.8	0.33	0.13	307.6	108.0	25.5	19.0	0.08	0.19
SD		84.4	28.1	28.5	1.9	0.09	0.02	30.2	28.8	5.2	0.6	0.02	0.05

Remark: A = TBOD/TCOD, B=SBOD/SBOD

Table B.16 Experimental results of TCOD, TBOD, SCOD and SBOD concentrations in segment 4 effluent of two DHS systems (RUN III)

DHS profiles	DATE	BDHS						FDHS					
		TCOD (mg/L)	SCOD (mg/L)	TBOD ₅ (mg/L)	SBOD ₅ (mg/L)	A*	B*	TCOD (mg/L)	SCOD (mg/L)	TBOD ₅ (mg/L)	SBOD ₅ (mg/L)	A*	B*
Segment 4	12 Jan 09	654.0	184.0	135.0	29.0	0.21	0.16	289.0	110.0	20.0	18.0	0.07	0.16
	15 Jan 09	546.0	126.0	129.0	26.0	0.24	0.21	265.0	133.8	19.4	16.0	0.07	0.12
	25 Feb 09	436.0	135.0	109.0	26.0	0.25	0.19	254.0	93.6	25.3	18.5	0.10	0.20
	15 Mar 09	397.0	189.0	98.0	27.0	0.25	0.14	216.0	149.6	34.0	19.0	0.16	0.13
	17 Mar 09	395.0	174.0	114.0	19.0	0.29	0.11	274.0	107.0	25.0	17.0	0.09	0.16
AVE		485.6	161.6	117.0	25.4	0.25	0.16	259.6	118.8	24.7	17.7	0.10	0.15
SD		112.4	29.1	15.0	3.8	0.03	0.04	27.5	22.5	5.9	1.2	0.04	0.03

Remark: A = TBOD/TCOD, B=SBOD/SBOD

APPENDIX C

EXPERIMENTAL DATA OF NITROGEN

REMOVAL EFFICIENCY

Table C.1 Nitrogen concentrations of influent of two DHS systems during RUN I

DHS profiles	DATE	BDHS (mg-N/L)					FDHS (mg-N/L)				
		Org-N	NH ₄ -N	NO ₂ -N	NO ₃ -N	Total-N	Org-N	NH ₄ -N	NO ₂ -N	NO ₃ -N	Total-N
Inlet	10 Dec 08	38.9	156.0	0.1	0.1	195.1	38.9	156.0	0.1	0.1	195.1
	23 Feb 08	45.0	175.0	0.1	0.1	220.2	45.0	175.0	0.1	0.1	220.2
	4 Mar 08	25.9	145.0	0.1	0.1	171.1	25.9	145.0	0.1	0.1	171.1
	18 Mar 08	18.0	169.0	0.1	0.1	187.2	18.0	169.0	0.1	0.1	187.2
	7 Jun 08	38.0	184.0	0.1	0.1	222.2	38.0	184.0	0.1	0.1	222.2
	30 May 08	15.6	132.0	0.1	0.1	147.8	15.6	132.0	0.1	0.1	147.8
	7 Jul 08	28.9	165.0	0.1	0.1	194.1	28.9	165.0	0.1	0.1	194.1
	8 Jul 08	42.0	185.0	0.1	0.1	227.2	42.0	185.0	0.1	0.1	227.2
	9 Jul 08	38.5	175.8	0.1	0.1	214.5	38.5	175.8	0.1	0.1	214.5
	10 Jul 08	35.8	166.0	0.1	0.1	202.0	35.8	166.0	0.1	0.1	202.0
AVE		32.7	165.3	0.1	0.1	198.1	32.7	165.3	0.1	0.1	198.1
SD		10.1	16.9	0.0	0.0	25.0	10.1	16.9	0.0	0.0	25.0

Table C.2 Nitrogen concentrations of segment 1 effluent of two DHS systems during RUN I

DHS profiles	DATE	BDHS (mg-N/L)					FDHS (mg-N/L)				
		Org-N	NH ₄ -N	NO ₂ -N	NO ₃ -N	Total-N	Org-N	NH ₄ -N	NO ₂ -N	NO ₃ -N	Total-N
Segment 1	10 Dec 08	25.0	125.0	0.3	0.7	151.0	96.0	184.0	0.1	0.1	280.2
	23 Feb 08	29.0	145.0	0.2	0.6	174.8	95.0	171.0	0.1	0.1	266.2
	4 Mar 08	15.0	123.0	0.3	0.8	139.1	87.0	175.0	0.1	0.1	262.2
	18 Mar 08	12.0	137.0	0.2	0.9	150.1	94.3	166.0	0.1	0.1	260.5
	7 Jun 08	25.0	142.0	0.4	0.4	167.8	97.0	174.0	0.1	0.1	271.2
	30 May 08	9.0	104.0	0.6	0.5	114.1	92.0	171.0	0.1	0.1	263.2
	7 Jul 08	20.5	123.0	0.1	0.6	144.2	94.0	173.0	0.1	0.1	267.2
	8 Jul 08	16.0	142.0	0.3	0.8	159.1	99.0	172.0	0.1	0.1	271.2
	9 Jul 08	22.0	134.0	0.3	0.7	157.0	102.0	171.0	0.1	0.1	273.2
	10 Jul 08	19.0	136.0	0.3	0.7	156.0	97.0	168.0	0.1	0.1	265.2
AVE		19.3	131.1	0.3	0.7	151.3	95.3	172.5	0.1	0.1	268.0
SD		6.3	12.5	0.1	0.1	16.7	4.0	4.8	0.0	0.0	6.0

Table C.3 Nitrogen concentrations of segment 2 effluent of two DHS systems during RUN I

DHS profiles	DATE	BDHS (mg-N/L)					FDHS (mg-N/L)				
		Org-N	NH ₄ -N	NO ₂ -N	NO ₃ -N	Total-N	Org-N	NH ₄ -N	NO ₂ -N	NO ₃ -N	Total-N
Segment 2	10 Dec 08	23	86.0	4.1	0.6	113.7	71.0	195.0	0.1	0.1	266.2
	23 Feb 08	25	89.0	5.2	0.5	119.7	85.0	178.0	0.1	0.1	263.2
	4 Mar 08	19	96.0	2.3	0.8	118.1	74.0	210.0	0.1	0.1	284.2
	18 Mar 08	19	68.0	1.3	0.4	88.7	70.0	212.0	0.1	0.1	282.2
	7 Jun 08	22	75.0	3.0	0.3	100.3	69.0	190.0	0.1	0.1	259.2
	30 May 08	26	83.0	3.0	0.7	112.7	65.0	189.0	0.1	0.1	254.2
	7 Jul 08	28	87.0	1.9	0.9	117.8	71.0	187.0	0.1	0.1	258.2
	8 Jul 08	26	94.0	2.9	0.4	123.3	69.0	195.0	0.1	0.1	264.2
	9 Jul 08	22	93.0	3.6	0.7	119.3	67.0	196.0	0.1	0.1	263.2
	10 Jul 08	21	88.0	4.1	0.5	113.6	69.0	198.0	0.1	0.1	267.2
AVE		23.1	85.9	3.1	0.6	112.7	71.0	195.0	0.1	0.1	266.2
SD		3.1	8.7	1.2	0.2	10.5	5.5	10.2	0.0	0.0	9.8

Table C.4 Nitrogen concentrations of segment 3 effluent of two DHS systems during RUN I

DHS profiles	DATE	BDHS (mg-N/L)					FDHS (mg-N/L)				
		Org-N	NH ₄ -N	NO ₂ -N	NO ₃ -N	Total-N	Org-N	NH ₄ -N	NO ₂ -N	NO ₃ -N	Total-N
Segment 3	10 Dec 08	12.0	59.0	12.0	6.0	89.0	60.0	189.0	0.1	0.1	266.2
	23 Feb 08	13.0	65.0	20.0	3.0	101.0	52.0	175.0	0.1	0.1	263.2
	4 Mar 08	9.0	63.0	23.0	2.0	97.0	67.0	179.0	0.1	0.1	284.2
	18 Mar 08	8.0	62.0	25.0	6.0	101.0	57.0	186.0	0.1	0.1	282.2
	7 Jun 08	13.0	54.0	15.0	5.0	87.0	50.0	179.0	0.1	0.1	259.2
	30 May 08	14.0	55.0	19.0	3.9	91.9	63.0	189.0	0.1	0.1	254.2
	7 Jul 08	12.0	57.0	20.0	4.2	93.2	62.0	192.0	0.1	0.1	258.2
	8 Jul 08	15.0	54.0	24.0	4.6	97.6	56.0	174.0	0.1	0.1	264.2
	9 Jul 08	11.0	52.0	19.0	4.9	86.9	62.0	176.0	0.1	0.1	263.2
	10 Jul 08	9.0	46.0	17.0	4.8	76.8	61.0	177.0	0.1	0.1	267.2
AVE		11.6	56.7	19.4	4.4	92.1	59.0	181.6	0.1	0.1	240.8
SD		2.3	5.7	4.0	1.2	7.5	5.2	6.7	0.0	0.0	9.8

Table C.5 Nitrogen concentrations of segment 4 effluent of two DHS systems during RUN I

DHS profiles	DATE	BDHS (mg-N/L)					FDHS (mg-N/L)				
		Org-N	NH ₄ -N	NO ₂ -N	NO ₃ -N	Total-N	Org-N	NH ₄ -N	NO ₂ -N	NO ₃ -N	Total-N
Segment 4	10 Dec 08	15.0	36.0	7.8	9.6	68.4	52.0	198.0	0.1	0.1	195.1
	23 Feb 08	11.0	31.0	8.9	9.6	60.5	56.0	165.0	0.1	0.1	220.2
	4 Mar 08	11.0	37.0	6.0	6.7	60.7	59.0	174.0	0.1	0.1	171.1
	18 Mar 08	14.0	41.0	9.0	7.5	71.5	68.0	169.0	0.1	0.1	187.2
	7 Jun 08	9.0	39.0	6.0	5.7	59.7	49.0	162.0	0.1	0.1	222.2
	30 May 08	17.0	28.0	7.0	9.6	61.6	39.0	170.0	0.1	0.1	147.8
	7 Jul 08	8.0	29.0	10.2	8.2	55.4	53.0	185.0	0.1	0.1	194.1
	8 Jul 08	22.0	32.0	6.0	10.1	70.1	33.0	186.0	0.1	0.1	227.2
	9 Jul 08	9.2	37.0	9.0	8.6	63.8	52.0	183.0	0.1	0.1	214.5
	10 Jul 08	8.5	38.0	8.0	7.9	62.4	55.0	186.0	0.1	0.1	202
AVE		12.5	34.8	7.8	8.4	63.4	51.6	177.8	0.1	0.1	229.6
SD		4.5	4.5	1.5	1.4	5.1	9.8	11.5	0.0	0.0	13.6

Table C.6 Nitrogen concentrations of influent of two DHS systems during RUN II

DHS profiles	DATE	BDHS (mg-N/L)					FDHS (mg-N/L)				
		Org-N	NH ₄ -N	NO ₂ -N	NO ₃ -N	Total-N	Org-N	NH ₄ -N	NO ₂ -N	NO ₃ -N	Total-N
Inlet	2 Sep 08	46.0	77.0	0.1	0.1	123.2	46.0	77.0	0.1	0.1	123.2
	3 Sep 08	39.0	164.9	0.1	0.1	204.1	39.0	164.9	0.1	0.1	204.1
	11 Sep 08	37.0	187.0	0.1	0.1	224.2	37.0	187.0	0.1	0.1	224.2
	15 Sep 08	32.0	168.0	0.1	0.1	200.2	32.0	168.0	0.1	0.1	200.2
	20 Sep 08	48.2	252.0	0.1	0.1	300.4	48.2	252.0	0.1	0.1	300.4
AVE		40.4	169.8	0.1	0.1	210.4	40.4	169.8	0.1	0.1	210.4
SD		6.6	62.6	0.0	0.0	63.3	6.6	62.6	0.0	0.0	63.3

Table C.7 Nitrogen concentrations of segment 1 effluent of two DHS systems during RUN II

DHS profiles	DATE	BDHS (mg-N/L)					FDHS (mg-N/L)				
		Org-N	NH ₄ -N	NO ₂ -N	NO ₃ -N	Total-N	Org-N	NH ₄ -N	NO ₂ -N	NO ₃ -N	Total-N
Segment 1	2 Sep 08	10.0	86.0	0.0	7.3	103.3	20.5	193.0	0.1	0.1	123.2
	3 Sep 08	16.0	71.5	0.3	4.6	92.4	20.1	180.0	0.1	0.1	204.1
	11 Sep 08	11.5	64.7	0.5	9.2	85.9	21.1	179.0	0.1	0.1	224.2
	15 Sep 08	7.6	79.5	0.3	8.4	95.8	24.0	195.7	0.1	0.1	200.2
	20 Sep 08	10.4	81.0	0.4	7.1	98.9	17.0	188.0	0.1	0.1	300.4
AVE		11.1	76.5	0.3	7.3	95.3	20.5	187.1	0.1	0.1	207.9
SD		3.1	8.4	0.2	1.7	6.6	2.5	7.5	0.0	0.0	8.7

Table C.8 Nitrogen concentrations of segment 2 effluent of two DHS systems during RUN II

DHS profiles	DATE	BDHS (mg-N/L)					FDHS (mg-N/L)				
		Org-N	NH ₄ -N	NO ₂ -N	NO ₃ -N	Total-N	Org-N	NH ₄ -N	NO ₂ -N	NO ₃ -N	Total-N
Segment 2	2 Sep 08	10.7	71.0	0.2	9.0	90.9	13.0	201.0	0.1	0.1	214.2
	3 Sep 08	14.9	62.0	0.2	7.5	84.6	16.0	198.0	0.1	0.1	214.2
	11 Sep 08	8.9	79.0	0.2	6.7	94.8	12.7	185.0	0.1	0.1	197.9
	15 Sep 08	6.7	62.0	0.3	8.1	77.1	11.0	198.0	0.1	0.1	209.2
	20 Sep 08	12.3	66.0	0.1	7.9	86.3	12.5	210.0	0.1	0.1	222.7
AVE		10.7	68.0	0.2	7.8	86.7	13.0	198.4	0.1	0.1	211.6
SD		3.1	7.2	0.1	0.8	6.7	1.8	9.0	0.0	0.0	9.1

Table C.9 Nitrogen concentrations of segment 3 effluent of two DHS systems during RUN II

DHS profiles	DATE	BDHS (mg-N/L)					FDHS (mg-N/L)				
		Org-N	NH ₄ -N	NO ₂ -N	NO ₃ -N	Total-N	Org-N	NH ₄ -N	NO ₂ -N	NO ₃ -N	Total-N
Segment 3	2 Sep 08	14.0	64.2	0.3	9.0	87.5	15.0	194.0	0.1	0.1	209.2
	3 Sep 08	15.0	61.0	0.3	7.2	83.5	25.0	180.0	0.1	0.1	205.2
	11 Sep 08	12.0	69.0	0.2	9.2	90.4	14.0	179.0	0.1	0.1	193.2
	15 Sep 08	16.0	62.8	0.1	7.9	86.8	13.0	191.5	0.1	0.1	204.7
	20 Sep 08	13.8	66.0	0.5	7.4	87.7	15.0	168.0	0.1	0.1	183.2
AVE		14.2	64.6	0.3	8.1	87.2	16.4	182.5	0.1	0.1	199.1
SD		1.5	3.1	0.1	0.9	2.5	4.9	10.5	0.0	0.0	10.7

Table C.10 Nitrogen concentrations of segment 4 effluent of two DHS systems during RUN II

DHS profiles	DATE	BDHS (mg-N/L)					FDHS (mg-N/L)				
		Org-N	NH ₄ -N	NO ₂ -N	NO ₃ -N	Total-N	Org-N	NH ₄ -N	NO ₂ -N	NO ₃ -N	Total-N
Segment 4	2 Sep 08	9.0	63.0	0.4	7.5	79.9	17.0	186.7	0.1	0.1	203.9
	3 Sep 08	14.0	64.0	0.1	7.9	86.0	15.0	178.0	0.1	0.1	193.2
	11 Sep 08	3.0	62.0	0.3	6.8	72.1	18.0	174.0	0.1	0.1	192.2
	15 Sep 08	14.0	57.0	0.3	7.2	78.5	14.0	183.5	0.1	0.1	197.7
	20 Sep 08	10.0	64.0	0.3	7.0	81.3	17.0	179.4	0.1	0.1	196.6
AVE		10.0	62.0	0.3	7.3	79.6	16.2	180.3	0.1	0.1	196.7
SD		4.5	2.9	0.1	0.4	5.0	1.6	4.9	0.0	0.0	4.6

Table C.11 Nitrogen concentrations of influent of two DHS systems during RUN III

DHS profiles	DATE	BDHS (mg-N/L)					FDHS (mg-N/L)				
		Org-N	NH ₄ -N	NO ₂ -N	NO ₃ -N	Total-N	Org-N	NH ₄ -N	NO ₂ -N	NO ₃ -N	Total-N
Inlet	12 Jan 09	36.0	179.0	0.1	0.1	215.2	36.0	179.0	0.1	0.1	215.2
	15 Jan 09	36.0	156.0	0.1	0.1	192.2	36.0	156.0	0.1	0.1	192.2
	25 Feb 09	32.0	165.0	0.1	0.1	197.2	32.0	165.0	0.1	0.1	197.2
	15 Mar 09	34.0	156.0	0.1	0.1	190.2	34.0	156.0	0.1	0.1	190.2
	17 Mar 09	37.0	167.0	0.1	0.1	204.2	37.0	167.0	0.1	0.1	204.2
AVE		35.0	164.6	0.1	0.1	199.8	35.0	164.6	0.1	0.1	199.8
SD		2.0	9.5	0.0	0.0	10.2	2.0	9.5	0.0	0.0	10.2

Table C.12 Nitrogen concentrations of segment 1 effluent of two DHS systems during RUN III

DHS profiles	DATE	BDHS (mg-N/L)					FDHS (mg-N/L)				
		Org-N	NH ₄ -N	NO ₂ -N	NO ₃ -N	Total-N	Org-N	NH ₄ -N	NO ₂ -N	NO ₃ -N	Total-N
Segment 1	12 Jan 09	15.0	86.0	0.3	7.5	108.8	12.0	195.0	0.1	0.1	207.20
	15 Jan 09	16.0	77.0	0.2	6.8	100.0	9.0	174.0	0.1	0.1	183.20
	25 Feb 09	14.0	95.0	0.4	9.5	118.9	8.0	179.0	0.1	0.1	187.20
	15 Mar 09	12.0	75.0	0.3	6.8	94.1	14.0	181.0	0.1	0.1	195.20
	17 Mar 09	17.0	90.0	0.3	7.1	114.4	9.0	197.0	0.1	0.1	206.20
AVE		14.8	84.6	0.3	7.5	107.2	10.4	185.2	0.1	0.1	195.80
SD		1.9	8.5	0.1	1.1	10.2	2.5	10.2	0.0	0.0	10.85

Table C.13 Nitrogen concentrations of segment 2 effluent of two DHS systems during RUN III

DHS profiles	DATE	BDHS (mg-N/L)					FDHS (mg-N/L)				
		Org-N	NH ₄ -N	NO ₂ -N	NO ₃ -N	Total-N	Org-N	NH ₄ -N	NO ₂ -N	NO ₃ -N	Total-N
Segment 2	12 Jan 09	12.0	85.0	0.2	7.9	105.1	10.0	182.0	0.1	0.1	192.20
	15 Jan 09	11.0	77.0	0.2	7.5	95.7	16.0	174.0	0.1	0.1	190.20
	25 Feb 09	9.6	68.0	0.1	9.3	87.0	8.0	196.0	0.1	0.1	204.20
	15 Mar 09	8.5	64.0	0.3	7.4	80.2	7.0	164.0	0.1	0.1	171.20
	17 Mar 09	17.0	79.0	0.2	9.1	105.3	10.0	176.0	0.1	0.1	186.20
AVE		11.6	74.6	0.2	8.2	94.7	10.2	178.4	0.1	0.1	188.80
SD		3.3	8.5	0.1	0.9	11.1	3.5	11.8	0.0	0.0	11.91

Table C.14 Nitrogen concentrations of segment 3 effluent of two DHS systems during RUN III

DHS profiles	DATE	BDHS (mg-N/L)					FDHS (mg-N/L)				
		Org-N	NH ₄ -N	NO ₂ -N	NO ₃ -N	Total-N	Org-N	NH ₄ -N	NO ₂ -N	NO ₃ -N	Total-N
Segment 3	12 Jan 09	12.0	71.0	0.2	10.6	93.8	9.0	198.0	0.1	0.1	207.2
	15 Jan 09	14.0	68.0	0.1	9.5	91.6	7.0	191.0	0.1	0.1	198.2
	25 Feb 09	19.0	54.0	0.3	8.3	81.6	12.0	187.0	0.1	0.1	199.2
	15 Mar 09	15.0	64.5	0.3	8.2	88.0	7.0	185.0	0.1	0.1	192.2
	17 Mar 09	13.0	67.5	0.1	9.5	90.1	11.0	201.0	0.1	0.1	212.2
AVE		14.6	65.0	0.2	9.2	89.0	9.2	192.4	0.1	0.1	201.8
SD		2.7	6.6	0.1	1.0	4.7	2.3	6.9	0.0	0.0	7.9

Table C.15 Nitrogen concentrations of segment 4 effluent of two DHS systems during RUN III

DHS profiles	DATE	BDHS (mg-N/L)					FDHS (mg-N/L)				
		Org-N	NH ₄ -N	NO ₂ -N	NO ₃ -N	Total-N	Org-N	NH ₄ -N	NO ₂ -N	NO ₃ -N	Total-N
Segment 4	12 Jan 09	12.0	67.0	0.2	7.8	87.0	6.0	189.0	0.1	0.1	195.2
	15 Jan 09	11.0	63.0	0.3	6.4	80.7	5.0	175.0	0.1	0.1	180.2
	25 Feb 09	9.0	58.0	0.1	8.5	75.6	8.0	194.0	0.1	0.1	202.2
	15 Mar 09	6.0	56.0	0.4	7.1	69.5	9.0	176.0	0.1	0.1	185.2
	17 Mar 09	4.0	67.0	0.1	7.2	78.3	7.0	185.0	0.1	0.1	192.2
AVE		8.4	62.2	0.2	7.4	78.2	7.0	183.8	0.1	0.1	191.0
SD		3.4	5.1	0.1	0.8	6.4	1.6	8.2	0.0	0.0	8.58

APPENDIX D

EXPERIMENTAL RESULT OF

COD FRACTION STUDY

Table D.1 Experimental results of COD fractionation of BDHS system during RUN I

Profiles	COD Concentrations (mg/L)						Soluble COD (mg/L)		Particulate COD (mg/L)		Soluble COD (%)		Particulate COD (%)	
	TCOD	SCOD	PCOD	TBOD ₂₀	SBOD ₂₀	PBOD	USCOD	BSCOD	UPCOD	BPCOD	USCOD	BSCOD	UPCOD	BPCOD
Inlet	1,273	439	834	335	211	124	228	211	710	124	18	17	56	10
Segment 1	776	291	485	234	115	119	176	115	366	119	23	15	47	15
Segment 2	807	231	577	552	93	459	138	93	117	459	17	12	15	57
Segment 3	446	206	240	260	75	185	131	75	55	185	29	17	12	42
Segment 4	634	201	432	76	68	8	133	68	50	382	21	11	8	60

Table D.2 Experimental results of COD fractionation of FDHS system during RUN I

Profiles	COD Concentrations (mg/L)						Soluble COD (mg/L)		Particulate COD (mg/L)		Soluble COD (%)		Particulate COD (%)	
	TCOD	SCOD	PCOD	TBOD ₂₀	SBOD ₂₀	PBOD	USCOD	BSCOD	UPCOD	BPCOD	USCOD	BSCOD	UPCOD	BPCOD
Inlet	1,273	439	834	335	211	124	228	211	710	124	18	17	56	10
Segment 1	427	328	99	138	93	45	236	93	53	45	55	22	13	11
Segment 2	356	292	64	101	45	56	247	45	8	56	69	13	2	16
Segment 3	469	240	229	96	56	39	184	56	190	39	39	12	40	8
Segment 4	256	222	34	65	56	8	166	56	26	8	65	22	10	3

Table D.3 Experimental results of COD fractionation of BDHS system during RUN II

Profiles	COD Concentrations (mg/L)						Soluble COD (mg/L)		Particulate COD (mg/L)		Soluble COD (%)		Particulate COD (%)	
	TCOD	SCOD	PCOD	TBOD ₂₀	SBOD ₂₀	PBOD	USCOD	BSCOD	UPCOD	BPCOD	USCOD	BSCOD	UPCOD	BPCOD
Inlet	1,528	429	1,099	550	379	171.0	49.8	379.0	928.2	171.0	3.3	24.8	60.7	11.2
Segment 1	410	192	219	95	82	13.0	109.6	82.0	205.8	13.0	26.7	20.0	50.1	3.2
Segment 2	286	194	92	65	56	9.0	137.6	56.0	83.0	9.0	48.2	19.6	29.1	3.2
Segment 3	269	193	76	57	45	12.0	147.6	45.0	64.2	12.0	54.9	16.7	23.9	4.5
Segment 4	236	111	125	55	45	10.0	65.6	45.0	115.4	10.0	27.8	19.1	48.9	4.2

Table D.4 Experimental results of COD fractionation of FDHS system during RUN II

Profiles	COD Concentrations (mg/L)						Soluble COD (mg/L)		Particulate COD (mg/L)		Soluble COD (%)		Particulate COD (%)	
	TCOD	SCOD	PCOD	TBOD ₂₀	SBOD ₂₀	PBOD	USCOD	BSCOD	UPCOD	BPCOD	USCOD	BSCOD	UPCOD	BPCOD
Inlet	1,528	429	1,099	520	379	141	50	379	958	141	3	25	63	9
Segment 1	383	161	222	42.0	42	0.0	119	42	222	0	31	11	58	0
Segment 2	291	141	151	35.0	25	10	116	25	140	10	40	9	48	3
Segment 3	286	143	143	32.0	25	7	118	25	136	7	41	9	48	2
Segment 4	229	102	127	32.0	25	7	77	25	120	7	34	11	52	3

Table D.5 Experimental results of COD fractionation of BDHS system during RUN III

Profiles	COD Concentrations (mg/L)						Soluble COD (mg/L)		Particulate COD (mg/L)		Soluble COD (%)		Particulate COD (%)	
	TCOD	SCOD	PCOD	TBOD ₂₀	SBOD ₂₀	PBOD	USCOD	BSCOD	UPCOD	BPCOD	USCOD	BSCOD	UPCOD	BPCOD
Inlet	1,106	449	656	508	242	266	208	242	390	266	19	22	35	24
Segment 1	580	372	208	305	111	193	261	111	14	193	45	19	2	33
Segment 2	326	251	76	122	98	24	153	98	52	24	47	30	16	7
Segment 3	432	222	210	138	28	111	194	28	100	111	45	6	23	26
Segment 4	486	162	324	117	25	92	136	25	232	92	28	5	48	19

Table D.6 Experimental results of COD fractionation of FDHS system during RUN III

Profiles	Concentrations (mg/L)						Soluble COD (mg/L)		Particulate COD (mg/L)		Soluble COD (%)		Particulate COD (%)	
	TCOD	SCOD	PCOD	TBOD ₂₀	SBOD ₂₀	PBOD	USCOD	BSCOD	UPCOD	BPCOD	USCOD	BSCOD	UPCOD	BPCOD
Inlet	1,106	449	656	508	242	266	208	242	390	266	19	22	35	24
Segment 1	462	135	326	44	29	15	106	29	311	15	23	6	67	3
Segment 2	349	107	242	27	19	9	88	19	233	9	25	5	67	2
Segment 3	308	108	200	26	19	7	89	19	193	7	29	6	63	2
Segment 4	260	119	141	25	18	7	101	18	134	7	39	7	52	3

APPENDIX E

**EXPERIMENTAL DATA OF BIOKINETIC
PARAMETERS**

Table E.1 Experimental data of biokinetic parameters of BDHS system

DHS profiles	S_0/X_0	S (mg/L)	DATE	OUR _{x,t} (mgO ₂ /mgVSS-h)	OUR _{x,e} (mgO ₂ /mgVSS-h)	OC (mgO ₂ /L)	OUR _{x,ox} (mgO ₂ /mgVSS-h)	OC/S	rx (mgCOD/mgVSS-h)	Y _{vss} (mgVSS/mgCOD)	μ (d ⁻¹)
Segment 1	0.05	20	24 May 08	0.011610	0.003000	5.72	0.00861	0.286	0.030	0.638	0.461
	0.10	40	24 May 08	0.011464	0.003900	6.58	0.00756	0.165	0.046	0.746	0.823
	0.20	80	24 May 08	0.014470	0.008100	7.02	0.00637	0.088	0.073	0.815	1.419
	0.30	120	24 May 08	0.017800	0.010650	7.61	0.00715	0.063	0.113	0.836	2.263
	0.50	200	24 May 08	0.020740	0.016950	8.28	0.00379	0.041	0.092	0.856	1.880
	0.80	320	3 Jun 08	0.021300	0.019200	8.30	0.00210	0.026	0.081	0.870	1.690
Segment 2	0.05	20	29 May 08	0.005870	0.001230	4.77	0.00464	0.239	0.019	0.680	0.317
	0.10	40	29 May 08	0.012590	0.007020	6.03	0.00557	0.151	0.037	0.758	0.672
	0.20	80	29 May 08	0.014040	0.007800	6.68	0.00624	0.084	0.075	0.818	1.468
	0.30	120	29 May 08	0.016890	0.008900	7.02	0.00799	0.059	0.137	0.841	2.756
	0.40	160	29 May 08	0.017890	0.010580	7.22	0.00731	0.045	0.162	0.853	3.315
	0.50	200	29 May 08	0.018200	0.012600	7.52	0.00560	0.038	0.149	0.859	3.071
Segment 3	0.80	320	3 Jun 08	0.019260	0.016580	7.66	0.00268	0.024	0.112	0.871	2.342
	0.05	20	2 Jun 08	0.00766	0.00240	5.13	0.00526	0.257	0.021	0.664	0.327
	0.10	40	2 Jun 08	0.00900	0.00480	5.22	0.00420	0.131	0.032	0.776	0.600
	0.20	80	3 Jun 08	0.00905	0.00600	5.40	0.00305	0.068	0.045	0.833	0.903
	0.30	120	3 Jun 08	0.01044	0.00630	5.69	0.00414	0.047	0.087	0.851	1.782
	0.40	160	3 Jun 08	0.01130	0.00860	6.03	0.00270	0.038	0.072	0.859	1.477
	0.50	200	3 Jun 08	0.01218	0.00990	6.13	0.00228	0.031	0.074	0.865	1.545
Segment 4	0.80	320	3 Jun 08	0.01309	0.01234	6.35	0.00075	0.020	0.038	0.875	0.794
	0.05	20	3 Jun 08	0.00748	0.00150	4.82	0.00598	0.241	0.025	0.678	0.404
	0.10	40	3 Jun 08	0.00831	0.00330	5.13	0.00420	0.131	0.032	0.776	0.600
	0.20	80	3 Jun 08	0.00962	0.00360	5.27	0.00305	0.068	0.045	0.833	0.903
	0.30	120	3 Jun 08	0.00985	0.00390	5.59	0.00595	0.047	0.128	0.851	2.610
	0.40	160	3 Jun 08	0.01198	0.00640	5.91	0.00558	0.037	0.151	0.860	3.118
	0.50	200	3 Jun 08	0.01605	0.01160	5.99	0.00445	0.030	0.149	0.866	3.089
0.8	320	3 Jun 08	0.01890	0.01650	6.33	0.00240	0.020	0.121	0.875	2.551	

Table E.2 Experimental data of biokinetic parameters of FDHS system

DHS profiles	S_0/X_0	S (mg/L)	DATE	OUR _{x,t} (mgO ₂ /mgVSS-h)	OUR _{x,e} (mgO ₂ /mgVSS-h)	OC (mgO ₂ /L)	OUR _{x,ox} (mgO ₂ /mgVSS-h)	OC/S	rx (mgCOD/mgVSS-h)	Y _{vss} (mgVSS/mgCOD)	μ (d ⁻¹)
Segment 1	0.05	20	29 May 08	0.005550	0.000730	6.03	0.00482	0.151	0.032	0.551	0.423
	0.10	40	29 May 08	0.007180	0.000900	6.16	0.00628	0.154	0.041	0.549	0.538
	0.20	80	29 May 08	0.007640	0.000920	6.35	0.00672	0.079	0.085	0.598	1.215
	0.30	120	29 May 08	0.010350	0.001500	6.37	0.00885	0.053	0.167	0.615	2.460
	0.40	160	3 May 08	0.011310	0.003700	6.64	0.00761	0.042	0.183	0.622	2.739
	0.50	200	29 May 08	0.013370	0.006240	6.88	0.00713	0.034	0.207	0.627	3.119
	0.80	320	3 Jun 08	0.014225	0.010135	7.25	0.00409	0.023	0.181	0.635	2.750
Segment 2	0.05	20	3 May 08	0.003920	0.000923	5.86	0.00300	0.293	0.010	0.459	0.113
	0.10	40	3 May 08	0.004950	0.001200	5.88	0.00375	0.147	0.026	0.554	0.339
	0.20	80	3 May 08	0.005020	0.001500	6.15	0.00352	0.077	0.046	0.599	0.659
	0.30	120	24 May 08	0.005329	0.001880	6.85	0.00345	0.057	0.060	0.612	0.888
	0.40	160	3 May 08	0.006675	0.002600	6.89	0.00408	0.043	0.095	0.621	1.411
	0.50	200	3 May 08	0.007670	0.004300	7.01	0.00337	0.035	0.096	0.627	1.446
Segment 3	0.05	20	2 Jun 08	0.005490	0.000670	5.83	0.00482	0.292	0.017	0.460	0.183
	0.10	40	2 Jun 08	0.006840	0.001570	5.90	0.00527	0.148	0.036	0.554	0.475
	0.20	80	2 Jun 08	0.008300	0.003330	6.30	0.00497	0.079	0.063	0.598	0.906
	0.30	120	2 Jun 08	0.008740	0.004870	6.51	0.00387	0.054	0.071	0.614	1.051
	0.40	160	3 Jun 08	0.009020	0.005980	6.80	0.00304	0.043	0.072	0.622	1.067
	0.50	200	3 Jun 08	0.010100	0.007200	6.85	0.00290	0.034	0.085	0.627	1.274
	0.80	320	3 Jun 08	0.012130	0.010811	7.56	0.00132	0.024	0.056	0.634	0.850
Segment 4	0.05	20	3 Jun 08	0.004230	0.001200	2.53	0.00303	0.127	0.024	0.567	0.326
	0.10	40	3 Jun 08	0.004350	0.001500	4.94	0.00285	0.124	0.023	0.569	0.315
	0.20	80	29 May 08	0.004450	0.001500	5.14	0.00295	0.064	0.046	0.608	0.670
	0.30	120	2 Jun 08	0.005050	0.001700	5.42	0.00335	0.045	0.074	0.620	1.104
	0.40	160	3 Jun 08	0.008290	0.004600	6.02	0.00369	0.038	0.098	0.625	1.471
	0.50	200	3 Jun 08	0.009600	0.006800	6.23	0.00280	0.031	0.090	0.629	1.357
	0.80	320	3 Jun 08	0.010500	0.008912	6.5	0.001588	0.020	0.078	0.636	1.194

APPENDIX F

EXPERIMENTAL DATA OF SLUDGE

CHARACTERISTICS

Table F.1 Experimental data of retained sludge concentrations during RUN I

DHS profiles	RUN I				
	Date	BDHS (g/L-sponge)		FDHS (g/L-sponge)	
		MLSS	MLVSS	MLSS	MLVSS
Segment 1	30 May 08	39.4	33.4	78.6	77.0
	7 Jul 08	39.0	34.0	79.4	78.0
	8 Jul 08	34.0	29.0	78.0	72.0
	9 Jul 08	42.0	28.0	76.0	74.0
	10 Jul 08	45.0	27.0	77.5	77.0
AVE		39.9	30.3	77.9	75.6
SD		4.1	3.2	1.3	2.5
Segment 2	30 May 08	36.0	24.0	13.9	13.2
	7 Jul 08	32.0	26.0	12.8	12.0
	8 Jul 08	26.0	20.0	10.8	10.0
	9 Jul 08	30.5	19.0	13.4	13.0
	10 Jul 08	24.0	18.0	12.9	12.5
AVE		29.7	21.4	12.8	12.1
SD		4.8	3.4	1.2	1.3
Segment 3	30 May 08	32.0	18.0	34.2	30.0
	7 Jul 08	29.0	22.0	32.0	29.0
	8 Jul 08	30.0	23.0	28.7	27.0
	9 Jul 08	28.0	18.0	31.0	28.4
	10 Jul 08	32.5	19.2	30.5	29.5
AVE		30.3	20.0	31.3	28.8
SD		1.9	2.3	2.0	1.2
Segment 4	30 May 08	62.5	52.0	48.9	46.0
	7 Jul 08	57.9	48.0	45.4	42.7
	8 Jul 08	61.0	54.0	42.0	39.5
	9 Jul 08	56.0	47.0	41.4	38.9
	10 Jul 08	58.9	51.0	45.3	42.6
AVE		59.3	50.4	44.6	41.9
SD		2.6	2.9	3.0	2.9

Table F.2 Experimental data of retained sludge concentrations during RUN II

DHS profiles	RUN II				
	Date	BDHS (g/L-sponge)		FDHS (g/L-sponge)	
		MLSS	MLVSS	MLSS	MLVSS
Segment 1	30 May 08	27.0	19.6	56.0	55.0
	7 Jul 08	29.0	18.4	58.3	48.0
	8 Jul 08	25.0	26.0	51.4	57.0
	9 Jul 08	24.0	17.0	57.4	47.0
	10 Jul 08	26.3	18.7	50.4	47.5
AVE		26.3	19.9	54.7	50.9
SD		1.9	3.5	3.6	4.7
Segment 2	30 May 08	28.0	21.0	11.5	11.2
	7 Jul 08	24.5	17.0	14.5	14.0
	8 Jul 08	26.0	17.0	13.7	13.5
	9 Jul 08	24.6	15.6	11.5	11.0
	10 Jul 08	27.5	22.1	12.4	12.0
AVE		26.1	18.5	12.7	12.3
SD		1.6	2.8	1.3	1.4
Segment 3	30 May 08	23.0	14.0	27.0	26.0
	7 Jul 08	24.0	19.0	28.0	27.0
	8 Jul 08	20.0	13.0	29.4	29.0
	9 Jul 08	24.4	15.0	22.0	22.0
	10 Jul 08	22.7	16.5	26.6	25.0
AVE		22.8	15.5	26.6	25.8
SD		1.7	2.3	2.8	2.6
Segment 4	30 May 08	36.0	32.0	39.4	37.0
	7 Jul 08	40.4	36.0	36.2	34.0
	8 Jul 08	27.0	24.0	38.3	36.0
	9 Jul 08	31.5	28.0	39.4	37.0
	10 Jul 08	34.8	31.0	36.2	34.0
AVE		33.9	30.2	37.9	35.6
SD		5.0	4.5	1.6	1.5

Table F.3 Experimental data of retained sludge concentrations during RUN III

DHS profiles	RUN III				
	Date	BDHS (g/L-sponge)		FDHS (g/L-sponge)	
		MLSS	MLVSS	MLSS	MLVSS
Segment 1	30 May 08	34.0	25.6	60.0	69.0
	7 Jul 08	42.0	24.0	58.9	57.0
	8 Jul 08	28.0	29.0	57.0	51.0
	9 Jul 08	33.5	22.0	62.0	47.0
	10 Jul 08	28.2	27.0	56.5	53.5
AVE		33.1	25.5	58.9	55.5
SD		5.7	2.7	2.2	8.4
Segment 2	30 May 08	26.0	21.0	13.4	13.0
	7 Jul 08	27.0	18.0	16.0	15.0
	8 Jul 08	25.0	22.0	13.0	12.0
	9 Jul 08	24.6	17.5	15.0	14.5
	10 Jul 08	26.0	18.5	13.0	12.4
AVE		25.7	19.4	14.1	13.4
SD		0.9	2.0	1.4	1.3
Segment 3	30 May 08	25.0	16.0	26.0	25.0
	7 Jul 08	19.0	14.0	27.4	26.7
	8 Jul 08	29.0	19.0	32.9	31.0
	9 Jul 08	29.6	21.5	28.0	27.0
	10 Jul 08	33.2	21.0	27.0	26.5
AVE		27.2	18.3	28.3	27.2
SD		5.4	3.2	2.7	2.2
Segment 4	30 May 08	50.2	42.7	40.6	39.0
	7 Jul 08	48.2	41.0	38.5	37.0
	8 Jul 08	58.8	50.0	42.7	41.0
	9 Jul 08	45.9	39.0	38.5	37.0
	10 Jul 08	47.1	40.0	40.1	38.5
AVE		50.0	42.5	40.1	38.5
SD		5.2	4.4	1.7	1.7

Table F.4 EPS concentrations in sludge during RUN I

DHS Profiles	DATE	Bound EPS (mg/mg-SS)						Soluble EPS (mg/mg-SS)					
		Protein (P)		Carbohydrate (C)		P/C		Protein (P)		Carbohydrate (C)		P/C	
		BDHS	FDHS	BDHS	FDHS	BDHS	FDHS	BDHS	FDHS	BDHS	FDHS	BDHS	FDHS
Segment 1	30 May 08	45.0	45.5	10.2	14.5	4.4	3.1	18.2	38.9	7.1	19.4	2.6	2.0
	7 Jul 08	56.0	38.0	11.5	13.0	4.9	2.9	15.6	35.4	8.5	17.5	1.8	2.0
	8 Jul 08	37.0	40.4	8.7	12.0	4.3	3.4	14.7	34.2	6.9	17.9	2.1	1.9
	9 Jul 08	37.4	40.0	9.4	14.0	4.0	2.9	19.7	37.2	6.5	16.1	3.0	2.3
	10 Jul 08	46.5	39.0	8.2	15.0	5.7	2.6	18.9	38.4	6.3	19.5	3.0	2.0
AVE		44.4	40.6	9.6	13.7	4.6	3.0	17.4	36.8	7.1	18.1	2.5	2.0
SD		7.8	2.9	1.3	1.2	0.7	0.3	2.2	2.0	0.9	1.4	0.5	0.2
Segment 2	30 May 08	26.4	32.0	11.6	12.0	2.3	2.7	13.8	32.0	7.0	19.4	2.0	1.6
	7 Jul 08	28.7	27.0	9.8	9.6	2.9	2.8	12.3	38.0	5.7	14.6	2.2	2.6
	8 Jul 08	30.2	29.0	8.7	12.0	3.5	2.4	14.5	39.0	4.8	13.0	3.0	3.0
	9 Jul 08	33.9	33.0	10.9	8.9	3.1	3.7	10.6	31.0	6.5	12.1	1.6	2.6
	10 Jul 08	25.2	28.7	10.7	9.9	2.4	2.9	12.3	35.0	6.0	16.7	2.1	2.1
AVE		28.9	29.9	10.3	10.5	2.8	2.9	12.7	35.0	6.0	15.2	2.2	2.4
SD		3.4	2.5	1.1	1.4	0.5	0.5	1.5	3.5	0.8	2.9	0.5	0.5

Table F.4 EPS concentrations in sludge during RUN I (Continued)

DHS Profiles	DATE	Bound EPS (mg/g-SS)						Soluble EPS (mg/g-SS)					
		Protein (P)		Carbohydrate (C)		P/C		Protein (P)		Carbohydrate (C)		P/C	
		BDHS	FDHS	BDHS	FDHS	BDHS	FDHS	BDHS	FDHS	BDHS	FDHS	BDHS	FDHS
Segment 3	30 May 08	40.2	19.5	14.6	10.6	2.8	1.8	18.9	24.2	7.8	13.5	2.4	1.8
	7 Jul 08	36.5	17.5	9.2	9.3	4.0	1.9	19.7	20.6	6.7	11.9	2.9	1.7
	8 Jul 08	35.1	16.7	8.7	10.5	4.0	1.6	19.4	20.1	6.9	14.2	2.8	1.4
	9 Jul 08	33.8	21.4	10.8	8.4	3.1	2.5	18.2	19.8	5.9	10.8	3.1	1.8
	10 Jul 08	39.8	18.4	13.2	8.9	3.0	2.1	16.8	27.6	7.0	13.0	2.4	2.1
AVE		37.1	18.7	11.3	9.5	3.4	2.0	18.6	22.5	6.9	12.7	2.7	1.8
SD		2.8	1.8	2.5	1.0	0.6	0.4	1.2	3.4	0.7	1.3	0.3	0.3
Segment 4	30 May 08	25.7	30.1	9.8	13.0	2.6	2.3	13.6	50.2	9.6	21.0	1.4	2.4
	7 Jul 08	21.3	28.3	8.5	10.5	2.5	2.7	14.9	43.1	8.7	23.0	1.7	1.9
	8 Jul 08	18.9	25.4	9.8	11.7	1.9	2.2	15.2	45.1	7.8	19.5	1.9	2.3
	9 Jul 08	17.6	26.4	9.2	13.7	1.9	1.9	13.6	39.7	8.2	18.0	1.7	2.2
	10 Jul 08	19.9	26.8	9.6	12.3	2.1	2.2	12.3	44.7	7.9	17.0	1.6	2.6
AVE		20.7	27.4	9.4	12.2	2.2	2.3	13.9	44.6	8.4	19.7	1.7	2.3
SD		3.1	1.8	0.5	1.2	0.3	0.3	1.2	3.8	0.7	2.4	0.2	0.3

Table F.5 EPS concentrations in sludge during RUN II

DHS Profiles	DATE	Bound EPS (mg/g-SS)						Soluble EPS (mg/g-SS)					
		Protein (P)		Carbohydrate (C)		P/C		Protein (P)		Carbohydrate (C)		P/C	
		BDHS	FDHS	BDHS	FDHS	BDHS	FDHS	BDHS	FDHS	BDHS	FDHS	BDHS	FDHS
Segment 1	2 Sep 08	15.0	17.5	5.6	10.2	2.7	1.7	2.6	11.6	3.0	9.7	0.9	1.2
	3 Sep 08	13.0	15.2	4.9	8.5	2.7	1.8	3.2	14.2	1.7	8.6	1.9	1.7
	11 Sep 08	12.0	14.8	6.3	10.2	1.9	1.5	1.9	9.6	2.3	8.7	0.8	1.1
	15 Sep 08	11.3	16.4	4.7	8.9	2.4	1.8	2.0	9.2	1.4	10.2	1.4	0.9
	20 Sep 08	14.0	14.9	5.9	9.3	2.4	1.6	1.8	12.9	1.7	9.4	1.1	1.4
AVE		13.1	15.8	5.5	9.4	2.4	1.7	2.3	11.5	2.0	9.3	1.2	1.2
SD		1.5	1.2	0.7	0.8	0.3	0.2	0.6	2.1	0.6	0.7	0.4	0.3
Segment 2	2 Sep 08	27.0	19.0	9.0	10.9	3.0	1.7	4.0	7.0	5.9	6.5	0.7	1.1
	3 Sep 08	22.0	24.0	8.7	10.4	2.5	2.3	4.8	4.0	5.4	4.7	0.9	0.9
	11 Sep 08	26.0	18.0	9.4	12.0	2.8	1.5	5.7	5.0	3.9	6.8	1.5	0.7
	15 Sep 08	21.0	26.0	10.8	9.4	1.9	2.8	6.2	7.0	4.2	4.9	1.5	1.4
	20 Sep 08	24.0	15.0	12.0	8.7	2.0	1.7	5.2	8.3	3.9	6.5	1.3	1.3
AVE		24.0	20.4	10.0	10.3	2.4	2.0	5.2	6.3	4.7	5.9	1.2	1.1
SD		2.5	4.5	1.4	1.3	0.5	0.5	0.8	1.7	0.9	1.0	0.4	0.3

Table F.5 EPS concentrations in sludge during RUN I(Continued)

DHS Profiles	DATE	Bound EPS (mg/g-SS)						Soluble EPS (mg/g-SS)					
		Protein (P)		Carbohydrate (C)		P/C		Protein (P)		Carbohydrate (C)		P/C	
		BDHS	FDHS	BDHS	FDHS	BDHS	FDHS	BDHS	FDHS	BDHS	FDHS	BDHS	FDHS
Segment 3	2 Sep 08	15.0	29.0	6.7	14.5	2.2	2.0	4.0	4.7	3.2	5.2	1.3	0.9
	3 Sep 08	16.0	21.0	5.5	9.8	2.9	2.1	2.9	6.0	3.1	4.9	0.9	1.2
	11 Sep 08	13.0	26.4	6.7	12.3	1.9	2.1	3.8	5.8	4.5	4.7	0.8	1.2
	15 Sep 08	12.5	24.0	7.1	11.7	1.8	2.1	4.1	3.4	3.2	4.8	1.3	0.7
	20 Sep 08	14.2	26.8	5.4	13.0	2.6	2.1	4.2	5.0	3.5	4.1	1.2	1.2
AVE		14.1	25.4	6.3	12.3	2.3	2.1	3.8	5.0	3.5	4.7	1.1	1.1
SD		1.4	3.1	0.8	1.7	0.5	0.1	0.5	1.0	0.6	0.4	0.2	0.2
Segment 4	2 Sep 08	36.0	29.0	14.0	12.0	2.6	2.4	9.7	8.4	9.3	7.4	1.0	1.1
	3 Sep 08	29.8	25.0	10.8	14.0	2.8	1.8	7.9	8.7	9.6	8.2	0.8	1.1
	11 Sep 08	29.7	30.0	17.0	9.4	1.7	3.2	10.9	7.4	7.5	6.2	1.5	1.2
	15 Sep 08	32.0	25.0	10.0	8.8	3.2	2.8	9.6	8.6	8.0	7.8	1.2	1.1
	20 Sep 08	31.9	24.0	10.7	9.9	3.0	2.4	8.7	8.3	9.8	6.7	0.9	1.2
AVE		31.9	26.6	12.5	10.8	2.7	2.5	9.4	8.3	8.8	7.3	1.1	1.1
SD		2.6	2.7	3.0	2.1	0.6	0.5	1.1	0.5	1.0	0.8	0.3	0.1

Table F.6 EPS concentrations in sludge during RUN III

DHS Profiles	DATE	Bound EPS (mg/g-SS)						Soluble EPS (mg/g-SS)					
		Protein (P)		Carbohydrate (C)		P/C		Protein (P)		Carbohydrate (C)		P/C	
		BDHS	FDHS	BDHS	FDHS	BDHS	FDHS	BDHS	FDHS	BDHS	FDHS	BDHS	FDHS
Segment 1	12 Jan 09	18.4	35.0	5.3	14.0	3.5	2.5	4.0	16.0	3.2	12.0	1.3	1.3
	15 Jan 09	21.2	30.1	5.6	10.0	3.8	3.0	7.5	17.2	3.0	14.0	2.5	1.2
	25 Feb 09	20.1	29.8	5.7	12.0	3.5	2.5	4.9	18.0	5.0	8.0	1.0	2.3
	15 Mar 09	18.0	34.3	6.3	11.0	2.9	3.1	5.6	21.0	3.8	12.0	1.5	1.8
	17 Mar 09	19.0	32.4	5.0	12.0	3.8	2.7	5.4	14.0	2.0	5.0	2.7	2.8
AVE		19.3	32.3	5.6	11.8	3.5	2.8	5.5	17.2	3.4	10.2	1.8	1.9
SD		1.3	2.4	0.5	1.5	0.4	0.3	1.3	2.6	1.1	3.6	0.8	0.7
Segment 2	12 Jan 09	36.0	22.0	10.1	14.0	3.6	1.6	6.7	8.9	4.9	6.0	1.4	1.5
	15 Jan 09	29.8	23.0	12.3	13.0	2.4	1.8	7.5	6.4	5.2	7.8	1.4	0.8
	25 Feb 09	32.0	28.0	11.4	11.0	2.8	2.5	5.8	9.7	3.8	5.6	1.5	1.7
	15 Mar 09	30.1	25.0	8.5	9.7	3.5	2.6	7.1	11.4	3.9	6.9	1.8	1.7
	17 Mar 09	32.0	24.0	9.4	16.0	3.4	1.5	5.9	8.4	4.5	5.6	1.3	1.5
AVE		32.0	24.4	10.3	12.7	3.1	2.0	6.6	9.0	4.5	6.4	1.5	1.4
SD		2.5	2.3	1.5	2.5	0.5	0.5	0.7	1.8	0.6	1.0	0.2	0.4

Table F.6 EPS concentrations in sludge during RUN III (Continued)

DHS Profiles	DATE	Bound EPS (mg/g-SS)						Soluble EPS (mg/g-SS)					
		Protein (P)		Carbohydrate (C)		P/C		Protein (P)		Carbohydrate (C)		P/C	
		BDHS	FDHS	BDHS	FDHS	BDHS	FDHS	BDHS	FDHS	BDHS	FDHS	BDHS	FDHS
Segment 3	12 Jan 09	19.2	38.0	4.9	17.0	3.9	2.2	7.9	6.0	3.7	4.5	2.1	1.3
	15 Jan 09	17.0	30.0	7.2	19.0	2.4	1.6	8.3	4.2	3.5	5.6	2.4	0.8
	25 Feb 09	15.0	31.0	6.7	16.0	2.2	1.9	5.9	5.8	4.1	3.9	1.4	1.5
	15 Mar 09	18.0	31.0	7.8	15.0	2.3	2.1	7.4	4.8	2.8	5.1	2.6	0.9
	17 Mar 09	16.4	29.0	5.2	15.0	3.2	1.9	8.5	5.2	3.9	4.9	2.2	1.1
AVE		17.1	31.8	6.4	16.4	2.8	2.0	7.6	5.2	3.6	4.8	2.2	1.1
SD		1.6	3.6	1.3	1.7	0.7	0.2	1.0	0.7	0.5	0.6	0.4	0.3
Segment 4	12 Jan 09	35.0	27.0	13.4	16.0	2.6	1.7	9.2	8.5	7.8	9.0	1.2	0.9
	15 Jan 09	28.0	19.4	14.1	13.0	2.0	1.5	7.9	7.4	8.4	9.7	0.9	0.8
	25 Feb 09	27.9	25.0	12.0	17.0	2.3	1.5	8.2	5.8	6.9	7.5	1.2	0.8
	15 Mar 09	35.0	21.0	13.4	12.0	2.6	1.8	8.3	8.7	7.4	7.4	1.1	1.2
	17 Mar 09	37.0	23.0	10.5	13.0	3.5	1.8	8.3	7.9	7.2	8.4	1.2	0.9
AVE		32.6	23.1	12.7	14.2	2.6	1.6	8.4	7.7	7.5	8.4	1.1	0.9
SD		4.3	3.0	1.4	2.2	0.6	0.1	0.5	1.2	0.6	1.0	0.1	0.2

APPENDIX G

THE UNIFIED MULTI-COMPONENT CELLULAR AUTOMATON (UMCCA) MODEL DATA

G.1 Part of the 2-D Physical Space of the Model

There are 150 compartments across the x direction and 70 compartments across the z direction. For the shaded element, $i=1$ since it is in the 1st row, and $j=2$ since it is in the 2nd column. Thus, the shaded element is compartment (2, 1).

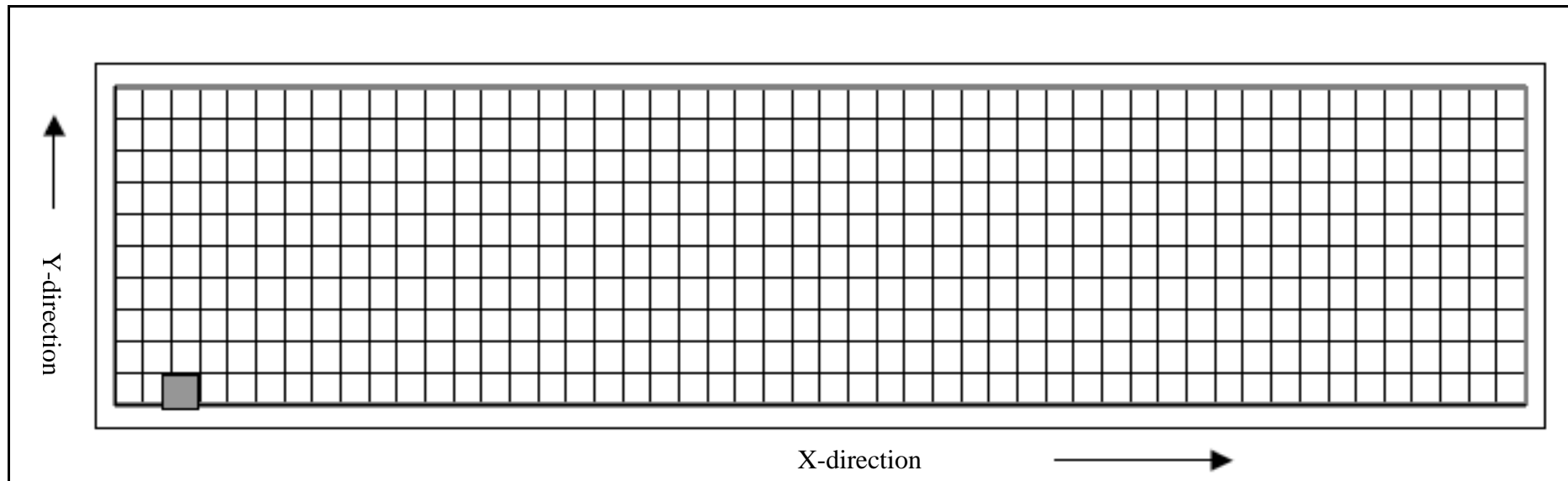


Figure G.1 Example of the part of 2-D physical space of the model

G.2 Statistical Analysis of Data Output for the UMCCA Model

Table G.1 Statistical analysis of data output for the segment 1 of FDHS system (*Bioage* 45 days)

Variables	Range of Values	Total Average	Average σ by row	% of average value	Average σ by column	% of average value
S	0.0703-1.0	0.2301	0.0023	1.00	0.1429	62.10
X _a	0-0.7189	0.3120	0.0121	3.88	0.2546	81.60
X _{res}	0-0.2624	0.1383	0.0098	7.09	0.0848	61.32
EPS	0-0.0555	0.0304	0.0038	12.50	0.0167	54.93
UAP	0-0.0102	0.0084	1.23×10 ⁻⁴	1.46	0.0027	32.14
BAP	0-1.06×10 ⁻⁴	8.72×10 ⁻⁴	3.12×10 ⁻⁶	0.36	2.79×10 ⁻⁴	32.00
CompDen (gCOD _x /L)	0-57.7	43.8	2.1	4.79	13.8	31.51

Table G.2 Statistical analysis of data output for the segment 2 of FDHS system (*Bioage* 180 days)

Variables	Range of Values	Total Average	Average σ by row	% of average value	Average σ by column	% of average value
S	0.0161-1.0	0.2412	0.0142	5.89	0.1465	60.73
X _a	0-0.2940	0.0699	0.0107	15.36	0.0578	82.69
X _{res}	0-0.1198	0.0683	8.43×10 ⁻³	12.34	0.0416	60.91
EPS	0-0.0048	2.63×10 ⁻³	2.41×10 ⁻⁴	9.85	1.45×10 ⁻³	55.13
UAP	0-0.0047	0.0038	1.70×10 ⁻⁴	4.48	1.22×10 ⁻³	32.11
BAP	0-1.31×10 ⁻⁵	1.07×10 ⁻⁵	3.67×10 ⁻⁷	3.43	3.44×10 ⁻⁶	32.15
CompDen (gCOD _x /L)	0-32.9	20.4	1.5	7.25	7.2	35.29

Table G.3 Statistical analysis of data output for the segment 3 of FDHS system (*Bioage* 180 days)

Variables	Range of Values	Total Average	Average σ by row	% of average value	Average σ by column	% of average value
S	0.1181-1.0	0.1793	0.5917	3.30	0.1192	66.48
X_a	0-0.1563	0.0526	7.78×10^{-3}	14.80	0.0479	91.06
X_{res}	0-0.1520	0.0852	0.0113	13.24	0.0522	61.27
EPS	$0-1.46 \times 10^{-3}$	7.24×10^{-4}	5.68×10^{-5}	7.85	4.90×10^{-4}	67.68
UAP	$0-4.23 \times 10^{-3}$	3.47×10^{-3}	1.91×10^{-5}	5.51	1.11×10^{-3}	31.98
BAP	$0-3.41 \times 10^{-3}$	2.79×10^{-4}	1.10×10^{-5}	3.95	8.92×10^{-5}	31.97
CompDen (gCOD _x /L)	0-33.1	22.7	1.9	8.30	9.5	41.85

Table G.4 Statistical analysis of data output for the segment 4 of FDHS system (*Bioage* 180 days)

Variables	Range of Values	Total Average	Average σ by row	% of average value	Average σ by column	% of average value
S	0.0957-1.0	0.1466	9.50×10^{-3}	6.48	0.1067	72.78
X_a	0-0.1269	0.0427	5.16×10^{-3}	12.08	0.0389	91.10
X_{res}	0-0.1851	0.1048	8.33×10^{-3}	7.95	0.0643	61.35
EPS	$0-1.29 \times 10^{-3}$	6.43×10^{-4}	5.39×10^{-3}	8.38	4.35×10^{-4}	67.65
UAP	$0-3.89 \times 10^{-3}$	3.18×10^{-3}	9.38×10^{-5}	2.95	1.09×10^{-3}	34.28
BAP	$0-3.02 \times 10^{-5}$	2.46×10^{-5}	1.30×10^{-6}	5.26	7.89×10^{-6}	32.07
CompDen (gCOD _x /L)	0-40.8	26.3	2.2	8.25	12.6	47.91

Table G.5 Statistical analysis of data output for the segment 1 of BDHS system (*Bioage* 245 days)

Variables	Range of Values	Total Average	Average σ by row	% of average value	Average σ by column	% of average value
S	0.2106-1.0	0.2909	0.0107	3.68	0.2028	69.74
X_a	0-0.1922	0.3365	0.0322	9.58	0.2169	64.47
X_{res}	0-0.0968	0.0543	7.47×10^{-4}	13.76	0.0334	61.51
EPS	0-0.0050	0.0012	2.23×10^{-4}	18.58	7.23×10^{-4}	60.24
UAP	0-0.0103	0.0103	3.89×10^{-4}	3.78	6.43×10^{-4}	6.24
BAP	$0-2.63 \times 10^{-5}$	2.15×10^{-5}	3.69×10^{-7}	2.49	6.89×10^{-6}	3.20
CompDen (gCOD _x /L)	0-170.5	99.0	9.4	9.45	35.5	35.81

Table G.6 Statistical analysis of data output for the segment 2 of BDHS system (*Bioage* 65 days)

Variables	Range of Values	Total Average	Average σ by row	% of average value	Average σ by column	% of average value
S	0.0502-1.0	0.2234	0.0028	1.25	0.1897	84.91
X_a	0-0.3107	0.1172	0.0215	18.34	0.1035	88.31
X_{res}	0-0.3074	0.1709	0.0215	12.58	0.1044	61.09
EPS	0-0.1235	0.0620	0.0102	16.47	0.0400	64.52
UAP	0-0.0167	0.0137	1.56×10^{-4}	1.14	0.0044	32.12
BAP	$0-1.53 \times 10^{-4}$	1.26×10^{-4}	2.26×10^{-6}	1.79	4.02×10^{-5}	31.90
CompDen (gCOD _x /L)	0-68.7	58.2	5.2	8.93	17.56	30.17

Table G.7 Statistical analysis of data output for the segment 3 of BDHS system (*Bioage* 145 days)

Variables	Range of Values	Total Average	Average σ by row	% of average value	Average σ by column	% of average value
S	0.0402-1.0	0.1820	0.0047	2.58	0.1560	85.71
X_a	0-0.2354	0.0889	0.0135	15.19	0.0780	87.74
X_{res}	0-0.4458	0.2491	0.0439	17.63	0.1516	60.86
EPS	0-0.0594	0.0326	2.61×10^{-3}	8.01	0.0179	54.91
UAP	0-0.0151	0.0124	3.98×10^{-4}	3.21	0.0039	31.45
BAP	2.39×10^{-4}	1.96×10^{-4}	3.12×10^{-6}	3.12	6.27×10^{-5}	31.99
CompDen (gCOD _x /L)	0-98.9	67.2	8.6	12.80	28.3	42.11

Table G.8 Statistical analysis of data output for the segment 4 of BDHS system (*Bioage* 105 days)

Variables	Range of Values	Total Average	Average σ by row	% of average value	Average σ by column	% of average value
S	0.0397-1.0	0.1815	0.0043	2.36	0.1081	59.56
X_a	0-0.3531	0.1332	0.0224	16.81	0.1176	88.29
X_{res}	0-0.3625	0.2015	0.0178	8.78	0.1231	61.09
EPS	0-0.0506	0.2780	0.0252	9.06	0.1821	65.50
UAP	0-0.0139	0.0114	0.68×10^{-4}	5.96	0.0036	31.58
BAP	$0-2.61 \times 10^{-4}$	2.14×10^{-4}	5.37×10^{-6}	2.51	6.84×10^{-5}	31.96
CompDen (gCOD _x /L)	0-81.2	59.2	6.2	10.47	20.1	33.95

APPENDIX H

EXPERIMENTAL DATA OF DISSOLVED OXYGEN, TOTAL SUSPENDED SOLIDS AND PH VALUES

Table H.1 TSS removal efficiency of FDHS and BDHS system during RUN I

Date	BDHS system			FDHS system		
	Influent	Effluent	% Removal	Influent	Effluent	% Removal
10 Dec 08	350	96	72.6	350	35.0	90.0
23 Feb 08	1,050	230	78.1	1,050	97.6	90.7
4 Mar 08	560	145	74.1	560	72.0	87.1
18 Mar 08	801	233	70.9	801	56.0	93.0
7 Jun 08	688	189	72.5	688	61.0	91.1
30 May 08	650	165	74.6	650	56.0	91.4
7 Jul 08	920	276	70.0	920	74.0	92.0
8 Jul 08	712	224	68.5	712	66.0	90.7
9 Jul 08	690	202	70.7	690	65.0	90.6
10 Jul 08	650	189	70.9	650	64.0	90.2
Average	707.1	194.9	72.4	707.1	64.7	90.9
S.D	190.9	51.0	2.8	190.9	15.9	91.7

Table H.2 TSS removal efficiency of FDHS and BDHS system during RUN II

Date	BDHS system			FDHS system		
	Influent	Effluent	% Removal	Influent	Effluent	% Removal
2 Sep 08	740	67	90.9	740	65	91.2
3 Sep 08	820	75	90.9	820	73	91.1
11 Sep 08	720	89	87.6	720	68	90.6
15 Sep 08	720	74	89.7	720	70	90.3
20 Sep 08	657	79	88.0	657	72	89.0
Average	731.4	76.8	89.4	731.4	69.6	90.4
S.D	58.6	8.1	1.6	58.6	3.2	0.9

Table H.3 TSS removal efficiency of FDHS and BDHS system during RUN III

Date	BDHS system			FDHS system		
	Influent	Effluent	% Removal	Influent	Effluent	% Removal
12 Jan 09	780	179	77.1	780	89	88.6
15 Jan 09	670	160	76.1	670	78	88.4
25 Feb 09	560	148	73.6	560	65	88.4
15 Mar 09	813	175	78.5	813	87	89.3
17 Mar 09	673	156	76.8	673	93	86.2
Average	699.2	163.6	76.4	699.2	82.4	88.2
S.D	100.5	13.0	1.8	100.5	11.2	1.2

Table H.4 pH values of FDHS and BDHS system during RUN I

Date	BDHS System		FDHS System	
	Influent	Effluent	Influent	Effluent
10 Dec 08	6.9	7.6	4.1	4.6
23 Feb 08	6.9	7.7	3.9	4.4
4 Mar 08	7.0	7.8	3.9	4.3
18 Mar 08	7.1	8.0	4.1	4.8
7 Jun 08	7.0	7.9	4.0	4.5
30 May 08	6.8	7.6	3.9	4.7
7 Jul 08	6.8	7.6	3.8	4.9
8 Jul 08	6.9	7.9	3.9	4.9
9 Jul 08	7.0	7.8	4.1	4.9
10 Jul 08	7.1	8.1	4.0	4.8
Average	6.95	7.80	3.97	4.68
S.D	0.11	0.18	0.11	0.22

Table H.5 pH values of FDHS and BDHS system during RUN II

Date	BDHS System		FDHS System	
	Influent	Effluent	Influent	Effluent
2 Sep 08	7.2	7.9	4.1	4.8
3 Sep 08	7.0	7.8	4.2	4.9
11 Sep 08	6.9	7.7	3.9	4.8
15 Sep 08	6.9	7.9	3.8	4.7
20 Sep 08	6.8	7.7	4.0	4.9
Average	6.96	7.79	4.00	4.81
S.D	0.15	0.11	0.16	0.08

Table H.6 pH values of FDHS and BDHS system during RUN III

Date	BDHS System		FDHS System	
	Influent	Effluent	Influent	Effluent
12 Jan 09	6.9	7.9	4.0	4.8
15 Jan 09	6.9	7.8	3.8	4.8
25 Feb 09	7.1	8.1	3.9	4.9
15 Mar 09	7.0	7.9	4.0	4.8
17 Mar 09	7.2	8.0	4.1	4.9
Average	7.02	7.93	3.96	4.84
S.D	0.13	0.13	0.11	0.06

Table H.7 Dissolved oxygen profiles of FDHS and BDHS effluent during RUN I

Date	FDHS Effluent				BDHS Effluent			
	Segment 1	Segment 2	Segment 3	Segment 4	Segment 1	Segment 2	Segment 3	Segment 4
10 Dec 08	4.2	4.3	4.8	3.2	0.2	1.0	2.2	2.9
23 Feb 08	3.1	3.8	4.3	2.4	0.1	0.3	2.7	3.1
4 Mar 08	2.9	3.9	4.5	2.5	0.3	0.5	2.6	3.2
18 Mar 08	3.4	4.2	4.6	2.4	0.2	0.6	2.9	3.0
7 Jun 08	3.2	4.4	4.9	3.0	0.2	0.4	2.7	3.4
30 May 08	2.8	4.1	4.5	2.6	0.1	0.6	3.1	3.3
7 Jul 08	3.1	3.8	4.3	2.3	0.2	0.5	2.8	3.5
8 Jul 08	3.2	4.2	4.5	2.2	0.3	0.7	2.5	3.2
9 Jul 08	3.5	4.2	4.5	2.4	0.1	0.8	2.4	3.3
10 Jul 08	3.3	4.3	4.7	2.5	0.1	0.9	2.5	3.4
Average	3.27	4.12	4.56	2.55	0.18	0.63	2.64	3.23
S.D	0.39	0.21	0.20	0.31	0.08	0.22	0.26	0.19

Table H.8 Dissolved oxygen profiles of FDHS and BDHS effluent during RUN II

Date	FDHS Effluent				BDHS Effluent			
	Segment 1	Segment 2	Segment 3	Segment 4	Segment 1	Segment 2	Segment 3	Segment 4
2 Sep 08	2.9	4.9	5.0	3.1	4.1	3.8	5.2	3.4
3 Sep 08	3.7	5.3	4.8	3.6	3.7	3.4	4.8	3.5
11 Sep 08	3.3	5.2	5.1	3.7	4.0	3.5	5.4	3.6
15 Sep 08	4.0	5.0	4.9	4.3	3.0	3.6	4.9	3.7
20 Sep 08	3.3	5.0	4.8	4.1	3.8	3.7	5.5	3.6
Average	3.44	5.08	4.92	3.76	3.72	3.60	5.16	3.56
S.D	0.42	0.16	0.13	0.47	0.43	0.16	0.30	0.11

Table H.9 Dissolved oxygen profiles of FDHS and BDHS effluent during RUN III

Date	FDHS Effluent				BDHS Effluent			
	Segment 1	Segment 2	Segment 3	Segment 4	Segment 1	Segment 2	Segment 3	Segment 4
12 Jan 09	2.9	4.2	5.2	3.7	2.6	3.1	3.6	3.4
15 Jan 09	3.3	3.9	4.9	3.9	2.8	3.2	3.5	3.2
25 Feb 09	2.9	4.1	5.3	3.7	2.9	3.4	3.3	3.3
15 Mar 09	3.1	4.6	5.4	3.9	2.7	3.1	3.6	3.3
17 Mar 09	3.2	4.5	4.9	3.8	2.5	3.4	3.4	3.4
Average	3.08	4.26	5.14	3.80	2.70	3.24	3.48	3.32
S.D	0.18	0.29	0.23	0.10	0.16	0.15	0.13	0.08

APPENDIX I

LIST OF PUBLICATIONS

Racho, P. and Wichitsathian, B. Feasibility of low cost post-treatment options for the anaerobic processes of tapioca starch wastewater: Fungal Down-flow Hanging Sponge (DHS) and Bacterial DHS systems. **KKU Res. J.** 13(10): 1-12.

KKU. Res. J. 13(10): November 2008

Feasibility of low cost post-treatment options for the anaerobic processes of tapioca starch wastewater: Fungal Down-flow Hanging Sponge (DHS) and Bacterial DHS systems

Presented in 12th International Conference on Integrated Diffuse Pollution Management (IWA DIPCON 2008).
Research Center for Environmental and Hazardous Substance Management (EHSM),

Patcharin Racho¹ and Boonchai Wichitsathian²

¹School of Environmental Engineering, Institute of Engineering,
Suranaree University of Technology, 111

Abstract

Aim of this research is to study the performances of the Downflow Hanging Sponge (DHS) systems using mixed fungal culture (FDHS) and mixed bacterial culture (BDHS) for treatment of UASB effluent of tapioca starch wastewater. This study attempted to compare the performance of the fungal and bacterial systems by systematically studying biokinetics coefficients by respirometry. Also, the influencing of sludge compositions to their microbial activity and effluent organic matter (EfOM) were evaluated. The remaining filtered COD in UASB effluent were about 45-50% removed in both of Bacterial DHS (BDHS) and Fungal DHS (FDHS) units and 71% and 48% filtered BOD₅ removed, respectively. Organic loading rate of in both of BDHS and FDHS reactors were 2.0-4.0 kgCOD/m³-d, at 7 h HRT. Values of biokinetic coefficients showed that substrate utilization rate and maximum specific growth rate were higher for the bacteria culture, which explained the higher COD removal rate for the bacterial culture. In steady state, the concentration of retained sludge in FDHS remained almost constant suggesting that the degradation of old biomass nearly balance the accumulation of the fresh one. Macromolecular compounds such as proteins and carbohydrate can comprise a significant portion of dissolved organic carbon in the DHS effluents.

Keyword: Downflow Hanging Sponge (DHS) system, Fungal culture, Bacterial culture, Post treatment system, Tapioca starch wastewater

Racho, P. and Wichitsathian, B. (2008). Feasibility of low cost post-treatment options for the anaerobic processes of tapioca starch wastewater: Fungal Down-flow Hanging Sponge (DHS) and Bacterial DHS systems. **12th International Conference on Integrated Diffuse Pollution Management (IWA DIPCON 2008)**, 25-29 August 2008. Research Center for Environmental and Hazardous Substance Management (EHSM), Khon Kaen University, Thailand.

12th International Conference on Integrated Diffuse Pollution Management (IWA DIPCON 2008).
Research Center for Environmental and Hazardous Substance Management (EHSM),
Khon Kaen University, Thailand ; 25-29 August 2008.

Feasibility of low cost post-treatment options for the anaerobic processes of tapioca starch wastewater: Fungal Down-flow Hanging Sponge (DHS) and Bacterial DHS systems

Patcharin Racho¹ and Boonchai Wichitsathian²

¹School of Environmental Engineering, Institute of Engineering,
Suranaree University of Technology, 111

Abstract

Aim of this research is to study the performances of the Downflow Hanging Sponge (DHS) systems using mixed fungal culture (FDHS) and mixed bacterial culture (BDHS) for treatment of UASB effluent of tapioca starch wastewater. This study attempted to compare the performance of the fungal and bacterial systems by systematically studying biokinetics coefficients by respirometry. Also, the influencing of sludge compositions to their microbial activity and effluent organic matter (EfOM) were evaluated. The remaining filtered COD in UASB effluent were about 45-50% removed in both of Bacterial DHS (BDHS) and Fungal DHS (FDHS) units and 71% and 48% filtered BOD₅ removed, respectively. Organic loading rate of in both of BDHS and FDHS reactors were 2.0-4.0 kgCOD/m³-d, at 7 h HRT. Values of biokinetic coefficients showed that substrate utilization rate and maximum specific growth rate were higher for the bacteria culture, which explained the higher COD removal rate for the bacterial culture. In steady state, the concentration of retained sludge in FDHS remained almost constant suggesting that the degradation of old biomass nearly balance the accumulation of the fresh one. Macromolecular compounds such as proteins and carbohydrate can comprise a significant portion of dissolved organic carbon in the DHS effluents.

Keyword: Downflow Hanging Sponge (DHS) system, Fungal culture, Bacterial culture, Post treatment system, Tapioca starch wastewater

Racho, P., Wichitsathian, B. and Jindal, R. (2009). Biokinetic parameters as an indicator to biodegradability assessment of down-flow hanging sponge (DHS) system. **Proceeding of the 8th National Environmental Conference**, 25-27 March, 2009. Suranaree University of Technology, Thailand.

**การประเมินการย่อยสลายทางชีวภาพในระบบ Down-flow Hanging Sponge (DHS)
ด้วยค่าคงที่ทางจลศาสตร์**

**Biokinetic Parameters as an Indicator to Biodegradability Assessment
of Down-flow Hanging Sponge (DHS) System**

พัชรินทร์ ราชโ¹ บุญชัย วิจิตรเสถียร² และ รัญจนา จิตดาล³

Patcharin Racho¹ Boonchai Wichitsathian² and Ranjna Jindal³

บทคัดย่อ

บทความนี้นำเสนอการอธิบายกลไกการย่อยสลายทางชีวภาพในระบบ Downflow Hanging Sponge (DHS) เพื่อบำบัดน้ำทิ้งจากระบบ UASB ในอุตสาหกรรมแป้งมันสำปะหลัง ด้วยการศึกษารอบคอบของค่าซีโอดีที่เป็นสารตั้งต้นและค่าคงที่ทางจลศาสตร์ของจุลชีพในระบบ DHS จากการศึกษาความสามารถในการย่อยสลายทางชีวภาพในระบบ DHS พบแนวโน้มการลดลงของ BSCOD ตามระดับความสูงของถังปฏิกรณ์ DHS แต่ BPCOD พบการเพิ่มขึ้นในน้ำเสียที่เข้าและออกจากระบบ DHS ใน segment ที่ 2 และ 4 โดยเพิ่มจาก 119 mg/L เป็น 456 mg/L และ 185 mg/L เป็น 382 mg/L ตามลำดับ ซึ่งการเพิ่มขึ้นของ PBOD เกิดเนื่องจากการสะสมและการหลุดของระบบฟิล์มชีวภาพและมีผลกระทบต่อค่าคงที่ทางจลศาสตร์ในระบบ DHS โดย BPCOD เป็นสารอินทรีย์ที่มีโมเลกุลขนาดใหญ่จึงต้องการกระบวนการไฮโดรไลซิสให้มีโมเลกุลขนาดเล็กก่อนจึงจะดูดซึมเข้าสู่เซลล์ได้ อีกทั้งจากการศึกษาพบว่าองค์ประกอบของ BSCOD ส่วนใหญ่ถูกกำจัดไปใน Segment ที่ 1 ของระบบ DHS โดยเมื่อพิจารณา ค่าคงที่ทางจลศาสตร์ของจุลชีพในกลุ่ม aerobic heterotrophs พบว่าค่า substrate utilization rate (r_{su}) และ maximum specific growth rate (μ_{max}) ของตะกอนในระบบ DHS กลับสูงสุดใน Segment ที่ 4 และ 2 ซึ่งอาจเกิดเนื่องจากการใช้ออกซิเจนของจุลชีพในกระบวนการไฮโดรไลซิสเพื่อเปลี่ยนรูปสารอินทรีย์ที่มีโมเลกุลขนาดใหญ่ให้มีขนาดเล็กลง

คำสำคัญ: ระบบ downflow hanging sponge (DHS), การย่อยสลายทางชีวภาพ, องค์ประกอบของซีโอดี, ค่าคงที่ทางจลศาสตร์, อุตสาหกรรมแป้งมันสำปะหลัง

¹Ph.D. candidate, ^{2*} Assistant Professor, School of Environmental Engineering, Institute of Engineering, Suranaree University of Technology, 111 University Avenue, Muang District, Nakhon Ratchasima, Thailand 30000

³Assistant Professor, School of Civil Engineering, Faculty of Engineering, Mahidol University, 25/25 Puthamonthon, Nakorn Pathom, Thailand, 73170.

* Corresponding author: Tel. 0-4422-4451, Fax. 0-4422-4606, Email: boonchai@sut.ac.th

Wichitsatian, B. and Racho, P. (2009). Quantification of Organic and Nitrogen Removal in Downflow Hanging Sponge (DHS) Systems as a Post-Treatment of UASB Effluent. **IWA Specialist Conference Chemical Industries**, November 30-December 2. Massey University, Palmerston North, New-Zealand.

IWA Specialist Conference Chemical Industries, November 30-December 2.

Massey University, Palmerston North, New-Zealand.

Quantification of Organic and Nitrogen Removal in Downflow Hanging Sponge (DHS) Systems as a Post-Treatment of UASB Effluent

B. Wichitsathian* and P. Racho**

*School of Environmental Engineering, Institute of Engineering, Suranaree University of Technology, 111 University Avenue, Muang District, Nakhon Ratchasima, Thailand 30000 (E-mail: *boonchai@sut.ac.th*)

**School of Environmental Engineering, Institute of Engineering, Suranaree University of Technology, 111 University Avenue, Muang District, Nakhon Ratchasima, Thailand 30000 (E-mail: *racho_p@hotmail.com*)

Abstract The aim of this research was to investigate the nature and composition of organic substrate in two down-flow hanging sponge (DHS) systems using mixed fungal (FDHS) and bacterial (BDHS) cultures treatment for UASB effluent of tapioca starch wastewater, evaluated by COD fractionations and two material balances. The random type DHS reactors were operated module column consisting of four identical segments connected vertically. Results of the wastewater characterization showed that carbonaceous fractions were varied on a function of DHS height. Two balances applied to experimental data were for chemical oxygen demand (COD) and nitrogen (N). Results of mass balance calculations can also be used to examine the process behavior of two DHS systems to improve the organic and nitrogen removal mechanisms.

KEYWORDS: downflow hanging sponge (DHS) system; biodegradation; COD fractions; COD mass balance; nitrogen mass balance; tapioca starch wastewater

BIOGRAPHY

Miss Patcharin Racho was born on October 28, 1974, in Roi-Et, a northeast province of Thailand. She studied at the Roi-Et Wittayalai School, Roi-Et for her secondary school education. She received her bachelor and master degrees in Environmental Engineering from Suranaree University of Technology (SUT). Following her master's degree graduation, she worked as Technical Engineer for two years at Hydrozone Co., Ltd., Bangkok. After that, she worked as Data and Technical Engineering Manager for three years at Toprich Corporation Co., Ltd. Subsequently, she interested to learn more about environmental section. She was going to study in doctoral program of Environmental Engineering at SUT, in 2004